UNIVERSIDAD AUTÓNOMA DE MADRID

PROGRAMA DE DOCTORADO EN BIOCIENCIAS MOLECULARES

REGULACIÓN EPIGÉNETICA DE LA EXPRESIÓN DE ARNs NO CODIFICANTES Y SU IMPLICACIÓN EN LA RESPUESTA TERAPÉUTICA EN CÁNCER DE PULMÓN NO MICROCÍTICO Y CÁNCER DE OVARIO

TESIS DOCTORAL

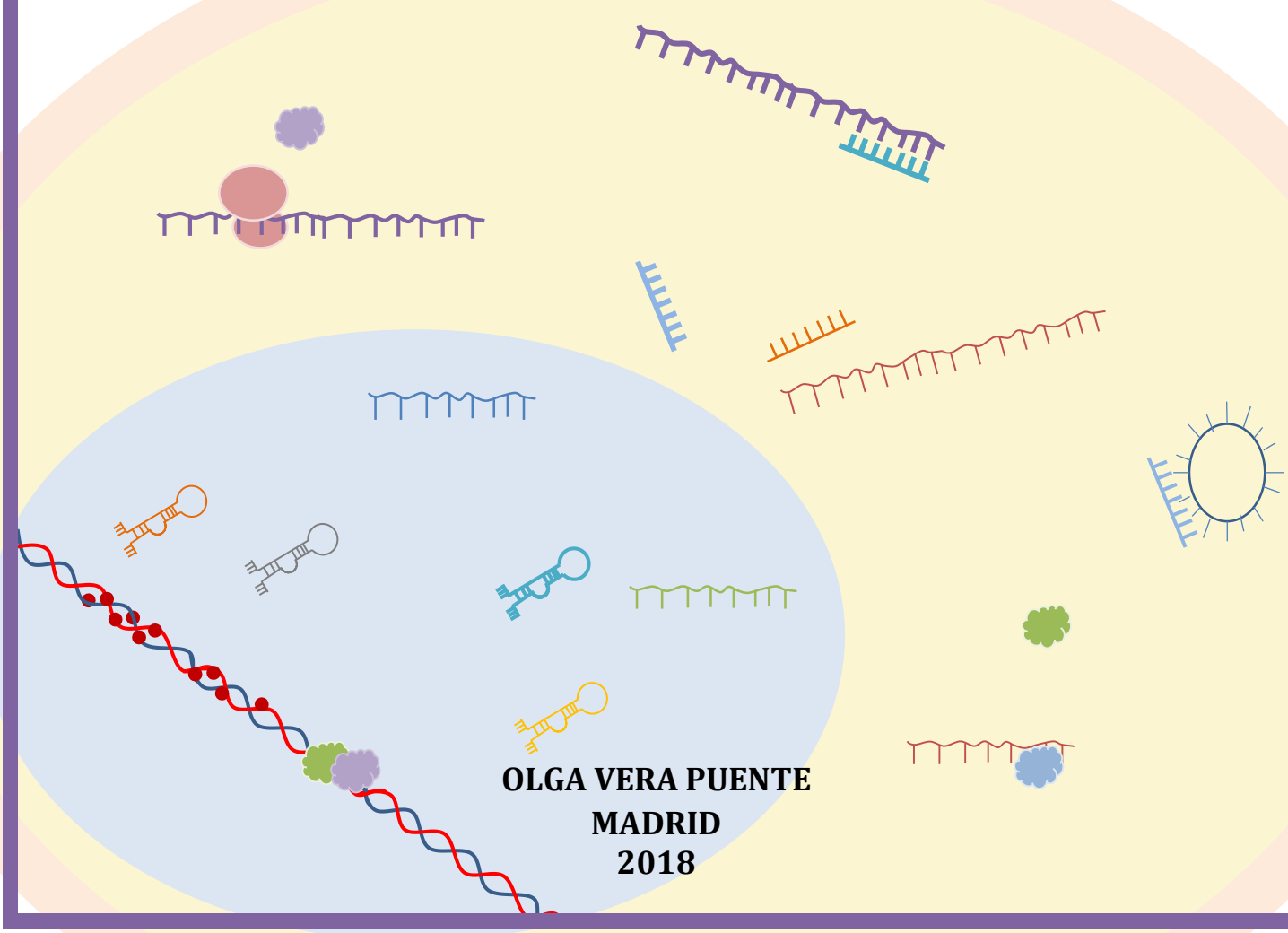

OLGA VERA PUENTE

MADRID

2018

Departamento de Bioquímica

Facultad de Medicina

Universidad Autónoma de Madrid

REGULACIÓN EPIGÉNETICA DE LA EXPRESIÓN DE ARNs NO CODIFICANTES Y SU IMPLICACIÓN EN LA RESPUESTA TERAPÉUTICA EN CÁNCER NO MICROCÍTICO DE PULMÓN Y CÁNCER DE OVARIO

Tesis Doctoral

Olga Vera Puente

Graduada en Biología por la Universidad Autónoma de Madrid

Directora de la Tesis:

Inmaculada Ibáñez de Cáceres

Fundación para la Investigación Biomédica del Hospital la Paz,

Laboratorio de Epigenética

"It is our choices, Harry, that
show what we truly are, far more
than our abilities."

A quien siempre creyó en mí

AGRADECIMIENTOS

AGRADECIMIENTOS

Qué gran tarea la de agradecer algo. Complicada, y seguramente injusta en algunos aspectos. Pues todos tenemos algo que agradecer a las personas de las que nos rodeamos. Y muchas veces, perdemos la noción de cuán agradecidos deberíamos estarle a todo el mundo. El primer profesor de instituto que creyó en ti, o la última persona con la que te tropezaste y que de algún modo te hizo llegar a donde estás "ahora". Si bien es cierto que hay unas cuantas personas de mi vida a las que estoy inmensamente agradecida, no son las únicas. Y quiero, por encima de todo, haceros saber que aunque no estéis aquí, en estas páginas, sí estáis en mi corazón.

Debo un GRACIAS inmenso y que jamás será suficiente a Inma. Gracias por darme esta oportunidad. Gracias por creer en mí. Gracias por haber luchado por que me quedara en el labo cada día de nuestras vidas científicas. Gracias por enseñarme no solo ciencia, sino también a moverme en la vida laboral. Por apoyarme, por aguantarme y por protegerme. Por ser buena, honesta y luchadora, en todos los aspectos. Por hacer que ir a trabajar sea más un juego que un trabajo. Por motivarnos. Por hacer que siempre reine un buen ambiente de trabajo, por confiar en nosotros, por darnos alas… Eres mi ejemplo a seguir. Y mi aspiración como investigadora. He sido muy afortunada de encontrarme contigo en esta vida y deseo con todo mi corazón que no sea la última vez que nos crucemos. Nada habría sido igual sin ti. Gracias.

Pero no solo Inma ha conseguido que yo haya llegado hasta aquí y esté escribiendo esto hoy. Esto no habría sido posible sin la inmensa ayuda de Olga Pernía. Gracias, Olga. Por haberme enseñado todo o casi todo lo que sé. Por haberme echado un cable cuando lo he necesitado y por ser un ejemplo de rigurosidad y

perfección en el trabajo. A ti y a Carmen os debo mil cosas, porque vuestra experiencia en este mundo es enorme y sois pozos de sabiduría inmensa. No he aprendido todo lo que debería, soy consciente. Pero espero al menos haber aprendido todo lo que necesito por ahora. Gracias a ambas.

Yo ya te dije esto en su día, pero teniendo esta oportunidad de dejarlo escrito, no la voy a dejar escapar. Eres un genio Carlos, un privilegiado. Tienes unas capacidades a un nivel que no tenemos los que trabajamos contigo. Entiendes la Biología desde un punto de vista de "comandos" y "algoritmos" que me da muchísima envidia. Te admiro infinito por esa habilidad de analizar ese mundo de la bioinformática. Y no solo por eso, sino porque eres una bellísima persona. De verdad, soy una afortunada por haber tenido la oportunidad de trabajar contigo. Y espero poder tenerla de nuevo en el futuro. Este trabajo no habría sido posible sin tu ayuda inicial. Gracias.

Quiero hacer, además una mención a esa gente tan maravillosa del Departamento de Farmacología y Terapéutica de la Facultad de Medicina que han aportado tanto a este trabajo. Patry, Rafa. Muchísimas gracias por vuestra ayuda, ganas y buena fe.

Podría escribir durante años y no podría agradecer todo lo que debo. Pero tengo que hacer un huequito especial para Álvaro y Darío – mis pequeños grandes aprendices – Rocío, Joan, Javi, Julia – por esas figuras tan maravillosas –, a todas las personas del INGEMM, y a la gran familia del iib, donde empecé en este mundo por problemas logísticos en nuestro laboratorio. Las Marías, las Lauras, Javi, Jaime, Carmen, Ana, Cristina, Leandro y Rosario. Aunque fue corto, guardo un recuerdo

muy bonito de haber trabajado y aprendido mis primeros pasos con vosotros. Gracias.

Por supuesto, nada de esto sería posible sin el apoyo incondicional de mis amigos y familia. Sí, esos amigos biólogos, cuya manera de apoyarme era sugerirme publicar mis artículos científicos en el "Hola" o el "20 Minutos" (la mejor forma de animar a alguien); Y sí, esa familia mía que sólo me preguntaba por "mis bichos" o si mis células "estaban más gordas". Les debo mucho a todos ellos. Por hacer que no decaiga el ánimo, por impulsarme a seguir adelante y por no dejarme tirar la toalla.

Y por último, pero no menos importante, querría agradecer parte de este trabajo a Chao. Puede parecer injusto e incluso inmerecido para muchos, pero ha sido testigo de los últimos pasos y el último esfuerzo en este largo camino. Me ha animado a seguir adelante cuando lo único que quería era abandonar, me ha apoyado y aconsejado en varias ocasiones cuando las cosas salían mal (es lo bueno de que entienda mi trabajo) y me ha dado siempre ese aliento de esperanza que en muchas ocasiones, era lo único que necesitaba. Gracias Chao, por seguir ahí en la distancia, por esperarme y por quererme.

ÍNDICE

ÍNDICE

RESUMEN

RESUMEN

Los ARNs no codificantes, incluyendo microARNs y ARNs no codificantes largos (lncRNAs), son reguladores fundamentales de la biología celular cuya alteración está relacionada con el desarrollo de enfermedades como el cáncer. Sin embargo su papel y regulación en respuesta al tratamiento es aún desconocida. El tratamiento de elección para el cáncer de pulmón no microcítico (CPNM) y el cáncer de ovario es la quimioterapia basada en compuestos de platino. El cisplatino, además de provocar la muerte celular, induce numerosos cambios moleculares que desembocan en el desarrollo de resistencia al fármaco. En el presente trabajo hemos abordado el estudio de la regulación epigenética de microARNs y lncRNAs en CPNM y cáncer de ovario, dos tipos tumorales que desarrollan frecuentemente resistencia al cisplatino. Hemos realizado un análisis a gran escala del transcriptoma, mediante microarrays de expresión y del metiloma, mediante la secuenciación del genoma modificado por bisulfito, en cuatro líneas celulares de CPNM y cáncer de ovario, seguido por la validación de la expresión mediante PCR a tiempo real y la validación epigenética a través de la secuenciación por bisulfito dirigida. De todos los microARNs analizados, el microARN-7 (miR-7) fue el único cuya expresión se encuentra inhibida por metilación de su región reguladora en líneas tumorales resistentes a cisplatino. Nuestros ensayos funcionales mediante mutagénesis dirigida y actividad luciferasa, la sobreexpresión de precursores del miR-7, su silenciamiento por antago-miRs y ensayos de viabilidad celular demuestran la regulación directa del gen *MAFG* por el miR-7 y su implicación en el desarrollo de resistencia a cisplatino en líneas celulares humanas. Además, hemos determinado el estado de metilación del miR-7 en 291 muestras tumorales quirúrgicas y controles de pacientes con CPNM y cáncer de ovario, lo que se asocia a un peor pronóstico. El análisis de la expresión de *MAFG* en 99 muestras quirúrgicas y 2505 pacientes con CPNM y cáncer de ovario de bases de datos públicas, ha permitido definir la implicación de *MAFG* en estas patologías. En este trabajo proponemos que la resistencia al cisplatino mediada por MAFG podría estar asociada con la detoxificación en la situación de estrés oxidativo generado tras el tratamiento con cisplatino. Por otro lado, nuestros resultados en relación con los lncRNAs muestran que la alteración de la expresión es más frecuente en lncRNAs que actúan en cis aunque los patrones de metilación se ven comúnmente más alterados en los solapantes. Además, éstos contienen más islas CpG que, en su mayoría, están compartidas con las de sus genes codificantes asociados. Validamos estos resultados a nivel de expresión y metilación y encontramos cinco lncRNAs con posible implicación en la aparición de resistencia. Globalmente, nuestros resultados ofrecen una nueva visión sobre los mecanismos epigenéticos reguladores de ARN no codificantes y su implicación en la resistencia a cisplatino en cáncer de pulmón y cáncer de ovario.

ABSTRACT

ABSTRACT

Non-coding RNAs, including microRNAs and long non-coding RNAs, are critical regulators of cell biology whose alteration can lead to the development of diseases such as cancer. However, the potential role of non-coding RNAs and their regulation in response to platinum treatment is largely unknown. Chemotherapy for solid tumors based on platinum-derived compounds, such as cisplatin, is the treatment of choice in most cases. Cisplatin triggers signaling pathways that lead to cell death, but it also induces changes in tumor cells that modify the therapeutic response, thereby leading to cisplatin resistance. In the current study, we sought to identify epigenetically regulated non-coding RNAs as novel biomarkers of platinum resistance in lung and ovarian cancers, the ones with highest ratios of associated chemo-resistance. We combined human microarray data on microRNAs, lncRNAs and mRNAs with whole genome bisulfite sequencing in a panel of four paired cisplatin-sensitive/resistant non-small cell lung cancer (NSCLC) and ovarian cancer cell lines, followed by real-time expression and epigenetic validations for accurate candidate selection. Firstly, among all the microRNAs candidates analyzed, only miR-7 was downregulated and presented specific methylation in resistant cell lines. Our experimental results from functional assays of site-directed mutagenesis and luciferase activity, miR-7 precursor overexpression, silencing by antago-miR and cell viability strongly support the direct regulation of *MAFG* through miR-7 and their involvement in the development of CDDP resistance in human tumor cells. We have also determined the methylation status of miR-7 in 291 tumor-surgical samples and controls from patients with NSCLC and ovarian cancer, which was associated with poorer prognosis in ovarian cancer patients. The analysis of the expression of MAFG in 99 surgical samples and 2505 patients with NSCLC and ovarian cancer from public databases allow us to define for the first time the implication of MAFG in these pathologies. We propose that MAFG mediates resistance by decreasing the reactive oxygen species (ROS) production after cisplatin exposure. Second, our results regarding lncRNAs show that differential expression in response to therapy is more frequent in cis-acting compared to overlapping lncRNAs, while significantly altered methylation profiles were more commonly associated with overlapping lncRNAs. Moreover, overlapping lncRNAs contain more CpG islands (CGIs) and the majority are shared with their associated coding genes CGIs. Validation in a selection of lncRNAs at methylation and expression levels showed five candidates under epigenetic regulation that appear to be involved in cisplatin resistance (AC091814.2, AC141928.1, RP11-65J3.1-002, BX641110 and AF198444). Finally, our novel findings provide new insights into epigenetic mechanisms regulators of non-coding RNAs and their implication in the acquired resistance to cisplatin in lung and ovarian cancer.

ABREVIATURAS

ABREVIATURAS

5Aza-dC	5Aza-2deoxycytidine
ABCA1	ATP-binding cassette transporter A1
ACG	Associated Coding Gene
ADN	Acido DesoxiRribonucleico
ALK	ALK Receptor Tyrosine Kinase
APC	Adenomatosis Polyposis Coli
ARE	Antioxidant Response Element
ARN	Acido RiboNucleico
ARNm	ARN mensajero
ASCO	American Society of Clinical Oncology
ATT	Adjacent Tumor Tissue
bp	base pair
BRAF	B-Raf Proto-Oncogene, Serine/Threonine Kinase
BRCA1/2	Breast Cancer 1/2 (DNA repair Associated
BS	Bisulfite sequencing
CBDCA	cis-diamino(ciclobutano-1,1-dicarboxilato-O,O')platino(II) (carboplatin)
CDDP	cis-diamminedicloroplatino (II)/cis-diamminedichloroplatinum (II) (Cisplatino/Cisplatin)
CGI	CpG Island
CHK2	Checkpoint Kinase 2
c-MYC	avian myelocytomatosis viral oncogene homolog (MYC proto-oncogene)
CNAG	Centro Nacional de Análisis Genómico
CNIO	Centro Nacional de Investigaciones Oncológicas
COPD	Chronic Obstructive Pulmonary Disease

CPM	Cancer de Pulmón Microcítico
CPNM	Cancer de Pulmón No Microcítico
CRNDE	Colorectal Neoplasia Differentially Expressed (lncRNA)
DDR2	Discoidin Domain Receptor Tyrosine Kinase 2
DM	Differential Methylation
DNA	Deoxiribonucleic Acid
DNMT	DNA Methyl Transferase
ECOG	Eastern Cooperative Oncology Group
EGFR	Epidermal Growth Factor Receptor
ELK-1	ETS domain-containing protein Elk-1
ENCODE	Encyclopedia of DNA Elements
EPOC	Enfermedad Pulmonar Obstructiva Crónica
ERN	Especies Reactivas de Nitrógeno
EROs	Especies Reactivas de Oxígeno
ESMO	European Society of Medical Oncology
FBS	Fetal Bovine Serum/Suero Fetal Bovino
FFPE	Formalin-Fixed Paraffin Embedded
FGFR1	Fibroblast Growth Factor Receptor 1
GADPH	Glyceraldehyde-3-Phosphate Dehydrogenase (Human)
GATA-4	GATA Binding Protein 4
GEO	Gene Expression Onmibus
GOTM	Gene Ontology Tree Machine
GPX7	Glutathione Peroxidase 7
GSTO2	Glutathione S-Transferase Omega 2
H2DCFDA	2',7'-dichlorodihydrofluorescein diacetate
H3K4	Histona 3, Lisina 4/Histone 3 Lysine 4

HAT	Histone Acetyl Transferase
HDAC	Histone Deacetylase
HGS	High Grade Serous (ovarian cancer)
HIF-1	Hypoxia Inducible Factor 1
HMOX1	Heme Oxygenase (decycling) 1
HMT	Histone Methyl Transferase
HOTTIP	HOXA Distal Transcript Antisense RNA
HOXA	Homeobox A Cluster
HULP	Hospital Universitario La Paz
IC50	Inhibitory Concentration that kills 50% of the cell population
ICG	Isla CpG
IDIS-CHUS	Instituto de Investigación Sanitaria de Santiago de Compostela
IGFBP-3	Insulin-like Growth Factor Binding Protein 3
IVD	*In vitro* Methylated DNA
KEAP1	Kelch Like ECH Associated Protein 1
KRAS	KRAS Proto-Oncogene, GTPase
LB	Luria-Bertani (LB) broth
LC	Lung Control
lncRNA	long non-coding RNA
MAFG	Musculo-Aponeurotic Fibrosarcoma oncogene amily, protein G
MALAT1	Metastases Associated Lung Adenocarcinoma Transcript 1
MAPKAP1	Mitogen-Activated Protein Kinase Associated Protein 1
MBP	Methyl-CpG binding protein
miR-7	microRNA-7
miRNAs	microRNAs
MLH1/6	MutL Homolog 1/6

MMR	Missmatch Repair
mRNA	messenger RNA
MSH2	MutS Homolog 2
MSP	Methylation Specific PCR
MTT	3-(4,5-Dimethylthiazol-2-yl)-2,5-Diphenyltetrazolium Bromide)
NER	Nucleotide Escision Repair
NF-κB	Nuclear Factor Kappa B Subunit 1
nM	nano Molar
NQO1	NAD(P)H Quinone Dehydrogenase 1
NRF2	*Nuclear factor erythroid related factor-2*
NSCLC	Non-Small Cell Lung Cancer
OC	Ovary Control
ORFs	Open Reading Frame
OS	Overall Survival
p16 (CDKN2A)	Cyclin Dependent Kinase Inhibitor 2A
PBMC	peripheral blood mononuclear cell
PCR	Polymerase Chain Reaction
PDE11A	Phosphodiesterase 11A
PFS	Progression Free Survival
PIK3CA	Phosphatidylinositol-4,5-Bisphosphate 3-Kinase Catalytic Subunit Alpha
PLCE	Phospholipase C Epsilon 1
PMS1/2	PMS1 Homolog 1, Mismatch Repair System Component
PTEN	Phosphatase And Tensin Homolog
qMSP	quantitative Methylation Specific PCR
qRT-PCR	quantitative Real-Time PCR

R	Resistat cells
RAD51	RAD51 Recombinase
RET	Ret Proto-Oncogene
RI	Resistant Index
RISC	RNA-induced silencing complex
RNA	Ribonucleic Acid
RNS	Reactive Nitrogen Species
ROS	Reactive Oxygen Species
ROS	ROS Proto-Oncogene 1, Receptor Tyrosine Kinase
RPMI	Roswell Park Memorial Institute (Medium)
RT	Resistant treated with epigenetic reactivation drugs
RT-PCR	Real Time Polymerase Chain Reaction
RUNX3	Runt Related Transcription Factor 3
S	Sensitive cells
TCC	MOFFITT's Total Cancer Care
TCGA	The Cancer Genome Atlas
TET	Tet Methylcytosine Dioxygenase
TNM	Tumor Node Metastases
TSA	trichostatin A
TSS	Transctription Start Site
TT	Tumor Tissue
UTR	Untranslated Region
WGBS	Whole Genome Bisulfite Sequencing
WT	Wild Type

INTRODUCCIÓN

INTRODUCCIÓN

1. Cáncer

1.1 Definición y estadísticas.

Cáncer es un término genérico que define un amplio y heterogéneo grupo de enfermedades que puede afectar a cualquier parte del organismo. Se considera una enfermedad multifásica, caracterizada por la aparición de células anormales en los tejidos, que crecen de forma descontrolada, más allá de sus límites, y que pueden invadir partes adyacentes del cuerpo, diseminándose a otros órganos (http://www.who.int/cancer/en/, 2018).

Según la Organización Mundial de la Salud, el cáncer es una de las principales causas de muerte siendo responsable de 8,8 millones de defunciones en 2015, lo que constituye un 17% del total ocurridas en todo el mundo. Según la Organización Mundial de la salud, en su revisión más actual de 2014 los cinco tipos tumorales diagnosticados más frecuentemente a nivel mundial entre los hombres fueron el cáncer de pulmón, próstata, colorectal, estómago e hígado, mientras que entre las mujeres destacaron los cánceres de mama, colorectal, pulmón, cérvix y estómago (http://www.who.int/cancer/en/, 2018, Ferlay et al., 2015).

El cáncer se origina como consecuencia de la suma de alteraciones moleculares de origen genético y/o epigenético. Estas pueden ser iniciadas por la acumulación de daños en el ADN de tipo genético, afectando a la secuencia del ADN (como mutaciones y reorganizaciones cromosómicas) o bien modificaciones en el ADN, histonas y el ARN no codificante que no conllevan cambio en la secuencia original (modificaciones epigenéticas). Todos estos cambios promueven la selección clonal de aquellas células que presentan un comportamiento cada vez más agresivo.

En el año 2000 se establecieron las principales alteraciones que definen a las células cancerosas: autosuficiencia en señales de crecimiento, insensibilidad a señales de antiproliferativas, evasión de la apoptosis, potencial replicativo ilimitado, mantenimiento de la angiogénesis e invasión celular y metástasis (Hanahan and Weinberg, 2000). Posteriormente, en 2009 se establecieron otras cinco, relacionadas con el estrés metabólico, proteotóxico, mitótico, oxidativo y por daño en el ADN (Luo et al., 2009). En el año 2011, Hanahan y Weinberg determinaron nuevas características y delimitaron la existencia de un microambiente tumoral que las células generan durante los múltiples pasos de los que

consta el proceso de tumorogénesis (Hanahan and Weinberg, 2011). En conjunto, todas estas propiedades definen, a día de hoy, la célula cancerosa.

1.2 Cáncer de pulmón

El cáncer de pulmón engloba aquellos tumores que surgen del epitelio respiratorio. Constituye una de las neoplasias más frecuentemente diagnosticadas y representa la principal causa de muerte en ambos sexos por cáncer en todo el mundo (Kasper, 2015). La incidencia del cáncer de pulmón en hombres ha disminuido en las últimas décadas, mientras que se ha incrementado en mujeres (Figura 1). Según el Cancer Statistics del año 2014, tiene una incidencia de 14% y 13% en hombres y mujeres, respectivamente, y constituye entre un 26% y un 28% de las muertes por cáncer (Kasper, 2015).

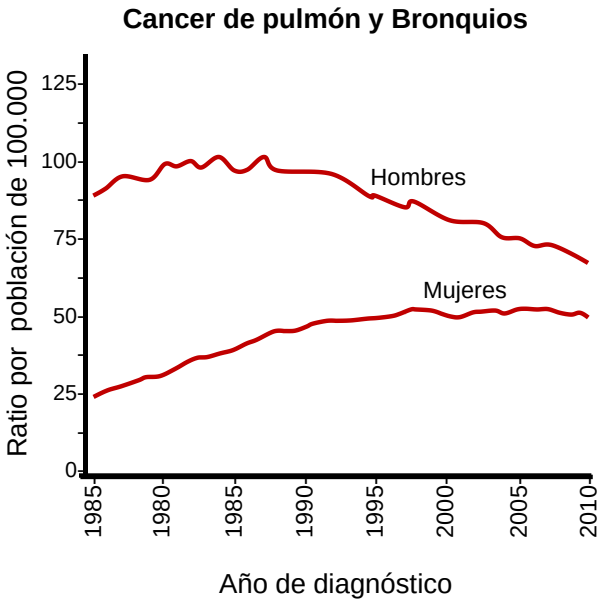

Figura 1. Evolución de la incidencia de cáncer de pulmón en los últimos 35 años en hombres y mujeres. Modificado de (Kasper, 2015).

Entre los factores de riesgo que se relacionan con la aparición del cáncer de pulmón, destaca el hábito tabáquico. Se ha demostrado que existe una relación dosis dependiente entre el riesgo de desarrollar un cáncer de pulmón y el número de cigarrillos consumidos. Existen otros carcinógenos pulmonares relacionados con la exposición a ciertos compuestos, como el asbesto, la radiación ionizante o la predisposición genética (Kasper, 2015). Otros factores de riesgo están relacionados con ciertas enfermedades respiratorias como puede ser la enfermedad pulmonar obstructiva crónica (EPOC) (Takiguchi et al., 2014, Young et al., 2009, Ytterstad et al., 2016).

Clasificación

El cáncer de pulmón se clasifica en dos tipos principales: el cáncer de pulmón de células pequeñas o microcítico (CPM) y el cáncer de pulmón no microcítico (CPNM), siendo este último el de mayor incidencia, ya que da cuenta de aproximadamente el 85% de todos los cánceres de pulmón (Detterbeck et al., 2017, Kasper, 2015). Históricamente, el CPNM se subdivide en tres tipos histológicos: adenocarcinoma, el carcinoma escamoso o epidermoide y el carcinoma de células grandes (Herbst et al., 2008).

El adenocarcinoma surge de las células que recubren los alveolos, se caracteriza por diferenciación glandular o producción mucinosa y puede presentar patrones acinares, papilares, sólidos o una mezcla de todos ellos. El carcinoma epidermoide o escamoso surge de las células escamosas de los bronquios, muestra una disposición en capas celulares y un proceso de queratinización. Está relacionado mayoritariamente con el hábito tabáquico. Es por ello que durante la primera mitad del siglo 20, éste era el tipo de CPNM más común entre la población. La disminución del número de fumadores a nivel global está haciendo que cambie esta tendencia, incrementando los casos de adenocarcinoma diagnosticados. El carcinoma de células grandes incluye todos aquellos CPNM no clasificables en los otros subtipos, ya que no presenta características citológicas o arquetípicas (Kasper, 2015, Herbst et al., 2008). Sin embargo, en la actualidad las nuevas técnicas diagnósticas han permitido su clasificación dentro de uno de los dos subtipos mayoritarios, disminuyendo el porcentaje de tumores inclasificables.

La patología molecular del cáncer de pulmón es múltiple y variada. Entre las anormalidades cromosómicas destaca la sobreexpresión de los factores de transcripción de la familia *MYC* como consecuencia de amplificaciones cromosómicas o la alteración transcripcional. En adenocarcinomas destacan las mutaciones en el receptor del factor de crecimiento epidérmico (EGFR), KRAS, BRAF y PIK3CA, así como reordenamientos de ALK, ROS y RET. Los carcinomas epidermoides se caracterizan por la amplificación del gen FGFR1, la pérdida de PTEN, y mutaciones en DDR2 o PIK3CA. Sumado a ello, durante la patogénesis del cáncer de pulmón se producen numerosos cambios que derivan en la inactivación de genes supresores tumorales o la activación de genes oncogénicos (Herbst et al., 2008, Kasper, 2015).

Estadificación y tratamiento

El cáncer de pulmón también se clasifica según la nomenclatura TNM, que indica el tamaño del tumor (T), la afectación ganglionar (N) y la presencia de metástasis (M), y según esta clasificación se distinguen distintos estadios tumorales.

Tabla 1. Estadificación del cáncer de pulmón según la nomenclatura TNM (Kasper, 2015, Detterbeck et al., 2017)

Estadio	T	N	M
Estadio IA	T1a-T1c	N0	M0
Estadio IB	T2a-T2b	N0	M0
Estadio IIA	T2b	N0	M0
Estadio IIB	T1-T2 T3	N1 N0	M0 M0
Estadio IIIA	T1-T2 T3 T4	N2 N1 N0, N1	M0 M0 M0
Estadio IIIB	T1-T2 T3-T4	N3 N2	M0 M0
Estadio IVA	Cualquier T	Cualquier N	M1a-M1b
Estadio IVB	Cualquier T	Cualquier N	M1c

El tratamiento del cáncer de pulmón varía en función del estadio tumoral diagnosticado. En la Tabla 2 se muestran los esquemas básicos de tratamiento según el estadio.

Tabla 2. Régimen de tratamiento del Cáncer de pulmón (Kasper, 2015)

Estadio I	Ia	Cirugía
	Ib	Cirugía + Quimioterapia en pacientes seleccionados
Estadio II		Cirugía + Quimioterapia postquirúrgica
Estadio III	IIIa – T3N1	Quimioterapia neoadyuvante + Cirugía
	IIIa – T3N2	Quimioterapia neoadyuvante + Cirugía (si baja a estadio N1-N0)
	IIIa – T4	Quimioterapia neoadyuvante + Cirugía
	IIIa – T4	Quimioterapia + Radioterapia (Tratamiento paliativo)
	IIIb	Quimioterapia + Radioterapia
Estadio IV		Quimioterapia + Radioterapia

El esquema quimioterapéutico por excelencia para el CPNM se basa en una combinación de un fármaco derivado del platino (cisplatino o carboplatino) junto con otro fármaco antitumoral de acción concreta (Paclitaxel, Docetaxel, Gemcitabina, Vinorelbina, Irinotecan, Etoposido o Pemetrexed entre otros).

1.3 Cáncer de ovario

Clasificación

El cáncer de ovario es la malignidad ginecológica con mayor prevalencia causante aproximadamente de 152.000 muertes por cáncer en mujeres. (Kasper, 2015, McGuire, 2016). Entre los factores de riesgo de padecer cáncer de ovario se encuentran la exposición a ciertos compuestos químicos como el asbesto, la historia familiar y la predisposición genética asociada a los genes *BRCA1* y *BRCA2*.

La gran mayoría de los carcinomas ováricos se encuentran representados por el cáncer del epitelio del ovario, generado a partir del epitelio superficial de este órgano. La clasificación actual de los tumores epiteliales del ovario atiende a la histología, pudiendo ser de tipo seroso (60-80%), mucinoso (25%), endometrioide (20%) o de células claras (5%) (Kasper, 2015). Los carcinomas de tipo seroso se relacionan con la nuliparidad, la obesidad y tratamientos hormonales. Recientemente su origen se ha asociado con el epitelio de la fimbria de la trompa de Falopio (Jazaeri et al., 2011, Karst and Drapkin, 2010). Los carcinomas mucinosos están asociados con una historia fumadora y los endometrioides y los de células claras con una historia de endometriosis.

Como toda neoplasia, hay factores genéticos que contribuyen a la aparición y el desarrollo del cáncer de ovario. Un 10% de las mujeres que cursan con esta enfermedad presentan mutaciones germinales o somáticas en el gen *BRCA1* o en *BRCA2*; también son frecuentes mutaciones en genes asociados a las roturas de cadena del ADN y que se encuentran relacionados con el síndrome de Lynch (*MSH2, MLH1, MLH6, PMS1* o *PMS2*); un pequeño grupo de cánceres de ovario presentan mutaciones en genes asociados a *BRCA,* como *RAD51* o *CHK2* (Kasper, 2015, Amin et al., 2017). Además, recientemente se ha identificado que el 95% de las pacientes con carcinomas ováricos de mal pronóstico presentan mutaciones en el gen *TP53* (Cancer Genome Atlas Research, 2011).

Estadificación y tratamiento

La estadificación se realiza siempre de forma postquirúrgica clasificándose según la Tabla 3. Pero además, la malignidad del tumor puede clasificarse por su similitud con las células normales según el grado de diferenciación. Así, tumores diferenciados o de grado bajo son más parecidos a las células normales y de mejor pronóstico, mientras que los tumores indiferenciados o de grado alto son más agresivos y en general poco respondedores al tratamiento quimioterapéutico (Kasper, 2015).

Tabla 3. Estadificación del cáncer de ovario y su relación con la supervivencia (Kasper, 2015)

Estadio	Localización	Supervivencia a 5 años (%)
I	Confinado al ovario	90-95
II	Confinado a la pelvis	70-80
III	Diseminación intraabdominal	20-25
IV	Diseminación fuera del abdomen	1-5

La cirugía es la primera opción de tratamiento en el cáncer de ovario y es necesaria para poder realizar la clasificación por estadios de la enfermedad. Con la cirugía se realiza una citorreducción que puede ser óptima, cuando el tamaño del tumor residual es < 1cm, o subóptima, cuando el tamaño es ≥ 1cm. En el primer caso, se realiza una cirugía completa y en el segundo caso se procede a la administración de una quimioterapia neoadyuvante para, posteriormente reintentar la cirugía completa.

En ambos casos, la cirugía se complementa con un régimen de quimioterapia basado en una combinación de compuestos derivados del platino junto con taxanos. Las tasas iniciales de respuesta a quimioterapia son de un 60 a un 75%. Sin embargo, aproximadamente un 75% de las pacientes respondedoras recaen en los primeros cuatro años tras el tratamiento. La enfermedad recurrente es tratada con una variedad de agentes quimioterapéuticos, aunque no se llega a conseguir la remisión completa (Kasper, 2015)

1.4 Mecanismos de acción del tratamiento con cisplatino

El cisplatino, cis-diamminedichloroplatino (II) o CDDP, es un agente reactivo derivado del platino, ampliamente utilizado como parte del tratamiento quimioterapéutico de múltiples tumores sólidos y es terapia de primera línea en cáncer de pulmón y de ovario, incluyendo cáncer de testículo y colorectal, entre otros. El cisplatino actúa entrando en la célula, formando especies acuosas que reaccionan con sitios nucleofílicos de las macromoléculas celulares, como son el ADN, ARN y las proteínas. En el ADN, reacciona con los sitios N7 de las purinas formando los denominados aductos, que consisten en la aparición de uniones cruzadas, principalmente entre guaninas, de tipo inter o intracatenario. La presencia de estos aductos induce una contorsión del ADN y desencadena múltiples vías de señalización que culminan en la reparación del ADN o en la apoptosis de la célula (Sanchez-Perez et al., 1998, Siddik, 2003, Kartalou and Essigmann, 2001). A nivel celular, el evento más característico de la acción del cisplatino es el aumento de estrés oxidativo mediante el incremento de los niveles de aniones superóxido, peróxido de hidrógeno y radicales hidroxilo (Deavall et al., 2012). En muchos tipos celulares, las

numerosas respuestas de estrés oxidativo parecen estar mediadas por el elemento de respuesta antioxidante (ARE, por sus siglas en inglés) y el factor de transcripción NRF2 (*Nuclear factor erythroid related factor-2*). Este factor es un sensor redox que regula la activación transcripcional a través de ARE. En condiciones normales, NRF2 se encuentra secuestrado por KEAP1, quien media la ubiquitinación de NRF2, provocando su degradación. Cuando la célula se ve sometida al estrés oxidativo derivado de la acumulación de especies reactivas de oxígeno o de nitrógeno, NRF2 se trasloca al núcleo, donde se forma un heterodímero con una proteína Maf pequeña, activando la transcripción de genes implicados en la respuesta oxidativa (Kilic et al., 2013, Katsuoka et al., 2005). Sin embargo, se ha descrito la alteración de numerosas vías de señalización que contribuyen a la acción citotóxica del cisplatino (Dasari and Tchounwou, 2014).

2. Epigenética y cáncer

La epigenética es la disciplina que estudia los cambios heredables en la expresión génica que se producen sin que exista un cambio en la secuencia de bases del ADN, sino en alteraciones químicas de éste y en las histonas, así como la implicación de ARNs no codificantes, que provocan la remodelación de la cromatina, facilitando o impidiendo la expresión génica. El silenciamiento de la expresión génica a nivel de cromatina, es necesario para la vida de los organismos eucarióticos y es particularmente importante en la regulación de procesos biológicos como el desarrollo embrionario, la diferenciación o la impronta genómica.

2.1 Mecanismos Epigeneticos

Metilación del ADN

La metilación del ADN es el mecanismo mejor estudiado y más asociado con la maquinaria epigenética. Por norma general, la metilación del ADN es sinónimo de silenciamiento génico, ya que conlleva a un estado de la cromatina difícilmente accesible para el proceso de transcripción. Esta modificación química consiste en la adición de un grupo metilo (CH_3) en el carbono 5 de la citosina, preferiblemente en regiones de dinucleótidos CpG. La distribución de los dinucleótidos CpG es asimétrica a lo largo del genoma y su acumulación preferencial en regiones promotoras de los genes es denominada Isla CpG (Stirzaker et al., 2014, Moore et al., 2013). En el genoma humano, hay aproximadamente 30.000 islas CpG no metiladas que garantizan la configuración potencialmente activa de los genes constitutivos. El patrón de metilación del ADN es

responsable de la diferenciación celular y su desregulación conlleva a numerosas enfermedades, entre ellas el cáncer (Zampieri et al., 2015).

Este proceso de metilación del ADN está catalizado por las ADN-metil transferasas (DNMTs, por sus siglas en inglés). Hay cuatro tipos de DNMTs, dos encargadas la metilación de novo durante el desarrollo (DNMTs 3A y 3B), una involucrada en el mantenimiento de dichos patrones de metilación tras la replicación del ADN (DNMT1), y una sin sitio catalítico que actúa junto con las metil-transferasas de novo para el reclutamiento de complejos remodeladores de la cromatina (Moore et al., 2013, Deplus et al., 2002). Este proceso es fundamental en el desarrollo embrionario, principalmente relacionado con la compensación de dosis cromosómica (inactivación del cromosoma X) (Brown, 1991, Ng et al., 2007, Boumil et al., 2006) y la impronta genómica (inactivación selectiva de genes según su procedencia parental) (Reik and Walter, 2001). El silenciamiento en estos mecanismos se encuentra mediado por la metilación del ADN, aunque es necesaria la participación del resto de la maquinaria epigenética para que se lleven a cabo correctamente.

Modificaciones de histonas

Otro de los grandes conocidos mecanismos epigenéticos consiste en la modificación química de las histonas que forman parte de los nucleosomas de la cromatina. Las principales modificaciones de las histonas consisten en la adición de grupos NH_3, mediante la acción de las Acetilasas de histonas (HAT, por sus siglas en inglés) y en la adición de grupos CH_3, gracias a la acción de las Metilasas de histonas (HMTs, por sus siglas en inglés), en residuos concretos de las histonas. La cooperación entre la metilación del ADN y las modificaciones de histonas inducen el reclutamiento de otras enzimas modificadoras de la cromatina y, de esta forma, promueven la conformación activa o inactiva de la cromatina (Tabla 4) (Bannister and Kouzarides, 2011):

Tabla 4. Relación entre las modificaciones epigenéticas y el estado de la cromatina.

	Cromatina potencialmente activa	Cromatina potencialmente inactiva
ADN	• Metilación en citosinas fuera de islas CpG	• Metilación de citosinas en islas CpG de regiones promotoras
Histonas	• Acetiladas • No metiladas • Metilación en H3K4	• Deacetiladas • Metiladas • No metilación en H3K4
Conformación de la cromatina	• Extendida, abierta	• Condensada • Heterocromatina constitutiva

ARNs no codificantes

Desde el establecimiento del denominado "Dogma central de la Biología molecular", en el que se establece que la información genética se almacena en genes codificadores y considera que las proteínas son los elementos protagonistas en la biología de la célula, la molécula de ARN ha sido considerada como un simple intermediario entre el ADN y las proteínas. Esta idea se trasladó al proyecto genoma humano en el año 2001, mediante el cual se identificaron unos 20.000 genes codificantes, que constituyen aproximadamente un 1,5% del genoma humano. A pesar de ello, el 98.5% restante que no codificaba para proteínas, se consideró ADN basura por no verse incluido dentro de este Dogma.

Posteriormente, en el año 2011, con el desarrollo de proyectos como el ENCODE que permitieron dilucidar el transcriptoma humano, se estimó que entre un 70 y un 90% del genoma sufre una transcripción activa no codificante. A esa región del genoma que se la ha denominado ARN no codificante.

Dentro del grupo de los transcritos de ARN no codificantes, podemos encontrar dos grandes grupos. Aquellos ARNs constitutivos, fundamentales para la célula y que incluye los ARNs ribosómicos, los transferentes, los nucleares y nucleolares pequeños. Por otro lado, encontramos los ARNs no codificantes reguladores, que se subdividen en pequeños (microARNs, los siARNs, los piwiARNs entre otros) y los largos o lncRNAs (por sus siglas en inglés) (Djebali et al., 2012, Ponting et al., 2009).

2.2. Implicación de la epigenética en la aparición de cáncer

Numerosos estudios muestran que las células cancerosas presentan cambios globales en la cromatina que afectan, por un lado, al epigenoma completo a través de un proceso de hipometilación generalizado, derivando en una inestabilidad genómica, y por otro llevan a la pérdida de función por hipermetilación de determinados genes que regulan vías de señalización implicadas en procesos de diferenciación celular, como son APC, GATA-4 o p16, permitiendo el crecimiento clonal y la supervivencia anormal de las células (Sanchez-Perez et al., 1998).

Respecto a la implicación de los ARNs no codificantes y su regulación en cáncer, ese conocimiento es más limitado, aunque en los últimos años se ha ampliado considerablemente (Gulyaeva and Kushlinskiy, 2016, Ha and Kim, 2014).

microARNs

Los microARNs (miARNs) son genes pequeños de ARN, no codificantes, de entre 19-23 nucleótidos en su forma madura, que regulan la expresión génica mediante complementariedad de bases, principalmente, con la región no traducible 3' (3'UTR) de un ARN mensajero, al que se denomina "gen diana".

Los miARN se transcriben como miARN primarios (pri-miARN) por la acción de la ARN polimerasa II a partir de la secuencia de ADN. Después siguen un procesamiento especial, por el cual sufren dos cortes endonucleásicos mediados por las enzimas Drosha, en el núcleo, y Dicer, en el citoplasma. El corte mediado por Drosha genera una horquilla de 60-100 nucleótidos, denominado precursor de miARN (pre-miARN), que sale al citoplasma por el transportador de membrana nuclear, Exportina-5. Una vez allí, Dicer corta esta estructura y genera ARN de doble cadena de 19-23 nucleótidos. El complejo RISC (RNA-induced silencing complex) selecciona una de las dos cadenas, provocando la degradación de la otra, y busca la zona de homología en algún ARN mensajero, para impedir su traducción o favorecer su degradación (Davis and Hata, 2009).

La primera vez que se describió la relación entre miARNs y cáncer fue en el año 2002. Se definieron como miARNs supresores de tumores a aquellos miARNs que se encuentran frecuentemente delecionados o con expresión disminuida en distintos tipos de cáncer. Este es el caso del clúster de los miR-15a/16-1en la leucemia linfocítica crónica (Calin et al., 2002). Pero además, hay otro tipo de miARNs, como el clúster de los miR-17-92, cuya inducción resulta en un aumento de la proliferación celular, la supervivencia y la angiogénesis tumoral. La ganancia o pérdida de estos miARNs, por lo tanto, aumenta o disminuye la actividad de múltiples vías de señalización en las células cancerosas (Mendell and Olson, 2012). Por otro lado, los miARNs pueden estar implicados en la regulación epigenética mediante la activación o inactivación de las ADN-metiltransferasas. Un ejemplo de ello es el caso de la familia de los miR-29s (miR-29a, miR-29b y miR-29c) en cáncer de pulmón no microcítico, donde se ha visto que la disminución de la expresión de estos miARN está inversamente correlacionada con la expresión de las DNMT-3A y -3B, genes diana de los miR-29s. La inducción de la sobreexpresión de esta familia de miARNs produce la demetilación de distintos genes supresores de tumores, frenando de esta forma la tumorogénesis en ratones inyectados con líneas celulares de cáncer de pulmón (Fabbri et al., 2007).

Se conoce poco acerca de la regulación existente sobre la síntesis de los miRNAs, algunos de los miARNs conocidos se encuentran regulados por c-MYC, un oncogen que

codifica para un factor de transcripción implicado en cáncer. Parece ser que Myc contribuye a la oncogénesis mediante la inducción o represión de determinados miARNs, provocando alteraciones como la progresión del ciclo celular (miR-17, let-7), la inhibición de la apoptosis (miR-19a, miR-26a), variaciones en el metabolismo (miR-23a/b), angiogénesis (miR-18a) o metástasis (miR-9) (Bui and Mendell, 2010). También se ha descrito como mecanismo regulador de su expresión la metilación de islas CpGs cercanas al lugar de codificación de los miRNAs en regiones intrónicas o bien localizadas en regiones promotoras reguladoras de la expresión del gen en el que se encuentran codificados (Furuta et al., 2010, Balaguer et al., 2010).

ARNs no codificantes largos

Los lncRNAs son aquellos ARNs transcritos que tienen una longitud mayor de 200 nucleótidos y que no codifican para proteínas o no tienen evidentes Pautas de Lectura Abierta (ORFs, por sus siglas en inglés) (Dey et al., 2014). Muchos se transcriben por la ARN polimerasa II y algunos sufren el procesamiento característico de los ARNs mensajeros como el procesamiento de regiones intrónicas (splicing) y la poliadenilación, aunque otros son funcionales sin sufrir estos procesos. Los lncRNAs se transcriben en niveles mucho menores que los ARN mensajeros, están pobremente conservados durante la evolución y su expresión parece ser más específica a nivel celular y tisular que la de los ARNm. Tienen una actividad dual, que les permite interaccionar tanto con proteínas como con otros ácidos nucleicos, y forman estructuras complejas que les permiten aumentar su capacidad regulatoria. Su implicación en la regulación génica es mucho más amplia que la que llevan a cabo los miARNs, por lo que su regulación también es mucho más estricta (Wilusz et al., 2009, Mercer et al., 2009).

Los lncRNAs se pueden clasificar según su posición cromosómica, localización y tipo de regulación con respecto a los genes codificantes asociados. Aquellos lncRNAs cuya secuencia coincide con la de un gen codificante se denominan solapantes u "overlapping", pudiendo ser exónicos o intrónicos; por el contrario, aquellos lncRNAs que se encuentran entre genes son denominados intergénicos (lincARNs) (Wang and Chang, 2011, Ma et al., 2013, Chen, 2016, Guttman and Rinn, 2012). La forma de acción de los lncRNAs puede ser en "cis", cuando regulan la expresión de otro gen que se encuentra en el mismo cromosoma que el lncRNA, o en "trans", cuando además pueden regular genes que se encuentren en cromosomas diferentes (Guttman and Rinn, 2012, Chen, 2016). Además, los lncRNAs cuya función se limita exclusivamente al núcleo celular, se encargan de guiar elementos modificadores de la cromatina, como las DNMTs, los complejos Polycomb o las HAT, para

reprimir o activar la transcripción. Hay además, otro grupo de lncRNAs que ejercen su función en el citoplasma, para regular la expresión de ARNm y microARNs de diversas formas (Wang and Chang, 2011, Ponting et al., 2009, Fatica and Bozzoni, 2014).

La regulación de la transcripción de los lncRNAs es muy similar a la que ocurre para los ARN mensajeros y sus funciones son tan extensas en la biología celular que su desregulación conlleva al desarrollo de enfermedades como el cáncer. Uno de los lncRNA asociados al desarrollo de cáncer más estudiado es MALAT1 (Metastases Associated Lung Adenocarcinoma Transcript 1), un lncRNA involucrado en el proceso de splicing de los ARNm (Tripathi et al., 2010). MALAT1 se encuentra sobreexpresado en tumores metastásicos de CPNM y puede utilizarse como biomarcador pronóstico en estadios I de la enfermedad (Ji et al., 2003). Además se ha visto que la sobreexpresión de MALAT1 tiene un papel oncogénico en cáncer de ovario, aumentando la viabilidad, formación de colonias y migración, así como la aparición de fenotipos metastásicos en pacientes con cáncer de ovario (Zhou et al., 2016).

3. Resistencia al tratamiento quimioterapéutico

3.1 Mecanismos de resistencia a cisplatino

La mayor limitación del uso del cisplatino como quimioterapéutico se debe a que, a pesar ser un potente inductor de la apoptosis, en muchos casos las células tumorales la evitan, apareciendo resistencia al fármaco. Los mecanismos por los cuales aparece resistencia a cisplatino, se agrupan en cuatro categorías: aumento de la reparación del ADN mediante el mecanismo de escisión de nucleótidos (NER) o la reparación de apareamientos erróneos (MMR); descenso en la retención del fármaco por aumento de la salida o por disminución de la entrada de éste al interior celular, como consecuencia de la presencia o ausencia de los transportadores de membrana encargados de su transporte; inactivación del cisplatino o imposibilidad de alcanzar el ADN, debido al incremento de moléculas implicadas en su detoxificación como son el glutatio y las metalotioneínas; y activación de factores de transcripción que inducen la proliferación celular, el aumento de proteínas antiapoptóticas como bcl-2 o la activación de ADN-metiltransferasas que modifican epigenéticamente la expresión de numerosos genes (Kartalou and Essigmann, 2001, Rabik and Dolan, 2007, Holzer et al., 2004, Wu et al., 2005). A pesar de que no se conoce el mecanismo concreto por el cual las células cancerosas desarrollan resistencia a cisplatino, se cree que se trata de un proceso multifactorial que incluye varios de los mecanismos mencionados.

3.2 Epigenética y resistencia a tratamiento

Como se ha mencionado, la aparición de resistencia al cisplatino está relacionada con la activación de DNMTs. Este proceso de metilación del ADN en las células tumorales provoca el silenciamiento de determinados genes, necesarios en condiciones normales para el correcto funcionamiento celular. Este silenciamiento puede considerase directo, si se hipermetila el promotor del gen que se inactiva, o indirecto, en caso de que se hipermetilen genes reguladores del gen que se silencia, o bien regiones reguladoras de los miARNs y lncRNAs, silenciándolos y provocando la sobreexpresión de sus genes diana.

Se ha descrito que el silenciamiento transcripcional de algunos genes, como el de la arginino-succinato-sintetasa, mediado por hipermetilación de los dinucleótidos CpG de su promotor, es un evento epigenético frecuente asociado al desarrollo de resistencia a cisplatino en cáncer de ovario (Nicholson et al., 2009). Otros estudios describen la pérdida de expresión del gen IGFBP-3 (Insulin-like Growth Factor Binding Protein-3) en células de CPNM, como efecto producido por la administración de CDDP. El silenciamiento de este gen se produce por la hipermetilación de su promotor en los fenotipos de células resistentes a cisplatino, lo que indica que la metilación del promotor de IGFBP-3 está mediando la aparición de resistencia a este fármaco (Ibanez de Caceres et al., 2010). Cada vez se conocen mejor los genes cuyos promotores están hipermetilados en cáncer y que se relacionan con la resistencia a cisplatino como consecuencia del silenciamiento epigenético al que están sometidos, sin embargo el número de genes identificados hasta la fecha es aún muy reducido (Chang et al., 2010).

Las alteraciones en la expresión de las histona-desacetilasas y demetilasas, también contribuyen al desarrollo de resistencia a cisplatino en determinados tipos de cáncer. Un ejemplo de ello se produce en CPNM, en el que el aumento de expresión de estas enzimas, en concreto la Histona-Deacetilasa-6 (HDAC6), genera fenotipos resistentes además de disminuir la apoptosis en estas células (Wang et al., 2012). Por otro lado, el estrés oxidativo provocado por el cisplatino, también induce cambios a nivel de histona-demetilasas, que alteran los patrones de metilación de las histonas y constituye un mecanismo de silenciamiento génico en algunos tipos de cáncer (Cortes-Sempere et al., 2013).

La importancia de estudiar la relación que parece haber entre las modificaciones epigenéticas de los promotores de los ARNs no codificantes y el desarrollo de fenotipos resistenets a fármacos quimioterapéuticos, como el cisplatino, ha crecido enormemente en los últimos años. De hecho, uno de los mecanismos reguladores de la expresión de miARNs, es su silenciamiento debido a la metilación de sus regiones reguladoras que resulta en la

sobreexpresión de sus genes diana (Gulyaeva and Kushlinskiy, 2016, Ha and Kim, 2014). La hipermetilación del promotor del miR-200c es un ejemplo de este hecho. Estudios en líneas de CPNM, relacionan la disminución de la expresión de este miARN con la resistencia a cisplatino, como consecuencia de la hipermetilación de su promotor (Ceppi et al., 2010). Por otro lado, estudios recientes han descrito por primera vez la relación entre la expresión de lncRNAs y la aparición de resistencia en distintos tumorales. Ejemplo de ello son HOTTIP, un lncRNA que regula la transcripción del grupo de genes de la familia HOXA en el extremo 5', y que se ha asociado a proliferación celular, invasión y quimioresistencia en osteosarcoma y cáncer de hígado y páncreas (Li et al., 2015, Quagliata et al., 2014). UCA1 o ROR son otros ejemplos de lncRNAs relacionados con la resistencia a compuestos derivados del platino en cáncer de vejiga y nasofaríngeos, respectivamente (Fan et al., 2014, Li et al., 2016).

3.3. Efecto del estrés oxidativo en la maquinaria epigenética

El estrés oxidativo es un fenómeno común en múltiples tipos de cáncer que deriva del metabolismo aumentado de las células para promover y mantener su potencial tumorogénico. Por otro lado, se ha demostrado que el estado hipóxico de las células tumorales aumenta la situación de estrés oxidativo, lo que conlleva a cambios estructurales y epigenéticos mediados por el factor de hipoxia HIF-1 (Nishida and Kudo, 2013, Kreuz and Fischle, 2016). Otro de los elementos que más cambios provoca en el estrés oxidativo, y por tanto en la modificación de la maquinaria epigenética, es el humo del tabaco (Arita and Costa, 2014). Además, como consecuencia de la administración de cisplatino a las células tumorales, se producen elevadas cantidades de especies reactivas de oxígeno (EROs) y de nitrógeno (ERNs) que aumentan el estrés oxidativo (Marullo et al., 2013, Martins et al., 2008, Schaaf et al., 2002). Todos estos cambios en el estado de oxidación de la célula conllevan a la remodelación de la maquinaria epigenética a todos los niveles.

Efecto en la metilación del ADN

Los cambios en la metilación del ADN derivados del estrés oxidativo radican principalmente en la alteración de la actividad y la función de las ADN-metil transferasas. Varios estudios sugieren que la inducción de estrés oxidativo mediada por peróxido de hidrógeno provoca el incremento de la actividad de la ADN-metil transferasa 1 y su unión a promotores de genes supresores tumorales como RUNX3 (Nishida and Kudo, 2013). Por otro lado, se ha descrito que el estado de estrés oxidativo provoca cambios en el ciclo catalítico del hierro que conlleva a la inhibición de las demetilasas de la familia TET, incrementando de esta forma los niveles de metilación del ADN (Kreuz and Fischle, 2016).

Como se ha mencionado con anterioridad, uno de los compuestos oxidantes a los que más se exponen las células epiteliales de los pulmones es el humo del tabaco. A parte de ser un potente carcinógeno, el humo del tabaco provoca elevados niveles de especies reactivas de oxigeno que tienen como consecuencia la aparición de enfermedades como la EPOC, lo que conlleva a la alteración de los patrones de metilación del ADN (Sundar et al., 2013, Arita and Costa, 2014).

Efecto en las modificaciones de histonas

Es también sabido que el estrés oxidativo induce alteraciones en la acetilación y metilación de las histonas al actuar sobre las enzimas que mantienen el estado de la cromatina. Se ha descrito que el estrés oxidativo inducido por el peróxido de hidrógeno puede reclutar moduladores de histonas a promotores de genes supresores tumorales activos para inhibirlo (Nishida and Kudo, 2013, Kreuz and Fischle, 2016). A pesar de que el estrés oxidativo influye en las modificaciones postraduccionales de las histonas que regulan el estado de la cromatina, no actúa sobre ellas de la misma forma, debido a la distinta sensibilidad de las enzimas metilasas, demetilasas y acetilasas de histonas a los productos derivados del estrés oxidativo (Kreuz and Fischle, 2016). Al igual que ocurre con la metilación del ADN, uno de los cambios más llamativos a nivel de las desacetilasas de histonas, reduciendo su actividad, se produce como consecuencia del humo del tabaco (Yao and Rahman, 2012). En pacientes con EPOC, se ha descrito un descenso de la actividad de la HDAC2 que aumenta la acetilación de las histonas H3 y H4 en el promotor de gen NF-κB, y por tanto la desregulación de genes proinflamatorios (Arita and Costa, 2014).

Efecto sobre los ARNs no codificantes

Igual que el estrés oxidativo se ha visto implicado en la remodelación de la cromatina a nivel de modificaciones en el ADN y las histonas, la regulación de la transcripción por parte de los ARNs no codificantes también se ve alterada de diversas formas por este estímulo.

Hasta la fecha se han identificado varios microARNs cuya alteración del patrón de expresión viene dado por cambios en el estrés oxidativo celular (Fuschi et al., 2017). Uno de ellos es el miR-200c cuya expresión aumenta en células epiteliales debido al incremento de las especies reactivas de oxígeno, lo que conlleva al aumento de la apoptosis y la senescencia celular (Magenta et al., 2011). Otros microARNs cuya expresión está inducida por la presencia de especies reactivas de oxígeno y nitrógeno son el miR-21 (Weber et al., 2010), el miR-24 (Bu et al., 2016) o el miR-181 (Liu et al., 2016). Sin embargo, hasta la fecha todas

estas alteraciones se han descrito en enfermedades vasculares o asociadas al estrés oxidativo como la diabetes o la aterosclerosis, sin estudiar el papel concreto de las EROs en cáncer y en la respuesta a cisplatino.

Por otro lado, y a pesar de que los ARNs no codificantes largos son un descubrimiento relativamente reciente, se ha relacionado la alteración de algunos de estos ARNs no codificantes con el estrés oxidativo. OxyS es uno de estos ARNs no codificantes reguladores de la expresión que media la adaptación al peróxido de hidrógeno en situaciones de estrés oxidativo debido a su inducción como consecuencia del aumento de EROs (Amaral et al., 2013). De hecho, el estrés oxidativo parece inducir la transcripción de cientos de lncRNAs antisentido en detrimento de sus genes codificantes (Fuschi et al., 2017). Sin embargo, hasta la fecha, la regulación detallada de estos ARNs no codificantes mediante las especies reactivas de oxígeno y su papel en la transcripción global, así como su relación con la aparición de resistencia al tratamiento con quimioterapia es aún objeto de estudio.

El estudio de los ARNs no codificantes y su relación con el cáncer y la quimioresistencia, están aumentando considerablemente el conocimiento que se tiene hasta la fecha de estos elementos reguladores de la expresión génica. Sin embargo, se necesita abordar su estudio de forma global a nivel del transcriptoma y el metiloma para poder implicar a estos elementos y a sus propios mecanismos de regulación epigenética en la respuesta a quimioterapia.

Por todo ello, en este trabajo nos centramos en la importancia de estudiar la relación que parece haber entre las modificaciones epigenéticas, tanto a nivel de metilación como de ARNs no codificantes, y el desarrollo de fenotipos resistentes a quimioterapia, para contribuir a perfilar patrones de expresión e identificar posibles nuevas dianas diagnósticas y terapéuticas que permitirán el desarrollo de nuevas terapias para el tratamiento de esta enfermedad.

OBJECTIVES

OBJECTIVES

The main objective of the present work is to deepen on the molecular mechanisms underlying cisplatin resistance mediated by epigenetic changes that occurs at DNA methylation and non-coding RNAs levels, as well as the signaling pathways involved in the development of resistance to platinum-based chemotherapy. To that end, the specific objectives of the present work are:

Objective 1: To study the role of the epigenetic regulation of miRNome in the acquired resistance to cisplatin in lung and ovarian cancer.

- Identification of microRNAs under potential epigenetic regulation in the acquired resistance to cisplatin.
- Identification of potential candidate target genes under microRNA regulation in the acquired resistance to cisplatin.
- To study the molecular pathways regulated by the microRNAs target genes as a mechanism of cisplatin resistance.
- To study the potential clinical applicability of identified microRNAs and target genes.

Objective 2: Epigenetic characterization of lncRNAs in the acquired resistance to cisplatin in lung and ovarian cancer.

- Transcriptome profiling of lncRNAs under epigenetic regulation in resistance to cisplatin.
- To characterize the epigenetic regulation of lncRNAs involved in cisplatin resistance.

MATERIALS and METHODS

MATERIALS AND METHODS

1. Cell culture, treatments and viability to CDDP

Seventeen human cancer cell lines were purchased from ATCC (Manassas, VA) or ECACC (Sigma-Aldrich, Spain) and cultured as recommended. Cisplatin (CDDP) was purchased from Farma Ferrer (Spain). The CDDP-resistant variants H23R and H460R were established previously in our laboratory from the parental sensitive cell lines (Ibanez de Caceres et al., 2010); OVCAR3R and A2780R variants were established using the same procedure (Levina et al., 2008, Plasencia et al., 2006). Briefly, cells were exposed to increasing doses of CDDP over the time until reaching a significant resistant index, calculated as the Inhibitory Concentration 50 (IC50) of the resistant over the IC50 of the sensitive cell line. The resistant variants H23R, H460R, A2780R and OVCAR3R were selected after a final exposure to 0.7, 0.5, 0.5 and 0.05 μg/ml cisplatin, respectively. The additional 13 human cell lines, PC-3, LNCAP, H727, H1299, HT29, HEK-293T, A549, BT474, LoVo, IMIM-PC-2, SKOV3, SW780 and IMR90, were used to validate the results obtained from the paired sensitive-resistant cell lines established in our laboratory. All cell lines used were authenticated at the Genomics Core Facility of the 'Instituto de Investigaciones Biomédicas Alberto Sols CSIC-UAM'. Authentication was performed by amplification SRT (Short Tandem Repeat) using the GenePreintR10 System kit (Promega, USA). This methodology allows co-amplification and three-color detection of ten human loci: TH01, TPOX, vWA, Amelogenin, CSF1PO, D16S539, D7S820, D13S317, D21S11 and D5S818. These loci collectively provide a genetic profile with a random match probability of 1 in 2.92 × 109 and are used for human cell line and tissue authentication and identification and human cell line cross-contamination determination. Results of the Authentication are shown in Table 5.

Table 5. Cell Authentication. Genomics Core Facility. IIBm CSIC-UAM.

Name of Cell line	Cancer type	*M musculus*	D5S818	D13S317	D7S820	D16S539	VWA	TH01	AMEL	TPOX	CSF1PO	D21S11	REF	Match/ Not Match
REF NCI-H23		Negative	12,13	12	9,10	11	16,17	6	X	8,9	10		ATCC ® CRL-5800	
H23	Lung	********	12,13	12	9,10	11	16,17	6	X	8,9	10	*30*		Match
REF NCI-H460		Negative	9,10	13	9,12	9	17	9.3	X,Y	8	11,12		ATCC ® HTB-177	
H460	Lung	********	9,10	13	9,12	9	17	9.3	X,Y	8	11,12	*30*		Match
REF A2780		Negative	11,12	12,13	10	11,13	15,16	6	X	8,10	10,11	*27,28*	SIGMA	
A2780	Ovary	********	11,12	12,13	10	11,12,13	15,16	6	X	8,10	10,11	*28*		Match
REF OVCAR3		Negative	11,12	12	10	12	17	9,9,3	X	8	11,12		ATCC ® HTB-161	
OVCAR3	Ovary	********	11,12	12	10	12	17	9,9,3	X	8	11,12	*29,31,2*		Match
REF PC3		Negative	13	11	8,11	11	17	6,7	X	8,9	11	*29,31,2*	ATCC ® CRL-1435	
PC3	Prostate	********	13	11	8,12	11	17	6,8	X	8,10	12	*29,31,2*		Match
REF LNCAP		Negative	11,12	10,12	9.1,10.3	11	16,18	9	X,Y	8,9	10,11		ATCC ® CRL-1740	
LNCAP	Prostate	********	11,12	10,12	9.1,10.4	11	16,18	9	X,Y	8,9	10,11	*29,31,2*		Match
REF H727		Negative	11,12	11	8,10	11,13	14,15	8	X	8	11,12		ATCC ® CRL-5815	
H727	Lung	********	11,12	11	8,10	11,13	14,15	8	X	8	11,12	*29,32,2*		Match
REF HT29		Negative	11,12	11,12	10	11,12	17,19	6,9	X	8,9	11,12	*29,30*	ATCC ® HTB-38	
HT29	Colorectal	********	11,12	11	10	11,12	17	6,9	X	8,9	11,12	*29*		Match
REF A549		Negative	11	11	8,11	11,12	14	8,9.3	X,Y	8,11	10,12	*29*	ATCC ® CCL-185	
A549	Lung	********	11	11	8,11	11,12	14	8,9.3	X,Y	8,11	10,12	*29*		Match
REF BT474		Negative	11,13	11	9,12	9,11	15,16	7	X	8	10,11	*28,32.2*	ATCC® HTB-20	
BT474	Mama	********	11,13	11	9,12	9,11	15,16	7	X	8	10,11	*28,32.2*		Match
REF LoVo		Negative	11,12,13	8,11	9.3,10,11	9,12	17,18	9.3	X,Y	8,9	11,13,14		ATCC® CCL-229	
LoVo	Colorectal	********	11,13	8,11	10,11	9,12	17,18	9.3	X,Y	8,9	10,11,13, 14	*29,31,2*		Match
REF IMIM PC2		Negative											Dr. F.X. Real (#)	No Match neither in ATCC nor the DSMZ
IMIM PC2	Pancreas	********	12	11	8,1	11	14,16	7,9	X	11	11	*29,30*		
REF SKOV3		Negative	11	8, 1	13, 14	12	17, 18	9, 9.3	X	8, 11	11		ATCC® HTB-77	
SKOV3	Ovary	********	11	8, 1	13, 14	12	17, 18	9, 9.3	X	8, 11	11	*30,31.2*		Match
REF SW780		Negative	11,12	11,12	9,10	9,11	16,19	6	X	8	10,11	*29,30*	ATCC ® CRL-2169	
SW780	Bladder	********	11,12	11,12	9,10	9,11	16,19	6	X	8	10,11	*29,30*		Match
REF IMR90		Negative	12,13	11,13	9,12	10,13	16,19	8,9.3	X	8,9	11,13	30.2, 31	ATCC ® CRL-186	
IMR90	Lung fibroblast	********	12,13	11,13	9,12	10,13	16,19	8,9.3	X	8,9	11,13	*30.2, 31*		Match
REF IMR90		Negative	12,13	11,13	9,12	10,13	16,19	8,9.3	X	8,9	11,13	30.2, 31	ATCC ® CRL-186	
IMR90	Lung fibroblast	********	12,13	11,13	9,12	10,13	16,19	8,9.3	X	8,9	11,13	*30.2, 31*		Match
REF IMR90		Negative	12,13	11,13	9,12	10,13	16,19	8,9.3	X	8,9	11,13	30.2, 31	ATCC ® CRL-186	
IMR90	Lung fibroblast	********	12,13	11,13	9,12	10,13	16,19	8,9.3	X	8,9	11,13	*30.2, 31*		Match
REF-HEK293T		Negative	8.9	12.14	11	9.13	16.19	7,9.3	X	11	11.12	*28,30,2*	ATCC®CRL-3216	
HEK-293T	Kidney embryo	********	8.9	12.14	11	9.13	16.19	7,9.3	X	11	11.12	*28,30,2*		Match
REF-H1299		Negative	11	12	10	12.13	16,17,18	6,9.3	X	8	12		ATCC®CRL-5803	
H1299	Lung cancer	********	11	12	10	12.13	16,17,18	6,9.3	X	8	12	*32.2*		Match

Note. # (Vila et al., 1995)

For viability assays cells were seeded in 24-well plates at 40,000 cells/well, then treated with increasing doses of CDDP (0, 0.5, 1, 1.5, 2 and 3 µg/ml) over the next 72 hours and stained following a previously described method (Chattopadhyay et al., 2006). Briefly, cells were washed with PBS 1X, fixed with glutaraldehyde 1% (Sigma Aldrich, USA) and stained with crystal violet 0.1% (Sigma Aldrich, USA). Afterwards, cells were discolored with acetic acid 10% (Merck, USA) and the extract was measured by colorimetry at 595 nm. Cell viability comparing sensitive with resistant cell lines was estimated relative to the density recorded over the same experimental group without drug exposure during the same period of time (0 µg/ml).

5Aza-2deoxycytidine (5Aza-dC) and trichostatin A (TSA) (Sigma-Aldrich, Spain) are epigenetic reactivation drugs that were used for the reexpression studies following a previously described methodology (Ibanez de Caceres et al., 2006). TSA is a pharmacological treatment that inhibits the action of histone deacetylases (HDAC); 5Aza-dC is a cytosine analogue that sequesters the DNMTs, blocking their action. The combination of both treatments facilitate the open conformation of chromatin and the transcriptional activation. The concentration of these drugs used in the present work are based on previous studies from our group, in which SW480 cells were treated with increasing doses of 5Aza-dC (2.5 and 5 μM) and TSA (150, 300 and 500 nM) to determine that the best re-expression/less mortality ratio was for 300 nM of TSA and 5Aza-dC at 5 μM. This study also studied the re-expression potential of both drugs alone or in combination, showing that combining both drugs produced higher re-expression levels (Ibanez de Caceres et al., 2006). For the present study, the resistant cancer cell lines H23R, H460R, OVCAR3R and A2780R were maintained in the absence of cisplatin for 20 days before the epigenetic treatment to avoid making note of transcriptional changes caused by the effects of the drug itself and to ensure that the resistance remained stable. The 4 resistant cell lines were seeded at 700,000 cells/p60 and exposed to 5Aza-dC (5μM) and TSA (300nM), named therefore Resistant Treated cells (RT). Simultaneously, the 8 matched sensitive and resistant cell lines were seeded at the same concentration and treated with PBS and ethanol (mock cells). DNA and RNA were extracted from all the experimental groups to perform the miRNA/mRNA expression array assays, the confirmation of the expression changes by qRT-PCR and the epigenetic validations.

2. Plasmids and bacteria transformation

To carry out the outlined experimental functional assays, we used two types of plasmids: overexpressing and 3'UTR-region plasmids. Overexpression vectors carry the cDNA sequence of the genes *MAFG* (RC221486, OriGene), *ELK-1* (RC208921, OriGene) or *ABCA1* (RC221861, OriGene) followed by the coding sequence of an epitope of Myc for the C-terminus of the protein, to be subsequently detected with antibodies for western blot. The vector PCMV5 was generously donated by Dr. R. Perona (Centro de Investigación Biomédica Alberto Sols, CSIC-UAM) and used as negative control. 3'UTR-region plasmids carry the sequence of the Luciferase reporter gene followed by the 3'UTR region of *MAFG* (SC221766, OriGene), *ELK-1* (SC213985, OriGene) or *ABCA1* (SC220652, OriGene). A vector with a 3'UTR region not regulated by any microRNA (PS100062, OriGene) was used as control.

In order to have enough amount of every vector for the efficient cellular transfection, we transformed *E. coli* DH5α cells with 100ng of each plasmid followed by incubation on ice at 30 minutes and thermal shock at 42ºC for 2 minutes. Transformed cells were incubated 1 hour at 37ºC in LB broth medium (Thermofisher, USA) prior to seeding in LB-agar (Sigma Aldrich, USA) + kanamycin or ampicillin (Roth, Alemania) plates. The next morning, colonies were collected and growth overnight in 400 ml of LB medium + kanamycin or ampicillin (10 ng/ml) at 37ºC and shaking at 200 RPM. 16-20 hours later, the plasmidic DNA isolation and purification was performed with the Plasmid Maxi Kit (Qiagen, USA) following the manufacturer's indications with minor modifications.

3. Site-directed mutagenesis assay

The full length MAFG-3'-UTR sequence (NM_002359.3 OriGene, USA) was used as a template to generate the mutants MAFG 3´UTR. Two different regions were identified as seed region of miR-7 binding site by more than six bioinformatic algorithms (diana, miranda, targetscan, miRmap and pita). Seven nucleotides within each seed region were mutated. Site-directed mutagenesis was carried out with QuikChange lightning site-directed mutagenesis kit (Stratagene, USA) according to the manufacturer´s instructions. The presence of both mutated seed regions and the integrity of the remaining MAFG 3'UTR sequence of all constructs were validated by Sanger sequencing. The primers designed to introduce mutations were for Region2: Fw-5'-caagtaaaccatgatatat**agtgcta**cttccaccttaactttgcc-3'; Rv-5'-ggcaaagttaaggtggaag**tagcact**atatatcatggtttacttg-3'; and for Region8: Fw-5'-ggccaagcgttccctggcc**agtgcta**tctggcctcagctttgttc-3', Rv-5'-gaacaaagctgaggccaga**tagcact**ggccagggaacgcttggcc-3'.

4. Cell Transfection and lentiviral transduction.

cDNA plasmids transfection: a Myc-DDK-tagged ORF clone of *MAFG*, *ELK-1* or *ABCA1* and the negative control pCMV6 were used for in transient transfection (OriGene, USA). H23 and A2780 cells were plated onto 60-mm dishes at 6x105 cells/dish and transfected with a negative control, *MAFG*, *ELK-1* or *ABCA1* vectors using jet-PEI DNA Transfection Reagent (PolyPlus Transfection, USA). For stable overexpression, lentiviruses carrying *ELK-1* cDNA (Applied Biological Materials, Canada) were obtained by cotransfecting 15 µg of the specific lentiviral vector (pGIPZ-nonsilencing or pLenti-GIII-CMV-h*ELK-1*-GFP-2A-Puro) and 5 µg of each packaging vector (pCD-NL-BH and pMD2-VSV-G) in 10 million HEK 293T cells using Lipofectamine 2000 (Invitrogen, USA). Supernatants were taken at 48 hours posttransfection. A2780S cells were plated onto 60-mm dishes at 1x105 cells/dish and

transduced with supernatant carrying nonsilencing or *ELK-1* lentivirus, and polybrene was added (5 μg/ml).

Luciferase assay: HEK-293T cells were transfected with MAFG-3'-UTR, MAFG-3'-mutated-UTR, ABCA1-3'-UTR or ELK-1-3'-UTR plasmids (OriGene, USA), and PremiR-hsa-miR-7 or Negative Control as described above. Luminiscence was assayed 24 hours later using the Kit Renilla Luciferase Assay System (Promega, USA), according to the manufacturer's instructions. Results were normalized to the Renilla luminescence from the same vector and shown as the ratio between the various treatments and cells transfected with control vector.

miR-7 overexpression and silencing: Cell lines were seeded at 500,000 cells/p60 plate, then transfected with 40 or 50 nM of miR-7 precursor, anti-miR-7 or negative controls (AM17100, AM 17110, AM10047 and AM17010 Ambion, USA) and using Lipofectamine 2000 (Invitrogen, USA) according to the manufacturer's protocol.

Transfection efficacy was measured by qRT-PCR, using the sensitive cell line transfected with the negative control as a calibrator. Two independent experiments were performed in quadruplicate.

5. Clinical sample and data collection

Formalin-Fixed Paraffin embedded (FFPE) and fresh-frozen ovarian cancer samples were collected from untreated patients and associated clinical data were obtained from Hospital Parc de Salut Mar (83 patients) and Biobank of IDIS-CHUS-HULP (55 patients) representing the most frequent ovarian cancer subtypes; all the patients underwent chemotherapy treatment after sample collection. In addition, 22 high-grade serous carcinoma (HGSOC), were obtained from the National Cancer Research Centre (CNIO) biobank in collaboration with Dr. J. Benitez, from a previously reported cohort of patients (Gayarre et al., 2016). Seven patients were also selected from stage III/IV patients from Hospital Madrid Clara Campal with a platinum treatment response classified as refractory or resistant..

Formalin-Fixed Paraffin embedded (FFPE) and fresh-frozen tumor (T) and Adjacent-tumor tissues (ATT) paired samples were obtained from 36 and 22 patients with NSCLC, respectively, from La Paz University Hospital. In addition, FFPE samples were obtained from 39 patients with NSCLC from Hospital Parc de Salut Mar. All patients had both a perioperative PET-CT scan showing localized disease and a pathological confirmation of

stages after having undergone a complete resection for a histologically confirmed early NSCLC.

We also collected 10 normal ovarian samples from patients who had undergone a sex reassignment surgery or tubal ligation and 10 peripheral blood mononuclear cells (PBMCs) to discard genomic imprinting. In addition, five saliva samples from healthy donors and two samples from non-neoplastic origin were used as controls. Follow-up was conducted according to the criteria of the medical oncology divisions from each institution. All samples were collected after the approval of the appropriate Human Research Ethics Committee at the contributing center, including an informed consent within the context of research. Clinical, pathological and therapeutic data were recorded by an independent observer, and a blind statistical analysis was performed on the data. Table 6 summarizes the total number of samples obtained and used in this work.

Table 6. Summary of the samples obtained for this study including the tissue type, center of origin and sample preservation type.

Tissue Type	Hospital/Biobank	Number of Samples	Sample Type	Characteristics
Ovarian cancer	Hospital Parc de Salut Mar	83	FFPE	Representation of the most frequent ovarian cancer subtypes. All the patients underwent chemotherapy treatment
Ovarian cancer	Biobank of IDIS-CHUS	55	Fresh-Frozen	Representation of the most frequent ovarian cancer subtypes. All the patients underwent chemotherapy treatment
Ovarian Cancer	National Cancer Research Centre (CNIO) biobank	22	FFPE	High-Grade Serous carcinoma from a previously reported cohort of patients (Gayarre et al., 2016)
Ovarian cancer	Hospital Madrid Clara Campal	7	FFPE	Stages III/IV with a platinum treatment response classified as refractory or resistant
NSCLC	La Paz University Hospital	36	FFPE	Lung cancer cohort of confirmed stages I/II from a previously reported cohort of patients (Ibanez de Caceres et al., 2010)
NSCLC	Hospital Parc de Salut Mar	39	FFPE	Lung cancer cohort of confirmed stages I-IV from a previously reported cohort of patients (Pernia et al., 2014)
NSCLC	La Paz University Hospital	22	Fresh-Frozen	Lung cancer cohort of paired samples Tumor and Tissue Adjacent to the Tumor
Peripheral Blood Mononuclear Cells	La Paz University Hospital	10	Blood	Negative Control cohort
Normal Ovarian	La Paz University Hospital	10	Fresh-Frozen	Negative Control cohort belonging to patients who had undergone a sex reassignment surgery or tubal ligation
Normal Lung /Normal saliva	La Paz University Hospital	2/5	FFPE/Bucal Swab	Negative Control cohort of lung and saliva samples from non-neoplastic disease

Note: FFPE, Formalin-Fixed Parafin Embedded; NSCLC, Non-Small Cell Lung Cancer

6. *In silico* databases: The Cancer Genome Atlas (TCGA) and Total Cancer Care (TCC)

The Cancer Genome Atlas (TCGA) data: We obtained RNA sequencing data for the *MAFG* of 984 NSCLC tumors and 312 ovarian tumors from the TCGA. The raw reads were quantified by RSEM (Li and Dewey, 2011) in order to determine the read counts for each gene (calculated separately). Then, we filtered out genes having less than one count-per-million reads in all samples. The normalization process was performed with trimmed mean of M-values (Robinson and Oshlack, 2010) to obtain the *MAFG* sequence count data in all patients.

Total Cancer Care (TCC): We obtained *MAFG* gene expression data for 1035 lung cancer and 174 ovarian cancer samples from the Moffitt Cancer Center Total Cancer Care Biorepository (Fenstermacher et al., 2011) that were assayed on a custom Affymetrix 2.0 microarray. Normalized intensity values for *MAFG* probe sets were obtained and the probe with highest average intensity was retained for gene expression analysis.

7. RNA isolation

Total RNA from sensitive (S), resistant (R) and resistant under epigenetic reactivation treatment (RT) cells was extracted by the guanidine thiocyanate method using TRIZOL reagent (Invitrogen, CA) and purified with the miRNeasy mini kit (Quiagen, CA), combined with DNAsa treatment as recommended by Agilent. RNA Integrity was determined by running samples in a 2100 Bioanalyzer (Agilent Technologies).

8. miRNA/mRNA and lncRNAs array preprocessing

miRNA microarrays: Labeling Kit (Agilent Technologies) was used to label RNA. Basically, 100 ng of total RNA were dephosphorylated and Cyanine 3-pCp molecule was ligated to the 3′ end of each RNA molecule by using T4 RNA ligase. For hybridization, 100 ng of Cy3 labelled RNA were hybridized onto Human miRNA Microarray v2, 8x15K (G4470B) for 20 hours at 55ºC in a hybridization oven (G2545A, Agilent Technologies) set to 15 rpm in a final concentration of 1X GE Blocking Agent and 1X Hi-RPM Hybridization Buffer, according to manufacturer's instructions (miRNA Microarray System Protocol, Agilent Technologies). Arrays were washed according to manufacturer's instructions (miRNA Microarray System Protocol, Agilent Technologies) and dried out using a centrifuge at 1000 rpm for 2 min. Finally, arrays were scanned at 5mm resolution on an Agilent DNA Microarray Scanner (G2565BA, Agilent Technologies) using the default settings for miRNA Microarray (miRNA

Microarray System Protocol, Agilent Technologies) and image provided by the scanner was analyzed using Feature Extraction software version 10 (Agilent Technologies).

mRNA microarrays: One-Color Microarray-Based Gene Expression Analysis Protocol (Agilent Technologies, Palo Alto, CA, USA) was used to amplify and label RNA. Briefly, 1 μg of total RNA was reverse transcribed using T7 promoter Primer and MMLV-RT. Then cDNA was converted to aRNA using T7 RNA polymerase, which simultaneously amplifies target material and incorporates cyanine 3-labeled CTP. Subsequently, samples were hybridized to Whole Human Genome Microarray 4 x 44K (G4112F, Agilent Technologies). 1.65 mg of Cy3 labeled aRNA were hybridized for 17 hours at 65ºC in a hybridization oven (G2545A, Agilent) set to 10 rpm in a final concentration of 1X GEx Hybridization Buffer HI-RPM, according to manufacturer's instructions (One-Color Microarray-Based Gene Expression Analysis, Agilent Technologies). Arrays were washed according to manufacturer's instructions (One-Color Microarray-Based Gene Expression Analysis, Agilent Technologies) and were dried out using a centrifuge. Finally, arrays were scanned at 5mm resolution on an Agilent DNA Microarray Scanner (G2565BA, Agilent Technologies) using the default settings for 4x44k format one-color arrays and the images provided by the scanner were analyzed using Feature Extraction software (Agilent Technologies).

mRNA array data were normalized using quantiles normalization (Bolstad et al., 2003) while miRNA array data were normalized using the VSN method (Huber et al., 2002) which preserves the biological characteristics of the data while stabilizing the variance across the entire intensity range. Quality control was based on statistical outlier criteria implemented in the Bioconductor package ArrayQualityMetrics; there were no statistical outliers in terms of MA plots, dendrogram or boxplots. After normalization, only those probes present in at least one sample from the microRNA-microarrays and at least 50% of all the samples from the mRNA-microarrays were considered for further analysis. Fifteen different bioinformatics algorithms were developed from GeneCard (www.genecards.org), miRBase (www.mirbase.org), mirwalk (www.umm.uni-heidelberg.de/apps/zmf/mirwalk) and Web gestalt (www.bioinfo.vanderbilt.edu/webgestalt) databases for studying the *in silico* complementarity between miRNAs/mRNA (Wang et al., 2013, Dweep and Gretz, 2015, Kozomara and Griffiths-Jones, 2014). (GEO reference: GSE84201).

The criteria used for filtering the miRNA/mRNA data were according to the packages recommended by Agilent, and were analyzed by two independent bioinformaticians. miRNA/mRNA experiments had an average expression over the 20th percentile of all average expressions and changed across the different conditions (i.e. with a coefficient of

variation [CV] >5% across all samples). Global data were combined to identify those miRNAs, with inhibited expression after cisplatin treatment that were re-expressed after epigenetic reactivation, together with those genes that have *in silico* mRNA complementary sequences and opposite expression. Genes were considered as targets if selected with at least one of the 10 methods described by Alexiou *et al* (Alexiou et al., 2009). For the inverse expression profiles, only those pairs (miRNA, gene) with a negative Spearman correlation coefficient and a p-value for this correlation <0.1 were considered as potential targets. The databases GeneCard (http://www.genecards.org) miRBase (www.mirbase.org), mirwalk (www.umm.uni-heidelberg.de/apps/zmf/mirwalk) and Web gestalt (www.bioinfo.vanderbilt.edu/webgestalt) were used for bioinformatics analysis (Wang et al., 2013, Dweep and Gretz, 2015, Kozomara and Griffiths-Jones, 2014). (GEO reference: GSE84201).

lncRNAs microarray: mRNA and lncRNA expression profiling was performed using the Arraystar Human LncRNA Microarray V3.0 (Arraystar) in two independent biological replicates per sample (GSE108139). This lncRNA microarray interrogates lncRNAs, together with mRNAs on the same chip, which are labeled along the entire length without 3' bias, even for degraded RNA at low amounts. LncRNAs as a population are ~10x less represented than mRNA. The overlapping lncRNAs have partial or total regions in common with their host gene (Ning et al., 2017). Thus, strand and transcript-specific detection is crucial to accurate detection of multiple transcript isoforms. The use of a specific exon or splice junction probe can specifically detect transcripts that overlap with other transcripts on the sense strand. The expression profiling was based on the manufacturer's standard protocols with minor modifications. Briefly, mRNA was purified from total RNA after removal of rRNA (mRNA-ONLY™ Eukaryotic mRNA Isolation Kit, Epicentre). Next, each sample was amplified and transcribed into fluorescent cRNA along the entire length of the transcripts without 3' bias, using a random priming method (Arraystar Flash RNA Labeling Kit, Arraystar). The labeled cRNAs were hybridized onto the Human LncRNA Array v3.0 (8 x 60 K, Arraystar). The slides were washed and the arrays were scanned by the Agilent Scanner G2505C. Agilent Feature Extraction software (version 11.0.1.1) was used to analyze acquired array images. Quantile normalization and subsequent data processing were performed using the GeneSpring GX v12.1 software package (Agilent Technologies). After quantile normalization of the raw data, lncRNAs and mRNAs that, in at least 1 of 16 samples, had flags in Present or Marginal ("all targets value") were chosen for further data analysis. Differentially expressed lncRNAs and mRNAs with statistical significance between the two groups were identified through fold change ≥1.5, p-value ≤ 0.05

9. Whole genome bisulfite sequencing

The DNA from H23S/R, H460S/R, A2780S/R and OVCAR3S/R was isolated as described (Pernia et al., 2014) and sent to the National Centre for Genome Analysis (Centro de Nacional de Análisis Genómico [CNAG]) for WGBS (GSE109317). Briefly, 2 μg of genomic DNA was mixed with unmethylated DNA from lambda phage in a proportion of 5 ng for each μg of genomic DNA. Libraries were prepared using the "preparation samples kit" TruSeqTM DNA v2 (Illumina Inc.) following the manufacturer's indications with minimum changes. DNA was sonicated using Covaris E220 (Covaris Inc.) to generate fragments of 50-500 bp. The selected size for library preparation was 150-300 bp. These fragments were purified using AMPure XP spheres (Agencourt Bioscience Corp). Following methodologies included end repair, adenylation and pairing with specific adaptors for the "paired-end" methodology from Illumina (Illumina Inc.) as described previously in-depth (Soto et al., 2014). After ligation, fragments were sodium-bisulfite modified using the EpiTect Bisulfite kit (Qiagen) following the manufacturer's protocol. DNA was amplified in 7 PCR cycles using DNA polymerase PfuTurboCx Hotstart (Agilent Technologies). Quality control of the library was performed by Bioanalyzer 75000 (Agilent Technologies). The library was sequenced on HiSeq2000 (Illumina, Inc.) following the manufacturer's protocol, in paired end mode with a read length of 2x101bp. Images analysis, base calling and quality scoring of the run were processed using the manufacturer's software Real Time Analysis (RTA 1.13.48). The average million read-pairs was ~500 reads and the mean coverage was ~30X per sample. The mapping was carried out using GEM 1.242 and the methylation calling with BScall.

10. RT-PCR and qRT-PCR

Total RNA from cells and surgical samples was reverse transcribed and quantitative RT-PCR analysis were performed as previously described (Ibanez de Caceres et al., 2010, Ibanez de Caceres et al., 2006). Briefly, 500 ng of total RNA isolated from cell lines were used for RT reaction using PrimeScript™ RT Master (Clontech-Takara, USA) and 5ul of the RT product was used for subsequent qPCR using Solis Biodyne Master Mix (Genycell, Spain) Samples were analyzed in triplicate using the HT7900Real-Time PCR system (Applied Biosystems, USA), and relative expression levels were calculated according to the comparative threshold cycle method ($2^{-\Delta\Delta Ct}$) using RNU48 or RNU6B as an endogenous control miRNAs and GADPH or β-actin as an endogenous control genes. Primers and probes for expression analysis were purchased from Applied Biosystems. miRNAs probes are detailed in Table 7. Probes for gene expression are as follows: *MAFG*: Hs 01034678_g1; *ELK-1*: Hs 00901847_m1; *MAPKAP1*: Hs 01118091_m1; *ABCA1*: Hs 01059118_m1; *GADPH*:

Hs03929097_g1; *β-actin*: Hs99999903_m1. Data are presented as the "change of expression in number of times" (Log10-RQ) and the error bars are expressed as the maximum estimate (RQmax) and the minimum estimate (RQmin) expression levels, representing the standard deviation of the average expression level RQ. miRNAs from human HEK-293T cell line were isolated using the miRNeasy kit (Quiagen, USA) and miR-7 expression analysis was carried out as described before, using RNU48 as endogenous control and the experimental groups transfected with 3'-UTR plasmid control and miR-NC as calibrators.

Table 7. Baseline and statistical characteristics associated with the selected miRNAs.

miRNA Name	Accession Number	Statistical contrast	FDR RvsS	FDR RTvsR	Assay Number	Validation confirmed	CpG Island position / Methylation Status
hsa-miR-7-5p	MIMAT0000252	Lung & Ovarian	0.0000	0.0000	268	H23/A2780	Intergenic / M
hsa-miR-132-3p	MIMAT0000426	Lung & Ovarian	0.0207	0.0000	457	H23/A2780	Intergenic / U
hsa-miR-335-5p	MIMAT0000765	Lung & Ovarian	0.0013	0.0048	546	H23/H460	Gene promoter / M
hsa-miR-148a-3p	MIMAT0000243	Lung	0.0017	0.1007	470	H23/H460	Intergenic / U
hsa-miR-10a-5p	MIMAT0000253	Lung & Ovarian	0.0159	0.0761	387	A2780	Gene promoter
hsa-miR-124-3p	MIMAT0000422	Lung & Ovarian	0.0442	0.0000	1182	H23	Intergenic
hsa-miR-9-5p	MIMAT0000441	Lung	0.0067	0.0112	583	H23	Intergenic

Note: The table shows the list of miRNAs with accession number, selected following the cut off indicated in the FDR columns according to the statistical analysis performed in two contrasts: For both tumor types (Lung and Ovarian) or for each tissue origin (Lung or Ovarian). It is also indicated the assays numbers for the qRT-PCR validation and the confirmed cell lines. Finally, the CpG islands positions were obtained from CpG Island Searcher (http://cpgislands.usc.edu) and the ENCODE annotation data (http://www.genome.ucsc.edu/index.html).

For semiquantitative RT-PCR, 500 ng of total RNA isolated from cell lines was used to generate cDNA with the High Capacity cDNA Reverse Transcription Kit (Life Technologies) and PrimeScript™ RT Master (Clontech-Takara). Briefly, 500 ng of total RNA were used for RT reaction, and 2 µl of the RT product (diluted 1:5) was used for subsequent semi-quantitative PCR or qPCR reactions with either Promega Green Mix or Promega PCR Mix (Promega) and SYBR Green PCR Mix (Applied Biosystems), respectively. Real-Time PCR was performed under the following conditions: (a) 1 cycle of 95ºC for 2 min; (b) Number of amplification cycles are between 25 to 37 at 95°C for 1 minute and annealing temperatures between 56°C to 62°C for 1 min depending on each pair of primers (detailed in Table 8) and then 72ºC for 1 min; (c) an extension of 5 min at 72ºC. RT-PCR products were run on a 1.5% agarose gel, using the 100 bp Molecular size Marker (New England Biolabs) for appropriate identification of band size. Relative quantification was performed by measuring the intensity of band amplified using ImageJ software.

qRT-PCR relative quantification was calculated according to the $2^{-\Delta\Delta Ct}$ using *GAPDH* as endogenous control and the sensitive-parental cell line as a calibrator and represents the change of expression in Log10. Deviation bars show the maximum estimate (RQ Max) and the minimum estimate (RQ Min) expression levels, representing the standard deviation of the average expression levels. Primers were designed flanking the probe on the array, when possible, in order to assure the correct transcript identification and for specific mRNAs and lncRNAs transcripts that significantly showed changes in the arrays; *GAPDH* was used as an endogenous control; all primers are listed in Table 8. The RNA obtained from the paired A2780/A2780CP and OV2008/OVC13 cell lines was generously donated from Dr. Cheng (Moffitt Cancer Center) and was used for further validations.

Table 8. List of designed primers used for RT-PCR, indicating the length amplified and the PCR conditions

GeneSymbol	cDNA Primer Forward (5' → 3')	cDNA Primer Reverse (5' → 3')	cDNA Amplification Length (bp)	Annealing Temperature	Cycles of amplification
MAFG	TCAGATTTCAGAGGAATACCCAGCAG	TGATCACCAGTCAGAAGTGTACACAC	149	60ºC	30
HMOX1	TGAGTTTCAAGTATCCTTGTTGACAC	CTTGGTCTAACTTTTGTGTGAAATAA	270	60ºC	30
AC091814.2	AGGATTATTCCAGCCTCTGTGATCAC	AGTTCCAGCCTTGTGGACACATAGTC	285	59ºC	37
RP11-65J3.1 002	AGAAAGTTCTTTCCCTGAGGACCATC	TTTTGCAGATGTGAGAACTGAGGCTC	417	59ºC	36
AC141928.1	AGGATGAAAACCATGGAAGGAAAGAGG	TTTCACTTACAAGGACCCTGATGACAC	258	59ºC	36
AF198444	TTTCTTGTTGGTTTGCAAGAGCTCTTTG	TGTGTTAGGCAGAAAATGAATGGTAGG	283	59ºC	34
BX641110	TAAAAAGCAGTCCACACTAACTTGTC	TATAATCACTTTCTGCTAGAACGTGG	306	58ºC	31
RP11-522B15.3	ATCGTTTGGGTAAACAGCCAAGCTTC	TCACATGAATTCACATGTCTGGGCAG	353	59ºC	36
RP11-532F12.5	TCCAAGATCCCTTCAGTGAACATGG	TTCCTTTAGAGTCTCTCATCCTCCAG	190	59ºC	36
RP11-65J3.1 003	AATACCCACCTTTCTGGTAATGCAGC	AAGAACTTTCTCCACACGGTCATGTG	249	58ºC	36
AC007040.5	AAAATCAACCAGACCCAAAACAGAGG	TAAACTGTTGGGATTACAGGTGTGAG	368	62ºC	34
RP11-1A16.1	TTTTCCACATCAGCCACAAGAATGACC	AGAAAATTTAGGGTCAGAGCGAATCTTC	220	57ºC	34
GS1-600G8.5	TTTGTCTTCTGCCGTGATTGTGAG	TTCTGAGTCCATAGTCCATTCTGG	151	57ºC	34
LA16c-83F12.6	TAAAGAGAGGTTATGGAGTCTGTAGC	ACATCATGTTCTTCATTCTGCCCTTGC	156	57ºC	34
TUBA4B	AAGCAATCTATGACATCTGCCACTGC	TACCTTTTCTGCAGAGATGACTGGTG	224	57ºC	34
CTD-2026G22.1	ATTCAAGACTGTTTCTTGGACGTCCTC	TATTCTTTGGCATAACACAGCTGTCTG	291	57ºC	34
AP001439.2	AAAGCATTTCCTACCTCCTCCTCTG	TAATCATGTCCTTCTGTCTTGGAGG	174	57ºC	34
RP11-874J12.4	TCATCAAGAGATAGTGTCCGACACAC	TTCCTTTACTGTTGTCCGTGTCAGTG	193	57ºC	34
AC000035.3	TTAACCAGGAATGTCTCGATCTCCTG	AAGGACATGGAGGATGAGGGAGAAAG	274	60ºC	30
XLOC_005125	TCCATTTACCTCTGCCTGAACACAAG	TCAAGTAGAGGATTTGTCAGCACAGTC	259	58ºC	34
RP11-100E13.1	AGGAAACTTGAAGCCAGCAGTACAAG	TGAAGTTCTCTCTGGAATGACTGGAC	266	59ºC	32
CRNDE	AAGTTCACTTCTGAACTAAGGGGTTCC	ATATTTAAACCACTCGAGCACTTTG	269	56ºC	33
PLAC2	TTTGCATGTCCCACCTTCTTTGTTTG	TTTTATTCAGTACACTCTCAAAACAGC	283	57ºC	36
RP11-6N17.4	TTGTCCTCATCTAATCCGTCAGTACC	TACATAGGTATACATGTGCCATGTTG	259	56ºC	30
ZNFX1-AS1	AGGCTTTGATTGAACCAGGATGAATG	AGATCTTCACTTTCATGAAAGCACAG	272	61ºC	27
AC007566.10	TAGAACCACCATCAAGTGAAAATTGCC	AGTGACCTAAGTCTGTCTTCAATGGTC	276	56ºC	34
HOXC-AS3	AGGCCACGAGCAAAGGCTGTTTCGGTCC	TAGGCATAGGCATAGGTGTCTCAGC	263	56ºC	33
RP11-333A23.4	AGTATAACCAGGTGCCAGATCTAAAG	ATATTTGGAAAGGACACTGTTCCTCAG	326	57ºC	33
RP11-384P7.7	TGTAAAACCATCAGATCTCGTGAGAC	AGTATGTCCTTCTCAGTACCCAACTG	195	56ºC	32
RP11-561O23.8	AAGAAATTAATGGTGAAGTGGTGACG	AAAGTTAACAGTTGATTTGCCTGAGG	261	56ºC	32
RP11-760H22.2	AGATTAGATGTGATCAACCTCACAC	ACTTTTGGCTACATAGGAGAATCAG	321	57ºC	36
AC003986.7	TCTCAAAAAATGGCTGGAGCTAGATAC	TCTTTCATCAGTTATTCCAGCAACTC	271	57ºC	34
GAPDH	GAGAGACCCTCACTGCTG	GATGGTACATGACAAGGTGC	135	58ºC	25

11. Epigenetic validation: CpG island identification, DNA extraction, bisulfite modification, bisulfite sequencing, methylation-specific PCR and quantitative MSP

The occurrence of CpG islands (CGIs) encompassing microRNA genes or being located nearby (2000 bp 5-upstream) was assessed using various CGI-revealing programs; we first used CGI Searcher, (http://bioinfo.itb.cnr.it/cgi-bin/wwwcpg.pl) under Takai and Jones parameters: GC ≥55%; Obs/Exp ≥65; and length ≥200 bp, because these situations exclude

most of the Alu- repetitive elements (Takai and Jones, 2002, Takai and Jones, 2003). To confirm the CGI position, we used ENCODE annotation data (http://www.genome.ucsc.edu/index.html). CGIs containing repetitive elements were detected using the RepeatMasker Web Server (http://www.repeatmasker.org) and then excluded from the study. The possible gene in which the miRNA was encoded was also analyzed, followed by an analysis of the presence of 5´ CGIs located in the transcriptional site and at least 1000 bp upstream.

The DNA from a total of 308 samples, including tumors, controls and cultured cell was isolated, bisulfite modified and used for Bisulfite Sequencing (BS), Methylation Specific PCR (MSP) and quantitative MSP (qMSP), as previously described (Ibanez de Caceres et al., 2006). Briefly, 1 µg of DNA was denaturalized using NaOH (0.2 mol/l) (Sigma-Aldrich, Spain) for 10 minutes at 37ºC and bisulfite modified with Sodium Bisulfite and Hydroquinone (Sigma-Aldrich, Spain) for 16-18 hours at 50ºC. Sample was protected from evaporation with mineral oil (Sigma-Aldrich, Spain). Afterwards, modified DNA was purified using the Wizard DNAClean-Up system (Promega, USA) following an incubation with NaOH 0.3 mol/l for 10 minutes at room temperature, to maintain the single-strand DNA molecules. Modified DNA was precipitated with 100% Ethanol (Merk, USA), glycogen 20 mg/ml (Roche, Spain) and Ammonium Acetate 10 mol/l (Sigma-Adrich, Spain) overnight at -20ºC. Finally, sample was centrifuged at 14,000RPM for 45 minutes at 4ºC and modified DNA was washed with 70% Ethanol following another centrifugation of 5 minutes. Modified DNA pellet was resuspended in 25 µl of DNase and RNase free water (Thermofisher, USA).

Bisulfite Sequencing (BS) is an epigenetic validation technique that allows to analyze the methylation status of every cytosine in a specific region of the genome no larger than 500 bp. For BS, primers were designed, when possible, to exclude binding to any CpG dinucleotide to ensure amplification of either methylated or unmethylated sequences. Primers are listed in Table 9. PCR reactions were used for cell lines and control studies, performed under the following conditions: (a) 1 cycle of 95ºC for 5 min; (b) 40–42 cycles of 95ºC for 1 min, 56°C–62ºC for 1 min, 72ºC for 1 min; (c) an extension of 8 min at 72ºC. The PCR products were run on a 1.5% agarose gel, using the 100 bp Molecular size Marker (New England Biolabs) for appropriate identification of band size, then cut and cleaned by the MinElute gel extraction kit (Qiagen). Direct sequencing was performed on all the genes, rather than subcloning of a mixed population of alleles, to avoid potential cloning efficiency bias (Grunau et al., 2001) and artefacts (Sandovici et al., 2003).

Table 9. List of designed primers used Bisulfite Sequencing, indicating the length amplified and the PCR conditions.

GeneSymbol	Bisulfite sequencing Primer Forward (5' → 3')	Bisulfite sequencing Primer Reverse (5' → 3')	Bisulfite Amplification Length (bp)	Annealing Temperature	Cycles of amplification
miR-7.3 A1	TTAGGAAGAAGTTAGGAGGGGAAA	CAAACACCTCAAACCACCCTCT	372	60ºC	40
miR-7.3 A2	TAGTTGGGGAAGTTTTTTTTAGGA	TTTCCCCTCCTAACTTCTTCCT	428	60ºC	40
miR-132 A1	GTTTTAGGTTTTTAYGGGAGTTTA	TACRACCRCRACTCCTACACACT	441	60ºC	40
miR-132 A2	AGGAGTYGYGGTYGTATGAATGA	GTCTCCTAAAACRCCAACACCTT	441	60ºC	40
miR-335	TGGGAAAGAGGAGGTGAGAAA	CGCTTCCTAAAACCAAAAATTCT	528	60ºC	40
miR-148	GTYGTTTTTTTTTTAGTTAGGAGATA	CCRCTCCCTTCCATCTTAACT	560	60ºC	40
C19MC	GTAAGGTTGGTTTTTTTATTTGTAAA	ATTCCAATTAAACAAATTCTAATCCCT	394	60ºC	42
AC091814.2	GTAAATTGTTAAGTATATTTGGTGA	AAAACTCCCCATTCTCTACTCT	374	62ºC	42
RP11-65J3.1	GTTTTYGTAGGTAGATGGATAGA	TTTTACATATATTTAAATCTCCTCT	408	56ºC	41
AC141928.1	TGTATTTGTGTGTTATTAGTTTGGA	CRTACRCAACTTAACCACT	305	63ºC	41
AF198444	GTTTTTYGGGTTTTGGGATGGA	RCRCRACACATACAACCCACT	422	64ºC	42
BX641110	GGTYGGTTTTTATYGYGTAGGA	ACCAACRCRATAAACCCRAACT	446	62ºC	42

Methylation Specific PCR (MSP) is a methodology that allows to detect DNA methylation or unmethylation in an order of one methylated allele over 1,000 unmethylated ones (Herman et al., 1996). Primers were design based on the results from the sequences obtained after BS and are specifically designed to bind methylated (F: 5'-GGGTGGGGTTTTTTAAGAATC-3'; R: 5'-ACATTCTCCTCCTTCGATCG-3') or unmethylated (F: 5'-GGGGTGGGGTTTTTTAAGAATT-3'; R: 5'-ATAACATTCTCCTCCTTCAATCA-3') modified DNA. PCR reactions were used for the primary tumor and control samples and performed for 35 cycles at 95°C denaturing, 57–59°C annealing and 72°C extension with a final extension step of 5 minutes. Each set of DNAs modified and PCR amplified, includes lymphocyte DNA from healthy donors as a negative control, and as a positive control DNA *in vitro* methylated with *Sss* I methylase (IVD) (New England Biolabs, USA). Water with no DNA template was used as a control for contamination. After PCR, samples were run on a 6% nondenaturing acrylamide gel with 10 bp Molecular size marker (Invitrogen, USA), and the presence or absence of a PCR product was analyzed. For Image acquisition we used the Vision-Capt Software v16.11a.

Quantitative methylation-specific PCR (qMSP) is an improved version of the MSP technique that allows to detect one single methylated allele over 10,000 unmethylated ones (Eads et al., 2000). This assay is based on a quantitative real time PCR by simultaneously using specific unmethylated and methylated probes in combination with the previously designed primers for MSP. We used the primer/probe set to detect levels of either methylation (F: 5'-GGGTGGGGTTTTTTAAGAATC-3'; R: 5'-ACATTCTCCTCCTTCGATCG-3'; Probe: 5'-FAM-ACCCCTCTTCGTTCTCGAT-3') or unmethylation (F: 5'-GGGGTGGGGTTTTTTAAGAATT-3'; R: 5'-ATAACATTCTCCTCCTTCAATCA-3'; Probe: 5'-VIC-ACCCCTCTTCATTCTCAAT-3'). All assays were performed in duplicate using the QuantiTect Multiplex PCR Kit (Qiagen, USA), which allows running the methylated and unmethylated reactions in the same well of a PCR plate, and the HT7900 Applied Biosystems. The

percentage of methylation of each sample was calculated according to previously published reports (Eads et al., 2000).

12. Western blot analysis

Cell lines were cultured at a density of 600,000 cells per 60-mm plate, shifted into medium containing 10% fetal bovine serum for 24 h and 72 h. Twenty micrograms (20 μg) of whole-cell extracts were subjected to Western blot, performed as previously described (Sanchez-Perez et al., 1998). The primary antibodies employed were the c-Myc-A14 (Santa Cruz, USA) and β-tubulin (Sigma, Spain) antibodies. Western blot were performed to double check the transfection efficacy.

13. ROS measurement

H23/A2780 cells were cultured in 96-well black plates at density of 10,000 cells/well. Cells were treated with 6 different doses of CDDP for 24, 48 and 72 h in Roswell Park Memorial Institute (RPMI) medium, containing 10% fetal bovine serum (FBS). Then treatments were removed and cells were incubated with the fluorescent probe 2',7'-dichlorodihydrofluorescein diacetate (H2DCFDA) (10 μM) for 45 minutes in RPMI medium (FBS-free). Cells were washed twice with RPMI (10% FBS), and fluorescence was recorded in a Fluostar Optima at 520 nm after excitation at 485 nm, each hour, over a 4-hour period. At the end of the experiment, solutions were replaced for fresh media containing MTT (0.5 mg/ml concentration) in order to determinate viability. ROS production was calculated dividing the mean H2DCFDA fluorescence by the mean viability. Data were normalized with respect to basal conditions that were considered as 100%. All experiments included cells treated with RPMI alone and one well without cells as basal fluorescence.

14. Bioinformatics and statistical analysis of expression and methylation

For the identification of differentially expressed miRNAs and genes from the microarray data, we used linear models (Smyth, 2004) as implemented in the Limma Bioconductor package. The fixed effects were the origin of the tissue (lung/ovarian), the cell line (H460, H23, OVCAR3, A2780) and the condition (sensitive, resistant, resistant treated). The replicate is the random effect. To identify the downregulated miRNAs in resistant cells and their opposite expressed target genes, we performed the following contrasts for all the tissues (lung and ovarian) or for each tissue origin (lung or ovarian): resistant vs. sensitive and resistant-treated vs. resistant. We then selected the candidates that fulfill the following conditions in at least 2 of the 4 cell lines interrogated: Log2(R/S) <0 AND Log2 (RT/R) >0;

RvsS or RTvsR statistically different $p<0.05$. As a statistical method we used the unpaired T-test algorithm with Benjamini Hochberg (BH) as the FDR correction method for multiple testing corrections with statistical significance of $p<0.1$ in the miRNA approach and $p<0.05$ in the gene approach as an adjusted p-value.

To identify differentially expressed lncRNAs and mRNAs with *in silico* complementarity and under potential epigenetic regulation, we interrogated the available databases with lncRNAs annotations (GENCODE (Harrow et al., 2012); RNAdb (Pang et al., 2007); NRED (Dinger et al., 2009); LncRNAdb (Amaral et al., 2011); LNCipedia (Volders et al., 2015), lncRNome (Bhartiya et al., 2013); NONCODE (Bu et al., 2012); fRNAdb (Kin et al., 2007); lncrna2target (Jiang et al., 2015b)) and selected those lncRNAs and mRNAs that changed significantly at three different contrasts: (1) resistant vs. sensitive for each cell line; (2) resistant vs. sensitive for each tumor type; and (3) resistant vs. sensitive for all. Based on the chromosomal relationship of the lncRNA with the mRNA, we defined as overlapping lncRNAs those within the body of the gene or oriented head to head with a protein-coding gene within 1 kb; and as cis-acting lncRNAs those at least 1 kb away from the nearest protein-coding gene but no more than 300 kb (Guttman and Rinn, 2012, Chen, 2016), including enhancer-like function LncRNAs (Orom et al., 2010) – excluding overlapping lncRNAs of this group. Finally, for the identification of CGIs based on the characteristics of Takai and Jones (Takai and Jones, 2003) in our WGBS data, we interrogated a region from 5000 bp upstream to the end of lncRNAs or mRNAs regions, and for individual CpGs from 2000 bp upstream to 500 bp downstream of TSS (Supporting Dataset, Sheets 2-5). The selection of differentially methylated (DM) CpG positions was based on previous results from our laboratory that established an experimentally validated cut-off point for the CpG site methylation level (ratio of reads with methylation out of the total number of reads covering this position). To be selected, the candidates must had to have a ratio of resistance > 0.4 and sensitivity < 0.23, with a minimum coverage of 10X, and at least five individuals DM CpGs. The association between qualitative variables was studied with the Chi-squared test with Yate's continuity correction and was considered statistically significant with p-value < 0.05.

Patient's clinical characteristics were described for the complete series with mean and standard deviation values or relative frequencies. The data were stratified for patients carrying methylated or unmethylated DNA, and their distributions compared with the Chi-squared test or Fisher's exact test for qualitative variables, and Student's t test or the Wilcoxon-Mann-Whitney test (non-normal distribution) for quantitative variables. For *in silico* databases, the data were stratified for patients with high or low expression of *MAFG*

according to the median of the gene expression. Overall survival (OS) and Progression free survival (PFS) were estimated according to the Kaplan-Meier method and compared between groups by means of the Log-Rank test. All the p-values were two-sided, and the type I error was set at 5 percent. Statistical analyses were performed using Stata 10 software.

RESULTS

RESULTS

1. Establishment of ovarian human cancer cell lines resistant to CDDP

To perform our *in vitro* studies, we worked with four human cancer cell lines: two NSCLC, H23 and H460; and two ovarian cancer cell lines, A2780 and OVCAR3. We first confirmed that the CDDP-resistant subtypes, H23R and H460R, maintained their status of resistance to CDDP as previously described (Ibanez de Caceres et al., 2010). The two human ovarian cancer cell lines resistant to CDDP, A2780R and OVCAR3R, were selected after a final exposure to 0.5 and 0.05 μg/ml CDDP, respectively, showing approximately 2.5 times more drug resistance than the matched parental cell line (2.47 and 2.50 resistant index; $p<0.001$). Both cell lines showed a lower CDDP-resistant index than H23R and H460R NSCLC cancer cells (5.00 and 3.85, respectively; $p<0.001$) but enough to assume that similar events would follow (Figure 2).

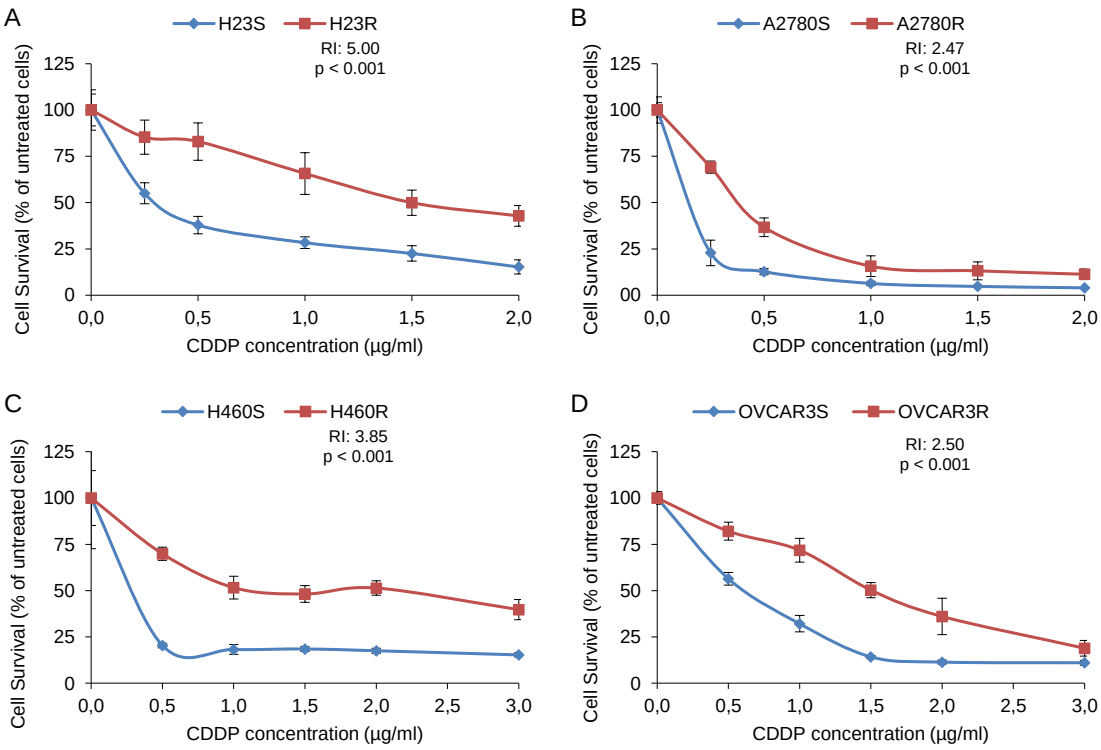

Figure 2 Effect of cisplatin on cell viability. Viability curves showing the acquired resistance of H23, H460, A2780 and OVCAR3 cell lines; Cells were exposed for 72 h to each drug concentration. Data were normalized to the untreated control, which was set at 100% and represent the mean + SD of at least 3 independent experiments performed in quadruplicate at each drug concentration tested for every one cell analyzed. IC50, is the inhibitory concentration that kills 50% of the cell population. Resistant index (RI) calculated as IC50 resistant / IC50 sensitive cell line. SD: standard deviation. P < 0.001 was considered as a significant change in drug sensitivity (Student's t-test).

2. Identification of candidate miRNAs under possible epigenetic regulation

As a first step to identify candidate miRNAs under epigenetic regulation and involved in the CDDP response, we searched for miRNAs showing a decrease of the expression in Resistant (R) *versus* Sensitive (S) cells and a recovered expression after epigenetic reactivation-treated (RT) *versus* R cells. First, 87 out of 723 miRNAs identified on the expression arrays showed a significant expression change ($p<0.05$) in at least one of the following conditions: $R < S$ or $RT > R$; while 28 changed their expression with a *False Discovery Rate (FDR)* < 0.1 simultaneously in both situations $R < S$ and $RT > R$. By analyzing the concurrence of CGIs with the characteristics described by Takai and Jones (Takai and Jones, 2003), candidates were reduced to 10 encompassing microRNA genes or being located nearby (less than 2000 bp 5´-upstream), together with the analysis of the presence of CGIs in the gene promoter region in which the miRNA is encoded. After a pair-base-complementarity analysis *in silico* between miRNA and the candidate target genes that showed opposite expression profiles (5170 mRNAs that assembled *in silico* and 2420 mRNAs that significantly changed expression) we made a functional web-based enrichment analysis with Gene Ontology Tree Machine (GOTM) tool and the selected genes. This approach identified seven miRNAs which potential target genes were involved in tumor progression: miR-7, miR-132, miR-335, miR-148a, miR-10a, miR-124 and miR-9 (Figure 3 and Figure 4). Mature miR-7 is generated from three different miRNA precursors in the human genome, miR-7-1, miR-7-2, and miR-7-3; we assumed expression changes were tightly associated to miR-7-3 (hereafter called miR-7) as no changes were identified on miR-7-1 and miR-7-2 probes represented in the array and it is the only precursor that presents two CGIs surrounding its genome location. We also found that some of the miRNAs showing the strongest upregulation were located at the C19MC cluster, previously linked with carcinogenesis (Augello et al., 2012). It presents a CGI located about 17kb from the first miRNA (Tsai et al., 2009) that was included to analyze its potential epigenetic regulation in drug resistance.

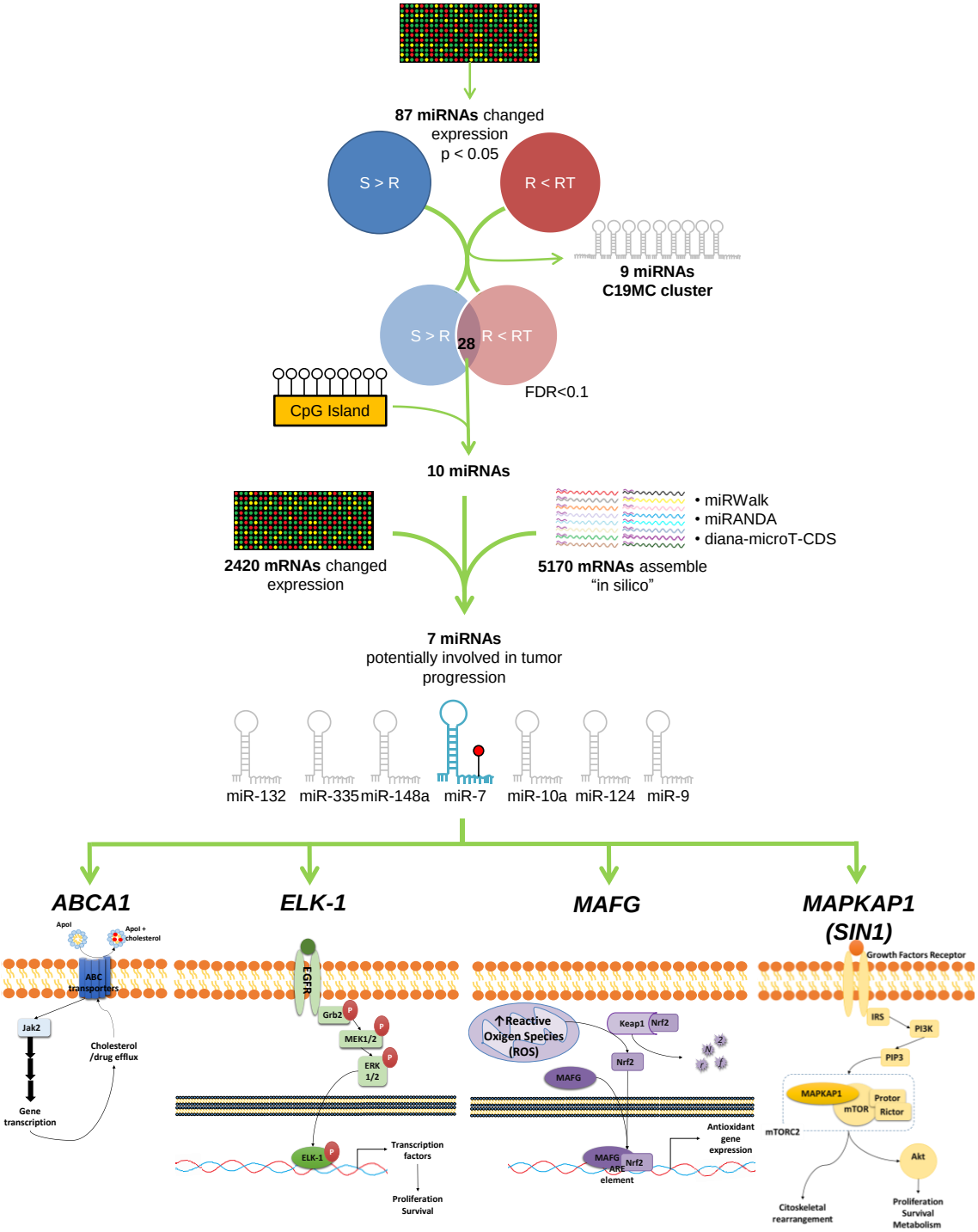

Figure 3. Selection of candidate miRNAs under epigenetic regulation and candidate target genes. The flowchart indicates the steps and criteria used for the selection of the final seven candidate miRNAs under epigenetic regulation and the final 4 candidate genes under possible regulation of miR-7.

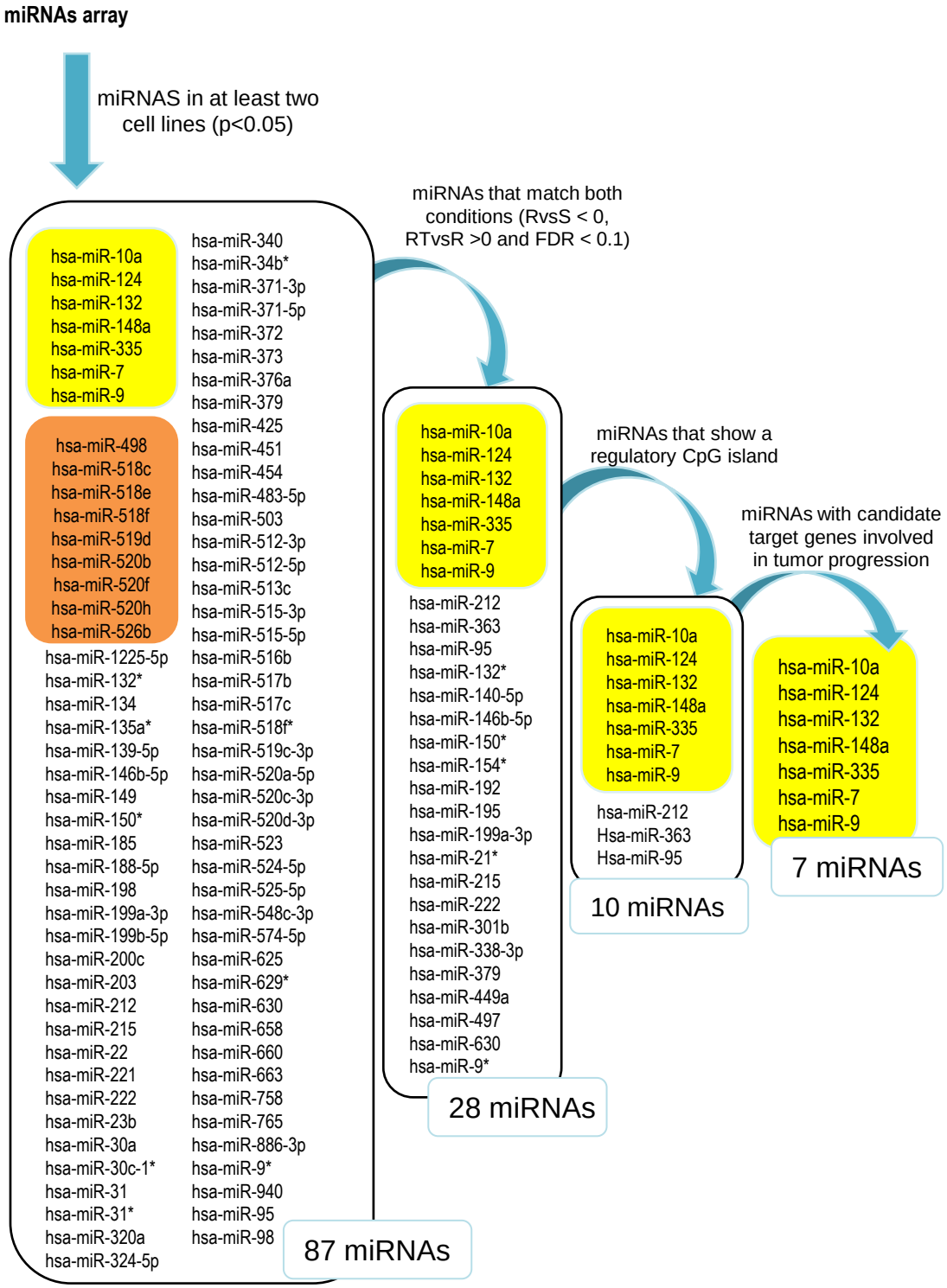

Figure 4. miRNAs selection process. Final miRNAs selected are highlighted in yellow; miRNAs from the C19MC cluster are highlighted in orange.

3. miRNA-7 as potential chemoresistance candidate under epigenetic regulation

For miRNA validation, we first tested the expression profile of the three experimental conditions (S, R and RT) from each cell line (H23, H460, A2780 and OVCAR3) by qRT-PCR

assay, confirming the results from the microarray analysis for all seven miRNAs in at least one of the cell lines analyzed (Figure 5).

Six of the seven miRNAs showed changes in their expression according to the microarray data in H23 cells, which were fully validated by qRT-PCR analysis (Figure 5A). In the H460 cell line, all the miRNAs selected after the analysis of the expression arrays accomplished the defined expression pattern; six shared with cell line H23. miR-335 and miR-148a were validated by qRT-PCR in both conditions, R vs. S and RT vs. R, whereas miR-7, miR-132, miR-9 and miR-10a were upregulated in RT, without significant changes in the experimental group R. Conversely, miR-124 was downregulated in R but no reexpression was observed after epigenetic treatment (Figure 5B). For the A2780 ovarian cancer cell line, the data from the arrays showed the defined expression pattern in 4 candidate miRNAs. Three were validated by qRT-PCR: miR-7, miR-132 and miR-10a, whereas no significant changes in expression between S and R cells were found for miR-124, although it was upregulated in the epigenetically reactivated RT cells (Figure 5C). Finally, the cell line OVCAR3 had less significant changes according to the array data, and in fact, in this cell line, the expression changes were only partially validated; the miRNAs -132 and -124 were reactivated in RT but there was no decreased expression in R (Figure 5D). Table 7 compiles the results obtained for each miRNA both in the arrays and in the qRT-PCR validation assays. Four miRNAs were validated in at least two cell lines: miR-7 and miR-132 in the H23 and A2780 cancer cell lines; and miR-335 and miR-148a in the NSCLC cell lines H460 and H23. These four miRNAs were the ones selected for the epigenetic validation step by bisulfite sequencing (BS), together with the C19MC cluster's CGI.

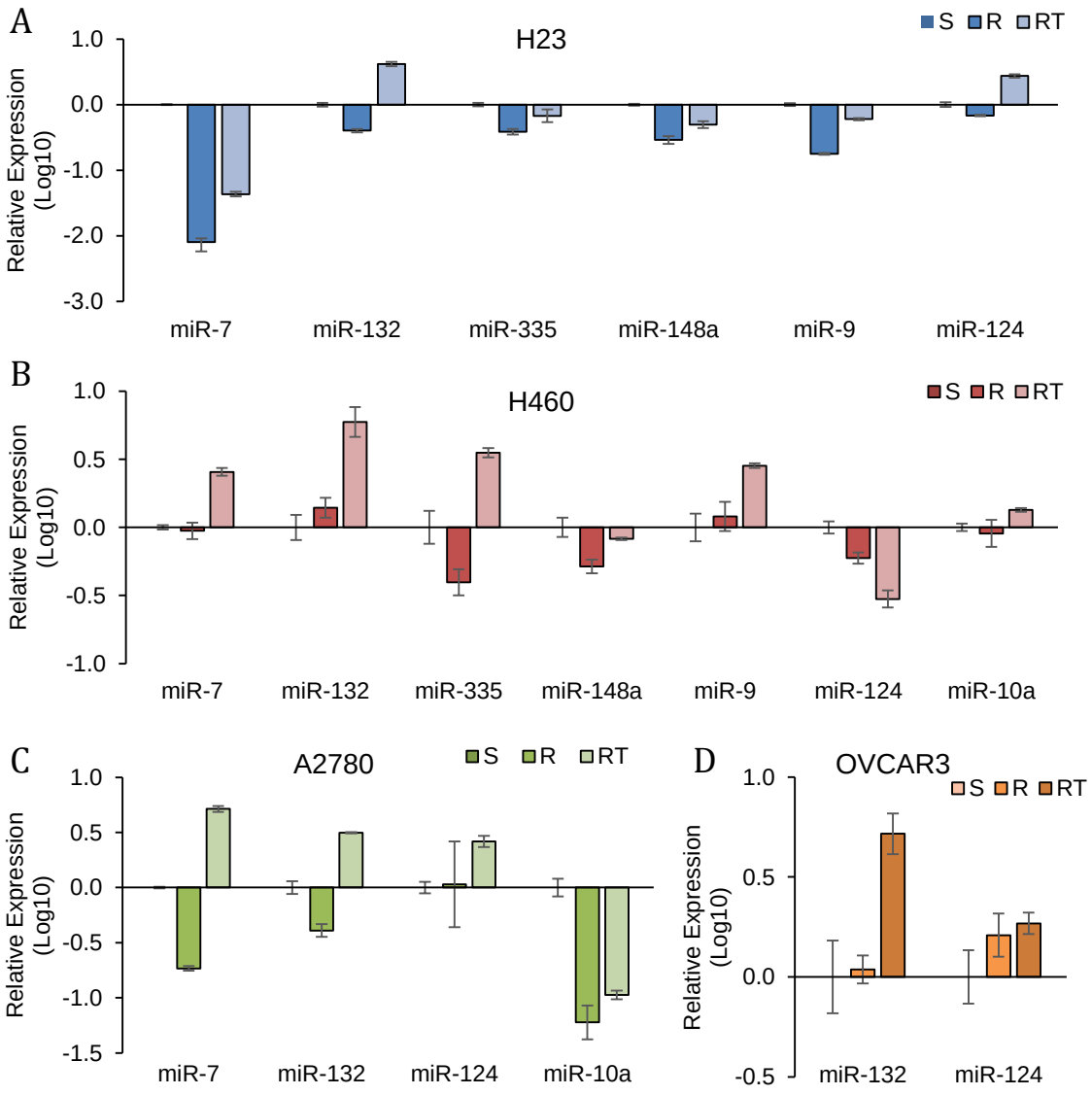

Figure 5. Relative expression levels of the selected miRNAs measured by qRT-PCR. Data are represented in log10 scale and are expressed using the corresponding sensitive (S) line as a calibrator. Each miRNA level was normalized to RNU48 as an endogenous control. Assays were made in the NSCLC cell lines H23 (A) and H460 (B); ovarian cancer cell lines A2780 (C) and OVCAR3 (D) in all experimental conditions: S, R and RT. S: sensitive; R: resistant; RT: resistant treated with epigenetic reactivation drugs (5-Aza and TSA).The expression number assays for each miRNA are indicated in Table 7.

The C19MC cluster's CGI is on the long arm of chromosome 19 and has a CGI of 2255 bp from which we analyzed 394 bp that comprises the area with the highest density of CG positions in H23, H460, A2780 and OVCAR3 cell lines. We also tested DNA from normal tissues from lung (LC), ovary (OC) and PMBCs to discard imprinting. All analyzed CpG positions were densely methylated (Figure 6A), confirming a possible role in embryonic development as described (Court et al., 2014, Noguer-Dance et al., 2010), but excluding a relation between acquisition of DNA hypermethylation and drug-response.

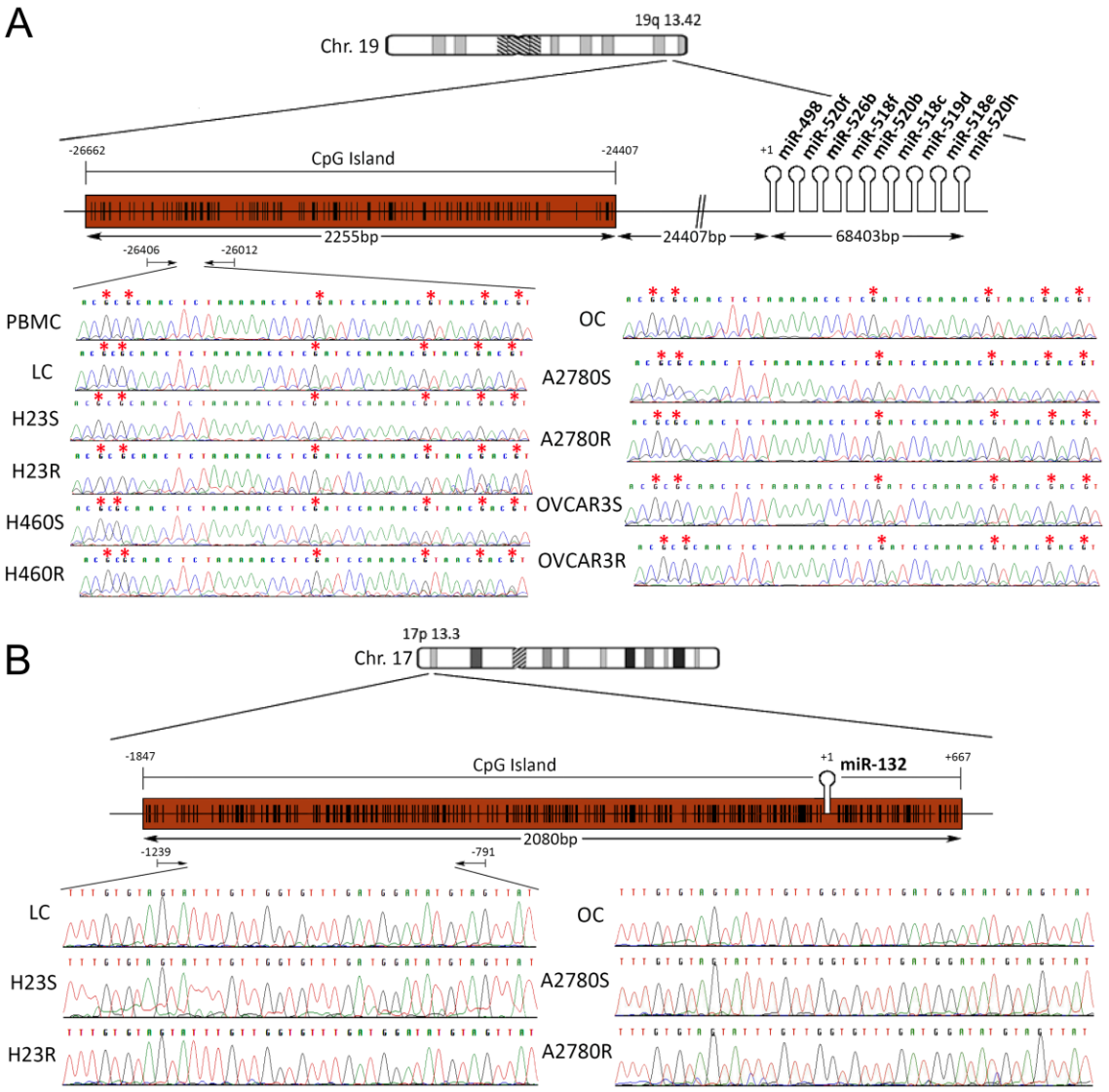

Figure 6. Bisulfite sequencing (BS) of the miRNA potential regulatory CGIs. The figure shows the schemas of chromosome CGIs and miRNA location as well as representative images of corresponding BS. CGIs are represented in red boxes; each CpG position is represented by vertical black lines inside the boxes. The first nucleotide of each miRNA is indicated by +1. Facing arrows mark the primers position. Asterisks indicate methylated positions. LC: lung control; OC: ovary Control (A) Analysis of the potential regulatory C19MC cluster's CGI. All the samples were fully methylated in all tested CpG positions. (B) The miR-132 CGI was unmethylated in all samples tested, with the presence of a T instead of a C previous to G.

Referred to miR-132, the area analyzed was 866 bp in length, at a CGI comprising -1847/+667bp at the short arm of chromosome 17 (Figure 6B). miR-148a is located on the short arm of chromosome 7, with a nearby CGI of 1663, located 137 bp upstream from the miRNA. A 560 bp area of the CGI was analyzed (Figure 7A). No methylation was found for both miRNAs either on the tumor cell lines or controls samples analyzed. miR-335 is located on the long arm of chromosome 7, on the second intron of the MEST002 gene transcript. A 1123 bp CGI is located in the promoter region of this transcript. We analyzed a fragment of

528 bp initially in the H23S/R, H460S/R cells and LC. The results showed methylation only in H460S/R subtypes. We extended the analysis to the additional cell lines LoVo, OVCAR3 and PC-3, and control samples, and no methylation was found in any of them (Figure 7B). Pairs of primers are listed in Table 9.

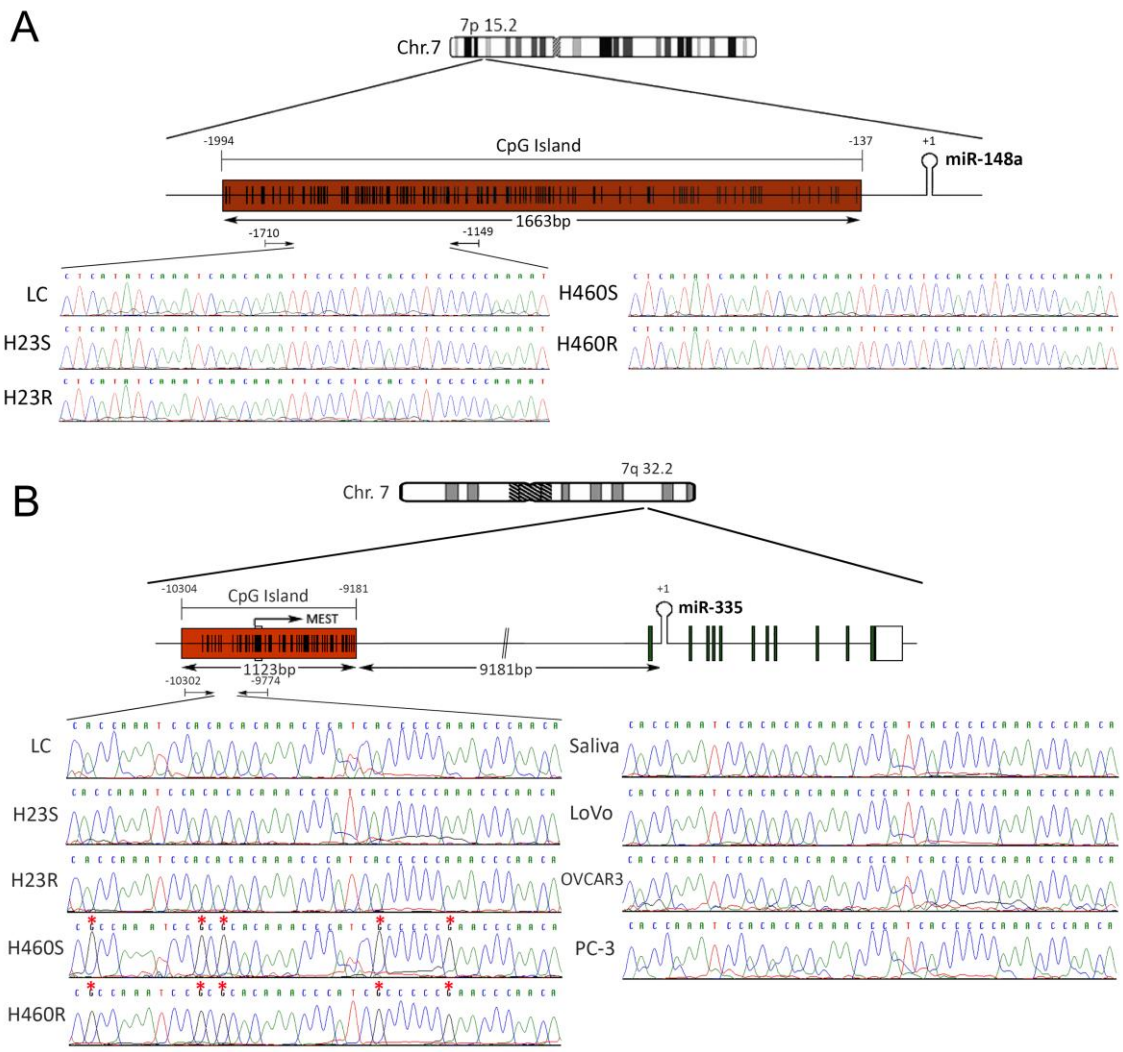

Figure 7. Bisulfite sequencing of the miRNA potential regulatory CGIs. (A) The CGI located near miR-148a was also unmethylated in all analyzed positions. (B) The miR-335 CGI was methylated in H460 cells. Figure legend is described in Figure 6.

miR-7 is located on the short arm of chromosome 19, with two potential regulatory CGIs: one located 861 bp before the first nucleotide of the miRNA sequence with a length of 667 bp; the second has an extension of 269 bp and comprises the miRNA sequence (Figure 8). Two overlapping pairs of primers were used to analyze the first CGI, covering 776 bp, which included the entire CGI and adjacent areas (Table 9). The analysis was performed on the ovarian cancer cells A2780S and A2780R. We found the presence of methylation specifically in the resistant cells. The specific aberrant methylation of miR-7 in resistance

was confirmed in H23R cells as well as in the cisplatin resistant cell lines IMIM-PC2 and LoVo, which present an IC_{50} over 2µg/ml CDDP (Figure 9). OC and LC were used as controls as well as nine additional tumor cell lines. In fact, the sensitive subtypes and controls presented an absence of methylation. A selection of these results is shown in Figure 8, left. This methylation pattern was used to design the MSP primers for the analysis of FFPE primary tumors. The second CGI, was fully methylated for all the samples tested (Figure 8, right). Therefore, the upstream CpG island of miRNA-7 was selected for our translational approach as it was the hypermethylated island in the platinum-resistant cells and therefore the candidate one regulating miR-7 expression.

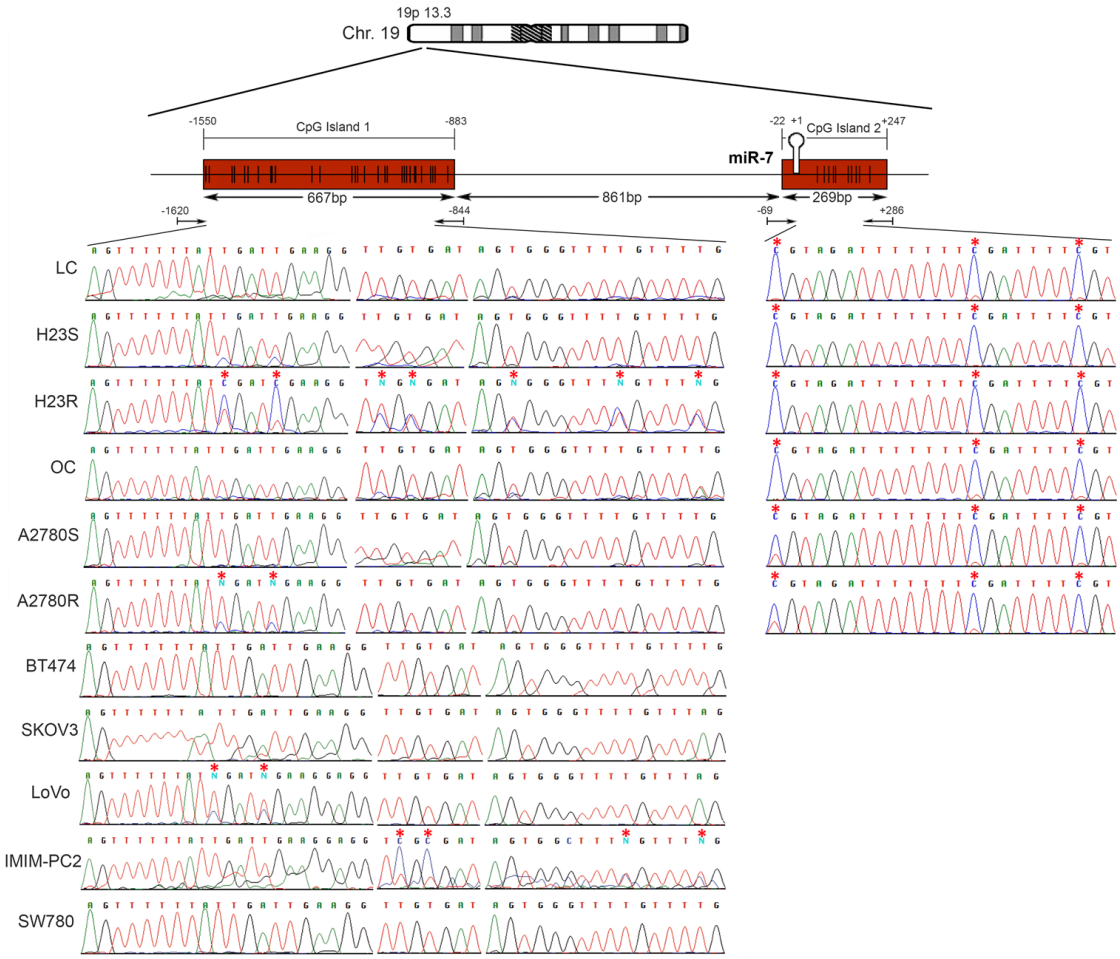

Figure 8. Bisulfite sequencing of miRNA-7 regulatory CGIs. Chromosomal location of miR-7 and their nearby CGIs, as well as representative images of corresponding bisulfite sequences (BS). CGIs are represented in red boxes; each CpG position is characterized by vertical black lines inside the boxes. The first nucleotide of each miRNA is indicated by +1. Facing arrows mark the primer positions used for BS. It is shown the methylation analysis of the two CGIs closely related to the encoded miR-7 region. For the first CGI, the three different fragments (left half of the Figure) corresponding to the most frequently methylated positions are shown. A representation of five of the 11 additional tumor cell lines interrogated, BT474, SKOV3, LoVo, IMIMPC2 and SW780, is also shown. All CpG positions interrogated at the second CGI were fully methylated in all the samples analyzed (right half of the Figure), as indicated by the presence of C preceding a G in the sites indicated by the asterisks. OC: ovary control; LC: lung control. Asterisks indicate methylated positions.

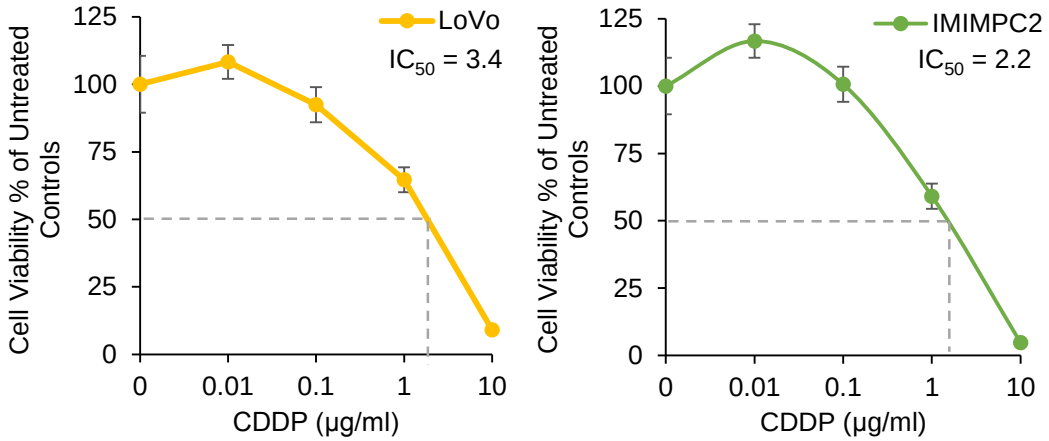

Figure 9. Effect of cisplatin on cell viability. Viability curves showing the acquired resistance of LoVo and IMIM-PC2 cell lines; Cells were exposed for 72 h to each drug concentration. Data were normalized to the untreated control, which was set at 100% and represent the mean ± SD of at least three independent experiments performed in quadruplicate at each drug concentration tested for every one cell analyzed. IC50, is the inhibitory concentration that kills 50% of the cell population

4. *MAFG* is a direct target gene of miRNA-7

To analyze if the methylation of miR-7 is affecting the cisplatin-cell viability through the silencing of its expression, we overexpressed miR-7 in the resistant subtypes at a final concentration of 40 nM (Figure 10A). No effect on drug sensitivity was observed although efficiency of the transfection was validated by qRT-PCR, confirming the miR-7 overexpression after 72h in both cell lines (Figure 10B). The overexpression of higher concentration of pre-miR-7 (50 nM) resulted in a decrease in basal cell viability, reaching levels of 63% and 52%, respectively, compared with their parental sensitive and resistant cell lines, transfected with the mimic negative control (Figure 10C), making unfeasible to evaluate the response to CDDP, given no representative cell population was left from the cell culture after the miR-7 precursor overexpression.

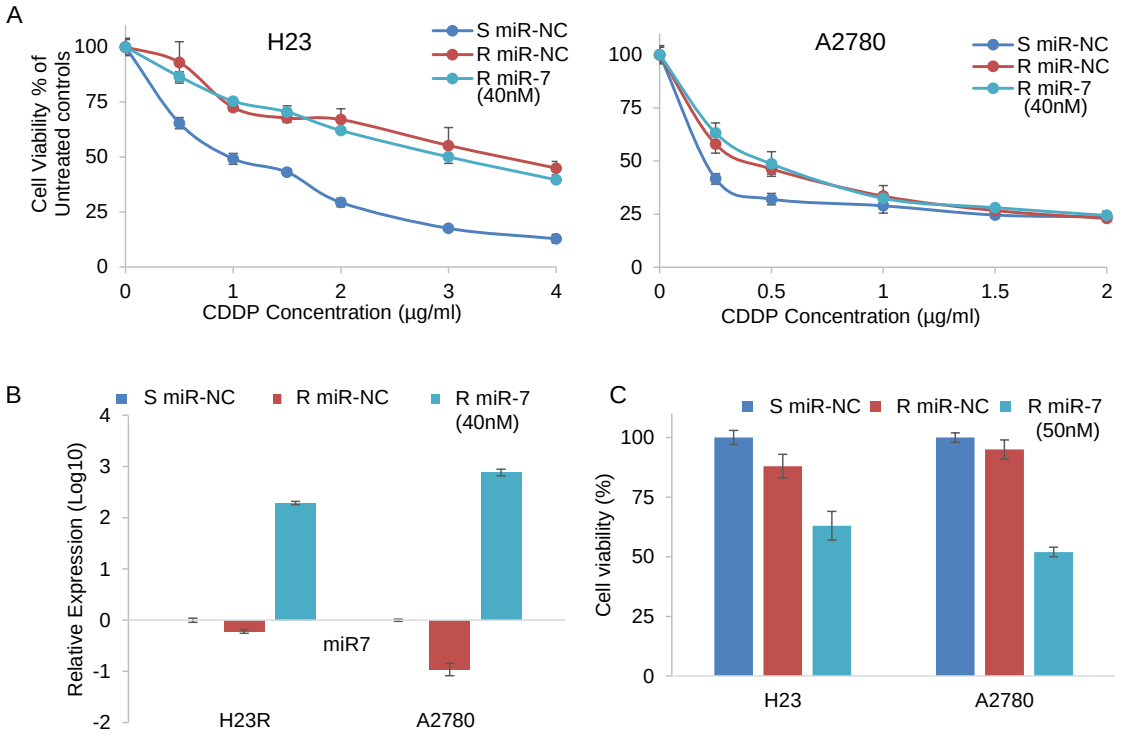

Figure 10. Effect of miRNA-7 overexpression on cell viability at 40 and 50nM of microRNA precursor. (A) Cell viability assay on A2780 and H23 cell lines transfected with 40 nM of the negative control (blue, S miR-Control; red, R miR-Control) and overexpressing miR-7 precursor (green, R miR-7). Data were normalized to each untreated control and represent the mean ± SD of at least 3 independent experiments performed in quadruplicate for each cell line analyzed. (B) Relative miR-7 expression levels measured by qRT-PCR in the A2780 and H23 cell lines, represented in log10 scale. The resistant cell line transfected with the mimic negative control was used as a calibrator. (C) Cell viability assay on A2780 and H23 cell lines transfected with 50 nM of the negative control (blue, S miR-Control; red, R miR-Control) and overexpressing miR-7 precursor (light blue, R miR-7). Data were normalized to each sensitive subtype and represent the mean ± SD of at least 3 independent experiments performed in quadruplicate for each cell line analyzed.

Thus, to fully understand the implication of miR-7 in the development of resistance, out of the 2420 genes that changed their expression in the arrays we investigated the role of the target candidate genes that showed a significant opposite expression to miR-7 and *in silico* complementarity (Figure 3). Out of the 1021 genes that accomplished both conditions we selected only those that were present in A2780 and H23 cell lines and which expression increased in R (resistant cells) compared to S (sensitive cells) and RT (resistant cells under epigenetic reactivation treatment) subtypes, with a p-value<0.05 adjusted by FDR correction. Further functional web-based annotation using the GOTM tool, grouped 149 genes in 20 significant functional groups, from which we selected *MAFG*, *MAPKAP1*, *ELK*-1 and *ABCA1* genes because of their implication in biological functions related to tumor progression (Figure 3). The changes on the expression were confirmed by qRT-PCR in H23 cells for *MAFG* and *ABCA1* (Figure 11A left) and in A2780 cells for *MAFG* and slighter but following the expected expression pattern for *ELK*-1 (Figure 11A right). To probe whether

MAFG, *ELK*-1 and/or *ABCA1* are target genes of miR-7, we overexpressed a precursor of miR-7 in the resistant subtypes to assess the changes in expression of the candidate target genes by qRT-PCR. As expected, the overexpression of miR-7 in H23R resulted in a decrease of the expression of *MAFG* and *ABCA1*, compared with the resistant cell line transfected with the negative control (Figure 11B). *MAFG* regulation was also confirmed in A2780R cells, in which the miR-7 precursor lead also to the decrease of the potential candidate gene *ELK-1* (Figure 11B). Efficiency of the miR-7 overexpresion was validated by qRT-PCR (Figure 11B, right). A summary of this selection in shown in Table 10.

Table 10. Summary of the main characteristics of the candidate target genes and the followed selection steps. Note. In bold X are indicated the three validations needed as a criteria for inclusion for further analysis

Gene		***MAFG***	***ELK-1***	***ABCA1***	***MAPKAP1***
Accession Number		NM_002359	NM_005229	NM_005502	NM_001006617
Name/ Function		v-maf musculoaponeurotic fibrosarcoma	ETS domain-containing protein Elk-1	ATP-binding cassette transporter A1	Mitogen-Activated Protein Kinase Associated Protein 1
Correlation		-0.4266	-0.4545	-0.4615	-0.5175
miR-7 FDR		0.0845	0.0702	0.0669	0.0443
H23	Array	**X**	**X**	**X**	**X**
	qRT-PCR	**X**	-	**X**	-
	After miR-7 Overexpression	**X**	-	**X**	-
A2780	Array	**X**	**X**	**X**	**X**
	qRT-PCR	**X**	**X**	-	-
	After miR-7 Overexpression	**X**	**X**	-	-

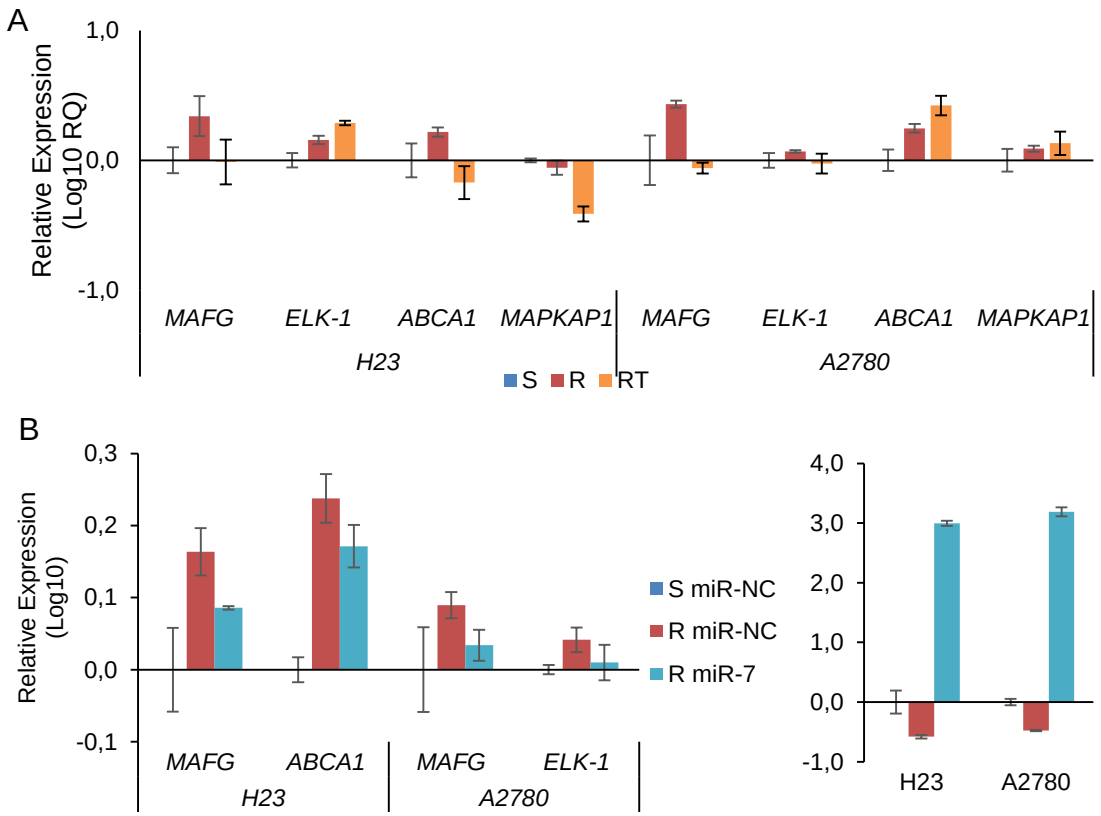

Figure 11. Candidate target genes under regulation of miR-7. (A) Relative expression levels of the selected genes measured by qRT-PCR. Data are represented in Log10 scale and are expressed using the corresponding sensitive (S) line as a calibrator. Each gene level was normalized to GAPDH or B-actin as an endogenous control. Assays were made in the NSCLC cell lines H23 (left) and ovarian cancer cell lines A2780 (right) in all experimental conditions: S, R and RT. S: sensitive; R: resistant; RT: resistant treated with epigenetic reactivation drugs (5-Aza and TSA). (B) Effect of miRNA-7 overexpression on candidate target genes expression. Left, relative expression levels of MAFG, ELK-1 and ABCA1 measured by quantitative RT-PCR in the H23 and A2780 cell lines represented in Log10 scale. Right, relative miR-7 expression levels measured by qRT-PCR in the H23 and A2780 cell lines, represented in log10 scale. Each bar represents the combined relative expression of two independent experiments measured in triplicate. The sensitive cell line transfected with the mimic negative control was used as a calibrator (S miR-NC, blue); R miR-NC, H23R and A2780R cells with same transfection (red); R miR-7, H23R and A2780R cells overexpressing miR-7 precursor (blue).

Next, we cotransfected in HEK-293T cells the pre-miRNA-7 together with a luciferase reporter vector that carries the 3'-UTR region of each candidate gene as a functional study to identify real candidate genes under miR-7 regulation. The cotransfection with the 3'-UTR region of *MAFG*, induced a reduction of the luciferase activity at both concentrations, 15 and 30 nM of the precursor, effect that was not observed when cotransfecting 3'-UTR regions of *ELK*-1 and *ABCA1* (Figure 12A, upper panel). Simultaneously, we confirmed through qRT-PCR that the pre-miR-7 was successfully transfected in the 293T cell line, for every experimental group (Figure 12B, lower panel).

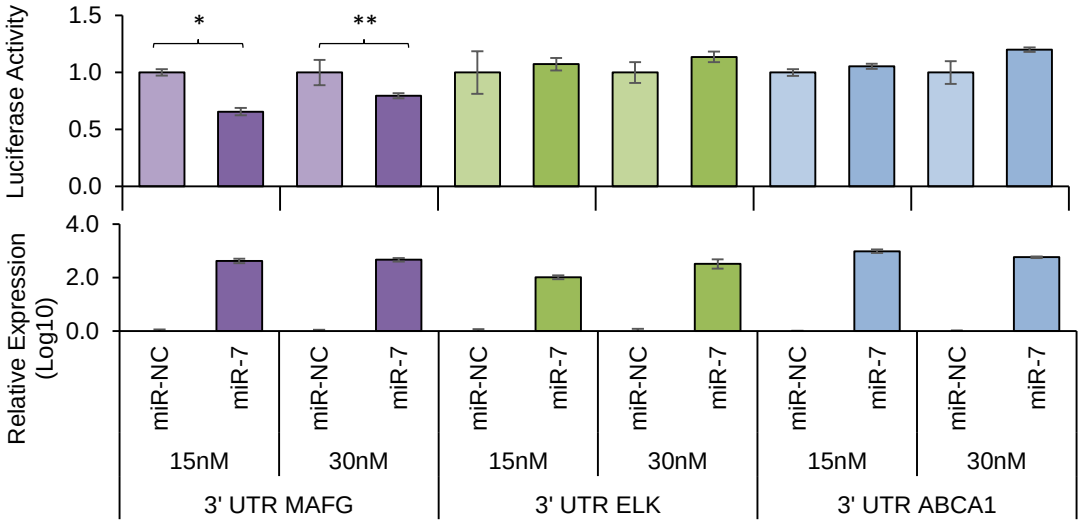

*Figure 12. Validation of the interaction of miR-7 and candidate target genes. Co-transfection of mimic miR-7 (miR-7) or mimic control (miR-NC) with the 3' UTR of MAFG, ELK-1 and ABCA1 at different concentrations (15nM and 30nM). Data was analyzed after 24h of co-transfection. The miR-NC co-transfected with the 3'-UTR of the candidate genes was used as calibrator. Top, Relative luciferase activity. The figures represent the mean ± SD of at least three independent experiments after data normalization with Renilla and the data a negative control 3'-UTR. *p=0.004; **p=0.003 (Student's t-test) p<0.01 was considered as significant change in Luciferase activity. Bottom, relative miR-7 expression levels measured by qRT-PCR in the after co-transfection. Each bar represents the combined relative expression of 2 independent experiments measured in triplicate.*

To fully confirm that *MAFG* is a target gene of miR-7, we performed directed-site mutagenesis at the predicted binding sites of miR-7 in the 3' UTR of *MAFG*, at two different regions (Figure 13A), followed by luciferase reporter assays. The significant decrease of luciferase activity observed when using the WT 3'UTR of *MAFG*, disappeared when we cotransfected pre-miR-7 with both constructs containing the mutated regions (Figure 13B).

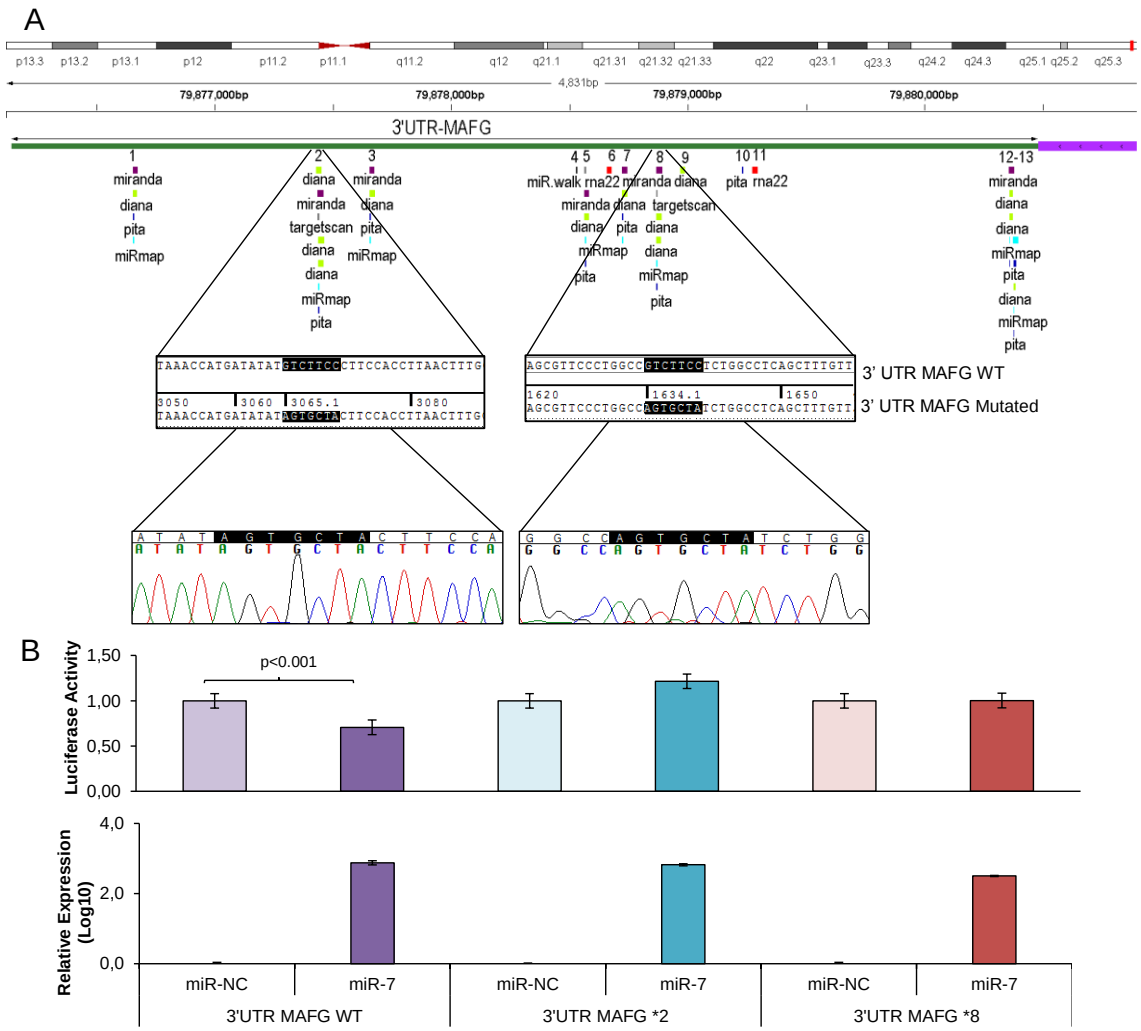

Figure 13 Site-directed mutagenesis for luciferase activity assay and effect of miR-7 silencing over MAFG expression. (A) Chromosomal localization of miR-7 predicted binding sites at 3'UTR of MAFG. Regions 2 and 8 were identified by six or more bioinformatic algorithms. Sanger sequencing showed that the seed sequence of miR-7 was fully mutated at regions 2 and 8 of the 3' UTR of MAFG. (B) Co-transfection of mimic miR-7 (miR-7) or mimic control (miR-NC) with the 3' UTR of MAFG WT, mutated on region 2 (MAFG 2) and mutated on region 8 (MAFG 8*). Experiments were performed at 15nM and data was analyzed after 24h of co-transfection. (Upper panel) Relative luciferase activity. The figures represent the mean ± SD of at least three independent experiments after data normalization with Renilla and the data from the negative control 3'-UTR; p<0.01 was considered as significant change in Luciferase activity (Student's t-test). (Lower panel) Relative miR-7 expression levels measured by qRT-PCR after co-transfection, as an internal control for the mimic transfection. Each bar represents the combined relative expression of two independent experiments measured in triplicate. The miR-NC co-transfected with the 3'-UTR of each tested group was used as calibrator.*

Moreover, to ultimately confirm this regulation, we silenced the expression of miR-7 in A2780S that resulted in increased levels of *MAFG* (Figure 14A). A2780 cells express miR-7 at a low level, as we can observe in Figure 14B compared with the control cell line HEK-293T, which explains the low efficiency decreasing the miR-7 levels at 48h, although it was sufficient enough to observe a strong change over *MAFG* expression.

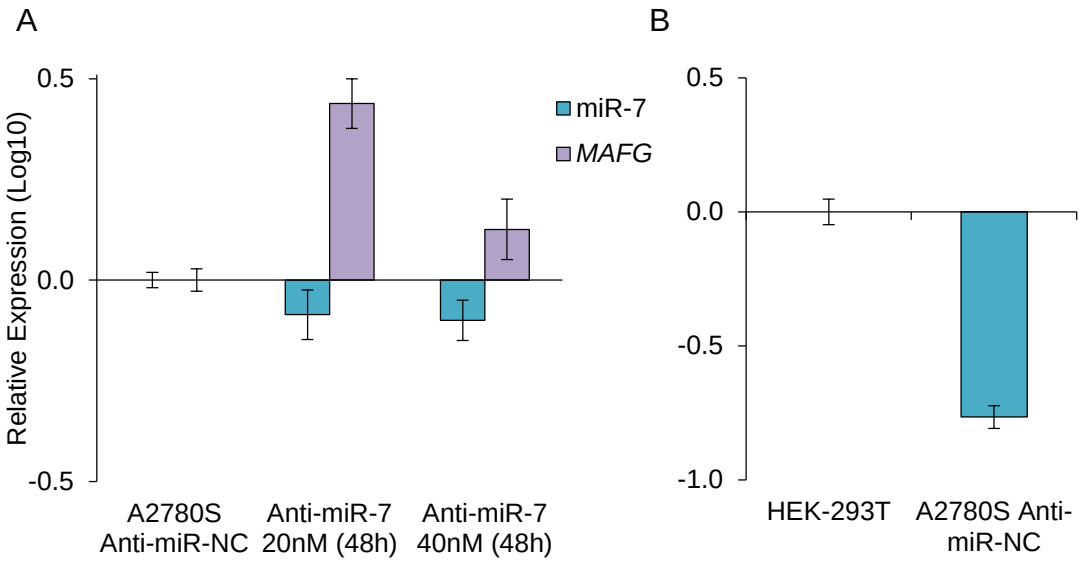

Figure 14. (A) Relative miR-7 and MAFG expression levels measured by qRT-PCR after silencing of miR-7 with antago-miR in A2780S cells. Two different concentrations of Anti-miR-7 were tested, 20nM and 40 nM. Data was analyzed at 48h after transfection. A2780S cells transfected with the Anti-miR Negative Control was used as calibrator. (B) Basal expression of miR-7 in HEK293T cells compared with A2780S cells. For (A) and (B) each bar represents the combined relative expression of two independent experiments measured in triplicate.

5. The response to cisplatin is mediated, at least in part, by MAFG expression in human cancer cell lines

To determine if the expression of the miR-7 candidate target genes was linked to CDDP response, we conducted their *in transient* overexpression in the sensitive cells comparing their response to CDDP with their parental resistant and sensitive cell lines, both transfected with an empty vector.

MAFG overexpression resulted in an increase in the resistance to CDDP in H23S cells compared with the sensitive cell line transfected with the empty vector, showing a resistance index of 1.7 ($p=0.01$) (Figure 15A). The same effect was also confirmed in the sensitive cell line A2780S reaching a similar CDDP-RI of 1.6 ($p<0.001$) (Figure 15B). The overexpression of *ABCA1* in H23S led to a RI of 1.5 compared with the sensitive cell line transfected with the empty vector, although it was not statistically significant ($p=0.796$) (Figure 15C). *ELK-1* overexpression in A2780S did not change the response to CDDP after 48 h of exposure to the drug (Figure 15D).

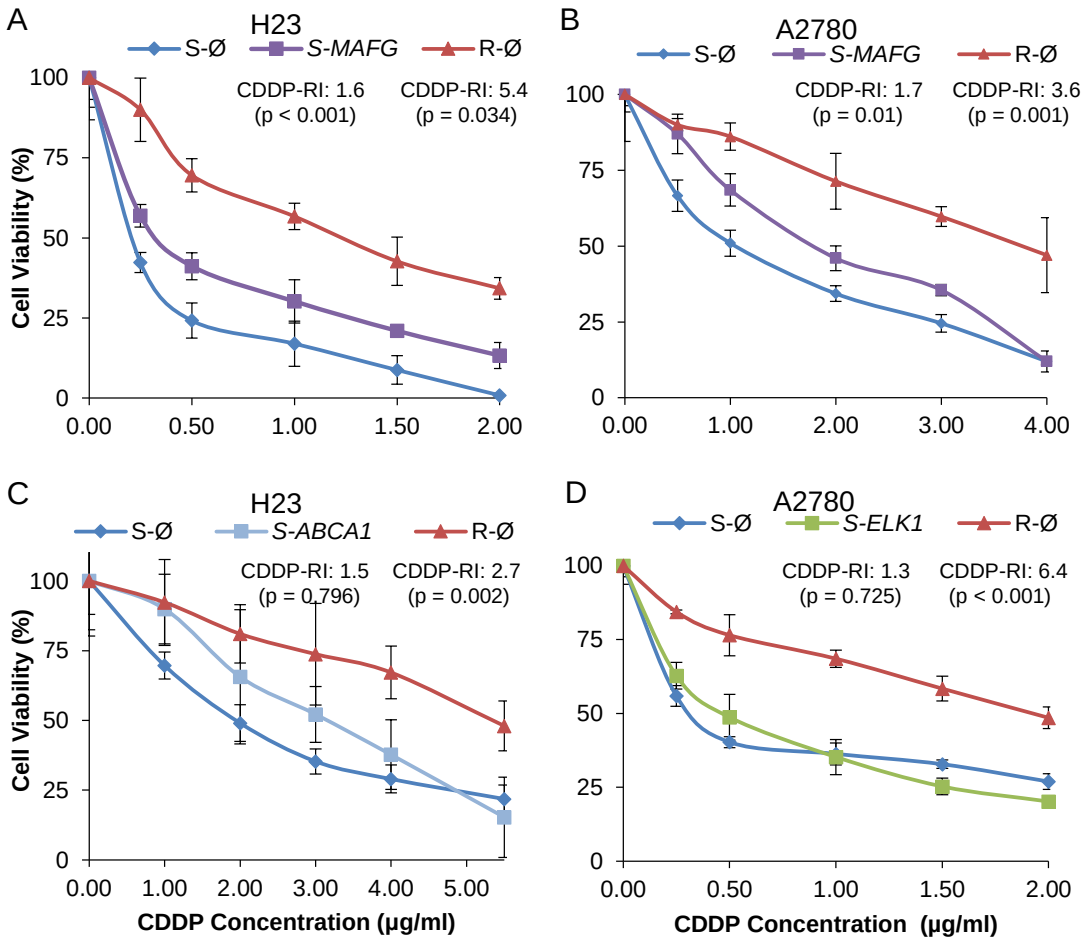

Figure 15. Effect of overexpression of MAFG, ABCA1 and ELK-1 on cell sensitivity to CDDP in H23 and A2780 cell lines. Viability curves of H23 and A2780 cell lines transfected with pCMV6 (S-Ø and R-Ø) and with the overexpression vectors (S-MAFG, S-ABCA1 and S-ELK-1). Each experimental group was exposed for 48 h to 6 different test CDDP concentrations, and data were normalized to each untreated control, set to 100%. The data represent the mean ± SD of at least three independent experiments performed in quadruplicate at each drug concentration for each cell line analyzed. CDDP-RI (Resistant Index to CDDP) was calculated as "IC50 from the R-Ø / IC50 from the S-Ø" and "IC50 from the S-transfected with the gene / IC50 from the S-Ø" ± SD. p<0.01 was considered as significant change in drug sensitivity (Student's t-test).

In order to confirm the efficiency of the transfection, we analyzed the mRNA and protein levels by qRT-PCR and western blot of the overexpressed genes. Results confirmed ectopic overexpression of *MAFG*, *ELK-1* and *ABCA1* at 72 h in both cell lines (H23S-*MAFG*, A2780S-*MAFG,* H23S-*ABCA1* and A2780S-*ELK-1*) with an increase of 0.2, 7, 6416 and 28-folds respectively, compared with the sensitive cell lines transfected with the control vector (Figure 16A). No changes at protein level were found between 24 and 72 hours when analyzing MAFG and ABCA1 overexpression (Figure 16B). However, we observed a slightly protein levels of ELK1 at 24h that was not maintained at 72 h (Figure 16B, right). Therefore, we performed the stable overexpression of *ELK-1* by transduction assays with a lentiviral vector and compare the response to CDDP with the parental-sensitive and resistant

subtypes harboring a nonsilencing vector (A2780S/R -NS). As previously observed in the "in transient" experimental assays, *ELK-1* overexpression did not change the sensitivity to CDDP; however, it induced an strongly increase in the number of cells at 0 µg/ml dose, that allowed to maintain higher ratios of survival fraction when treated with CDDP, compared with the control sensitive cell line. We also confirmed the success of the overexpression by qRT-PCR (Figure 16C).

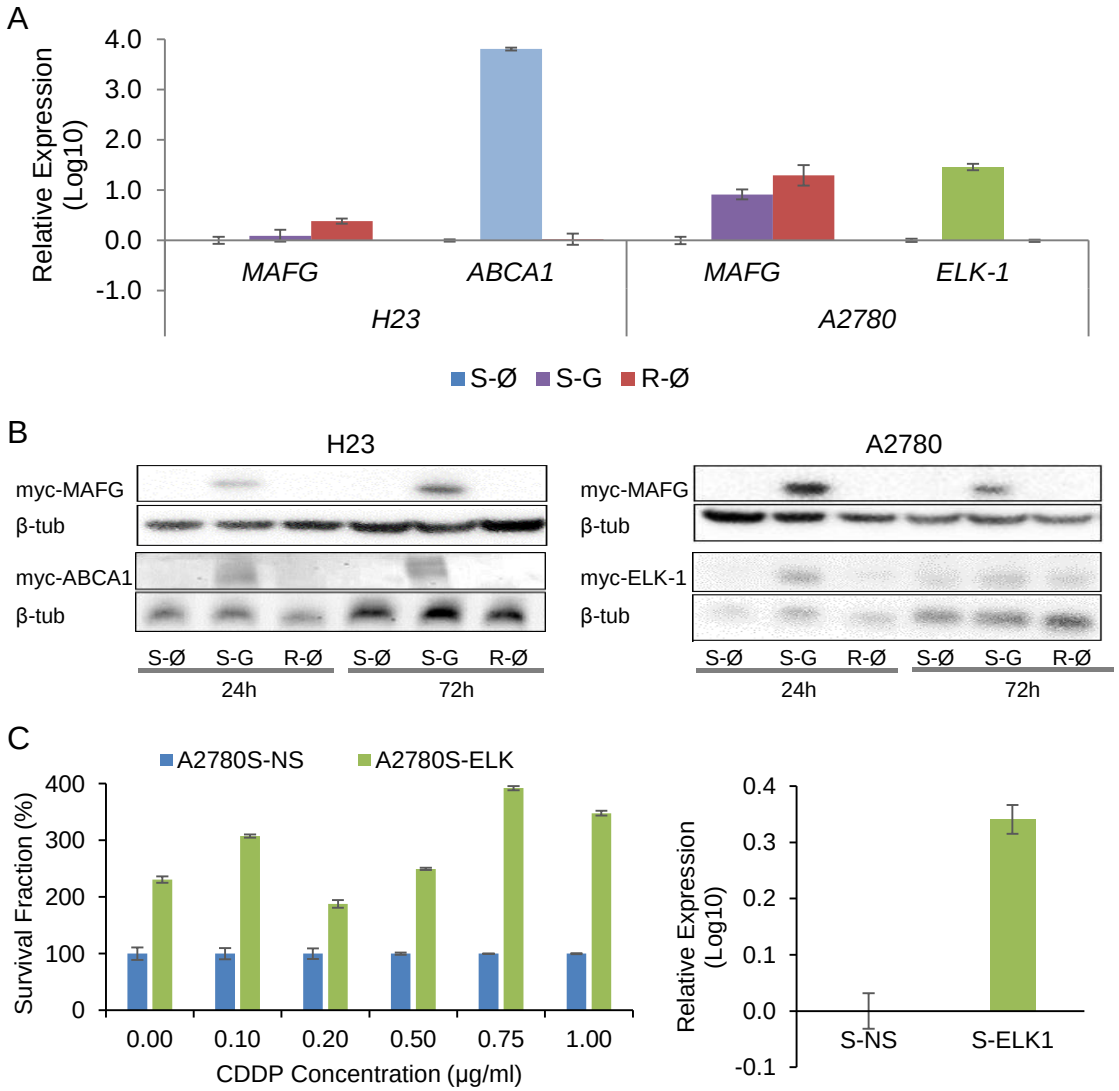

Figure 16. Validation of the transfection efficacy at mRNA and protein levels. (A) Relative expression levels of MAFG, ABCA1 and ELK-1 measured by quantitative RT-PCR, in the cell lines H23 and A2780, represented in Log10 scale; In each experimental group, the sensitive cell line transfected with pCMV6 plasmid was used as a calibrator. Each bar represents the combined relative expression of two independent experiments measured in triplicate. (B) Total cell protein extracted from cells at 24 and 72 hours was subjected to Western blot. The membranes were then hybridized with antibodies against c-Myc and β-tubulin as loading control. S: Sensitive; S-G: Sensitive transfected with the gene; R: Resistant; β-tub: β-tubulin. (C) Stable overexpression of ELK-1 in A2780S cell line. Left, Viability assay after the nonsilencing plasmid infections (S-NS blue) and overexpressing ELK-1 plasmid (S-ELK-1 green). Each experimental group was exposed for 72 h to six different test CDDP concentrations, and data were normalized to each sensitive subtype. Data represents the mean ± SD of at least three independent

experiments performed in quadruplicate at each drug concentration for each cell line analyzed. Right, relative ELK-1 expression levels measured by qRT-PCR and represented in Log10 scale. The sensitive cell line infected with nonsilencing vector was used as a calibrator. Each bar represents the combined relative expression of two independent experiments measured in triplicate.

6. MAFG overexpression might induce CDDP resistance, targeting ROS

As MAFG is a transcription factor involved in the detoxification of ROS, whose expression is increased in the resistant cell phenotypes H23R and A2780R we explored whether MAFG influenced oxidative stress in our experimental model of paired sensitive/resistant cells by analyzing ROS production in these cell lines after CDDP exposure.

First, we confirmed the response to CDDP at 24, 48 and 72 h after exposure to the drug for both cell lines H23S and H23R, analyzed by an MTT-based methodology rather than the traditional crystal-violet staining used previously in this work. H23R cells present a resistance index >3, in accordance with our previous results (Ibanez de Caceres et al., 2010) (Figure 17A). ROS levels were increased in sensitive cells after CDDP treatment compared with resistant cells, reaching 300% and 159% ROS production at 3.00 μg/ml CDDP, respectively, *versus* basal untreated cells, $p<0.001$ (Figure 17B). The response to CDDP and the differences in ROS production between sensitive and resistant cells were also confirmed in A2780S/R ovarian cancer cell lines (Figure 17C and 17D), in which we observed an effect of CDDP treatment after 48 h of exposure.

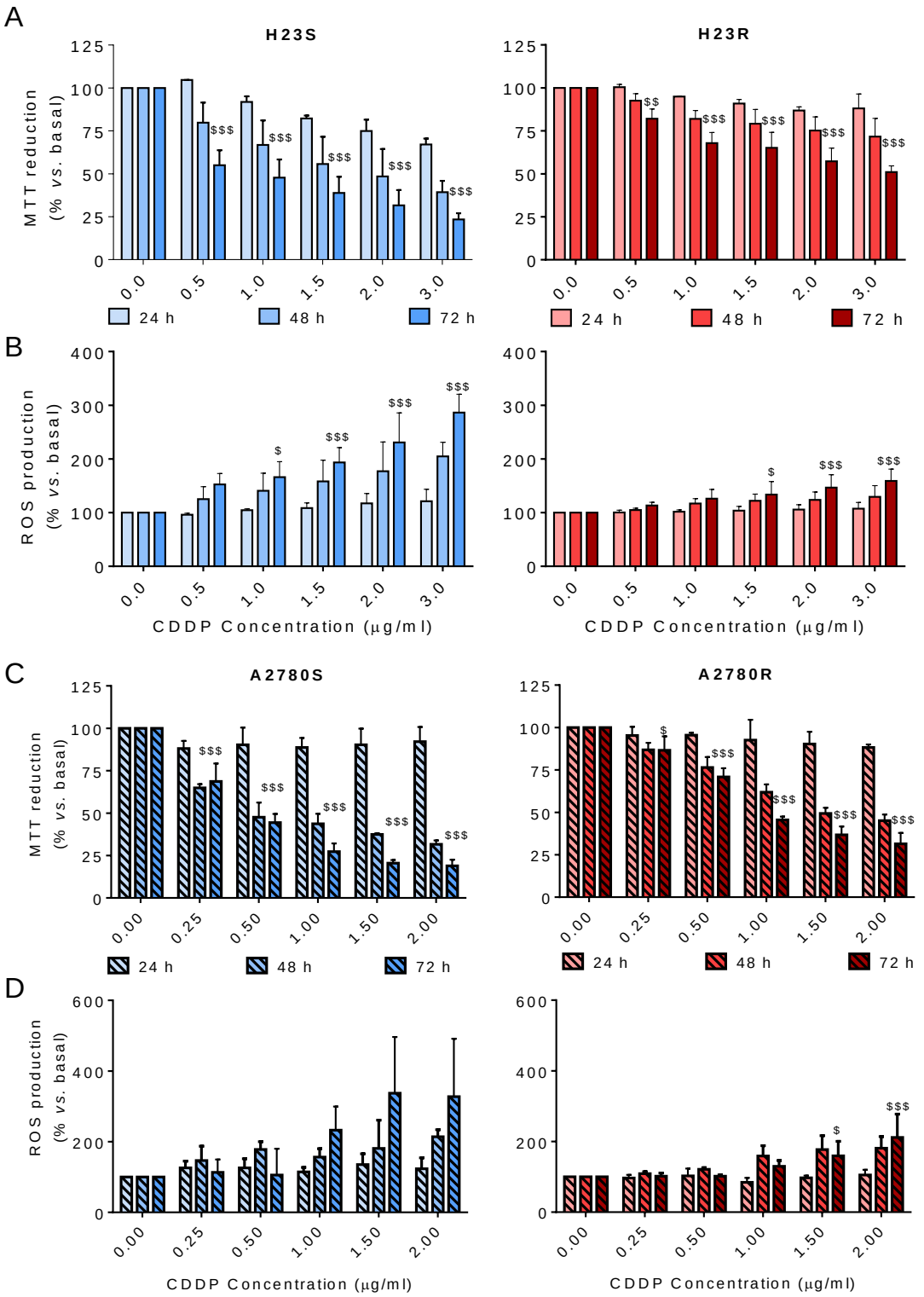

Figure 17. Viability assays and reactive oxygen species detection after CDDP treatment in H23 cell lines. (A and C) Viability to CDDP of H23 (A) and A2780 (C) in Sensitive (left) and Resistant (right) at 24, 48 and 72 hours and six concentrations of CDDP measured by MTT assay; (B and D) Increment of ROS production of H23 (B) and A2780 (D) in Sensitive (left) and Resistant (right) after 24, 48 and 72 hours of CDDP treatment; Each bar represents the mean of at least two independent experiments measured by duplicate ± SD. $: p≤0.05 versus basal; $$: p≤0.01 versus basal; $$$: p≤0.001 were considered as significant change in CDDP resistance and ROS production.

Moreover, we found that the expression of ROS-detoxifying genes, such as *HMOX1*, *NQO1*, *GSTO2* or *GPX7* (Table 11), was upregulated in these resistant cell lines ($p<0.05$), according to the gene expression arrays (GEO GSE84201). We selected *HMOX1* for semiquantitative real-time polymerase chain reaction (RT-PCR) expression pattern validation, which showed an increase in expression in resistant *versus* sensitive cells in H23SR and A2780S/R paired cells (Figure 18).

Table 11. Differences in expression of Redox-detoxifying related genes between cisplatin-resistant and sensitive cell lines.

Symbol	ALL RvsS	Lung RvsS	Ovarian RvsS	H23 RvsS	A2780 RvsS	H460 RvsS	OVCAR3 RvsS
HMOX1	1.459	1.292	1.626	1.070	0.369	1.514	2.884
GSTO2	0.777	0.830	0.723	1.965	1.461	-0.305	-0.015
GPX7	1.236	2.112	0.360	4.422	2.069	-0.199	-1.348
GPX1	0.658	0.487	0.830	1.111	-0.091	-0.137	1.751
MOSC1	0.360	0.334	0.386	0.930	-0.203	-0.262	0.975
PXDN	0.822	1.039	0.605	1.044	1.346	2.043	-0.136
GPX5	0.758	0.768	0.748	0.960	0.768	0.576	0.729
GPX4	0.222	0.146	0.299	0.319	-0.004	-0.027	0.601
GSTM3	0.478	-0.606	1.561	-1.059	1.143	-0.152	1.980
PRDX2	0.370	0.531	0.244	1.111	0.463	-0.118	-0.165
GPX3	0.565	0.098	1.032	-0.078	0.870	0.274	1.194
S100A9	1.266	0.091	2.441	-0.387	-0.745	0.568	5.628
GSTM1	0.699	-0.259	1.657	-0.475	0.550	-0.042	2.765
SOD3	0.662	-0.088	1.412	-0.703	0.759	0.526	2.064
GSTM2	0.315	-0.676	1.305	-0.903	1.061	-0.449	1.550
PTGS2	-0.604	-0.248	0.476	-1.688	3.646	1.192	-2.694
MGST1	-0.050	-1.243	1.143	-2.607	1.494	0.122	0.791
NXN	0.308	1.095	-0.478	2.310	-0.506	-0.121	-0.450
NOS3	0.339	0.324	0.355	0.527	0.402	0.121	0.307
LPO	0.534	0.389	0.678	0.902	0.300	-0.123	1.056
TXNRD2	0.134	0.544	-0.276	0.994	-0.404	-0.360	-0.148
NQO1	0.348	0.108	0.589	0.567	0.627	-0.352	0.551
GSTK1	0.206	0.070	0.343	0.300	0.058	-0.161	0.627
GSR	0.249	0.234	0.265	0.264	-0.558	0.204	0.948
HP	0.053	0.638	-0.533	1.216	-1.029	0.061	-0.038
APOE	0.080	0.359	-0.198	0.665	-0.770	0.052	0.374
MGST2	-1.649	-4.126	0.829	-8.084	1.757	-0.169	-0.100
APOA4	1.397	0.962	1.831	1.233	1.571	0.692	2.090
SRXN1	0.072	0.170	-0.026	0.190	-0.076	0.150	0.024
HBA2	0.452	0.556	-0.449	1.044	-1.114	0.312	0.632
SELS	0.116	0.050	0.182	-0.041	0.683	0.140	-0.318
TP53INP1	-0.513	-0.952	-0.073	-2.089	0.630	0.185	-0.777
DUOX2	0.293	0.444	-0.721	0.294	-1.166	0.594	-0.275
HBA1	-0.021	0.068	-0.109	-0.098	-1.082	0.233	0.863
SLC30A1	-0.103	0.062	-0.269	-0.304	-0.772	0.210	0.354
TXNRD1	-0.060	0.127	-0.247	0.019	0.193	0.235	-0.688
SOD2	-0.101	0.259	-0.460	0.000	-0.579	0.517	-0.341
C10orf58	-0.042	-0.093	0.010	-0.363	-0.185	0.177	0.204
MT3	-1.573	-1.108	-2.038	-1.376	-3.690	-0.840	-0.386

Note: Table shows the log Fold Change of those genes that are significantly overexpressed (green) or downregulated (red) in resistant (R) vs sensitive (S). Uncolored cells indicate no significant differences.

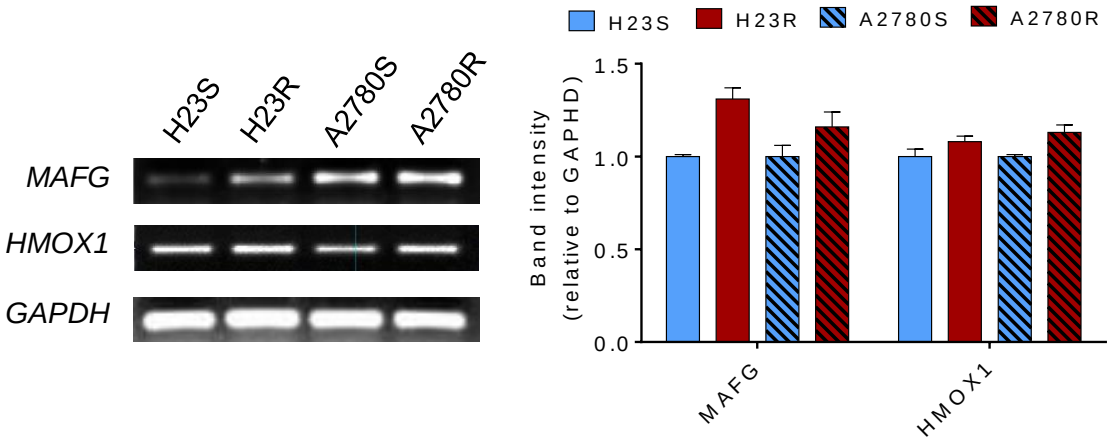

Figure 18. Semi-quantitative mRNA expression analysis of downstream genes involved in ROS detoxification regulated by MAFG, which showed expression changes for H23 and A2780 cell lines identified in the microarray data (GSE84201) (left panel). Representative images of MAFG and HMOX1 RT-PCR comparing sensitive and resistant subtypes. Each assay was performed at least three times to confirm the results. (Right panel) Relative intensity quantification of the amplified band for each gene measured by ImageJ Software. Bars represent the mean of the three independent experiments using the intensity of GAPDH as endogenous control and the sensitive subtype of each cell line as calibrator.

7. Clinical applicability of miR-7 methylation in NSCLC and ovarian cancer

Response rates, overall survival or progression free survival are recommended by ASCO and ESMO Clinical Practice Guidelines Committees to assess the clinical benefit of chemotherapy treatment in cancer (Wright et al., 2016) (Ledermann et al., 2013). In addition, the Ovarian Cancer Consensus Meeting, defines 'platinum-refractory' as patients progressing during therapy or within four weeks after the last dose; 'platinum-resistant' patients progressing within six months of platinum-based therapy; 'partially platinum-sensitive, patients progressing between six and 12 months; and 'platinum-sensitive' patients progressing with an interval of more than 12 months (GCIG Consensus) (Friedlander et al., 2011). Following the international guidelines, we compared the miR-7 methylation levels with the next clinical parameters: progression free survival (PFS) and the associated Overall survival (OS) on two cohorts of 83 and 55 ovarian cancer patients all of them treated with platinum (Table 6 and Figure 19). We studied the OS for all patients and the PFS in those patients that had recurred at the end of the study to analyze the relationship between platinum response and miR-7 methylation.

We observed a 29% of methylation (24 out of 83 samples) in the cohort from Hospital del Mar (Table 12), which increased to 36% (20 out of 55) in the CHUS-HULP biobank samples, a cohort enriched in serous resistant tumors (HGSOC) (Table 13). We also observed a higher percentage of methylation in HGSOC samples from an additional cohort

of patients from the CNIO (50% methylated samples 11 out of 22) (Table 14) and in a small group of additional seven resistant/refractory samples from H. Madrid (57%, four out of seven). We also tested 10 ovarian control samples, a non-tumor cell line (IMR90) and 10 PBMCs to discard imprinting. None of them were methylated (100% specificity) (Figure 19A).

Table 12. Demographic table with the clinicopathological characteristics of a cohort of 83 samples from Hospital del Mar

Characteristics		Complete series (n=83)		Unmethylated (n=59)		Methylated (n=24)		*p*
		No. of patients	%	No. of patients	%	No. of patients	%	
Age (median, range)		55 (17-84)		59 (17-80)		55 (18-84)		0.880
Menopausal status								0.565
	Premenopausal	34	41.0	23	39.0	11	45.8	
	Postmenopausal	49	59.0	36	61.0	13	54.2	
Parity								0.974
	No	24	28.9	17	28.8	7	29.2	
	Yes	59	71.1	42	71.2	17	70.8	
Familiar history								0.684
	No	58	69.9	42	71.2	16	66.7	
	Yes	25	30.1	17	28.8	8	33.3	
ECOG								0.025
	0	21	25.3	20	33.9	1	4.2	
	1	36	43.4	22	37.3	14	58.3	
	2	20	24.1	12	20.3	8	33.3	
	3	6	7.2	5	8.5	1	4.2	
Ascites								0.025
	No	47	56.6	38	64.4	9	37.5	
	Yes	36	43.4	21	35.6	15	62.5	
Tumor Grade								0.35
	I	34	41	27	45.8	7	29.2	
	II	24	28.9	15	25.4	9	37.5	
	III	25	30.1	17	28.8	8	33.3	
Histology								0.883
	Serous	40	48.2	27	45.8	13	54.2	
	Mucinous	9	10.8	7	11.9	2	8.3	
	Clear cell	8	9.6	5	8.5	3	12.5	
	Endometroid	4	4.8	3	5.1	1	4.8	
	Others	22	26.5	17	28.8	5	20.8	
Chemotherapy								0.956
	Adjuvant	59	71.1	43	72.9	16	66.7	
	Neoadjuvant	6	7.2	3	5.1	3	12.5	
	Metastatic	18	21.7	13	22.0	5	20.8	
Platinum sensitivity								0.196
	Sensitive	21	63.6	15	71.4	6	50.0	
	Resistant	12	36.4	6	28.6	6	50.0	
Relapse								0.286
	No	49	59.0	37	62.7	12	50.0	
	Yes	34	41.0	22	37.3	12	50.0	
Death								0.119
	No	49	59	38	64.4	11	45.8	
	Yes	34	41	21	35.6	13	54.2	

Table 13. Clinicopathological characteristics in 55 patients from IDIS-CHUS/HULP biobank with ovarian cancer.

	Complete Series (n=55)		Unmethylated (n=35)		Methylated (n=20)		
Characteristics	No. of Patients	%	No. of Patients	%	No. of Patients	%	*p*
Type							0.520
Adenocarcinoma	23	41.8	15	42.9	8	40.0	
Carcinoma	19	34.5	10	28.6	9	45.0	
Cystadenocarcinoma	12	21.8	9	25.7	3	15.0	
Undetermined	1	1.8	1	2.9	0	0.0	
Tumor Grade							0.483
I	5	9.1	2	5.7	3	15.0	
II	13	23.6	9	25.7	4	20.0	
III	13	23.6	7	20.0	6	30.0	
Undetermined	24	43.6	17	48.6	7	35.0	
Histology							0.125
Serous	30	54.5	19	54.3	11	55.0	
Mucinous	3	5.5	1	2.9	2	10.0	
Endometrioid	8	14.5	7	20.0	1	5.0	
Clear Cell	3	5.5	1	2.9	2	10.0	
Other	11	20.0	7	20.0	4	20.0	
Chemotherapy							0.474
Platinum+Taxane	37	67.3	23	65.7	14	70.0	
Platinum+CTX	8	14.5	7	20.0	1	5.0	
Platinum	3	5.5	1	2.9	2	10.0	
Other	3	5.5	2	5.7	1	5.0	
No	4	7.3	2	5.7	2	10.0	
Platinum Sensitivity							0.625
Sensitive	20	36.4	12	34.3	8	40.0	
Refractory/Resistant	26	47.3	16	45.7	10	50.0	
Undetermined	9	16.4	7	20.0	2	10.0	
Relapse							0.436
No	17	30.9	13	37.1	4	20.0	
Yes	29	52.7	19	54.3	10	50.0	
Death				0.0		0.0	0.438
No	23	41.8	16	45.7	7	35.0	
Yes	32	58.2	19	54.3	13	65.0	

Table 14 . Clinicopathological characteristics in 22 patients from National Cancer Research Center (CNIO) biobank with HGS ovarian cancer.

	Complete Series (n=22)		Unmethylated (n=11)		Methylated (n=11)		
Características	No. of Patients	%	No. of Patients	%	No. of Patients	%	*P*
Age (mean)	58.6		55.1		62.1		0.236
Familial Type							
Familial	7	31.2	5	45.5	2	18.2	0.360
Sporadic	15	68.2	6	54.5	9	81.8	
Grade							
I	3	13.6	1	9.1	2	18.2	0.070
II	4	18.2	0	0.0	4	36.4	
III	9	40.9	6	54.5	3	27.3	
IV	3	13.6	3	27.3	0	0.0	
Undetermined	3	13.6	1	9.1	2	18.2	
Relapse							
No	7	31.8	3	27.3	4	36.4	0.990
Yes	15	68.2	8	72.7	7	63.6	
Death							
No	11	50.0	4	36.4	7	63.6	0.394
Yes	11	50.0	7	63.6	4	36.4	

When correlating our results with the patient's clinical histories we obtained significant data correlating methylation and cisplatin response in the group of 33 patients that recurred. Kaplan-Meier curves show that patients relapsing before 10 months, carried preferentially methylated miR-7 tumors (80% methylated *versus* 14% unmethylated) (Figure 19B) (p=0.004). No differences were found in CDDP-refractory and resistant patients. Moreover, after three years of follow up over the 83 patients cohort, the overall survival was significantly higher in the group of patients with an unmethylated tumor in comparison with those with a methylated one (67% vs 35%, p=0.004) (Figure 19C). Similar results showing a tendency in terms of PFS and OS were also observed in the CHUS-HULP biobank cohort, although these last results were not statically significant mainly because of a size-limitation (Figure 19D and 19E).

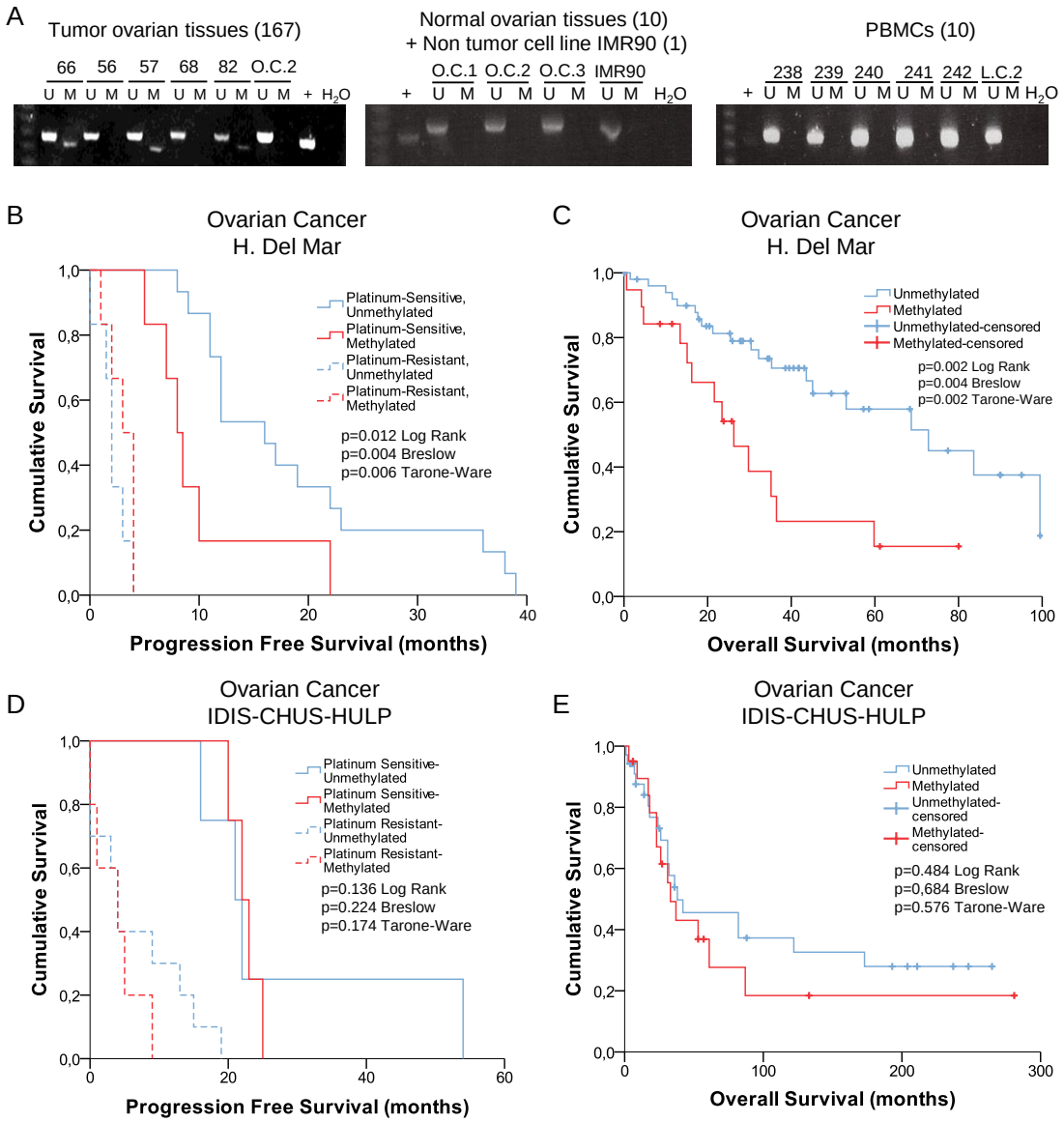

Figure 19. miRNA-7 methylation analysis in ovarian primary tumors and survival analysis. (A) Representative MSPs of miR-7 nearby CGI in DNA obtained from ovarian tumor tissues, normal ovarian tissues, non tumor cell line and PBMCs from healthy donors. For each sample, the PCR product in the M lane was considered as the presence of methylated DNA, whereas the amplification product in the U lane was considered as the presence of unmethylated DNA. In vitro methylated DNA was used as a positive control (+). (B) to (E) Kaplan-Meier comparison between cisplatin treatment and miR-7 proximal island methylation in ovarian cancer patients treated with platinum in terms of progression free survival (B and D) and overall survival in months (C and E). LogRank, Breslow and Tarone-Ware tests were used for comparisons and p<0.05 was considered as a significant change in OS or PFS. p values in (B) represent the significant difference between sensitive-unmethylated and sensitive-methylated patients.

Finally, we observed a decrease in the number of patients with higher ECOG status when the promoter region of miR-7 was unmethylated in the higher cohort of patients (p=0.025). Accordingly, 62.5% of the patients who harbored the methylated promoter presented ascites compared with 80% of the patients who did not develop ascites harboring an unmethylated promoter region (p=0.025) (Table 12). Those results indicate that patients

carrying an unmethylated sample tended to have less aggressive tumors, with better progression free survival after platinum treatment and overall survival rates than those who carried the methylated DNA.

To determine whether miR-7 methylation was also a frequent event in human lung primary tumors and was not limited or more common in tumor cell lines, we performed a methylation-specific PCR (MSP) analysis of 75 primary NSCLC tumors of the more common histologic cell types (adenocarcinoma and epidermoid carcinoma) from two different cohorts of patients belonging to La Paz University Hospital (Madrid) and Hospital del Mar (Barcelona). We first included 36 primarily organ-confined (stage I or II) NSCLC tumors in the study (Table 15), in which the response to CDDP had previously been measured *in vitro* (Ibanez de Caceres et al., 2010). We completed the analysis with a second cohort of 39 specimens from patients (Table 16), including late stages with a complete clinical history that we have recently published (Pernia et al., 2014).

Table 15. Clinicopathological characteristics in 36 patients from La PAZ University Hospital-NSCLC.

	Complete series (n=36)		Unmethylated (n=15)		Methylated (n=21)		
Characteristics	No. Of patients	%	No. Of patients	%	No. Of patients	%	p
Age (mean, range)	66 (49-79)		66 (54-79)	41.7	65 (49-79)	58.3	0.64
Gender							0.99
Male	34	94.4	14	93.3	20	95.2	
Female	2	5.6	1	6.7	1	4.8	
Histology							0.22
Adenocarcinoma	10	27.8	5	33.3	5	23.8	
Epidermoid carcinoma	22	61.1	10	66.7	12	57.1	
Large Cell	4	11.1	0	0.0	4	19.0	
Stage							
I	21	60.0	7	50.0	14	66.7	0.37
II	13	37.1	7	50.0	6	28.6	
III	1	2.9	0	0.0	1	4.8	
CDDP response							0.49
Sensitive	18	50.0	9	60.0	9	42.9	
Resistant	18	50.0	6	40.0	12	57.1	
Relapse							0.44
No	27	75.0	10	66.7	17	81.0	
Yes	9	25.0	5	33.3	4	19.0	
Death							0.99
No	24	66.7	10	66.7	14	66.7	
Yes	12	33.3	5	33.3	7	33.3	

Table 16. Clinicopathological characteristics in 39 patients witH NSCLC from Hospital del Mar.

Characteristics	Complete series (n=39)		Unmethylated (n=17)		Methylated (n=22)		
	No. Of patients	%	No. Of patients	%	No. Of patients	%	p
Age (mean, range)	63 (47-79)		63 (50-75)	43.6	64 (47-79)	56.4	0.78
Gender							0.63
Male	34	87.2	14	82.4	20	90.9	
Female	5	12.8	3	17.6	2	9.1	
Smoking		0.0					0.81
Smoker	19	48.7	8	47.1	11	50.0	
Ex-smoker	15	38.5	6	35.3	9	40.9	
Non-smoker	5	12.8	3	17.6	2	9.1	
Histology		0.0					0.68
Adenocarcinoma	24	61.5	9	52.9	15	68.2	
Epidermoid carcinoma	12	30.8	6	35.3	6	27.3	
Large Cell	2	5.1	1	5.9	1	4.5	
BAC	1	2.6	1	5.9	0	0.0	
Stage		0.0					0.63
I	8	20.5	3	17.6	5	22.7	
II	10	25.6	4	23.5	6	27.3	
III	19	48.7	10	58.8	9	40.9	
Chemotherapy		0.0					0.34
CDDP-Vinorelbine	23	59.0	11	64.7	12	54.5	
CBDCA-Vinorelbine	6	15.4	2	11.8	4	18.2	
CDPP-Gemcitabine	6	15.4	1	5.9	5	22.7	
CBDCA-Paclitaxel	4	10.3	3	17.6	1	4.5	
Radiotherapy		0.0					0.99
Yes	13	33.3	6	35.3	7	31.8	
No	26	66.7	11	64.7	15	68.2	
Death							0.52
No	21	53.8	8	47.1	13	59.1	
Yes	18	46.2	9	52.9	9	40.9	

Abbreviations: BAC, Bronchioalveolar carcinoma CDDP, Cisplatin; CBDCA, Carboplatin.

We found a similar and very high miR-7 percentage of methylation between both cohorts: 21 out of 36 and 22 out of 39, 58% and 56%, respectively. We then compared these results with 10 emphysema samples that are traditionally considered normal tissues for this disease; however, the assessment of these samples showed also a high rate of methylation for this miRNA (50%). In contrast, no hypermethylation was observed in control DNA obtained from lung samples from patients with other nonrespiratory diseases. A representative selection of the MSP results in shown in Figure 20A. No significance was found in terms of stage, sex, histology, therapy response or overall survival in both lung cancer cohorts (Figure 20B-E).

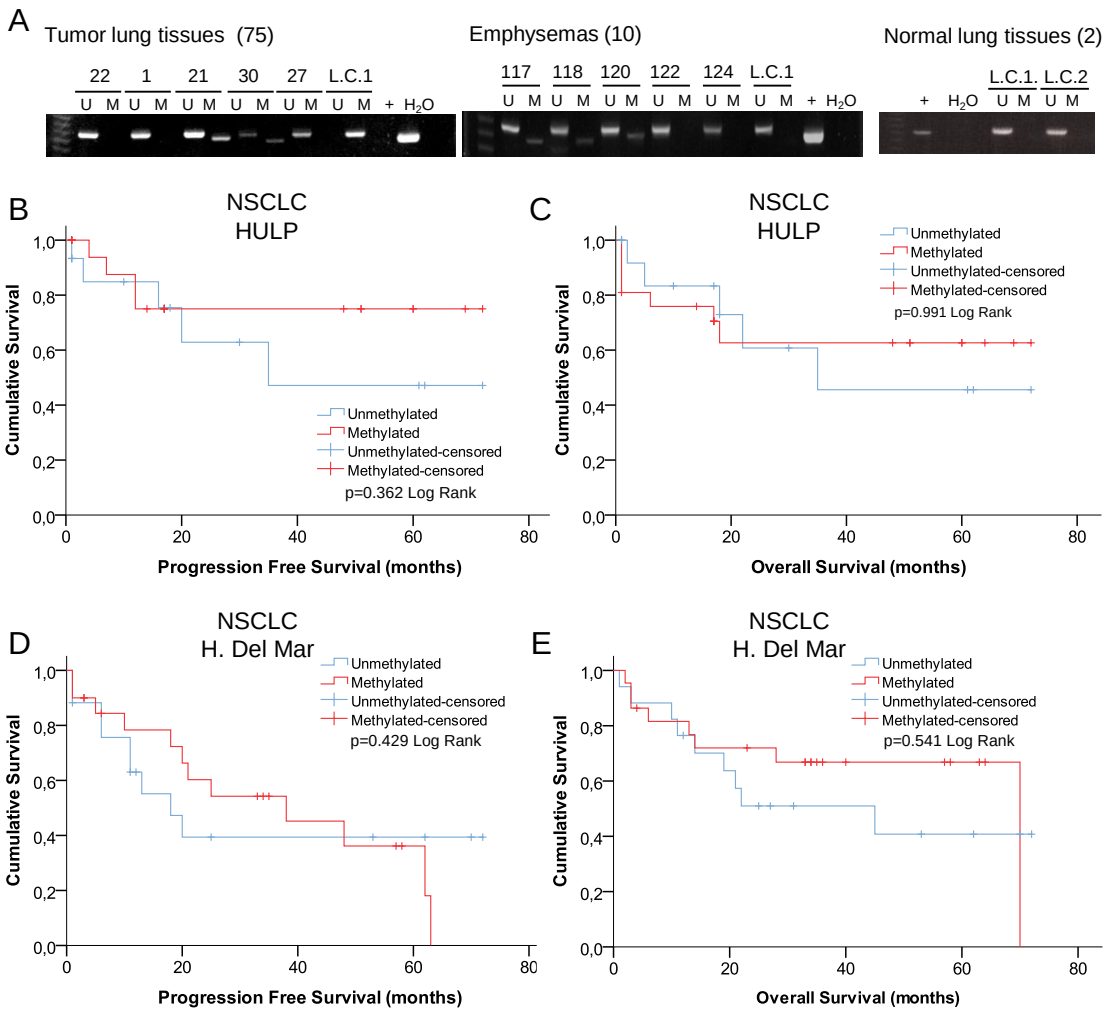

Figure 20. miRNA-7 methylation analysis in primary tumors of NSCLC patients and survival analysis. (A) Representative MSPs of miR-7 nearby CGI in DNA obtained from NSCLC tumor tissues, emphysemas and normal lung tissues from healthy donors. For each sample, the PCR product in the M lane was considered as the presence of methylated DNA, whereas the amplification product in the U lane was considered as the presence of unmethylated DNA. In vitro methylated DNA was used as a positive control (+). (B) to (E) Kaplan-Meier comparison between miR-7 proximal island methylation status in NSCLC patients in terms of progression free survival (B and D), and overall survival in months (C and E). LogRank test was used for comparisons and p<0.05 was considered as a significant change in OS or PFS.

8. Clinical applicability of *MAFG* in NSCLC and ovarian cancer

To explore the involvement of the miR-7/MAFG axis in primary tumors, we first analyzed the quantitative DNA methylation levels of miR-7 and RNA expression levels of miR-7 and *MAFG* in a cohort of 22 paired samples from fresh frozen tumors (T) and adjacent-tumor tissue (ATT) from patients with NSCLC (Table 17). We also interrogated the cohort of 55 fresh frozen tumors from ovarian cancer patients from IDIS-CHUS/HULP

described previously (Table 6 and Table 13). Ten tubal ligation and five normal saliva samples were used as controls.

Table 17. Clinicopathological data and hypermethylation frequency of 22 patients with NSCLC from La Paz University Hospital

						miR-7 methylation		miR-7 expression		MAFG expression				
Patient	Sex	Age, years	Histology	Stage	Chemotherapy	ATT (%)	T (%)	ATT ($2^{-\Delta Ct}$)	T ($2^{-\Delta Ct}$)	ATT ($2^{-\Delta Ct}$)	T ($2^{-\Delta Ct}$)	Last Contact	Status	Overall Survival, months
1	Female	56	Adenocarcinoma	IA	No	58.49	NA	0.50	0.19	0.62	0.43	18/05/2015	Alive	37
2	Male	69	Epidermoid	IB	No	5.63	5.35	1.71	2.61	0.65	0.53	15/10/2014	Exitus	34
3	Male	71	Adenocarcinoma	IB	No	14.98	13.12	1.16	0.31	0.59	0.28	01/08/2011	Exitus	1
4	Male	79	Adenocarcinoma	NA	No	12.47	26.06	1.11	0.51	0.43	4.37	21/03/2013	Exitus	20
5	Male	74	Large Cell	IIB	No	9.20	12.69	0.80	0.34	0.28	0.29	25/11/2011	Exitus	3
6	Male	62	Adenocarcinoma	IIIA	Other	7.28	3.74	2.33	0.38	0.31	2.12	10/11/2011	Exitus	8
7	Female	63	Epidermoid	IB	CDDP-other	8.47	5.69	1.65	1.77	0.58	0.05	29/04/2011	Exitus	7
8	Female	41	Adenocarcinoma	IIA	CDDP-other	8.37	28.94	0.70	2.42	0.91	0.13	17/09/2016	Alive	56
9	Male	86	Epidermoid	IB	No	9.41	8.09	1.07	1.17	5.59	0.29	04/05/2016	Alive	53
10	Male	58	Adenocarcinoma	IA	No	8.19	38.79	1.00	0.09	1.00	0.04	30/08/2011	Exitus	7
11	Female	61	Adenocarcinoma	IIIA	CBDCA-others	6.51	6.08	0.99	5.83	1.91	0.20	07/07/2016	Alive	53
12	Male	62	Epidermoid	IB	CDDP-other	7.59	30.28	0.92	0.75	2.24	0.81	18/03/2016	Alive	52
13	Male	79	Epidermoid	IIA	No	12.44	NA	0.77	1.51	0.70	0.09	07/11/2012	Exitus	10
14	Male	81	Epidermoid	IIA	No	12.66	10.98	2.21	2.07	0.73	0.84	01/01/2012	NA	4
15	Female	66	Adenocarcinoma	IIIA	CDDP-other	4.72	3.57	0.73	0.32	0.76	0.49	10/11/2016	Alive	57
16	Male	74	Adenocarcinoma	IIB	Other	35.35	10.00	0.80	0.31	1.03	0.78	06/08/2013	Exitus	29
17	Male	84	Epidermoid	IIB	CBDCA-others	8.24	53.19	1.35	1.05	0.57	0.03	10/12/2011	NA	9
18	Female	55	Adenocarcinoma	IB	CDDP-other	10.29	9.42	1.19	2.86	0.38	1.52	23/04/2014	Exitus	31
19	Male	57	Epidermoid	IIB	CDDP-other	13.67	9.52	1.50	2.87	0.99	0.50	27/05/2014	Exitus	40
20	Male	74	Epidermoid	IIIB	CBDCA-others	4.06	13.45	0.80	1.33	0.22	0.43	01/09/2012	NA	20
21	Male	65	Adenocarcinoma	IIIA	CDDP-other	9.55	63.07	1.14	0.65	1.11	2.57	25/03/2013	NA	14
22	Female	35	Adenocarcinoma	IIB	CDDP-other	4.43	6.84	0.50	2.07	0.26	2.35	27/11/2012	NA	18

Abbreviations: ATT, Adjacent Tumor Tissue; T, Tumor; CDDP, cisplatin; CBDCA, carboplatin; NA, Not Available

We observed an increase in the data dispersion for both tumor types *versus* the non-tumor samples, in miR-7 methylation and expression levels (Table 18). Moreover, there is a higher percentage of methylation levels (17.95% vs 2.3%, p=0.00001), and a lower miR-7 expression (1.43 vs 14.2, p=0.0001), in the NSCLC samples than in the ovarian ones. As expected, *MAFG* expression was higher in the NSCLC tissues compared to ovarian ones (0.9 vs 0.2, p=0.0001) (Figure 21). The higher dispersion was statistically significant in NSCLC groups only when compared with saliva samples from healthy donors (p=0.0002) (Figure 21A and Table 18).

Table 18. Comparison of methylation and expression levels among a cohort of 22 paired samples from patients with NSCLC and 55 samples from patients with ovarian cancer.

	miR-7 methylation (%)					
	Mean	**Median**	**Minimum**	**Maximum**	**Dispersion**	**p-value (Student's t-test)**
Saliva samples	0.54	0.69	0.18	0.88	0.7	0.0002 (Saliva vs ATT)
ATT (NSCLC)	12.36	8.83	4.06	58.5	54.44	.22 (ATT vs T)
Tumor (NSCLC)	17.95	10.49	3.57	63.08	59.5	0.0002 (Saliva vs T)
Tubal Ligation	1.31	1.10	0.03	3.23	3.20	0.5196 (Tubal vs Ovarian cancer)
Ovarian Tumors	2.31	0.13	0.01	70.30	70.29	

	miR-7 Expression ($2^{-\Delta Ct}$)					
	Mean	**Median**	**Minimum**	**Maximum**	**Dispersion**	**p-value (Student's t-test)**
ATT (NSCLC)	1.13	1.03	0.5	2.33	1.83	-
Tumor (NSCLC)	1.43	1.11	0.09	5.83	5.74	.34 (ATT vs T)
Tubal Ligation	29.03	23.93	6.24	75.74	69.51	0.02 (Tubal vs OvCa)
Ovarian Tumors	14.25	6.64	0.15	89.50	89.35	

	MAFG Expression ($2^{-\Delta Ct}$)					
	Mean	**Median**	**Minimum**	**Maximum**	**Dispersion**	**p-value (Student's t-test)**
ATT (NSCLC)	0.99	0.68	0.22	5.59	5.38	-
Tumor (NSCLC)	0.87	0.46	0.03	4.37	4.34	0.7146 (NT vs T)
Tubal Ligation	0.18	0.15	0.02	0.37	0.35	0.8205 (Tubal vs OvCa)
Ovarian Tumors	0.19	0.10	0.00	1.25	1.25	

Note: p<0.01 was considered as statistically significant changes between the groups compared (Student's t-test). ATT, Adjacent Tumor Tissue; T, Tumor.

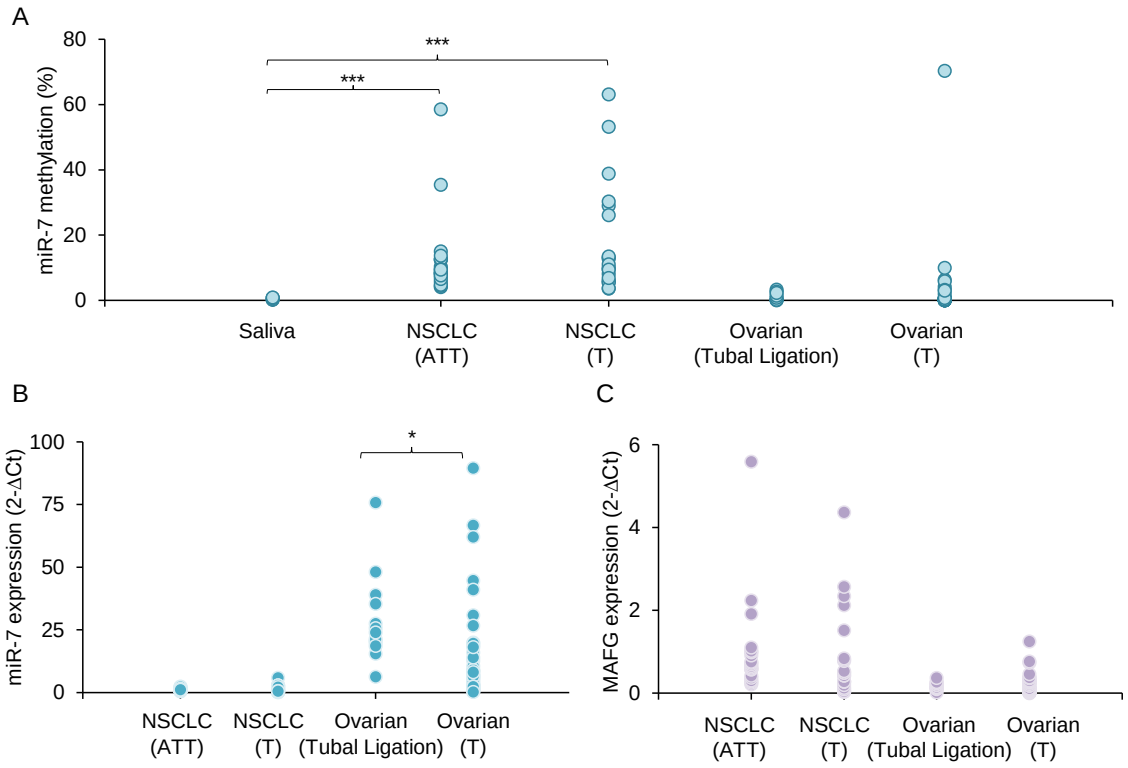

Figure 21. Involvement of miR-7 and MAFG in patients with NSCLC and ovarian cancer. Assessment of miR-7 methylation levels measured by qMSP (A) and expression levels of miR-7 (B) and MAFG (C) measured by qRT-PCR in fresh samples from a cohort of 22 patients with NSCLC and a cohort of 55 patients with ovarian cancer. Saliva and Tubal ligations were used as reference. ATT, Adjacent Tumor Tissue; T, Tumor. Asterisks are indicating the level of significance for each comparison according to table 22.

A negative correlation between the percentage of methylation and expression levels of miR-7 was found only in the T samples (Figure 22A). The opposite tendency was found, towards more expression of *MAFG* in T samples, when the percentage of miR-7 methylation increased (Figure 22B). Interestingly, the two samples that showed the highest dispersion for *MAFG* expression presented a miR-7 methylation level over 20%. No correlation or tendency was found in tubal ligation or ovarian cancer samples (Figure 22C and 22D).

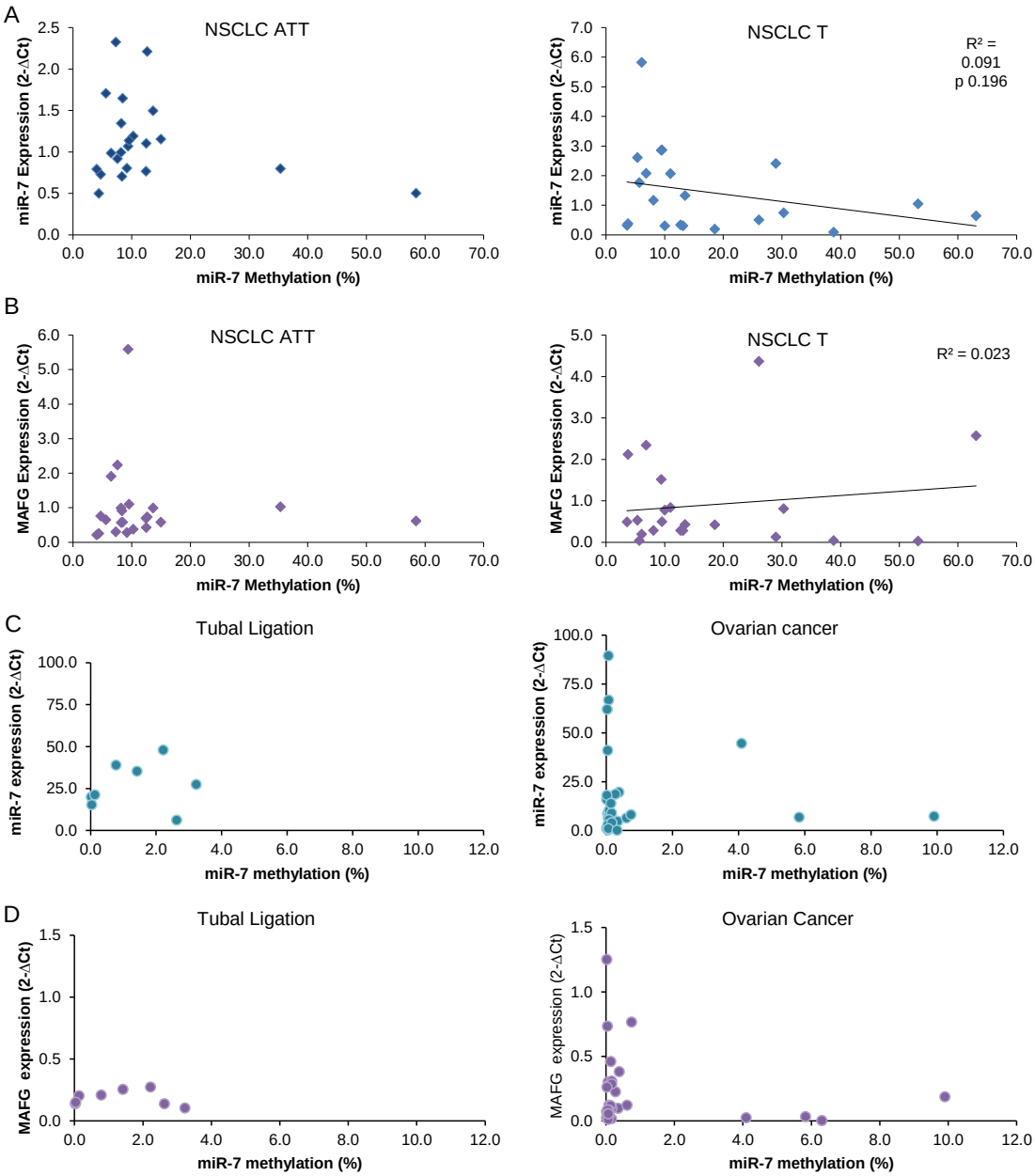

Figure 22. In vivo relationship between miR-7 and MAFG in patients with NSCLC and ovarian cancer. (A and C) Correlation between the methylation percentage of miR-7 and expression levels of miR-7 in 22 NSCLC ATT samples (A left) and Tumor (A, right) and 55 ovarian cancer samples (C, right) and controls (C, left). (B and D) Correlation between the methylation percentage of miR-7 and expression levels of MAFG in 22 NSCLC ATT samples (B left) and paired Tumors (B, right) and 55 ovarian cancer samples (D, right) and controls (D, left). For all the analyses, data represents the percentage of methylation according to a previous report (Eads et al., 2000) and expression levels in $2^{-\Delta Ct}$.

To determine whether *MAFG* expression correlated with clinical outcome in patients with NSCLC and ovarian cancer, we investigated the gene expression levels in 984 and 312 patients with NSCLC and ovarian cancer, respectively, from the TCGA database. In addition, we interrogated the gene expression of *MAFG* in 1035 and 134 patients with NSCLC and ovarian cancer, respectively, from the Total Cancer Care Biorepository at the Moffitt Cancer Center. When comparing data from both datasets, we observed statistical significance

according to the median level of *MAFG* expression in the group of NSCLC patients; patients with low expression levels had a clearly increased overall survival compared with the group of patients with high *MAFG* expression levels, with p-values of 0.020 and 0.011 for both cohorts, respectively (Figure 23A). We did not observed any significant differences between high or low expression of *MAFG* in ovarian cancer patients (Figure 23B)

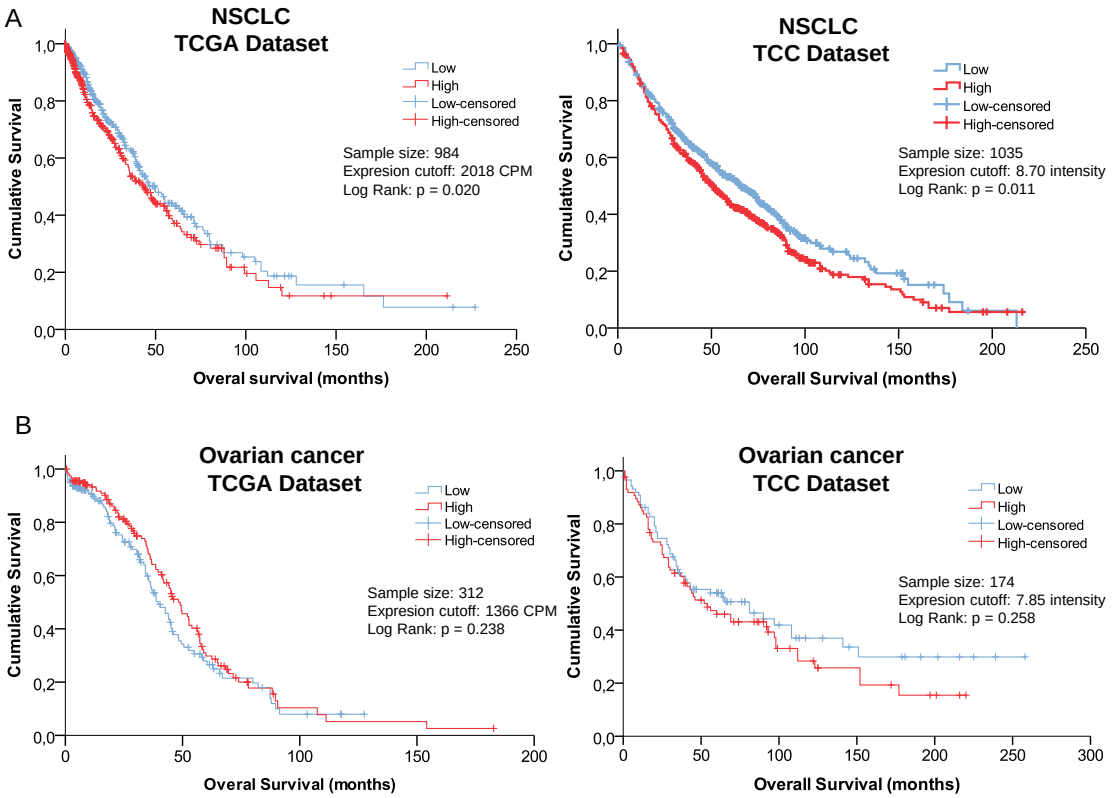

Figure 23. In silico analysis of mRNA expression of MAFG in two cohorts of patients with NSCLC and two cohorts of patients with ovarian cancer. (A) Survival analysis in 984 (left panel) and 1035 (right panel) NSCLC samples from the TCGA and TCC, respectively. (B) Survival analysis in 312 (left panel) and 174 (right panel) ovarian samples from the TCGA and TCC, respectively. LogRank test was used for comparisons and p<0.05 was considered as a significant change in OS. NSCLC: non-small cell lung cancer; CPM: counts per million; TCGA, The Cancer Genome Atlas; TCC, Total Cancer Care.

9. Approach followed for the epigenetic characterization of lncRNAs in the acquired resistance to cisplatin in lung and ovarian cancer.

In the present thesis we also aimed to gain insight into the epigenetic characterization of a recently discovered group of RNA regulators, the lncRNA. Although their function and the classification begin to be clarified candidate by candidate, still the information we have got from most of them is very poor, Furthermore, there hse not been any global approach to understand their potential epigenetic regulation in cancer nor in response to therapy. Therefore, to identify candidate long non-coding RNAs under epigenetic regulation as an alternative mechanism involved in the response to platinum, we first explored the global

profile of lncRNAs and mRNAs that change their expression after platinum treatment through the analysis of the transcriptome and DNA-methylome of these cancer cell lines (Figure 24).

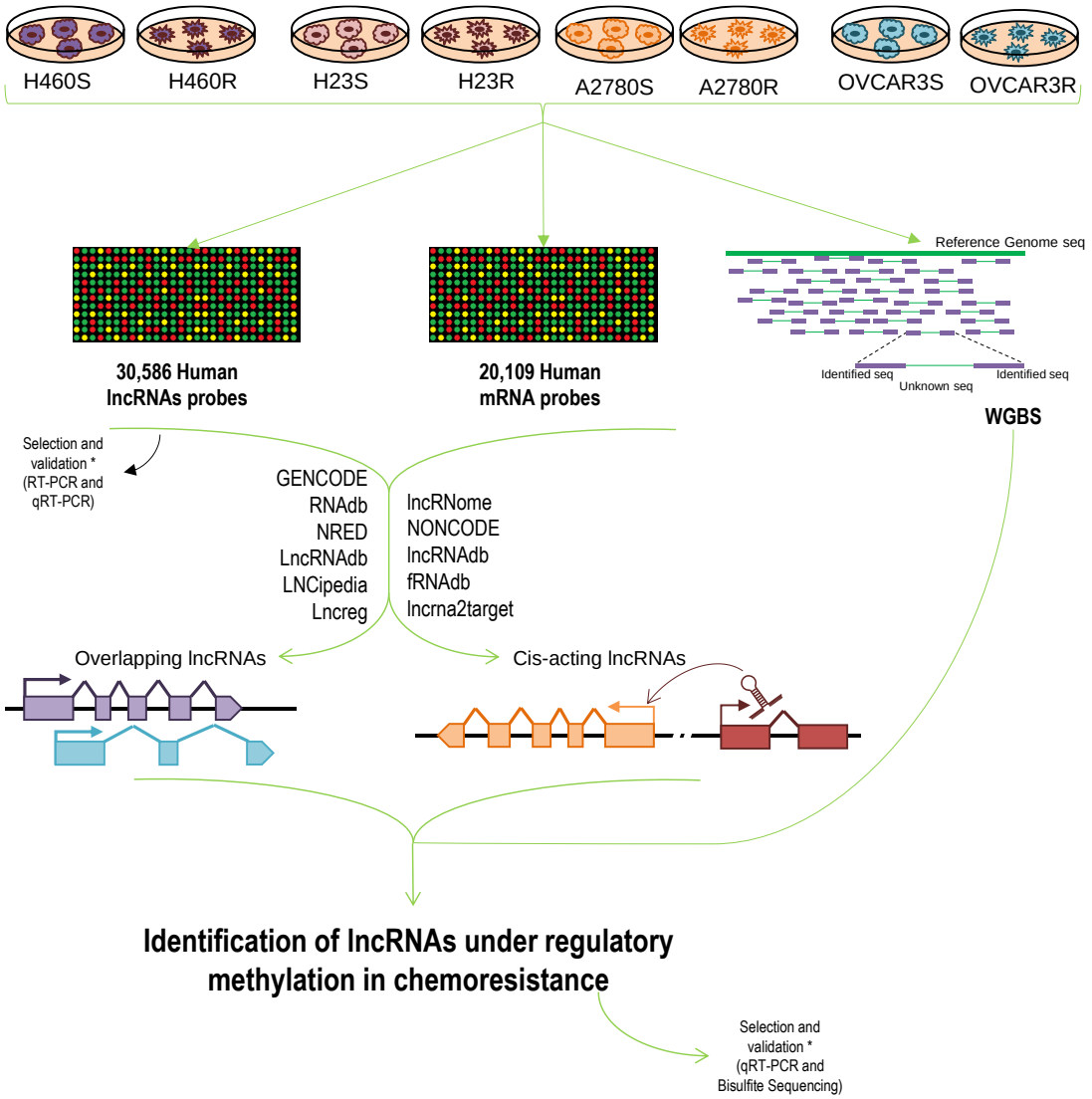

*Figure 24. Experimental design and general overview of expression changes. Pipeline of the steps followed for this study. Arrays combining lncRNAs and mRNAs probes were performed for four paired sensitive/resistant cell lines from lung and ovarian cancer. The threshold for selection was Fold Change ≥1.5. Inclusion of WGBS data was used to identify lncRNAs under epigenetic regulation by DNA methylation. Selection and further validation of lncRNAs was performed to confirm observed changes in expression and methylome analysis. * Fold Change ≥ 1.5*

10. Transcriptome profiling of lncRNAs in the acquired resistance to cisplatin treatment.

All data are based on eight CDDP-sensitive and CDDP-resistant NSCLC (H23S/R and H460S/R) and ovarian cancer (A2780S/R and OVCAR3S/R) cell lines previously established in our laboratory (Ibanez de Caceres et al., 2010, Vera et al., 2017) (Figure 2). We generated

a global transcriptome profile of lncRNAs and mRNAs to identify those that had a change in expression levels after the development of platinum resistance.

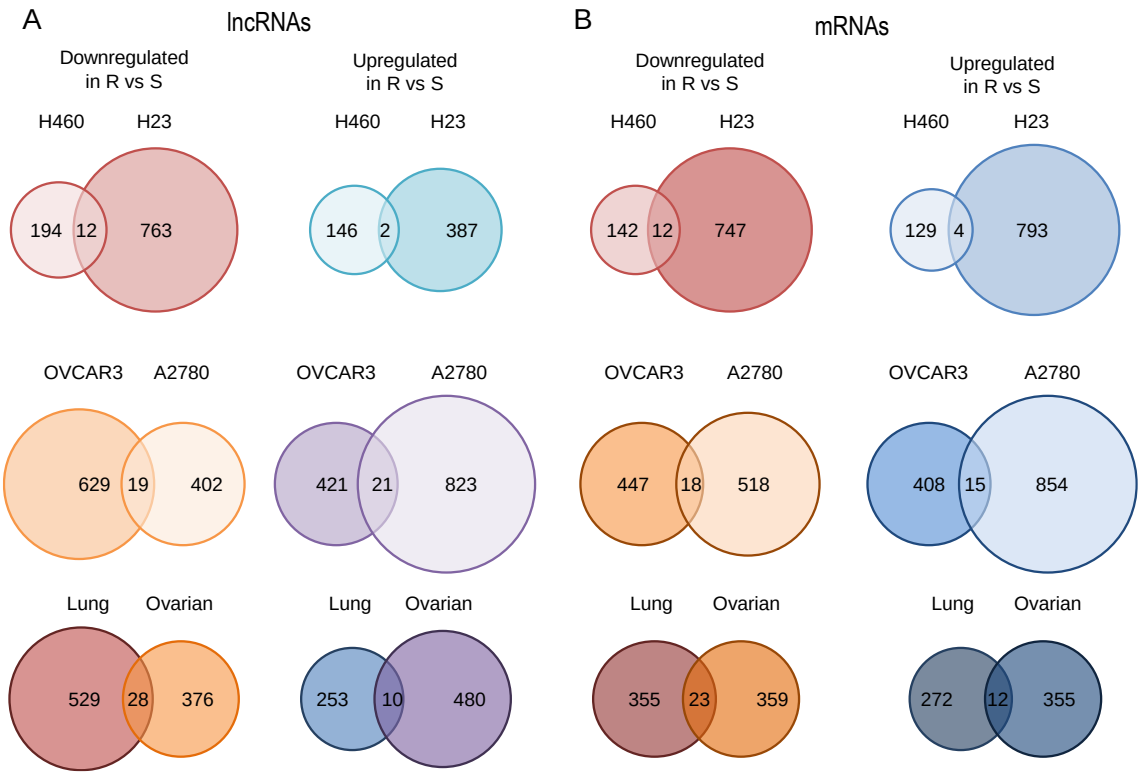

Figure 25. General overview of expression changes. Venn diagrams of shared lncRNAs (A) and mRNAs (B) that change in resistance in both lung cancer cell lines (top), both ovarian cancer cells (middle) or when comparing lung and ovarian cells (bottom).

Among the 30,586 lncRNAs (19,590 intergenic lncRNAs and 10,996 overlapping) and the 20,109 mRNA transcripts interrogated in the platform, we found a percentage of expression changes of approximately 1.5% and 2.0%, respectively, for all the contrasts analyzed, with a Fold Change ≥ 1.5 (Table 19). We also compared the common lncRNAs or mRNAs with detectable changes in expression between sensitive and resistant cell lines and tissue type, and found a similar percentage change (Figure 25A and 25B).

Table 19. Overall view of changes for lncRNAs (left) and mRNAs (right) observed in the arrays.

	lncRNAs				mRNAs			
Contrast	**Downregulated**		**Upregulated**		**Downregulated**		**Upregulated**	
H23R vs H23S	763	2.5%	387	1.3%	747	2.9%	793	3.0%
H460R vs H460S	194	0.6%	146	0.5%	142	0.5%	129	0.5%
A2780R vs A2780S	402	1.3%	823	2.7%	518	2.0%	514	2.0%
OVCAR3R vs OVCAR3S	629	2.1%	421	1.4%	447	1.7%	408	1.6%
Lung R vs Lung S	529	1.7%	253	0.8%	355	1.4%	272	1.0%
Ovarian R vs Ovarian S	376	1.2%	480	1.6%	359	1.4%	418	1.6%
All R vs All S	363	1.2%	257	0.8%	290	1.1%	250	1.0%

We next selected a representative group of 30 lncRNA transcripts to validate the expression changes between resistant and sensitive cells observed in the array analysis by semi-quantitative PCR. Validation was successful in 11 out of 15 downregulated and 14 out of 15 upregulated lncRNAs in the cancer cell lines used for the array (Figure 26A – 26C). We further tested the expression of six transcripts in a selection of two additional paired CDDP-resistant/sensitive cancer cell lines, a different pair A2780/A2780CP and the pair OV2008/OVC13 (Figure 26D). Table 20 summarizes the total lncRNAs analyzed and validated, as well as their associated coding genes.

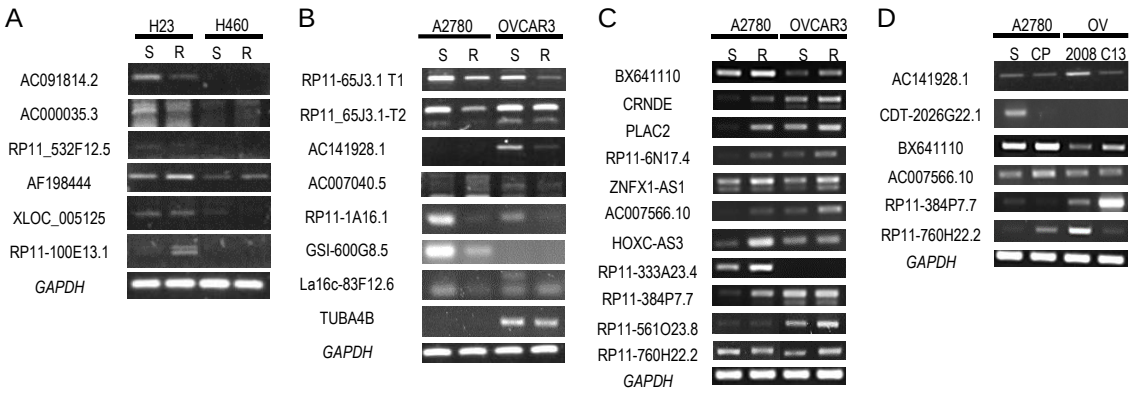

Figure 26. Semi-quantitative validation of lncRNA microarray in a selection of 30 lncRNAs based on statistical terms. Representative images of the downregulated and upregulated lncRNAs that were validated in the resistant subtypes compared with the expression of the sensitive parental cells in the lung cancer model, up and downregulated (A), in the ovarian model downregulated (B) and upregulated (C) and in two additional ovarian cancer cell lines (D). Each assay was performed at least three times to confirm the results.

Table 20. Summary of the selected lncRNAs

Contrast	Cell line	Seq.name	GeneSymbol	Chromosome	Strand	RNA Length	Validation in Original/ Additional Cells	Associated Coding Gene (ACG)
Downregulated	H23	ENST00000412084	AC091814.2	chr12	-	979	H23R	*OLR1*
Downregulated	H23	ENST00000563217	RP11-532F12.5	chr15	-	250	H23R	*DNAJC17*
Downregulated	H23	ENST00000558382	RP11-522B15.3	chr15	+	501	Undetermined	*NR2F2*
Downregulated	A2780	ENST00000423122	RP11-65J3.1-002	chr9	+	545	A2780R & OVCAR3R	*IER5L*
Downregulated	Ovarian	ENST00000444125	RP11-65J3.1-003	chr9	+	783	A2780R & OVCAR3R	*IER5L*
Downregulated	OVCAR3	ENST00000511928	AC141928.1	chr4	-	4525	OVCAR3R/A2780CP & OVC13	*LRPAP1*
Downregulated	OVCAR3	ENST00000449073	AC007040.5	chr2	+	625	OVCAR3R	*FIGLA*
Downregulated	A2780R&OVCAR3R	ENST00000556071	RP11-1A16.1	chr14	+	554	A2780R & OVCAR3R	-
Downregulated	A2780R	ENST00000412485	GS1-600G8.5	chrX	-	1497	A2780R	*EGFL6*
Downregulated	OVCAR3R	ENST00000453395	LA16c-83F12.6	chr22	-	624	OVCAR3R	-
Downregulated	OVCAR3R	ENST00000490341	TUBA4B	chr2	+	1380	OVCAR3R	*TUBA4*
Downregulated	A2780R&OVCAR3R	ENST00000529081	CTD-2026G22.1	chr11	+	578	Undetermined/A2780CP	*FOLH1*
Downregulated	A2780R	ENST00000455275	AP001439.2	chr21	+	392	Undetermined	*APP*
Downregulated	A2780R	ENST00000577848	RP11-874J12.4	chr18	+	1455	Undetermined	*DLGAP1*
Downregulated	AllR_vs_All-S	ENST00000419368	AC000035.3	chr22	-	570	H23R & OVCAR3R	*NF2*
Upregulated	H23	uc021sxs.1	AF198444	chr15	+	3890	H23R & H460R	*ALDH1A3*
Upregulated	H23	TCONS_00011636	XLOC_005125	chr6	+	1366	H23R	*FOXC1*
Upregulated	Lung	ENST00000437416	RP11-100E13.1	chr1	-	403	H23R	*CNIH3*
Upregulated	A2780R&OVCAR3R	uc003jsd.1	BX641110	chr5	-	3720	A2780R & OVCAR3R/A2780CP	*PDE4D*
Upregulated	A2780R&OVCAR3R	uc010vhb.2	CRNDE	chr16	-	838	A2780R & OVCAR3R	-
Upregulated	A2780R&OVCAR3R	NR_027064	PLAC2	chr19	-	3693	A2780R & OVCAR3R	*ZNRF4*
Upregulated	A2780R&OVCAR3R	ENST00000577279	RP11-6N17.4	chr17	-	374	A2780R & OVCAR3R	*SP2*
Upregulated	A2780R&OVCAR3R	ENST00000450535	ZNFX1-AS1	chr20	+	1075	A2780R & OVCAR3R	*ZNFX1*
Upregulated	OVCAR3R	ENST00000441539	AC007566.10	chr7	+	395	A2780R & OVCAR3R/A2780CP	*PEX1*
Upregulated	A2780R	ENST00000567780	HOXC-AS3	chr12	-	2816	A2780R	*HOXC10*
Upregulated	A2780R	ENST00000520259	RP11-333A23.4	chr8	+	2367	A2780R	-
Upregulated	A2780R	ENST00000566968	RP11-384P7.7	chr9	+	3528	A2780R/A2780CP	*PRSS3*
Upregulated	OVCAR3R	ENST00000425587	RP11-561O23.8	chr9	+	340	OVCAR3R	-
Upregulated	OVCAR3R	ENST00000574086	RP11-760H22.2	chr8	+	522	OVCAR3R/A2780CP	-
Upregulated	A2780R&OVCAR3R	ENST00000417460	AC003986.7	chr7	+	692	Undetermined	*HDAC9*

Note: Contrast indicates lncRNA changes with statistical significance; seq.name is the transcript name of the lncRNA; GeneSymbol is the name of the lncRNA.

We performed a gene ontology analysis with the described associated coding genes of the 25 validated lncRNAs, which are included into the Arraystar platform. Most of the lncRNA probes included in the array have at least one associated coding gene. Based on this GO analysis we selected 16 lncRNAs due to biological plausibility for their involvement in cancer, or published evidence of a role in cancer, as is the case of CRNDE (Ellis et al., 2012, Graham et al., 2011). We were able to confirm the expression changes by quantitative RT-PCR for six out of seven downregulated (Figure 27A) and eight out of nine upregulated lncRNA candidates (Figure 27B). A summary of the selection process is detailed in Figure 28.

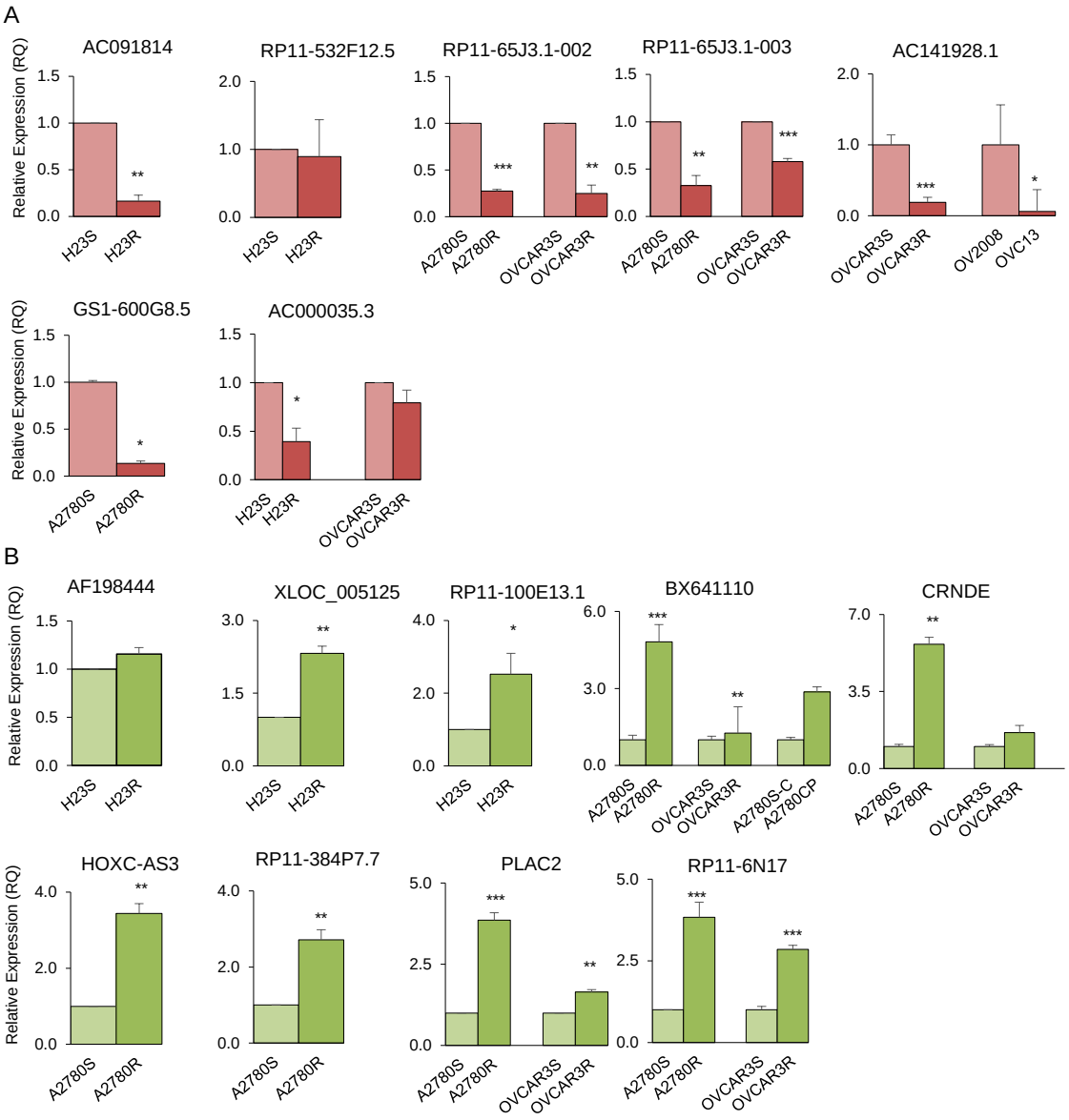

*Figure 27. Quantitative validation of lncRNA microarray expression changes in 15 lncRNAs based on their possible biological implication in cancer. qRT-PCR to confirm the quantitative expression changes of the downregulated (A) and upregulated (B) lncRNAs that were validated in the resistant subtypes compared with the expression of the sensitive parental cells in the lung cancer model (H23S/R and H460S/R), in the ovarian cancer model (A2780S/R and OVCAR3S/R) and two additional ovarian cancer cell lines (A2780S-C/A2780CP and OV2008/OVC13). The data represent the results from at least two different experiments measured by triplicate in Relative Quantification (RQ) scale ± SD. * p < 0.05; ** p < 0.01; *** p < 0.001 (Student's T-test).*

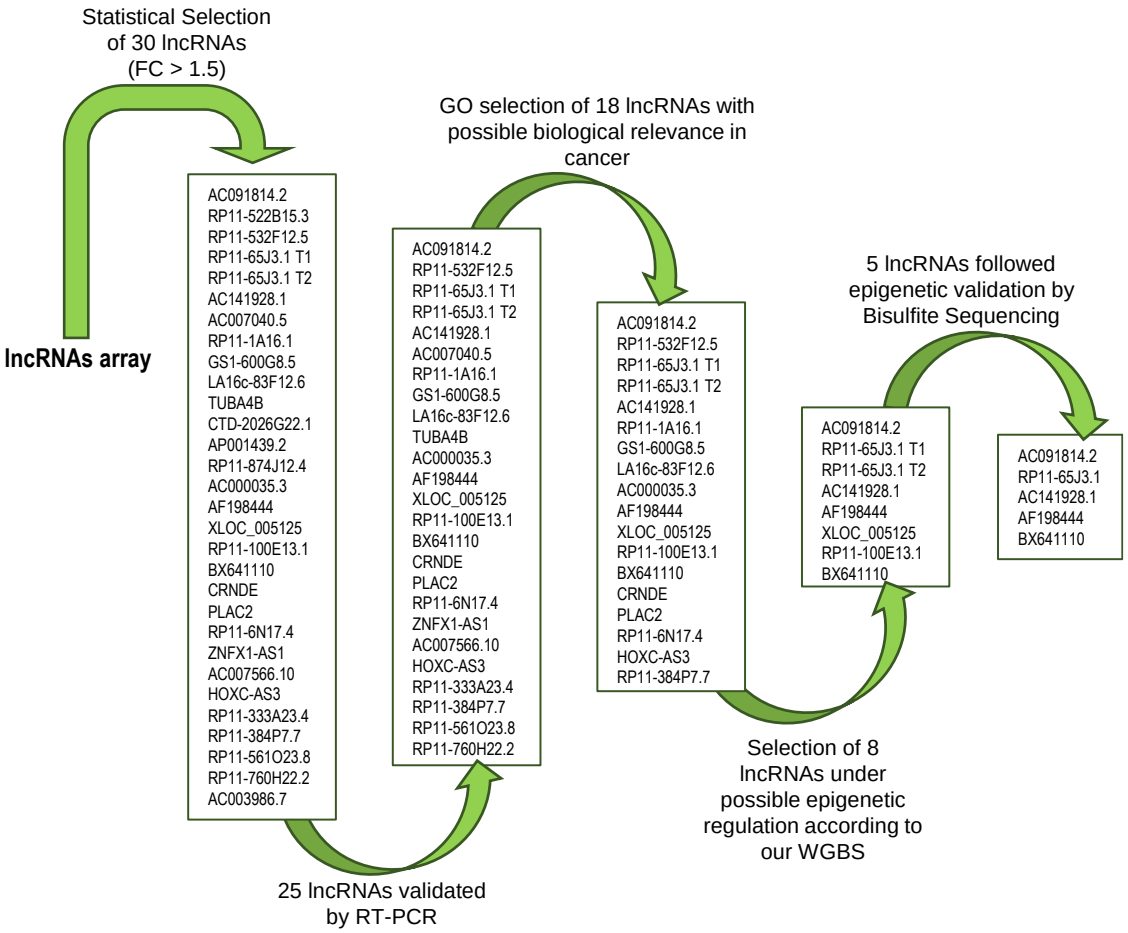

Figure 28. Summary of the selection and validation process followed in to identify lncRNAs under epigenetic validation involved in cancer.

11. Expression of cis-acting lncRNAs is frequently altered in CDDP resistant cells compared with overlapping lncRNAs

Further bioinformatics analyses allowed us to classify the lncRNAs that changed in resistance into two groups according to their relationship with the mRNA of a coding gene (Ma et al., 2013, Wang and Chang, 2011). These analyses included (a) transcript and lncRNA genomic annotations in order to designate their positional relation that could help determine their functional relationship with their possible associated coding gene (ACG) and (b) a restrictive statistical analysis selecting only those lncRNAs and mRNAs with statistically significant changes in expression (Figure 29). Those lncRNAs sharing a genomic location with an ACG and both showing statistically significant expression changes in the array were classified as "overlapping lncRNAs," including sense, antisense and bidirectional lncRNAs. This group was represented by 176 unique lncRNA transcripts, which were associated with 185 unique mRNA transcripts. lncRNAs encoded in the 1 kb – 300 kb

upstream region that did not overlap with another coding gene were included in the "cis-acting lncRNA" group (Guttman and Rinn, 2012, Chen, 2016). This group was represented by 613 lncRNA transcripts interacting with 662 mRNA transcripts (Figure 24). Among the lncRNAs represented on the arrays with known genomic location, the observed vs. expected ratio was increased for cis-acting lncRNA (78% vs. 64%) but decreased for the overlapping lncRNAs (22% vs. 36%). When analyzing the global expression changes from both groups, we observed that the majority of the overlapping lncRNAs showed the same expression pattern as the associated mRNA (Figure 29, top panel). For cis-acting lncRNAs, we observed both similar and opposing expression changes with their associated mRNAs in resistant compared to sensitive cell lines (Figure 29, bottom panel).

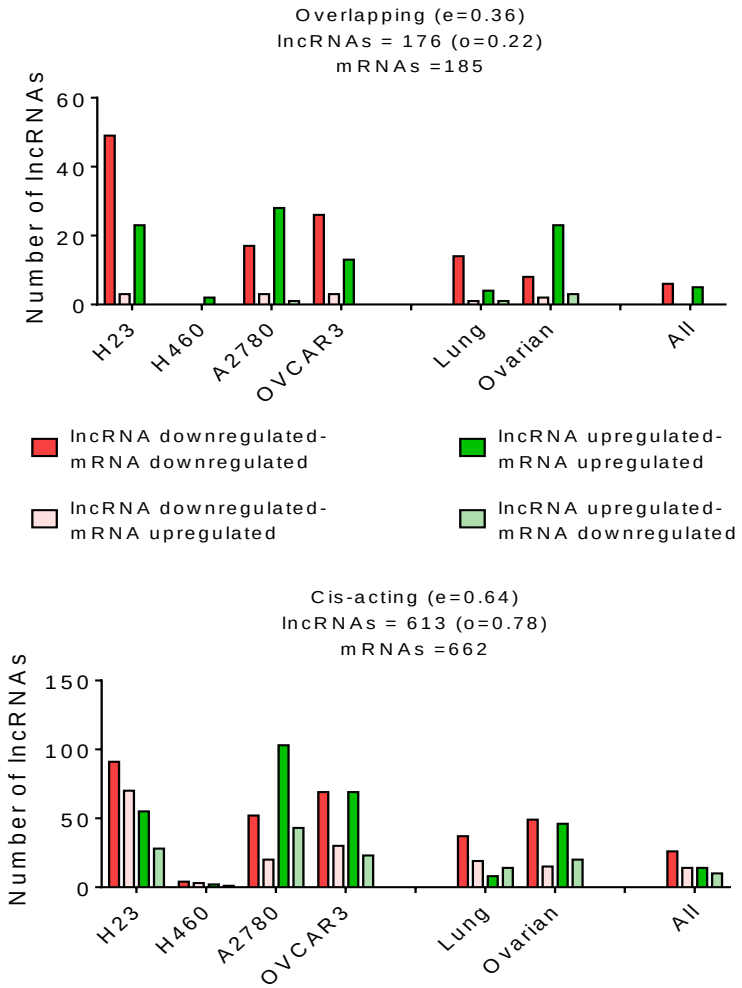

Figure 29. Overall view of the lncRNAs with significant changes in expression between resistant and sensitive cell lines, according to their relationship with the associated mRNA transcript identified in the array. The upper panel represents overlapping lncRNAs, whereas the lower panel represents cis-acting lncRNAs.

12. Presence of CpG islands and associated aberrant methylation are more frequent in overlapping than cis-acting lncRNAs in CDDP resistance

Next, we searched for canonical CpG islands (CGIs) by interrogating the WGBS data obtained from our experimental models, then classified the lncRNAs according to their CpG island position. We first observed that 44 of the 176 overlapping lncRNAs (25%) have a defined CGI for themselves or for their ACG, whereas a defined CGI was found in only 17% (105 of 613) of the cis-acting lncRNAs. It is interesting to highlight that the majority of the overlapping lncRNAs with a defined CGI share this island with their ACG (21%, in green). Those lncRNAs are increased in the downregulated group of lncRNAs (Figure 30A). Only 3% have an exclusive CGI and a small percentage of these lncRNAs (1%) belonged to a group with one CGI for the lncRNA and a different CGI for the ACG (Figure 30A, left bars). Conversely, among the cis-acting lncRNAs there was a small percentage of lncRNAs sharing the CGI with the ACG (1%), with 6% showing an exclusive CGI and the majority represented by lncRNAs that have CGIs different from the CGI of their ACG (10%). This association between the presence or absence of CGIs and the lncRNA location (overlapping or cis-acting) was statistically significant (Chi-square test, p = 0.02).

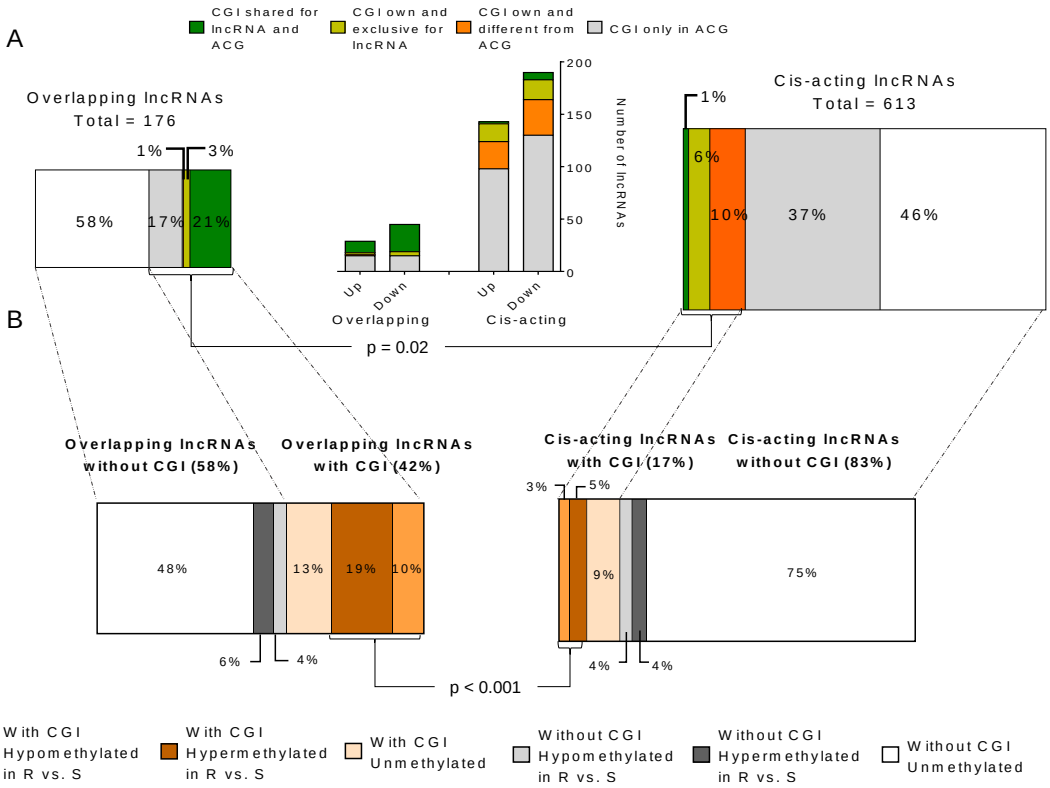

Figure 30. Bioinformatic and in silico analysis of lncRNA epigenetic regulation in resistance. (A) Identification of possible regulatory regions under CpG island methylation and distribution according to overlapping or cis-acting groups. The graphic in the middle represents the number of lncRNAs grouped by expression pattern and according to the location of their CGI. (B) Distribution of the

methylation detected by WGBS in the six possible groups indicated with squares and comparison between cis and overlapping lncRNAs. Chi-squared test was used for statistical analysis and $p < 0.05$ was considered statistically significant.

Thus, to identify whether CGI methylation was associated with the observed changes in lncRNA expression, we divided them into lncRNAs carrying or not a CGI and another group based on where the CGI was located (Figure 31A). For overlapping lncRNAs, we included all the lncRNAs with a possible CGI at their regulatory region or at their ACGs in the first group (Figure 31A, top). For cis-acting lncRNAs, we included only those lncRNAs with a possible CGI in their regulatory region (Figure 31A, bottom). This contrast revealed that the overlapping lncRNAs are similarly represented in both groups, with and without CGIs (42% and 58%, respectively) but cis-acting lncRNAs are richer in lncRNAs without CGIs (17% vs. 83%).

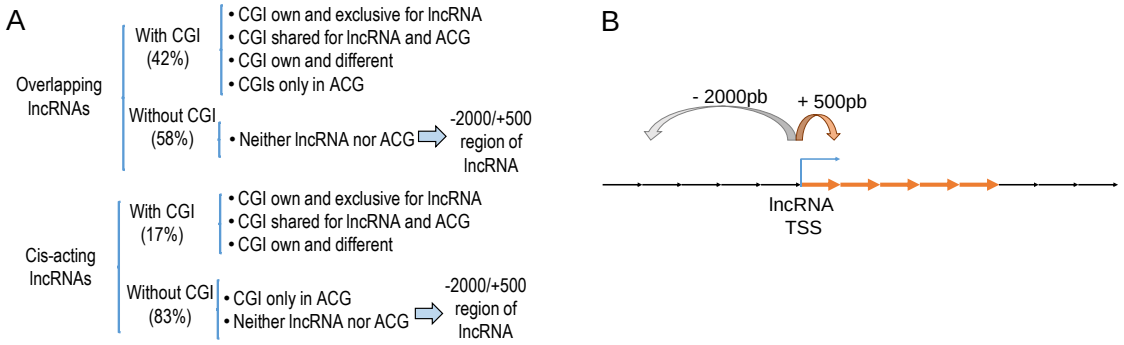

C

	Overlapping lncRNAs						Cis-acting lncRNAs					
	CGI			-2000/+500			CGI			-2000/+500		
	Global	Down	Up	Global	Down	Up	Global	Down	Up	Global	Down	Up
lncRNAs with CGI	74	45	29				105	60	45			
Differential methylation		73%	59%					50%	40%			
lncRNAs without CGI				102	56	46				508	275	273
Differential methylation				10%	11%	9%				8%	7%	8%

Figure 31. Bioinformatic and in silico analysis of lncRNA epigenetic regulation in resistance. (A) Experimental approach for the study of methylation in lncRNAs. For those lncRNAs without a described CGI, we explored a region comprising -2000 to +500 bp from the transcription start site represented in (B). (C) Presence of methylation detected by WGBS according to the expression pattern of the lncRNAs.

Following the identification of the potential CGIs that could be involved in the regulation of expression changes, we analyzed the differentially methylated CpG positions identified by WGBS. To avoid losing any possible methylated candidates, we also included in our bioinformatic study the analysis of a longer region starting at -2000 bp and ending at +500 bp from the lncRNA transcription start site (TSS) for those lncRNAs without a CGI (Figure 31B). Among the overlapping lncRNAs with a CGI, 29% demonstrated differential

methylation (DM) between resistant and sensitive cells at more than one position, compared with 8% of cis-acting lncRNAs (Figure 30B). The difference in methylation by location of the lncRNAs (overlapping or cis-acting) was statistically significant (Chi-square test p-value < 0.001). For overlapping lncRNAs, the methylation pattern is associated with downregulation in platinum resistance, 73% of all differentially methylated overlapping lncRNAs in comparison with the 50% observed for cis-acting lncRNAs (Figure 31C). The results show that the -2000/+500 bp region was essentially the same for overlapping lncRNAs and their ACG; while the -2000/+500 bp region for cis-acting lncRNAs is far away (> 100,000 bp) from the -2000/+500 bp region observed in their ACG, assuming that the gene´s DM does not interfere with the cis-lncRNA epigenetic regulation. Analyses of the -2000/+500 bp region for those lncRNAs without CGI revealed similar percentages of differential methylation for overlapping (10%) and for cis-acting (8%) lncRNAs (Figure 31C).

13. Whole-Genomic Bisulfite Sequencing validation confirms the selection criteria of our approach

Finally, we validated the methylation observed by WGBS by alternative bisulfite sequencing in our experimental model. We selected eight candidates out of the 14 lncRNAs, which expression was validated previously by qRT-PCR, in order to confirm the differentially methylated positions observed by WGBS (Figure 24 and Figure 28). These candidates were AC091814.2, AC141928.1, RP11-65J3.1-002, RP11-65J3.1-003, BX641110, AF198444, XLOC_005125 and RP11-100E13.1 (Table 21).

Table 21. Main characteristics of the selected lncRNAs for methylation validation.

			lncRNA								Differential Methylated Positions by WGBS			
lncRNA	mRNA	Contrast	Accession number	Symbol	Chromosomic location	Strand	ACG accession	ACG Symbol	Relationship	Possible Function	Analysed region	Chromosomic location	Cell line	Number
Down	Up	H23	ENST00000412084	AC091814.2	12: 10089177-10096094	-	NM_001172632	*OLR1*	Cis-acting	upstream enhancer	-2000/+500 region	12: 10095915-10096112	H23	7
Down	Down	OVCAR3	ENST00000511928	AC141928.1	4: 3760474-3765117	-	NM_002337	*LRPAP1*	Cis-acting	downstream	lncRNA CpGi	4: 3768571-3769414	OVCAR3	37
Down	Down	A2780	ENST00000423122	RP11-65J3.1-002	9: 132104121-132121817	+	NM_203434	*IER5L*	Cis-acting	upstream enhancer	lncRNA CpGi	9: 132099124-132099573	A2780	23
Down	Down	Ovarian	ENST00000444125	RP11-65J3.1-003	9:132099157-132109743									
Up	Up	H23	uc021sxs.1	AF198444	15: 101449472-101453362	+	NM_000693	*ALDH1A3*	Overlapping	intron sense-overlapping	mRNA CpGi	15: 101419262-101420165	H23	15
Up	Up	H23	TCONS_00011636	XLOC_005125	6: 1605723-1607305	+	NM_001453	*FOXC1*	Cis-acting	downstream	lncRNA CpGi	6: 1605010-1611693	H23	13
Up	Up	Lung	ENST00000437416	RP11-100E13.1	1:22480997-224803922	-	NM_152495	*CNIH3*	Overlapping	bidirectional	-2000/+500 region	1:224804032-224804373	H460	8
Up	Up	OVCAR3	uc003jsd.1	BX641110	5: 58567936-58571656	-	NM_006203	*PDE4D*	Overlapping	intron sense-overlapping	mRNA CpGi	5: 59189120-59189507	OVCAR3	6

Our first approach included the validation of general changes in expression after epigenetic reactivation treatment (RT) in the resistant cells. RT-PCR (Figure 32) and qRT-PCR (Figure 33) confirmed our first expression results observed in the cell lines for the six

candidates, AC091814.2, AC141928.1, RP11-65J3.1-002, BX641110, AF198444 and XLOC_005125.

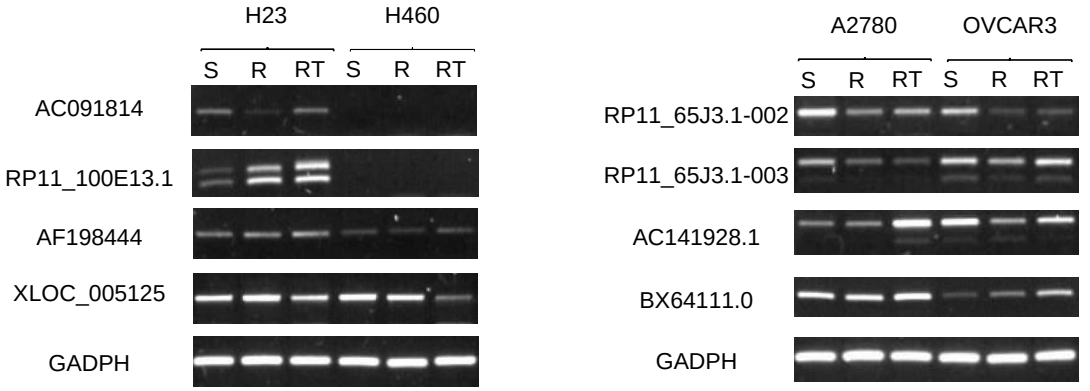

Figure 32. Validation of epigenetic reactivation treatment in lncRNA expression. RT-PCR comparing expression changes among sensitive (S), resistant (R), and resistant treated with epigenetic reactivation (RT). Each assay was performed at least three times to confirm the results.

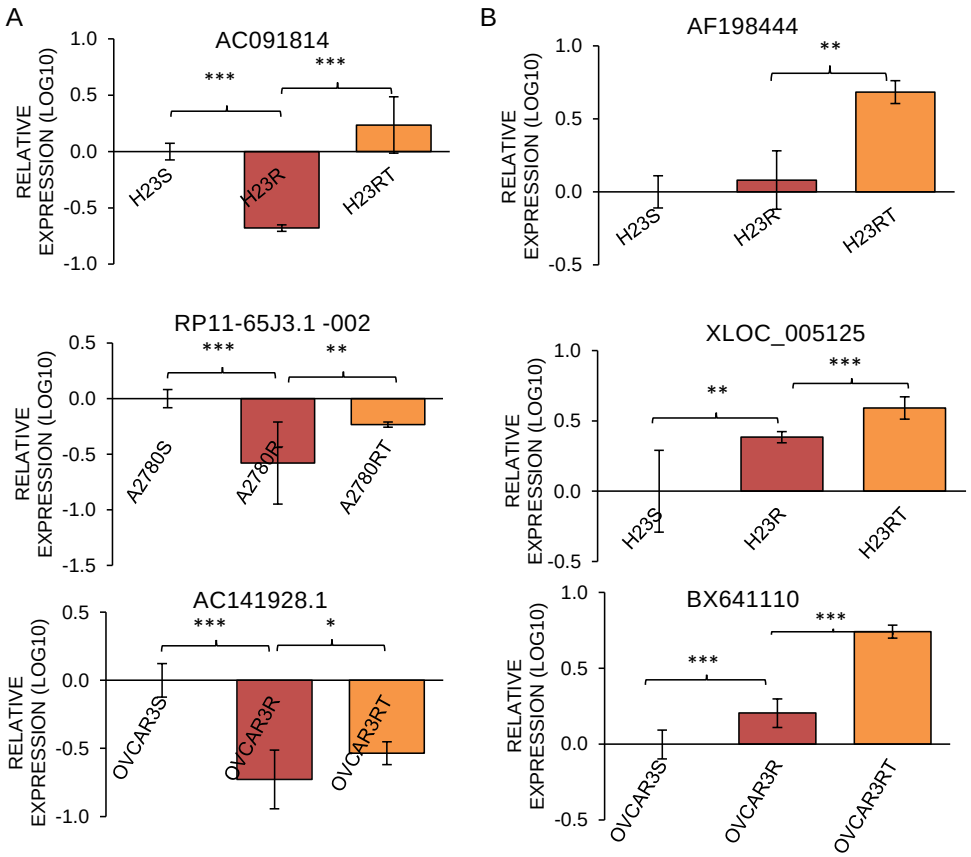

*Figure 33. Quantitative validation of epigenetic changes in lncRNA expression. qRT-PCR to confirm the quantitative expression changes for downregulated (A) and upregulated (B) lncRNAs in sensitive (S), resistant (R), and resistant treated with epigenetic reactivation (RT), only for those samples that showed differentially methylated positions by WGBS. The data represent the results from two different experiments in triplicate in Log10 scale ± SD. * p < 0.05; ** p < 0.01; *** p < 0.001 (Student's T-test).*

Bisulfite sequencing of the differentially methylated positions between sensitive (S) and resistant (R) cells confirmed the gain of methylation in the resistant subtypes for candidates AC091814.2, AC141928.1 and RP11-65J3.1-002, and loss of methylation for AF198444 and BX641110 (Figure 34).

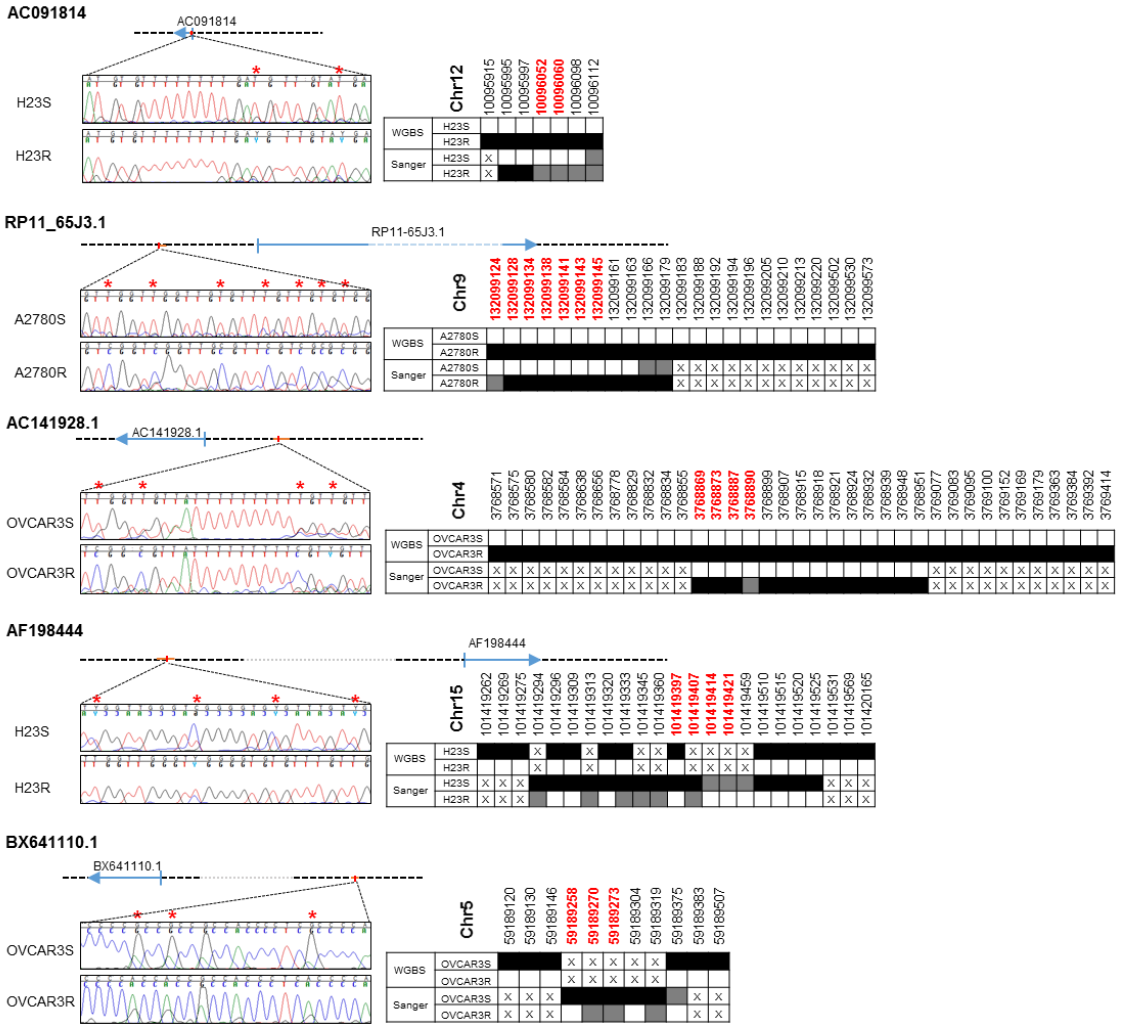

Figure 34. Bisulfite sequencing validation of the differentially methylated positions identified by WGBS. Figure shows the genomic location of lncRNAs interrogated and the most representative positions after Sanger sequencing (left). Red asterisks indicate those positions with differential methylation between S and R cells. The right part of the panel shows the comparison with WGBS, where white squares indicate unmethylation, grey hemimethylation and black shows methylated positions. The crosses indicate an absence of information. Red chromosomal positions are marked with a red asterisk in the sequence. Discontinued-grey line indicates a distance greater than 30,000 pb between the end of the CGI and the start of the lncRNA.

DISCUSSION

DISCUSSION

The search for new biomarkers for survival, prognosis and drug-resistance in cancer is a wide-open field for exploration and investigation. In fact, the findings described in the present work indicate that the function of a gene or a non-coding RNA cannot be considered uniquely responsible for the development, progression and resistance to chemotherapy drugs for cancer treatment.

Epigenetics provides a new scenario to study and understand the transcriptional and post-transcriptional regulatory mechanisms involved in carcinogenesis, increasing our knowledge of the genes and non-coding RNAs involved in these processes. It is therefore a novel source for potential new markers that can improve current treatments and may allow to find new ones based on the genetic and epigenetic profiles, thus leading to personalized therapies.

This study seeks to contribute to the understanding of drug-resistance and the identification of new epigenetic biomarkers in NSCLC and ovarian cancer, by studying the role and regulation of non-coding RNAs.

1. The epigenetic silencing of microRNA-7 contributes to the development of cisplatin resistance

The literature provides evidence that miRNA dysregulation can lead to the development of cancer (Calin et al., 2002, Mendell and Olson, 2012, Fabbri et al., 2007, Ceppi et al., 2010). Epigenetic alterations through DNA methylation can also regulate the expression of a number of microRNAs, diminishing in general and contributing to the onset of cancer (Wang et al., 2010). There are several studies that relate the dysregulation of various miRNAs to clinical outcomes. For tumor tissue, the expression of these regulators is generally downregulated (Gallardo et al., 2009, Jusufovic et al., 2012). To contribute to the molecular characterization of CDDP resistance in cancer, we intended to deepen our understanding of this aspect by approaching the regulation of microRNAs and their target genes with a large-scale expression study. For this type of studies, microarrays keep providing a powerful tool to specifically study the involvement of a large number of miRNAs simultaneously and their role in various tumor processes (Calura et al., 2013, Wang et al., 2015). In the current study, we used this technology in a miRNA-microarray based strategy combined with an epigenetic reactivation treatment. The differential miRNA expression profile from sensitive, resistant and pharmacological treated cells was correlated with gene

expression from the same experimental groups in four paired cell lines to identify new miRNA-targets of promoter hypermethylation potentially involved in the development of resistance in lung and ovarian cancer. We established the ovarian cancer cell lines A2780R and OVCAR3R with a CDDP-resistant index in accordance with the previously established NSCLC cancer cell lines H23R and H460R, assuming that similar resistant events could follow (Ibanez de Caceres et al., 2010).

We first identified 87 of the 723 miRNAs analyzed on the arrays (12%), whose potential epigenetic silencing could promote resistance. This percentage of miRNA epigenetic reactivation is in accordance with published data regarding when tumor cells are exposed to similar unmasking treatment using the same miRNA-expression-array technique (10%-15%) (Lujambio et al., 2008). In addition, some of the miRNAs showing the strongest upregulation were located in the miRNA cluster C19MC, results that are consistent with previous data and that support our experimental approach combining a microarray and pharmacologic unmasking strategy (Saito et al., 2009, Suzuki et al., 2010, Tsai et al., 2009). A restrictive statistical analysis simultaneously achieving both conditions (R *versus* S<0 and RT *versus* R>0) in at least one of the four cell lines analyzed identified 28 of the 87 miRNAs whose silencing could be a frequent event in CDDP-resistant cells, excluding those regulated by other non-epigenetic mechanisms. Of these miRNAs, we identified the presence of a CGI in the regulatory region in 36% (10 of 28), which is consistent with the results obtained in previous studies with a similar percentage of candidate miRNAs with proximal CGIs (Weber et al., 2007). In addition, regulation by promoter methylation has been described for two of 10 selected candidates, miR-200c and miR-23b, supporting again the strategy followed in our study (Ceppi et al., 2010, Geng et al., 2012). The potential epigenetic silencing of the selected candidates could, in fact, be involved in promoting resistance, given their expression levels were significantly lower in resistant cells than in sensitive ones, and these levels recovered after pharmacological treatment.

Additionally, during the initial screening process we found a group of nine miRNAs (miR-498, miR-520f, miR-526b, miR-518f, miR-520b, miR-518c, miR-519d, miR-518e and miR-520h) that did not initially show any CGI in the 2000 bp previous and subsequent to their sequence. However, they belong to the C19MC cluster, which has been reported to have a distant regulatory CGI. It has been reported that the epigenetic regulation by DNA methylation at this distant island controls the expression of the miRNAs located at the C19MC cluster (Noguer-Dance et al., 2010, Tsai et al., 2009). Several studies link expression changes in this miRNA-cluster with brain tumors and liver carcinomas (Augello et al., 2012); thus, it was selected for further validation studies. However, we found a constitutive

methylation in all the sensitive and resistant cells and also in normal lung and ovarin tissues and in PBMCs, suggesting a possible role of this cluster in embryonic development, as has previously been shown (Court et al., 2014, Noguer-Dance et al., 2010). Our results show that there is no correlation between the downregulation of the selected nine miRNAs from the cluster in the resistant phenotypes initially identified on the arrays and the acquisition of hypermethylation in NSCLC and ovarian cancer cell lines after exposure to CDDP.

Our screening included an ontological study of routes and processes related to the biological response to chemotherapy and tumor development for all target genes found in the mRNA expression strategy to be candidate target genes under epigenetic regulation by the 10 selected miRNAs. We identified a set of seven miRNAs containing a surrounding CGI that were complementary to target genes involved in cell growth, proliferation, cell migration, drug efflux, angiogenesis or apoptosis inhibition such *MAFG, ELK-1, RAB6B, CAMK2G, MAPKAP1, ABCA1, ABL1* or *STAT3* (Hanrahan et al., 2003, Iwasaki et al., 2010). All these processes might influence the acquisition of drug-resistance in the CDDP treated cells through the potential miRNA silencing.

Changes in expression were validated for all seven candidates, but not in all the expected paired cell lines, indicating that qRT-PCR is a valuable and necessary validation method more restrictive than microarray, that still keeps providing a powerful tool to study the involvement of a large number of miRNAs simultaneously (Calura et al., 2013, Wang et al., 2015). The expression changes were more significant after unmasking treatment, probably because the pharmacologic combination exerts a synergistic and specific influence in mRNA and miRNA global re-expression, as described in different tumor types (Adi Harel et al., 2015). This effect can be stronger than the silencing observed as a secondary effect of CDDP on DNA methylation.

The expression of miR-7, miR-132, miR-335 and miR-148a was validated in at least two cell lines, suggesting that their deregulation can be a common event in the development of CDDP resistance, which is why they were chosen for epigenetic validation. Although miR-124, miR-9 and miR-10a were validated in one of the cell lines, they could also play a possible role in cancer and chemoresistance, thus explaining the clinical heterogeneity that characterizes these two tumor types. In fact, there are previous studies describing an epigenetic silencing of miR-124 and miR-9 in colon, breast and gastric cancer and in T cell tumors (Bueno et al., 2008, Lujambio et al., 2007, Tsai et al., 2011), and a downregulation of miR-10a has been described in acute myeloid leukemia (Jongen-Lavrencic et al., 2008). Therefore, although we have focused on the epigenetic regulation at miR-7, miR-132, miR-

335 and miR-148, future studies are also warranted to explore their role in chemoresistance.

The absence of methylation found at miR-148a and miR-132 at sensitive and resistant cells indicates that its differential expression is not regulated by DNA methylation. Previous studies link their epigenetic silencing with the development of pancreatic cancer and metastasis in lymph nodes (Lujambio et al., 2008, Hanoun et al., 2010, Zhang et al., 2011). These results could be associated with a tumor-type specificity event; in fact, we have found the same unmethylated profile in lung and ovarian tumor cell lines and in normal tissues, suggesting no relationship between this epigenetic event and tumor progression and/or development of resistance in these malignancies. The expression of those miRNAs might be regulated by an upstream epigenetic mechanism or transcription factor reactivated by demethylation, as has been reported for gene expression upregulation in previous studies using similar epigenetic reactivation approaches (Ibanez de Caceres et al., 2006, Ibanez de Caceres et al., 2010).

miR-335 is located in the second intron of the *MEST* gene (Nishita et al., 1996), whose expression has been shown to be strongly regulated in cancer together with a silencing of miR-335 in different tumor types (Png et al., 2011, Sorrentino et al., 2008). We found specific methylation in the H460 cell line, in both sensitive and resistant cells. However, normal lung and H23 cells did not present this methylation pattern, suggesting that the downregulation for both resistant phenotypes compared with their parental sensitive is probably independent of the methylation profile, and therefore might be not related to the establishment of resistance. We also analyzed three additional cell lines from different tumor types and a saliva sample as an extra control. We found a lack of methylation in all of them, making methylation particular for H460 cells; nevertheless, miR-335 methylation is probably an event in these cells that could be related to the occurrence of that particular tumor. In fact, in a previous study, 5-Aza epigenetic reactivation reestablished miR335 expression in another lung cancer cell line, MDA-231, suggesting a potential role in tumor progression in lung cancer and confirming our results, which were obtained from the unmasking strategy used (Png et al., 2011).

The CpG island encompassing miR-7 showed constitutive methylation in all the normal and tumor samples analyzed. This result suggests the absence of a regulatory role, as has been reported for other potential regulatory CGIs in which the methylated status did not correlate with mRNA expression levels and that are preferentially methylated at nonregulating intergenic regions (Eckhardt et al., 2006, Lopez-Lera et al., 2014). However,

we found a specific methylation in the resistant A2780R and H23R subtypes at the distant CpG island compared with the parental cells and various controls from lung and ovarian control samples. This event appears not to be specific to ovarian and lung cancer resistant cells because we also found the same methylation profile in colon and pancreatic tumor cell lines (LoVo and IMIM-PC2) that also exhibit high resistance to cisplatin. These data suggest a potential epigenetic regulation of miR-7 at the DNA methylation level for this second CGI, a relatively common event in various tumor types, which can present intrinsic resistance to CDDP by epigenetic regulation.

We sought then to confirm the role of miR-7 in the response to CDDP, in order to explore the potential therapeutic effect of miR-7 overexpression, as it has been developed for miR-34, the first microRNA mimic to be used in clinical testing as a theranostic marker (http://mirnatherapeutics.com). However, the ectopically overexpression of miRNA-7 in resistant cells did not change their sensitivity to CDDP, although it induced an increase in cell mortality; probably, due to the multifactorial effect that overexpression of miRNAs may cause on the cellular processes by regulating a high number of potential candidates genes. These results validate previous studies, which have shown its possible tumor suppressor role in cancer (Ma et al., 2014). Its expression has been also linked with sensitization to paclitaxel (Liu et al., 2014), although miR-7 regulation in this process was not defined.

2. *MAFG* is directly regulated by miR-7 and it is potentially involved in cisplatin resistance through the modulation of reactive oxygen species.

Due to the possible multifactorial effects of microRNAs, we believe that miR-7 might be involved in these processes through the regulation of its target genes, whose overexpression has been found in our experimental approach. Using a transcriptomic profile together with the *in silico* assembling of sequences, we identified a group of genes candidate to be targets of miR-7 that could provide cells with the oncogenic capabilities described by Hanahan and Weinberg (Hanahan and Weinberg, 2011). Further analysis of molecular pathways and cellular functions, led us to the selection of *MAFG*, *ELK-1*, *ABCA1* and *MAPKAP1* genes. Validation by alternative techniques and overexpression of miR-7 in the resistant cell lines, revealed that *MAFG*, *ABCA1* and *ELK-1* recovered their levels of expression after epigenetic treatment and overexpression of miR-7, thus indicating a possible regulation of these genes by the methylation of this miRNA.

However, our functional studies performed with luciferase vectors carrying a mutation in the conserved miR-7 binding site, revealed that only *MAFG* seems to be a direct candidate target gene under miR-7 regulation. Moreover, the silencing of miR-7 expression resulted in increased levels of *MAFG* and its overexpression is able to strongly increase the resistance to CDDP in sensitive cells. miR-7 may be an indirect regulator of *ABCA1* and *ELK-1*, in fact, it has been reported that miR-7 could act as modulator of chemoresistance by targeting the *MRP1/ABCC1*, a member of the ABC family proteins, and being involved in lung tumorogenesis by directly regulating the *EGFR* expression (Liu et al., 2015, Chou et al., 2010, Webster et al., 2009). Moreover, *ABCA1* upregulation has been related to the decrease in chemotherapy response in breast cancer. However, we could not find a significant increase of resistance to CDDP after *ABCA1* overexpression, possibly because of the different schema of treatment used in this study, based on sequential paclitaxel/neoadjuvant chemotherapy (Park et al., 2006). The inhibition of *ELK-1* through the drug silodosin has been reported to increase the response to cisplatin in bladder cancer cells (Kawahara et al., 2015). Its overexpression in ovarian cancer cells did not change the sensitivity to CDDP; nevertheless, we observed an increase in the cell survival fraction. As *ELK-1* is a nuclear target of the MAP-kinases cascade and the EGFR-signaling pathway, and miR-7 is a direct regulator of EGFR gene, we believe that our results are a consequence of the highly implication of *ELK-1* in cell proliferation and apoptosis through these signaling routes (Smedberg et al., 2002).

MAFG is associated with detoxification in oxidative stress situations. This leads us to believe that its involvement in the acquired resistance to platinum resides in the protection it confers against free radicals generated in the cell after the administration of this drug (Katsuoka et al., 2005, Katsuoka and Yamamoto, 2016, Kilic et al., 2013, Li et al., 2008, Motohashi et al., 2006). Despite the fact that sMafs family, to which *MAFG* belongs, have been associated with cellular response, little is known about their involvement in human diseases. A number of studies have however linked these proteins with cancer, such as the study by Schembri et al. on *MAFG* regulation by miR-218 as an indicator of smoking-induced disease processes in the lungs (Schembri et al., 2009) and the study by Yang et al. on the relationship between increased *MAFG* and growth in colon cancer cell lines through the insulin-like growth factor-I actions (Yang et al., 2011). Taken together, our experimental results strongly support the direct regulation of *MAFG* through miR-7 and their involvement in the development of cancer. Moreover, the approach we used was aimed at directly linking the development of *in vitro* CDDP resistance with the overexpression of *MAFG* through the decrease of ROS production in our model of cancer cell lines. It has previously been shown that the resistance to CDDP in the A2780 cell line is an event caused by overactivation of the redox-detoxifying pathway (Bao et al., 2014). In line with these, the results obtained with

the ROS production assay in our experimental models indicate that CDDP-resistant subtypes have a lesser increase in ROS after CDDP exposure, probably due to its ability to detoxify the oxidative stress produced by the drug, as a consequence of an overexpression of *MAFG*. We also found a significant overexpression of reported redox-detoxifying-related genes in the resistant cell lines harboring an increased expression of *MAFG*, reinforcing the idea that MAFG mediates the resistance to CDDP through the modulation of ROS (Chen and Kunsch, 2004). These results are summarized in Figure 35.

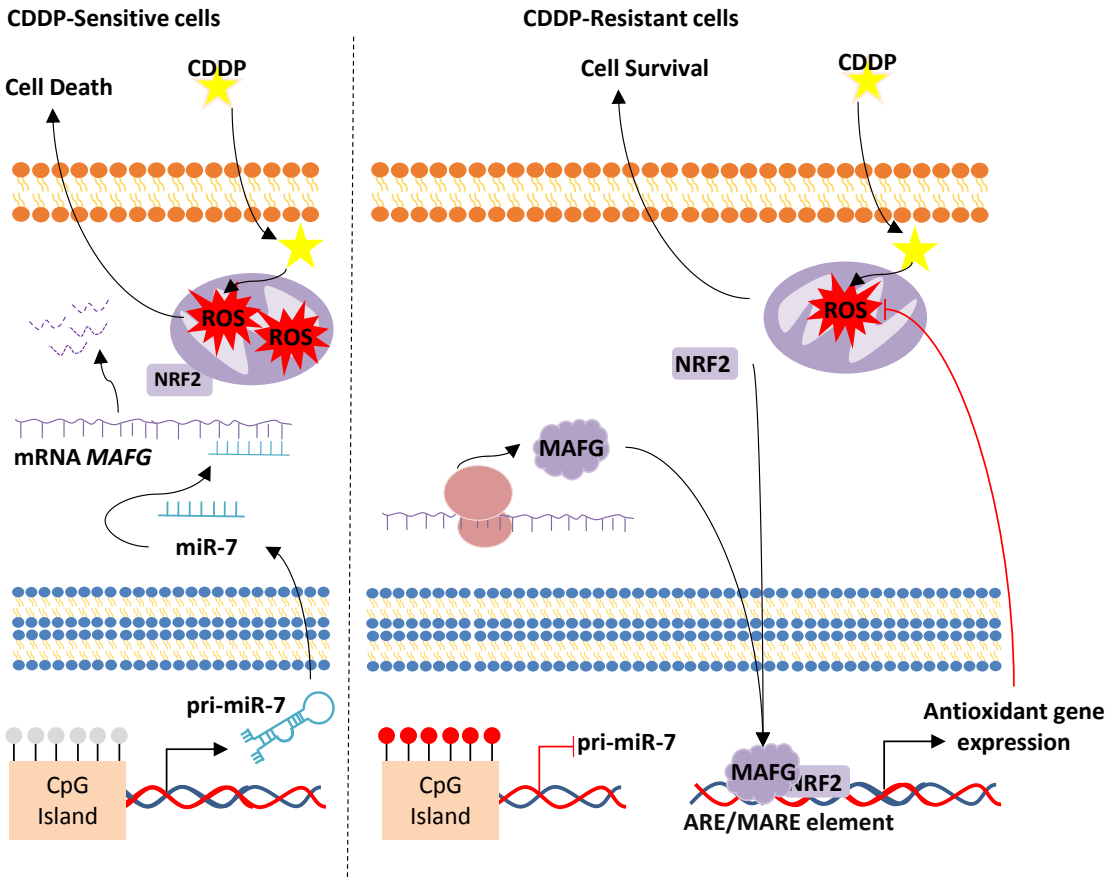

Figure 35. Proposed mechanism for the acquired resistance to cisplatin in NSCLC and ovarian cancer cells through miR-7 methylation and MAFG overexpression. CDDP, cisplatin; ROS, Reactive Oxigen Species.

3. miR-7 and MAFG are promising biomarkers and therapeutic targets in ovarian and NSCLC, respectively.

Our basic results describe that the epigenetic alteration by DNA methylation can reduce the expression of a miR-7, altering the response to CDDP and contributing to the onset of more aggressive phenotypes. We intended to deepen our understanding of this aspect, focusing on miR-7 epigenetic regulation and the clinical outcome for patients with lung and ovarian cancer. We tested the specificity of aberrant miR-7 hypermethylation as a

potential epigenetic biomarker to detect the response to chemotherapy on 167 ovarian cancer patients, all of them treated with platinum-based therapy. An extensive clinical follow-up of 83 of those patients showed that those considered platinum-sensitive, harboring an unmethylated miR-7 had a better progression free survival rates than those patients with a methylated marker. These differences were not observed in platinum-resistant patients, probably because in these patients the recurrence develop in short-time periods and in a small number of cases. We confirmed the same tendency in an additional smaller cohort of 55 patients. Furthermore, our analysis indicated that those patients carrying an unmethylated marker tended to have less aggressive tumors, with three times more overall survival after platinum treatment than those who carried the methylated DNA. In addition, the methylation percentage increased in tumor grades III/IV and when analyzing high-serous samples and Platinum-refractory/resistant tumors. Thus, miR-7 methylation could play a role as a clinical tool predicting the aggressive behavior of this malignancy and the poorer response to platinum-based treatment.

However, miR-7 silencing through DNA methylation appears to play a different role in lung cancer biology, primarily in terms of early development. We measured the methylation status of miR-7 in 75 NSCLC primary tumors from Hospitals la Paz and del Mar and correlated it with the patient's clinical history. Our data are consistent within both cohorts of paraffin samples obtained from distant regions, such as Madrid and Barcelona, in terms of percentage of methylation, confirming the robustness of the MSP technology management. For NSCLC, differential expressions have been reported for various miRNAs, such as miR-138 in CDDP-resistant cell lines (Wang et al., 2011); and the downregulation of several miRNAs has been related to clinical outcomes in many tumor tissues (Diaz-Garcia et al., 2013, Jusufovic et al., 2012). However, there are few studies linking the role of miRNA methylation in NSCLC with tumor development and clinical outcomes, as reported for miR-34a (Gallardo et al., 2009). Therefore, our results yielded remarkable data, enabling us to report for the first time that miR-7 methylation is occasional in normal DNA, whereas it is a common and relative early and frequent event in NSCLC samples, even at early stages I/II, which could play an important role in lung tumorigenesis. In addition, we found similar methylation levels of miR-7 in tumor samples and in normal adjacent tissues, and no association of methylation levels with therapy response or overall survival in a cohort of 22 paired samples from patients with NSCLC. We observed, however, a higher dispersion of methylation and expression of miR-7 and *MAFG* in the T than in the ATT and in the control samples, suggesting that different molecular changes in miR-7 and *MAFG* could be mediating the carcinogenic process, as has been observed for other markers (Schmidt et al., 2012). We have not specifically observed clear differences either in methylation or

expression of any candidate in NSCLC T vs. ATT samples, which could indicate that the samples adjacent to the tumor have already acquired molecular changes probably associated with tumor features. These results are similar to those of Jusufovic et al. who reported a lower expression of miRNAs let-7b and miR-126 in T and ATT from patients with NSCLC in comparison with corresponding non-tumor tissue (Jusufovic et al., 2012). Moreover, the methylation analysis of the ATT compared with the five normal saliva samples indicates that the methylation of this miRNA is an event that occurs in the early stages of the disease. This fact suggests that molecular changes such as miR-7 methylation within the tumor tissue and surrounding tissue generate the microenvironment necessary for tumor cells to grow and this event could be involved not only in tumorigenesis but also in other malignancies associated with smoking (Ostrow et al., 2013).

There is an intense cross-talk between epigenetics and the environment; in fact, tobacco smoke and other environmental hazards deregulate the epigenome profile, which is closely related to the development of lung cancer (Guida et al., 2015). We also found a clear relationship between methylation levels and expression of miR-7 and *MAFG*, which confirm our *in vitro* results and suggest a relationship with *MAFG* in NSCLC, and indicates that higher accumulation of molecular changes are necessary in ovarian cancer to observe the same alteration of miR-7 and *MAFG* expression. The small sample size of our cohorts affords limited statistical power; thus a strength of the current study is that results are based on analysis of fresh tissues from patients with NSCLC and ovarian cancer, whereas most of the data in the literature report the expression of miRNAs and candidate genes performed in cultured cell lines. In accordance with our results, we observed a significant relationship between the expression of *MAFG* and survival in both largest NSCLC cohorts analyzed from TCC and TCGA, with a clear trend towards higher Overall Survival when *MAFG* expression is low. This suggests an oncogenic role of *MAFG* in lung cancer, supporting its potential as a prognostic biomarker. Nevertheless, *MAFG* seems not to correlate with clinical history when analyzing public data bases of ovarian cancer. The differential clinical outcomes regarding the methylation and expression profiles for miR-7 and *MAFG* observed in this study between lung and ovarian cancers could be due, in part, to the differential biology of both tissues. Lung is a tissue continuously exposed to external agents, some of which are highly toxic, such as tobacco smoke, which is closely related to the development of DNA methylation in lung cancer patients (Guida et al., 2015, Jin et al., 2016). In fact, we observed a higher percentage of methylated samples from patients with NSCLC than from patients with ovarian cancer who are protected from external hazards until their exposure to the oxidative stress that arises from chemotherapy treatment. In NSCLC patients, those higher methylation levels correlate in fact with increased *MAFG* expression that may play a

significant role in carcinogenesis. This situation could in part influence a differential response to chemotherapy treatment from both tumor types, as in ovarian cancer patients the observed percentage of miR-7 methylation is probably not enough to induce significant changes in *MAFG* expression.

Taken together, in this work we introduce the epigenetic regulation of miR-7 as a mechanism involved in platinum-resistance in cancer cell lines directly regulating the action of *MAFG*, which is overexpressed in resistant phenotypes. Moreover, miR-7 methylation arises as a potential predictive biomarker for the identification of ovarian cancer patients that may present worst response to platinum-derived treatment in terms of OS and PFS. Furthermore, our functional assays strongly support the role of MAFG in the development of CDDP resistance through ROS detoxification. To the best of our knowledge, this is the first report linking the regulation of *MAFG* by miRNA-7 its role in chemotherapy response to CDDP and the possible role of *MAFG* expression as a potential therapeutic and diagnostic target in cancer and other pathologies.

4. The epigenetic regulation of lncRNAs depends on their chromosomic location.

To deepen in the molecular mechanism underlying CDDP resistance, we decided to complete our study by analyzing the expression patterns of other non-coding that could be under epigenetic regulation by comparing CDDP-resistant with their CDDP-sensitive parental cells.

Consistent with previous reports on NSCLC (Yang et al., 2013) we observed a small percentage of expression changes among all the transcripts investigated, results that were consistent across all bioinformatics contrasts. Moreover, we found a similar percentage change between ovarian and lung human cancer cell lines and limited to a relatively small number of transcripts. In fact, some of the common lncRNAs are associated with coding genes that belong to GO categories involved in cancer initiation and progression such as the *PLCE* and *PDE11A* genes (Cui et al., 2014, Pathak et al., 2015). The validation of the expression changes in a selected group of lncRNAs was successful in 87% of the candidates analyzed by quantitative methodology, which is similar to the percentage found in a previous study (Rajeevan et al., 2001). The remaining lncRNAs are novel, with unknown associated coding genes, highlighting the potential utility of the methodology employed. Although they were not included in the GO analysis, these lncRNAs cannot be completely refuted and additional research is needed to confirm the functional involvement of these candidates in cancer and chemoresistance. Some of the targets identified in the current study, AC091814.2; AC000035.3; XLOC_005125; BX641110 and RP11-384P7.7, are

associated with coding genes that have been previously reported in the cancer literature; however, they have not been previously related to cancer development or cisplatin-resistance, which increases their interest for further studies.

Our bioinformatics analyses classified the lncRNAs that changed in resistance into overlapping and cis-acting lncRNAs according to their relationship with the mRNA of a coding gene (Wang and Chang, 2011, Ma et al., 2013, Chen, 2016, Guttman and Rinn, 2012). One lncRNA transcript can be associated with one or more mRNA transcripts, and the number of cis-acting lncRNAs that change in the development of CDDP resistance is 3.5 times higher than the number of overlapping lncRNAs. This result is expected, because overlapping lncRNAs are encoded within the sequence of a coding gene, which represents less than 2% of the genome (Venter et al., 2001, Jiang et al., 2015a), whereas cis-acting lncRNAs can be found anywhere in a larger region (299 kb) on the same chromosome as an ACG. Trans-acting lncRNAs can exert a widespread action over the entire genome; thus, we limited our study to overlapping and cis-acting lncRNAs. The inclusion of trans-acting lncRNAs would necessitate a wider analysis in order to integrate all potential interactions between the transcriptome and the lncRNome, to discover new potential lncRNA-ACG pairs and to validate them. Therefore, this study is extensive and beyond the scope of the current work.

In terms of global expression changes, our results suggest that in the development of CDDP resistance the expression of a lncRNA overlapping with a coding gene is directly related to the expression of mRNA. Presumably this is because their transcription is controlled by the same regulatory mechanisms. Conversely, cis-acting lncRNAs may promote or interfere with the expression of their ACG, as has been previously shown (Ozes et al., 2016, Wang et al., 2014). These results are in accordance with our bioinformatics methylation analysis performed on the data obtained from the WGBS, suggesting that the possible epigenetic regulation of overlapping lncRNAs can be mediated by CGIs located in their regulatory region or in one of their ACGs. By contrast, cis-acting lncRNAs could be primarily regulated by their own CGIs. Therefore, as overlapping lncRNA have a higher fraction of CGI, they are more likely to be unmethylated in normal/sensitive cells and more likely to be silenced by aberrant DNA methylation. Indeed, we found that the methylation in overlapping lncRNAs was more frequent than the cis-acting lncRNAs, reinforcing the idea that cis-acting lncRNAs could be regulated by mechanisms different from those of overlapping lncRNAs during the development of resistance to CDDP.

Although we observed that the occurrence of CpG islands in overlapping lncRNAs is higher than in cis-acting IncRNAs, this result doesn't reach the estimated 50%–60% of coding genes showing defined CGIs (Deaton et al., 2011), suggesting that lncRNAs might be less regulated by DNA methylation. The inclusion of the -2000/+500 bp region surrounding the lncRNA and the mRNAs TSS in our analysis was an inefficient approach to increasing the number of possible candidates under epigenetic regulation because the scrutiny had to be extended to 508 cis-acting lncRNAs with a one-by–one candidate approach, to find only a 8% of potential epigenetically-regulated candidates. Altogether, these results suggest that the overlapping lncRNAs could be epigenetically regulated through the CGIs shared with their ACGs, thus implying that these lncRNAs would be acting on regulatory loops with their ACG due to sequence complementarity. Although various studies have *in silico* analyzed the epigenetic regulation by DNA methylation of lncRNAs in cancer (Yang et al., 2017, Hu et al., 2017), our experimental results obtained from *in vitro* assays are the first to identify differential epigenetic regulation for overlapping and cis-acting lncRNAs in cancer chemoresistance.

Experimental validation at the level of lncRNA expression was successful for all the selected candidates, suggesting an epigenetic regulation of these lncRNAs in resistance. Furthermore, bisulfite sequencing of the regions identified by WGBS confirmed hypermethylation in resistance for AC091814.2, AC141928.1 and RP11-65J3.1-002 lncRNAs. In addition, we identified several positions that lost methylation in the resistant subtypes of our models in the regulatory regions of AF198444 and BX641110, suggesting that CDDP also leads to epigenetic changes that decrease methylation levels. We found more differentially methylated positions by Sanger sequencing than those first identified by WGBS. The more restrictive analysis of coverage and reads for WGBS showed no information for various regions along the genome. However, it has been reported that the methylation patterns show the same behavior in proximal regions, explaining the results in our cell lines (Shoemaker et al., 2010, Guo et al., 2017). We could not validate the methylated positions of XLOC_005125, because they were widely separately located along the CGI and no pair of primers was available to cover more than two CGI positions in the entire region. However, we were able to validate the expected methylation pattern for 100% of the selected candidates.

Our approach has allowed us to identify and characterize the molecular behavior of lncRNAs in the development of CDDP resistance in cancer. We have first shown that variation in lncRNAs and mRNAs after CDDP treatment leads to similar ratios of differences, thus identifying a small group of candidates whose expression is altered in both NSCLC and

ovarian tumor types as a result of platinum treatment. This outcome is of interest for future studies focused on the potential role of lncRNAs and mRNAs in acquired resistance. Moreover, our bioinformatic analyses have identified two groups of lncRNAs according to the relationship with their associated coding gene, supporting previous findings in this field. This genomic distribution may reinforce that overlapping and cis-acting lncRNAs could play different regulatory roles in response to chemotherapy treatment. Further, the whole methylome scope of our study revealed differences in methylation patterns for overlapping and cis-acting lncRNAs. We clearly observed that overlapping and cis-acting lncRNAs are differentially regulated by DNA methylation, suggesting that overlapping lncRNAs that show a positive correlation of expression with their host gene are probably regulated by the shared CGI. This regulation has been shown for miRNAs such as miR-335 and its host gene *MEST* and miR-31 and its host lncRNA LOC554202 (Dohi et al., 2013, Augoff et al., 2012); however, to the best of our knowledge, this is the first report providing this finding for lncRNAs. Furthermore, our results indicate that cis-acting lncRNAs are probably regulated by transcriptional mechanisms other than DNA methylation and thus, alternative analyses are required to study the regulation of these lncRNAs. Our research could be of great importance for future analyses involving the identification of new diagnostic and predictive cancer biomarkers based on epigenetics and lncRNA regulation.

CONCLUSIONES

CONCLUSIONES

1. En este trabajo hemos identificado un grupo de siete microARNs (miR-7, miR-132, miR-335, miR-148a, miR-10a, miR-124 y miR-9) bajo potencial regulación epigenética que podrían estar jugando un papel en la aparición de resistencia a cisplatino.

2. A partir de la combinación de las técnicas de arrays de expresión y el tratamiento de reactivación epigenética en los modelos celulares de sensibilidad y resistencia establecidos en nuestro laboratorio, hemos identificado que la metilación de la región reguladora del miR-7 provoca su silenciamiento.

3. Además, describimos por primera vez que *MAFG* es un gen diana directo de la acción del microARN-7, cuya sobreexpresión induce el desarrollo de resistencia a cisplatino en las líneas celulares de cáncer de pulmón no microcítico y cáncer de ovario estudiadas.

4. La resistencia al cisplatino inducida por MAFG está mediada, al menos en parte, por la detoxificación de las especies reactivas de oxígeno generadas tras el tratamiento con cisplatino.

5. Nuestros resultados indican que la presencia de metilación en la región reguladora del miR-7 podrían utilizarse como un marcador predictivo de respuesta al tratamiento basado en platino en cáncer de ovario, prediciendo qué subgrupo de pacientes tienen mayor riesgo de recaída y por tanto habrían de someterse a un mayor seguimiento clínico o incluso beneficiarse de terapias alternativas.

6. Por otra parte, encontramos aplicabilidad clínica en los niveles de expresión de *MAFG* en cuanto a su potencial uso como biomarcador pronóstico en cáncer de pulmón no microcítico. Estos resultados abren las puertas al desarrollo de nuevas estrategias diagnósticas y opciones terapéuticas alternativas para el tratamiento del cáncer de pulmón.

7. Con este trabajo, hemos sentado las bases para el estudio bioinformático comparativo entre metiloma y transctriptoma, identificando y caracterizando por primera vez el perfil de regulación epigenética diferencial entre lncRNAs solapantes y los que actúan en cis, en el desarrollo de resistencia a cisplatino. Este resultado abre nuevas fronteras en el estudio de su posible papel como biomarcadores de respuesta a terapia en cáncer.

8. Nuestros resultados indican que los lncRNAs solapantes muestran una correlación positiva de la expresión con su gen hospedador, probablemente regulados por una Isla CpG común. Estos lncRNAs presentan mayor metilación diferencial en células resistentes a cisplatino comparados con los lncRNAs que actúan en cis.

9. Sin embargo, los lncRNAs que actúan en cis están probablemente regulados por otros mecanismos transcripcionales distintos a la metilación del ADN y por tanto se necesitarían aproximaciones distintas para estudiar su regulación transcripcional.

10. Finalmente, hemos identificado un grupo de lncRNAs bajo regulación epigenética cuya expresión se altera en respuesta a quimioterapia en nuestros modelos celulares de CPNM y cáncer de ovario. El interés clínico de estos lncRNAs así como de sus genes candidatos es prometedor, aunque aún queda por explorar en muestras clínicas.

CONCLUSIONS

CONCLUSIONS

1. In the present work we have identified a group of seven microRNAs (miR-7, miR-132, miR-335, miR-148a, miR-10a, miR-124 and miR-9) under potential epigenetic regulation that could be playing a role in the development of cisplatin resistance.

2. Based on a combination of expression microarray methodology and the epigenetic reactivation treatment in our cellular models of sensitive and resistant cell lines established in our laboratory, we have identified that the methylation of the regulatory region of miR-7 is involved in its silencing.

3. In addition, we describe for the first time that *MAFG* is a direct target gene of the miR-7 and how its overexpression induces the development of cisplatin resistance in the non-small cell lung cancer and ovarian cancer cell lines of study.

4. The cisplatin-resistant phenotype induced by MAFG is mediated, at least in part, by the detoxification of reactive oxygen species produced after cisplatin treatment.

5. Our results indicate that the presence of methylation in the regulatory region of miR-7 can be used as a predictive biomarker for the response to cisplatin-based therapy in ovarian cancer, predicting which group of patients is more likely to relapse and therefore should have an intense clinical follow up or could benefit from alternative therapies.

6. Additionally, we have found clinical applicability for *MAFG* expression levels as a prognostic biomarker in NSCLC, which have implication for the development of new therapeutic strategies for the treatment of lung cancer.

7. We have also set up the base for the bioinformatics comparative study between methylome and transcriptome, identifying and characterizing for the first time the epigenetic regulatory profile of lncRNAs during the development of cisplatin resistance. These results provide new insights into the study of the potential use of lncRNAs as biomarkers in response to chemotherapy in cancer.

8. Our results indicate that overlapping lncRNAs show a positive correlation with their associated coding genes, which are probably regulated by a common CpG island and present higher differential methylation in resistance *versus* sensitivity compared with cis-acting lncRNAs.

9. Nevertheless, cis-acting lncRNAs appear to be regulated by other transcriptional mechanisims different than DNA methylation and thus other approaches are needed for the study of their transcriptional regulation.

10. Finally, we have identified a group of lncRNAs under epigenetic regulation whose expression is altered in response to cisplatin treatment in our cellular models of sensitive and resistant NSCLC and ovarian cancer cell lines. The clinical interest of these lncRNAs and their associated coding genes is promising, although further exploration in clinical samples is still needed.

REFERENCES

REFERENCES

ADI HAREL, S., BOSSEL BEN-MOSHE, N., AYLON, Y., BUBLIK, D. R., MOSKOVITS, N., TOPEROFF, G., AZAIZA, D., BIAGONI, F., FUCHS, G., WILDER, S., HELLMAN, A., BLANDINO, G., DOMANY, E. & OREN, M. 2015. Reactivation of epigenetically silenced miR-512 and miR-373 sensitizes lung cancer cells to cisplatin and restricts tumor growth. *Cell Death Differ,* 22**,** 1328-40.

ALEXIOU, P., MARAGKAKIS, M., PAPADOPOULOS, G. L., RECZKO, M. & HATZIGEORGIOU, A. G. 2009. Lost in translation: an assessment and perspective for computational microRNA target identification. *Bioinformatics,* 25**,** 3049-55.

AMARAL, P. P., CLARK, M. B., GASCOIGNE, D. K., DINGER, M. E. & MATTICK, J. S. 2011. lncRNAdb: a reference database for long noncoding RNAs. *Nucleic Acids Res,* 39**,** D146-51.

AMARAL, P. P., DINGER, M. E. & MATTICK, J. S. 2013. Non-coding RNAs in homeostasis, disease and stress responses: an evolutionary perspective. *Brief Funct Genomics,* 12**,** 254-78.

AMIN, M. B., GREENE, F. L., EDGE, S. B., COMPTON, C. C., GERSHENWALD, J. E., BROOKLAND, R. K., MEYER, L., GRESS, D. M., BYRD, D. R. & WINCHESTER, D. P. 2017. The Eighth Edition AJCC Cancer Staging Manual: Continuing to build a bridge from a population-based to a more "personalized" approach to cancer staging. *CA Cancer J Clin,* 67**,** 93-99.

ARITA, A. & COSTA, M. 2014. Oxidative Stress and the Epigenome in Human Disease. *J Genet Genome Res*.

AUGELLO, C., VAIRA, V., CARUSO, L., DESTRO, A., MAGGIONI, M., PARK, Y. N., MONTORSI, M., SANTAMBROGIO, R., RONCALLI, M. & BOSARI, S. 2012. MicroRNA profiling of hepatocarcinogenesis identifies C19MC cluster as a novel prognostic biomarker in hepatocellular carcinoma. *Liver Int,* 32**,** 772-82.

AUGOFF, K., MCCUE, B., PLOW, E. F. & SOSSEY-ALAOUI, K. 2012. miR-31 and its host gene lncRNA LOC554202 are regulated by promoter hypermethylation in triple-negative breast cancer. *Mol Cancer,* 11**,** 5.

BALAGUER, F., LINK, A., LOZANO, J. J., CUATRECASAS, M., NAGASAKA, T., BOLAND, C. R. & GOEL, A. 2010. Epigenetic silencing of miR-137 is an early event in colorectal carcinogenesis. *Cancer Res,* 70**,** 6609-18.

BANNISTER, A. J. & KOUZARIDES, T. 2011. Regulation of chromatin by histone modifications. *Cell Res,* 21**,** 381-95.

BAO, L. J., JARAMILLO, M. C., ZHANG, Z. B., ZHENG, Y. X., YAO, M., ZHANG, D. D. & YI, X. F. 2014. Nrf2 induces cisplatin resistance through activation of autophagy in ovarian carcinoma. *Int J Clin Exp Pathol,* 7**,** 1502-13.

BHARTIYA, D., PAL, K., GHOSH, S., KAPOOR, S., JALALI, S., PANWAR, B., JAIN, S., SATI, S., SENGUPTA, S., SACHIDANANDAN, C., RAGHAVA, G. P., SIVASUBBU, S. & SCARIA, V. 2013. lncRNome: a comprehensive knowledgebase of human long noncoding RNAs. *Database (Oxford),* 2013**,** bat034.

BOLSTAD, B. M., IRIZARRY, R. A., ASTRAND, M. & SPEED, T. P. 2003. A comparison of normalization methods for high density oligonucleotide array data based on variance and bias. *Bioinformatics,* 19**,** 185-93.

BOUMIL, R. M., OGAWA, Y., SUN, B. K., HUYNH, K. D. & LEE, J. T. 2006. Differential methylation of Xite and CTCF sites in Tsix mirrors the pattern of X-inactivation choice in mice. *Mol Cell Biol,* 26**,** 2109-17.

BROWN, S. D. 1991. XIST and the mapping of the X chromosome inactivation centre. *Bioessays,* 13**,** 607-12.

BU, D., YU, K., SUN, S., XIE, C., SKOGERBO, G., MIAO, R., XIAO, H., LIAO, Q., LUO, H., ZHAO, G., ZHAO, H., LIU, Z., LIU, C., CHEN, R. & ZHAO, Y. 2012. NONCODE v3.0: integrative annotation of long noncoding RNAs. *Nucleic Acids Res,* 40**,** D210-5.

BU, H., BARALDO, G., LEPPERDINGER, G. & JANSEN-DURR, P. 2016. mir-24 activity propagates stress-induced senescence by down regulating DNA topoisomerase 1. *Exp Gerontol,* 75**,** 48-52.

BUENO, M. J., PEREZ DE CASTRO, I., GOMEZ DE CEDRON, M., SANTOS, J., CALIN, G. A., CIGUDOSA, J. C., CROCE, C. M., FERNANDEZ-PIQUERAS, J. & MALUMBRES, M. 2008. Genetic and epigenetic silencing of microRNA-203 enhances ABL1 and BCR-ABL1 oncogene expression. *Cancer Cell,* 13**,** 496-506.

BUI, T. V. & MENDELL, J. T. 2010. Myc: Maestro of MicroRNAs. *Genes Cancer,* 1**,** 568-575.

CALIN, G. A., DUMITRU, C. D., SHIMIZU, M., BICHI, R., ZUPO, S., NOCH, E., ALDLER, H., RATTAN, S., KEATING, M., RAI, K., RASSENTI, L., KIPPS, T., NEGRINI, M., BULLRICH, F. & CROCE, C. M. 2002. Frequent deletions and down-regulation of micro- RNA genes miR15 and miR16 at 13q14 in chronic lymphocytic leukemia. *Proc Natl Acad Sci U S A,* 99**,** 15524-9.

CALURA, E., FRUSCIO, R., PARACCHINI, L., BIGNOTTI, E., RAVAGGI, A., MARTINI, P., SALES, G., BELTRAME, L., CLIVIO, L., CEPPI, L., DI MARINO, M., FUSO NERINI, I., ZANOTTI, L., CAVALIERI, D., CATTORETTI, G., PEREGO, P., MILANI, R., KATSAROS, D., TOGNON, G., SARTORI, E., PECORELLI, S., MANGIONI, C., D'INCALCI, M., ROMUALDI, C. & MARCHINI, S. 2013. MiRNA landscape in stage I epithelial ovarian cancer defines the histotype specificities. *Clin Cancer Res,* 19**,** 4114-23.

CANCER GENOME ATLAS RESEARCH, N. 2011. Integrated genomic analyses of ovarian carcinoma. *Nature,* 474**,** 609-15.

CEPPI, P., MUDDULURU, G., KUMARSWAMY, R., RAPA, I., SCAGLIOTTI, G. V., PAPOTTI, M. & ALLGAYER, H. 2010. Loss of miR-200c expression induces an aggressive, invasive, and chemoresistant phenotype in non-small cell lung cancer. *Mol Cancer Res,* 8**,** 1207-16.

CORTES-SEMPERE, M., DE MIGUEL, M. P., PERNIA, O., RODRIGUEZ, C., DE CASTRO CARPENO, J., NISTAL, M., CONDE, E., LOPEZ-RIOS, F., BELDA-INIESTA, C., PERONA, R. & IBANEZ DE CACERES, I. 2013. IGFBP-3 methylation-derived deficiency mediates the resistance to cisplatin through the activation of the IGFIR/Akt pathway in non-small cell lung cancer. *Oncogene,* 32**,** 1274-83.

COURT, F., TAYAMA, C., ROMANELLI, V., MARTIN-TRUJILLO, A., IGLESIAS-PLATAS, I., OKAMURA, K., SUGAHARA, N., SIMON, C., MOORE, H., HARNESS, J. V., KEIRSTEAD, H., SANCHEZ-MUT, J. V., KANEKI, E., LAPUNZINA, P., SOEJIMA, H., WAKE, N., ESTELLER, M., OGATA, T., HATA, K., NAKABAYASHI, K. & MONK, D. 2014. Genome-wide parent-of-origin DNA methylation analysis reveals the intricacies of human imprinting and suggests a germline methylation-independent mechanism of establishment. *Genome Res,* 24**,** 554-69.

CUI, X. B., PENG, H., LI, S., LI, T. T., LIU, C. X., ZHANG, S. M., JIN, T. T., HU, J. M., JIANG, J. F., LIANG, W. H., LI, N., LI, L., CHEN, Y. Z. & LI, F. 2014. Prognostic value of PLCE1 expression in upper gastrointestinal cancer: a systematic review and meta-analysis. *Asian Pac J Cancer Prev,* 15**,** 9661-6.

CHANG, X., MONITTO, C. L., DEMOKAN, S., KIM, M. S., CHANG, S. S., ZHONG, X., CALIFANO, J. A. & SIDRANSKY, D. 2010. Identification of hypermethylated genes associated with cisplatin resistance in human cancers. *Cancer Res,* 70**,** 2870-9.

CHATTOPADHYAY, S., MACHADO-PINILLA, R., MANGUAN-GARCIA, C., BELDA-INIESTA, C., MORATILLA, C., CEJAS, P., FRESNO-VARA, J. A., DE CASTRO-CARPENO, J., CASADO, E., NISTAL, M., GONZALEZ-BARON, M. & PERONA, R. 2006. MKP1/CL100 controls tumor growth and sensitivity to cisplatin in non-small-cell lung cancer. *Oncogene,* 25**,** 3335-45.

CHEN, L. L. 2016. Linking Long Noncoding RNA Localization and Function. *Trends Biochem Sci,* 41**,** 761-72.

CHEN, X. L. & KUNSCH, C. 2004. Induction of cytoprotective genes through Nrf2/antioxidant response element pathway: a new therapeutic approach for the treatment of inflammatory diseases. *Curr Pharm Des,* 10**,** 879-91.

CHOU, Y. T., LIN, H. H., LIEN, Y. C., WANG, Y. H., HONG, C. F., KAO, Y. R., LIN, S. C., CHANG, Y. C., LIN, S. Y., CHEN, S. J., CHEN, H. C., YEH, S. D. & WU, C. W. 2010. EGFR promotes lung

tumorigenesis by activating miR-7 through a Ras/ERK/Myc pathway that targets the Ets2 transcriptional repressor ERF. *Cancer Res,* 70**,** 8822-31.

DASARI, S. & TCHOUNWOU, P. B. 2014. Cisplatin in cancer therapy: molecular mechanisms of action. *Eur J Pharmacol,* 740**,** 364-78.

DAVIS, B. N. & HATA, A. 2009. Regulation of MicroRNA Biogenesis: A miRiad of mechanisms. *Cell Commun Signal,* 7**,** 18.

DEATON, A. M., WEBB, S., KERR, A. R., ILLINGWORTH, R. S., GUY, J., ANDREWS, R. & BIRD, A. 2011. Cell type-specific DNA methylation at intragenic CpG islands in the immune system. *Genome Res,* 21**,** 1074-86.

DEAVALL, D. G., MARTIN, E. A., HORNER, J. M. & ROBERTS, R. 2012. Drug-induced oxidative stress and toxicity. *J Toxicol,* 2012**,** 645460.

DEPLUS, R., BRENNER, C., BURGERS, W. A., PUTMANS, P., KOUZARIDES, T., DE LAUNOIT, Y. & FUKS, F. 2002. Dnmt3L is a transcriptional repressor that recruits histone deacetylase. *Nucleic Acids Res,* 30**,** 3831-8.

DETTERBECK, F. C., BOFFA, D. J., KIM, A. W. & TANOUE, L. T. 2017. The Eighth Edition Lung Cancer Stage Classification. *Chest,* 151**,** 193-203.

DEY, B. K., MUELLER, A. C. & DUTTA, A. 2014. Long non-coding RNAs as emerging regulators of differentiation, development, and disease. *Transcription,* 5**,** e944014.

DIAZ-GARCIA, C. V., AGUDO-LOPEZ, A., PEREZ, C., LOPEZ-MARTIN, J. A., RODRIGUEZ-PERALTO, J. L., DE CASTRO, J., CORTIJO, A., MARTINEZ-VILLANUEVA, M., IGLESIAS, L., GARCIA-CARBONERO, R., FRESNO VARA, J. A., GAMEZ-POZO, A., PALACIOS, J., CORTES-FUNES, H., PAZ-ARES, L. & AGULLO-ORTUNO, M. T. 2013. DICER1, DROSHA and miRNAs in patients with non-small cell lung cancer: implications for outcomes and histologic classification. *Carcinogenesis,* 34**,** 1031-8.

DINGER, M. E., PANG, K. C., MERCER, T. R., CROWE, M. L., GRIMMOND, S. M. & MATTICK, J. S. 2009. NRED: a database of long noncoding RNA expression. *Nucleic Acids Res,* 37**,** D122-6.

DJEBALI, S., DAVIS, C. A., MERKEL, A., DOBIN, A., LASSMANN, T., MORTAZAVI, A., TANZER, A., LAGARDE, J., LIN, W., SCHLESINGER, F., XUE, C., MARINOV, G. K., KHATUN, J., WILLIAMS, B. A., ZALESKI, C., ROZOWSKY, J., RODER, M., KOKOCINSKI, F., ABDELHAMID, R. F., ALIOTO, T., ANTOSHECHKIN, I., BAER, M. T., BAR, N. S., BATUT, P., BELL, K., BELL, I., CHAKRABORTTY, S., CHEN, X., CHRAST, J., CURADO, J., DERRIEN, T., DRENKOW, J., DUMAIS, E., DUMAIS, J., DUTTAGUPTA, R., FALCONNET, E., FASTUCA, M., FEJES-TOTH, K., FERREIRA, P., FOISSAC, S., FULLWOOD, M. J., GAO, H., GONZALEZ, D., GORDON, A., GUNAWARDENA, H., HOWALD, C., JHA, S., JOHNSON, R., KAPRANOV, P., KING, B., KINGSWOOD, C., LUO, O. J., PARK, E., PERSAUD, K., PREALL, J. B., RIBECA, P., RISK, B., ROBYR, D., SAMMETH, M., SCHAFFER, L., SEE, L. H., SHAHAB, A., SKANCKE, J., SUZUKI, A. M., TAKAHASHI, H., TILGNER, H., TROUT, D., WALTERS, N., WANG, H., WROBEL, J., YU, Y., RUAN, X., HAYASHIZAKI, Y., HARROW, J., GERSTEIN, M., HUBBARD, T., REYMOND, A., ANTONARAKIS, S. E., HANNON, G., GIDDINGS, M. C., RUAN, Y., WOLD, B., CARNINCI, P., GUIGO, R. & GINGERAS, T. R. 2012. Landscape of transcription in human cells. *Nature,* 489**,** 101-8.

DOHI, O., YASUI, K., GEN, Y., TAKADA, H., ENDO, M., TSUJI, K., KONISHI, C., YAMADA, N., MITSUYOSHI, H., YAGI, N., NAITO, Y., TANAKA, S., ARII, S. & YOSHIKAWA, T. 2013. Epigenetic silencing of miR-335 and its host gene MEST in hepatocellular carcinoma. *Int J Oncol,* 42**,** 411-8.

DWEEP, H. & GRETZ, N. 2015. miRWalk2.0: a comprehensive atlas of microRNA-target interactions. *Nat Methods,* 12**,** 697.

EADS, C. A., DANENBERG, K. D., KAWAKAMI, K., SALTZ, L. B., BLAKE, C., SHIBATA, D., DANENBERG, P. V. & LAIRD, P. W. 2000. MethyLight: a high-throughput assay to measure DNA methylation. *Nucleic Acids Res,* 28**,** E32.

ECKHARDT, F., LEWIN, J., CORTESE, R., RAKYAN, V. K., ATTWOOD, J., BURGER, M., BURTON, J., COX, T. V., DAVIES, R., DOWN, T. A., HAEFLIGER, C., HORTON, R., HOWE, K., JACKSON, D. K., KUNDE, J., KOENIG, C., LIDDLE, J., NIBLETT, D., OTTO, T., PETTETT, R., SEEMANN, S., THOMPSON, C., WEST, T., ROGERS, J., OLEK, A., BERLIN, K. & BECK, S. 2006. DNA methylation profiling of human chromosomes 6, 20 and 22. *Nat Genet,* 38**,** 1378-85.

ELLIS, B. C., MOLLOY, P. L. & GRAHAM, L. D. 2012. CRNDE: A Long Non-Coding RNA Involved in CanceR, Neurobiology, and DEvelopment. *Front Genet,* 3**,** 270.

FABBRI, M., GARZON, R., CIMMINO, A., LIU, Z., ZANESI, N., CALLEGARI, E., LIU, S., ALDER, H., COSTINEAN, S., FERNANDEZ-CYMERING, C., VOLINIA, S., GULER, G., MORRISON, C. D., CHAN, K. K., MARCUCCI, G., CALIN, G. A., HUEBNER, K. & CROCE, C. M. 2007. MicroRNA-29 family reverts aberrant methylation in lung cancer by targeting DNA methyltransferases 3A and 3B. *Proc Natl Acad Sci U S A,* 104**,** 15805-10.

FAN, Y., SHEN, B., TAN, M., MU, X., QIN, Y., ZHANG, F. & LIU, Y. 2014. Long non-coding RNA UCA1 increases chemoresistance of bladder cancer cells by regulating Wnt signaling. *FEBS J,* 281**,** 1750-8.

FATICA, A. & BOZZONI, I. 2014. Long non-coding RNAs: new players in cell differentiation and development. *Nat Rev Genet,* 15**,** 7-21.

FENSTERMACHER, D. A., WENHAM, R. M., ROLLISON, D. E. & DALTON, W. S. 2011. Implementing personalized medicine in a cancer center. *Cancer J,* 17**,** 528-36.

FERLAY, J., SOERJOMATARAM, I., DIKSHIT, R., ESER, S., MATHERS, C., REBELO, M., PARKIN, D. M., FORMAN, D. & BRAY, F. 2015. Cancer incidence and mortality worldwide: sources, methods and major patterns in GLOBOCAN 2012. *Int J Cancer,* 136**,** E359-86.

FRIEDLANDER, M., TRIMBLE, E., TINKER, A., ALBERTS, D., AVALL-LUNDQVIST, E., BRADY, M., HARTER, P., PIGNATA, S., PUJADE-LAURAINE, E., SEHOULI, J., VERGOTE, I., BEALE, P., BEKKERS, R., CALVERT, P., COPELAND, L., GLASSPOOL, R., GONZALEZ-MARTIN, A., KATSAROS, D., KIM, J. W., MILLER, B., PROVENCHER, D., RUBINSTEIN, L., ATRI, M., ZEIMET, A., BACON, M., KITCHENER, H., STUART, G. C. & GYNECOLOGIC CANCER, I. 2011. Clinical trials in recurrent ovarian cancer. *Int J Gynecol Cancer,* 21**,** 771-5.

FURUTA, M., KOZAKI, K. I., TANAKA, S., ARII, S., IMOTO, I. & INAZAWA, J. 2010. miR-124 and miR-203 are epigenetically silenced tumor-suppressive microRNAs in hepatocellular carcinoma. *Carcinogenesis,* 31**,** 766-76.

FUSCHI, P., MAIMONE, B., GAETANO, C. & MARTELLI, F. 2017. Noncoding RNAs in the Vascular System Response to Oxidative Stress. *Antioxid Redox Signal*.

GALLARDO, E., NAVARRO, A., VINOLAS, N., MARRADES, R. M., DIAZ, T., GEL, B., QUERA, A., BANDRES, E., GARCIA-FONCILLAS, J., RAMIREZ, J. & MONZO, M. 2009. miR-34a as a prognostic marker of relapse in surgically resected non-small-cell lung cancer. *Carcinogenesis,* 30**,** 1903-9.

GAYARRE, J., KAMIENIAK, M. M., CAZORLA-JIMENEZ, A., MUNOZ-REPETO, I., BORREGO, S., GARCIA-DONAS, J., HERNANDO, S., ROBLES-DIAZ, L., GARCIA-BUENO, J. M., RAMON, Y. C. T., HERNANDEZ-AGUDO, E., HEREDIA SOTO, V., MARQUEZ-RODAS, I., ECHARRI, M. J., LACAMBRA-CALVET, C., SAEZ, R., CUSIDO, M., REDONDO, A., PAZ-ARES, L., HARDISSON, D., MENDIOLA, M., PALACIOS, J., BENITEZ, J. & GARCIA, M. J. 2016. The NER-related gene GTF2H5 predicts survival in high-grade serous ovarian cancer patients. *J Gynecol Oncol,* 27**,** e7.

GENG, J., LUO, H., PU, Y., ZHOU, Z., WU, X., XU, W. & YANG, Z. 2012. Methylation mediated silencing of miR-23b expression and its role in glioma stem cells. *Neurosci Lett,* 528**,** 185-9.

GRAHAM, L. D., PEDERSEN, S. K., BROWN, G. S., HO, T., KASSIR, Z., MOYNIHAN, A. T., VIZGOFT, E. K., DUNNE, R., PIMLOTT, L., YOUNG, G. P., LAPOINTE, L. C. & MOLLOY, P. L. 2011. Colorectal Neoplasia Differentially Expressed (CRNDE), a Novel Gene with Elevated Expression in Colorectal Adenomas and Adenocarcinomas. *Genes Cancer,* 2**,** 829-40.

GRUNAU, C., CLARK, S. J. & ROSENTHAL, A. 2001. Bisulfite genomic sequencing: systematic investigation of critical experimental parameters. *Nucleic Acids Res,* 29**,** E65-5.

GUIDA, F., SANDANGER, T. M., CASTAGNE, R., CAMPANELLA, G., POLIDORO, S., PALLI, D., KROGH, V., TUMINO, R., SACERDOTE, C., PANICO, S., SEVERI, G., KYRTOPOULOS, S. A., GEORGIADIS, P., VERMEULEN, R. C., LUND, E., VINEIS, P. & CHADEAU-HYAM, M. 2015. Dynamics of smoking-induced genome-wide methylation changes with time since smoking cessation. *Hum Mol Genet,* 24**,** 2349-59.

GULYAEVA, L. F. & KUSHLINSKIY, N. E. 2016. Regulatory mechanisms of microRNA expression. *J Transl Med,* 14**,** 143.

GUO, S., DIEP, D., PLONGTHONGKUM, N., FUNG, H. L., ZHANG, K. & ZHANG, K. 2017. Identification of methylation haplotype blocks aids in deconvolution of heterogeneous tissue samples and tumor tissue-of-origin mapping from plasma DNA. *Nat Genet,* 49**,** 635-642.

GUTTMAN, M. & RINN, J. L. 2012. Modular regulatory principles of large non-coding RNAs. *Nature,* 482**,** 339-46.

HA, M. & KIM, V. N. 2014. Regulation of microRNA biogenesis. *Nat Rev Mol Cell Biol,* 15**,** 509-24.

HANAHAN, D. & WEINBERG, R. A. 2000. The hallmarks of cancer. *Cell,* 100**,** 57-70.

HANAHAN, D. & WEINBERG, R. A. 2011. Hallmarks of cancer: the next generation. *Cell,* 144**,** 646-74.

HANOUN, N., DELPU, Y., SURIAWINATA, A. A., BOURNET, B., BUREAU, C., SELVES, J., TSONGALIS, G. J., DUFRESNE, M., BUSCAIL, L., CORDELIER, P. & TORRISANI, J. 2010. The silencing of microRNA 148a production by DNA hypermethylation is an early event in pancreatic carcinogenesis. *Clin Chem,* 56**,** 1107-18.

HANRAHAN, V., CURRIE, M. J., GUNNINGHAM, S. P., MORRIN, H. R., SCOTT, P. A., ROBINSON, B. A. & FOX, S. B. 2003. The angiogenic switch for vascular endothelial growth factor (VEGF)-A, VEGF-B, VEGF-C, and VEGF-D in the adenoma-carcinoma sequence during colorectal cancer progression. *J Pathol,* 200**,** 183-94.

HARROW, J., FRANKISH, A., GONZALEZ, J. M., TAPANARI, E., DIEKHANS, M., KOKOCINSKI, F., AKEN, B. L., BARRELL, D., ZADISSA, A., SEARLE, S., BARNES, I., BIGNELL, A., BOYCHENKO, V., HUNT, T., KAY, M., MUKHERJEE, G., RAJAN, J., DESPACIO-REYES, G., SAUNDERS, G., STEWARD, C., HARTE, R., LIN, M., HOWALD, C., TANZER, A., DERRIEN, T., CHRAST, J., WALTERS, N., BALASUBRAMANIAN, S., PEI, B., TRESS, M., RODRIGUEZ, J. M., EZKURDIA, I., VAN BAREN, J., BRENT, M., HAUSSLER, D., KELLIS, M., VALENCIA, A., REYMOND, A., GERSTEIN, M., GUIGO, R. & HUBBARD, T. J. 2012. GENCODE: the reference human genome annotation for The ENCODE Project. *Genome Res,* 22**,** 1760-74.

HERBST, R. S., HEYMACH, J. V. & LIPPMAN, S. M. 2008. Lung cancer. *N Engl J Med,* 359**,** 1367-80.

HERMAN, J. G., GRAFF, J. R., MYOHANEN, S., NELKIN, B. D. & BAYLIN, S. B. 1996. Methylation-specific PCR: a novel PCR assay for methylation status of CpG islands. *Proc Natl Acad Sci U S A,* 93**,** 9821-6.

HOLZER, A. K., SAMIMI, G., KATANO, K., NAERDEMANN, W., LIN, X., SAFAEI, R. & HOWELL, S. B. 2004. The copper influx transporter human copper transport protein 1 regulates the uptake of cisplatin in human ovarian carcinoma cells. *Mol Pharmacol,* 66**,** 817-23.

HTTP://WWW.WHO.INT/CANCER/EN/ 2018. *World Health Organization*.

HU, H., SHU, M., HE, L., YU, X., LIU, X., LU, Y., CHEN, Y., MIAO, X. & CHEN, X. 2017. Epigenomic landscape of 5-hydroxymethylcytosine reveals its transcriptional regulation of lncRNAs in colorectal cancer. *Br J Cancer,* 116**,** 658-668.

HUBER, W., VON HEYDEBRECK, A., SULTMANN, H., POUSTKA, A. & VINGRON, M. 2002. Variance stabilization applied to microarray data calibration and to the quantification of differential expression. *Bioinformatics,* 18 Suppl 1**,** S96-104.

IBANEZ DE CACERES, I., CORTES-SEMPERE, M., MORATILLA, C., MACHADO-PINILLA, R., RODRIGUEZ-FANJUL, V., MANGUAN-GARCIA, C., CEJAS, P., LOPEZ-RIOS, F., PAZ-ARES, L.,

DE CASTROCARPENO, J., NISTAL, M., BELDA-INIESTA, C. & PERONA, R. 2010. IGFBP-3 hypermethylation-derived deficiency mediates cisplatin resistance in non-small-cell lung cancer. *Oncogene,* 29**,** 1681-90.

IBANEZ DE CACERES, I., DULAIMI, E., HOFFMAN, A. M., AL-SALEEM, T., UZZO, R. G. & CAIRNS, P. 2006. Identification of novel target genes by an epigenetic reactivation screen of renal cancer. *Cancer Res,* 66**,** 5021-8.

IWASAKI, H., OKABE, T., TAKARA, K., YOSHIDA, Y., HANASHIRO, K. & OKU, H. 2010. Down-regulation of lipids transporter ABCA1 increases the cytotoxicity of nitidine. *Cancer Chemother Pharmacol,* 66**,** 953-9.

JAZAERI, A. A., BRYANT, J. L., PARK, H., LI, H., DAHIYA, N., STOLER, M. H., FERRISS, J. S. & DUTTA, A. 2011. Molecular requirements for transformation of fallopian tube epithelial cells into serous carcinoma. *Neoplasia,* 13**,** 899-911.

JI, P., DIEDERICHS, S., WANG, W., BOING, S., METZGER, R., SCHNEIDER, P. M., TIDOW, N., BRANDT, B., BUERGER, H., BULK, E., THOMAS, M., BERDEL, W. E., SERVE, H. & MULLER-TIDOW, C. 2003. MALAT-1, a novel noncoding RNA, and thymosin beta4 predict metastasis and survival in early-stage non-small cell lung cancer. *Oncogene,* 22**,** 8031-41.

JIANG, B. C., SUN, W. X., HE, L. N., CAO, D. L., ZHANG, Z. J. & GAO, Y. J. 2015a. Identification of lncRNA expression profile in the spinal cord of mice following spinal nerve ligation-induced neuropathic pain. *Mol Pain,* 11**,** 43.

JIANG, Q., WANG, J., WU, X., MA, R., ZHANG, T., JIN, S., HAN, Z., TAN, R., PENG, J., LIU, G., LI, Y. & WANG, Y. 2015b. LncRNA2Target: a database for differentially expressed genes after lncRNA knockdown or overexpression. *Nucleic Acids Res,* 43**,** D193-6.

JIN, Y., XU, P., LIU, X., ZHANG, C., TAN, C., CHEN, C., SUN, X. & XU, Y. 2016. Cigarette Smoking, BPDE-DNA Adducts, and Aberrant Promoter Methylations of Tumor Suppressor Genes (TSGs) in NSCLC from Chinese Population. *Cancer Invest,* 34**,** 173-80.

JONGEN-LAVRENCIC, M., SUN, S. M., DIJKSTRA, M. K., VALK, P. J. & LOWENBERG, B. 2008. MicroRNA expression profiling in relation to the genetic heterogeneity of acute myeloid leukemia. *Blood,* 111**,** 5078-85.

JUSUFOVIC, E., RIJAVEC, M., KESER, D., KOROSEC, P., SODJA, E., ILJAZOVIC, E., RADOJEVIC, Z. & KOSNIK, M. 2012. let-7b and miR-126 are down-regulated in tumor tissue and correlate with microvessel density and survival outcomes in non--small--cell lung cancer. *PLoS One,* 7**,** e45577.

KARST, A. M. & DRAPKIN, R. 2010. Ovarian cancer pathogenesis: a model in evolution. *J Oncol,* 2010**,** 932371.

KARTALOU, M. & ESSIGMANN, J. M. 2001. Mechanisms of resistance to cisplatin. *Mutat Res,* 478**,** 23-43.

KASPER, D. L. 2015. *Harrison's principles of internal medicine,* New York, McGraw Hill Education.

KATSUOKA, F., MOTOHASHI, H., ENGEL, J. D. & YAMAMOTO, M. 2005. Nrf2 transcriptionally activates the mafG gene through an antioxidant response element. *J Biol Chem,* 280**,** 4483-90.

KATSUOKA, F. & YAMAMOTO, M. 2016. Small Maf proteins (MafF, MafG, MafK): History, structure and function. *Gene,* 586**,** 197-205.

KAWAHARA, T., IDE, H., KASHIWAGI, E., PATTERSON, J. D., INOUE, S., SHAREEF, H. K., ALJARAH, A. K., ZHENG, Y., BARAS, A. S. & MIYAMOTO, H. 2015. Silodosin inhibits the growth of bladder cancer cells and enhances the cytotoxic activity of cisplatin via ELK1 inactivation. *Am J Cancer Res,* 5**,** 2959-68.

KILIC, U., KILIC, E., TUZCU, Z., TUZCU, M., OZERCAN, I. H., YILMAZ, O., SAHIN, F. & SAHIN, K. 2013. Melatonin suppresses cisplatin-induced nephrotoxicity via activation of Nrf-2/HO-1 pathway. *Nutr Metab (Lond),* 10**,** 7.

KIN, T., YAMADA, K., TERAI, G., OKIDA, H., YOSHINARI, Y., ONO, Y., KOJIMA, A., KIMURA, Y., KOMORI, T. & ASAI, K. 2007. fRNAdb: a platform for mining/annotating functional RNA candidates from non-coding RNA sequences. *Nucleic Acids Res,* 35**,** D145-8.

KOZOMARA, A. & GRIFFITHS-JONES, S. 2014. miRBase: annotating high confidence microRNAs using deep sequencing data. *Nucleic Acids Res,* 42**,** D68-73.

KREUZ, S. & FISCHLE, W. 2016. Oxidative stress signaling to chromatin in health and disease. *Epigenomics,* 8**,** 843-62.

LEDERMANN, J. A., RAJA, F. A., FOTOPOULOU, C., GONZALEZ-MARTIN, A., COLOMBO, N., SESSA, C. & GROUP, E. G. W. 2013. Newly diagnosed and relapsed epithelial ovarian carcinoma: ESMO Clinical Practice Guidelines for diagnosis, treatment and follow-up. *Ann Oncol,* 24 Suppl 6**,** vi24-32.

LEVINA, V., MARRANGONI, A. M., DEMARCO, R., GORELIK, E. & LOKSHIN, A. E. 2008. Drug-selected human lung cancer stem cells: cytokine network, tumorigenic and metastatic properties. *PLoS One,* 3**,** e3077.

LI, B. & DEWEY, C. N. 2011. RSEM: accurate transcript quantification from RNA-Seq data with or without a reference genome. *BMC Bioinformatics,* 12**,** 323.

LI, F., CAO, L., HANG, D., WANG, F. & WANG, Q. 2015. Long non-coding RNA HOTTIP is up-regulated and associated with poor prognosis in patients with osteosarcoma. *Int J Clin Exp Pathol,* 8**,** 11414-20.

LI, L., GU, M., YOU, B., SHI, S., SHAN, Y., BAO, L. & YOU, Y. 2016. Long non-coding RNA ROR promotes proliferation, migration and chemoresistance of nasopharyngeal carcinoma. *Cancer Sci,* 107**,** 1215-22.

LI, W., YU, S., LIU, T., KIM, J. H., BLANK, V., LI, H. & KONG, A. N. 2008. Heterodimerization with small Maf proteins enhances nuclear retention of Nrf2 via masking the NESzip motif. *Biochim Biophys Acta,* 1783**,** 1847-56.

LIU, G., LI, Y. & GAO, X. G. 2016. microRNA-181a is upregulated in human atherosclerosis plaques and involves in the oxidative stress-induced endothelial cell dysfunction through direct targeting Bcl-2. *Eur Rev Med Pharmacol Sci,* 20**,** 3092-100.

LIU, H., WU, X., HUANG, J., PENG, J. & GUO, L. 2015. miR-7 modulates chemoresistance of small cell lung cancer by repressing MRP1/ABCC1. *Int J Exp Pathol,* 96**,** 240-7.

LIU, R., LIU, X., ZHENG, Y., GU, J., XIONG, S., JIANG, P., JIANG, X., HUANG, E., YANG, Y., GE, D. & CHU, Y. 2014. MicroRNA-7 sensitizes non-small cell lung cancer cells to paclitaxel. *Oncol Lett,* 8**,** 2193-2200.

LOPEZ-LERA, A., PERNIA, O., LOPEZ-TRASCASA, M. & IBANEZ DE CACERES, I. 2014. Expression of the SERPING1 gene is not regulated by promoter hypermethylation in peripheral blood mononuclear cells from patients with hereditary angioedema due to C1-inhibitor deficiency. *Orphanet J Rare Dis,* 9**,** 103.

LUJAMBIO, A., CALIN, G. A., VILLANUEVA, A., ROPERO, S., SANCHEZ-CESPEDES, M., BLANCO, D., MONTUENGA, L. M., ROSSI, S., NICOLOSO, M. S., FALLER, W. J., GALLAGHER, W. M., ECCLES, S. A., CROCE, C. M. & ESTELLER, M. 2008. A microRNA DNA methylation signature for human cancer metastasis. *Proc Natl Acad Sci U S A,* 105**,** 13556-61.

LUJAMBIO, A., ROPERO, S., BALLESTAR, E., FRAGA, M. F., CERRATO, C., SETIEN, F., CASADO, S., SUAREZ-GAUTHIER, A., SANCHEZ-CESPEDES, M., GIT, A., SPITERI, I., DAS, P. P., CALDAS, C., MISKA, E. & ESTELLER, M. 2007. Genetic unmasking of an epigenetically silenced microRNA in human cancer cells. *Cancer Res,* 67**,** 1424-9.

LUO, J., SOLIMINI, N. L. & ELLEDGE, S. J. 2009. Principles of cancer therapy: oncogene and non-oncogene addiction. *Cell,* 136**,** 823-37.

MA, J., FANG, B., ZENG, F., PANG, H., ZHANG, J., SHI, Y., WU, X., CHENG, L., MA, C., XIA, J. & WANG, Z. 2014. Curcumin inhibits cell growth and invasion through up-regulation of miR-7 in pancreatic cancer cells. *Toxicol Lett,* 231**,** 82-91.

MA, L., BAJIC, V. B. & ZHANG, Z. 2013. On the classification of long non-coding RNAs. *RNA Biol,* 10**,** 925-33.

MAGENTA, A., CENCIONI, C., FASANARO, P., ZACCAGNINI, G., GRECO, S., SARRA-FERRARIS, G., ANTONINI, A., MARTELLI, F. & CAPOGROSSI, M. C. 2011. miR-200c is upregulated by oxidative stress and induces endothelial cell apoptosis and senescence via ZEB1 inhibition. *Cell Death Differ,* 18**,** 1628-39.

MARTINS, N. M., SANTOS, N. A., CURTI, C., BIANCHI, M. L. & SANTOS, A. C. 2008. Cisplatin induces mitochondrial oxidative stress with resultant energetic metabolism impairment, membrane rigidification and apoptosis in rat liver. *J Appl Toxicol,* 28**,** 337-44.

MARULLO, R., WERNER, E., DEGTYAREVA, N., MOORE, B., ALTAVILLA, G., RAMALINGAM, S. S. & DOETSCH, P. W. 2013. Cisplatin induces a mitochondrial-ROS response that contributes to cytotoxicity depending on mitochondrial redox status and bioenergetic functions. *PLoS One,* 8**,** e81162.

MCGUIRE, S. 2016. World Cancer Report 2014. Geneva, Switzerland: World Health Organization, International Agency for Research on Cancer, WHO Press, 2015. *Adv Nutr,* 7**,** 418-9.

MENDELL, J. T. & OLSON, E. N. 2012. MicroRNAs in stress signaling and human disease. *Cell,* 148**,** 1172-87.

MERCER, T. R., DINGER, M. E. & MATTICK, J. S. 2009. Long non-coding RNAs: insights into functions. *Nat Rev Genet,* 10**,** 155-9.

MOORE, L. D., LE, T. & FAN, G. 2013. DNA methylation and its basic function. *Neuropsychopharmacology,* 38**,** 23-38.

MOTOHASHI, H., KATSUOKA, F., MIYOSHI, C., UCHIMURA, Y., SAITOH, H., FRANCASTEL, C., ENGEL, J. D. & YAMAMOTO, M. 2006. MafG sumoylation is required for active transcriptional repression. *Mol Cell Biol,* 26**,** 4652-63.

NG, K., PULLIRSCH, D., LEEB, M. & WUTZ, A. 2007. Xist and the order of silencing. *EMBO Rep,* 8**,** 34-9.

NICHOLSON, L. J., SMITH, P. R., HILLER, L., SZLOSAREK, P. W., KIMBERLEY, C., SEHOULI, J., KOENSGEN, D., MUSTEA, A., SCHMID, P. & CROOK, T. 2009. Epigenetic silencing of argininosuccinate synthetase confers resistance to platinum-induced cell death but collateral sensitivity to arginine auxotrophy in ovarian cancer. *Int J Cancer,* 125**,** 1454-63.

NING, Q., LI, Y., WANG, Z., ZHOU, S., SUN, H. & YU, G. 2017. The Evolution and Expression Pattern of Human Overlapping lncRNA and Protein-coding Gene Pairs. 7**,** 42775.

NISHIDA, N. & KUDO, M. 2013. Oxidative stress and epigenetic instability in human hepatocarcinogenesis. *Dig Dis,* 31**,** 447-53.

NISHITA, Y., YOSHIDA, I., SADO, T. & TAKAGI, N. 1996. Genomic imprinting and chromosomal localization of the human MEST gene. *Genomics,* 36**,** 539-42.

NOGUER-DANCE, M., ABU-AMERO, S., AL-KHTIB, M., LEFEVRE, A., COULLIN, P., MOORE, G. E. & CAVAILLE, J. 2010. The primate-specific microRNA gene cluster (C19MC) is imprinted in the placenta. *Hum Mol Genet,* 19**,** 3566-82.

OROM, U. A., DERRIEN, T., BERINGER, M., GUMIREDDY, K., GARDINI, A., BUSSOTTI, G., LAI, F., ZYTNICKI, M., NOTREDAME, C., HUANG, Q., GUIGO, R. & SHIEKHATTAR, R. 2010. Long noncoding RNAs with enhancer-like function in human cells. *Cell,* 143**,** 46-58.

OSTROW, K. L., MICHAILIDI, C., GUERRERO-PRESTON, R., HOQUE, M. O., GREENBERG, A., ROM, W. & SIDRANSKY, D. 2013. Cigarette smoke induces methylation of the tumor suppressor gene NISCH. *Epigenetics,* 8**,** 383-8.

OZES, A. R., MILLER, D. F., OZES, O. N., FANG, F., LIU, Y., MATEI, D., HUANG, T. & NEPHEW, K. P. 2016. NF-kappaB-HOTAIR axis links DNA damage response, chemoresistance and cellular senescence in ovarian cancer. *Oncogene,* 35**,** 5350-5361.

PANG, K. C., STEPHEN, S., DINGER, M. E., ENGSTROM, P. G., LENHARD, B. & MATTICK, J. S. 2007. RNAdb 2.0--an expanded database of mammalian non-coding RNAs. *Nucleic Acids Res,* 35**,** D178-82.

PARK, S., SHIMIZU, C., SHIMOYAMA, T., TAKEDA, M., ANDO, M., KOHNO, T., KATSUMATA, N., KANG, Y. K., NISHIO, K. & FUJIWARA, Y. 2006. Gene expression profiling of ATP-binding cassette (ABC) transporters as a predictor of the pathologic response to neoadjuvant chemotherapy in breast cancer patients. *Breast Cancer Res Treat,* 99**,** 9-17.

PATHAK, A., STEWART, D. R., FAUCZ, F. R., XEKOUKI, P., BASS, S., VOGT, A., ZHANG, X., BOLAND, J., YEAGER, M., LOUD, J. T., NATHANSON, K. L., MCGLYNN, K. A., STRATAKIS, C. A., GREENE, M. H. & MIRABELLO, L. 2015. Rare inactivating PDE11A variants associated with testicular germ cell tumors. *Endocr Relat Cancer,* 22**,** 909-17.

PERNIA, O., BELDA-INIESTA, C., PULIDO, V., CORTES-SEMPERE, M., RODRIGUEZ, C., VERA, O., SOTO, J., JIMENEZ, J., TAUS, A., ROJO, F., ARRIOLA, E., ROVIRA, A., ALBANELL, J., MACIAS, M. T., DE CASTRO, J., PERONA, R. & IBANEZ DE CACERES, I. 2014. Methylation status of IGFBP-3 as a useful clinical tool for deciding on a concomitant radiotherapy. *Epigenetics,* 9**,** 1446-53.

PLASENCIA, C., MARTINEZ-BALIBREA, E., MARTINEZ-CARDUS, A., QUINN, D. I., ABAD, A. & NEAMATI, N. 2006. Expression analysis of genes involved in oxaliplatin response and development of oxaliplatin-resistant HT29 colon cancer cells. *Int J Oncol,* 29**,** 225-35.

PNG, K. J., YOSHIDA, M., ZHANG, X. H., SHU, W., LEE, H., RIMNER, A., CHAN, T. A., COMEN, E., ANDRADE, V. P., KIM, S. W., KING, T. A., HUDIS, C. A., NORTON, L., HICKS, J., MASSAGUE, J. & TAVAZOIE, S. F. 2011. MicroRNA-335 inhibits tumor reinitiation and is silenced through genetic and epigenetic mechanisms in human breast cancer. *Genes Dev,* 25**,** 226-31.

PONTING, C. P., OLIVER, P. L. & REIK, W. 2009. Evolution and functions of long noncoding RNAs. *Cell,* 136**,** 629-41.

QUAGLIATA, L., MATTER, M. S., PISCUOGLIO, S., ARABI, L., RUIZ, C., PROCINO, A., KOVAC, M., MORETTI, F., MAKOWSKA, Z., BOLDANOVA, T., ANDERSEN, J. B., HAMMERLE, M., TORNILLO, L., HEIM, M. H., DIEDERICHS, S., CILLO, C. & TERRACCIANO, L. M. 2014. Long noncoding RNA HOTTIP/HOXA13 expression is associated with disease progression and predicts outcome in hepatocellular carcinoma patients. *Hepatology,* 59**,** 911-23.

RABIK, C. A. & DOLAN, M. E. 2007. Molecular mechanisms of resistance and toxicity associated with platinating agents. *Cancer Treat Rev,* 33**,** 9-23.

RAJEEVAN, M. S., VERNON, S. D., TAYSAVANG, N. & UNGER, E. R. 2001. Validation of array-based gene expression profiles by real-time (kinetic) RT-PCR. *J Mol Diagn,* 3**,** 26-31.

REIK, W. & WALTER, J. 2001. Genomic imprinting: parental influence on the genome. *Nat Rev Genet,* 2**,** 21-32.

ROBINSON, M. D. & OSHLACK, A. 2010. A scaling normalization method for differential expression analysis of RNA-seq data. *Genome Biol,* 11**,** R25.

SAITO, Y., SUZUKI, H., TSUGAWA, H., NAKAGAWA, I., MATSUZAKI, J., KANAI, Y. & HIBI, T. 2009. Chromatin remodeling at Alu repeats by epigenetic treatment activates silenced microRNA-512-5p with downregulation of Mcl-1 in human gastric cancer cells. *Oncogene,* 28**,** 2738-44.

SANCHEZ-PEREZ, I., MURGUIA, J. R. & PERONA, R. 1998. Cisplatin induces a persistent activation of JNK that is related to cell death. *Oncogene,* 16**,** 533-40.

SANDOVICI, I., LEPPERT, M., HAWK, P. R., SUAREZ, A., LINARES, Y. & SAPIENZA, C. 2003. Familial aggregation of abnormal methylation of parental alleles at the IGF2/H19 and IGF2R differentially methylated regions. *Hum Mol Genet,* 12**,** 1569-78.

SCHAAF, G. J., MAAS, R. F., DE GROENE, E. M. & FINK-GREMMELS, J. 2002. Management of oxidative stress by heme oxygenase-1 in cisplatin-induced toxicity in renal tubular cells. *Free Radic Res,* 36**,** 835-43.

SCHEMBRI, F., SRIDHAR, S., PERDOMO, C., GUSTAFSON, A. M., ZHANG, X., ERGUN, A., LU, J., LIU, G., BOWERS, J., VAZIRI, C., OTT, K., SENSINGER, K., COLLINS, J. J., BRODY, J. S., GETTS, R.,

LENBURG, M. E. & SPIRA, A. 2009. MicroRNAs as modulators of smoking-induced gene expression changes in human airway epithelium. *Proc Natl Acad Sci U S A,* 106**,** 2319-24.

SCHMIDT, M., HELLWIG, B., HAMMAD, S., OTHMAN, A., LOHR, M., CHEN, Z., BOEHM, D., GEBHARD, S., PETRY, I., LEBRECHT, A., CADENAS, C., MARCHAN, R., STEWART, J. D., SOLBACH, C., HOLMBERG, L., EDLUND, K., KULTIMA, H. G., RODY, A., BERGLUND, A., LAMBE, M., ISAKSSON, A., BOTLING, J., KARN, T., MULLER, V., GERHOLD-AY, A., COTARELO, C., SEBASTIAN, M., KRONENWETT, R., BOJAR, H., LEHR, H. A., SAHIN, U., KOELBL, H., GEHRMANN, M., MICKE, P., RAHNENFUHRER, J. & HENGSTLER, J. G. 2012. A comprehensive analysis of human gene expression profiles identifies stromal immunoglobulin kappa C as a compatible prognostic marker in human solid tumors. *Clin Cancer Res,* 18**,** 2695-703.

SHOEMAKER, R., DENG, J., WANG, W. & ZHANG, K. 2010. Allele-specific methylation is prevalent and is contributed by CpG-SNPs in the human genome. *Genome Res,* 20**,** 883-9.

SIDDIK, Z. H. 2003. Cisplatin: mode of cytotoxic action and molecular basis of resistance. *Oncogene,* 22**,** 7265-79.

SMEDBERG, J. L., SMITH, E. R., CAPO-CHICHI, C. D., FROLOV, A., YANG, D. H., GODWIN, A. K. & XU, X. X. 2002. Ras/MAPK pathway confers basement membrane dependence upon endoderm differentiation of embryonic carcinoma cells. *J Biol Chem,* 277**,** 40911-8.

SMYTH, G. K. 2004. Linear models and empirical bayes methods for assessing differential expression in microarray experiments. *Stat Appl Genet Mol Biol,* 3**,** Article3.

SORRENTINO, A., LIU, C. G., ADDARIO, A., PESCHLE, C., SCAMBIA, G. & FERLINI, C. 2008. Role of microRNAs in drug-resistant ovarian cancer cells. *Gynecol Oncol,* 111**,** 478-86.

SOTO, J., RODRIGUEZ-ANTOLIN, C., VALLESPIN, E., DE CASTRO CARPENO, J. & IBANEZ DE CACERES, I. 2014. The impact of next-generation sequencing on the DNA methylation-based translational cancer research. *Transl Res,* 169**,** 1-18 e1.

STIRZAKER, C., TABERLAY, P. C., STATHAM, A. L. & CLARK, S. J. 2014. Mining cancer methylomes: prospects and challenges. *Trends Genet,* 30**,** 75-84.

SUNDAR, I. K., YAO, H. & RAHMAN, I. 2013. Oxidative stress and chromatin remodeling in chronic obstructive pulmonary disease and smoking-related diseases. *Antioxid Redox Signal,* 18**,** 1956-71.

SUZUKI, H., YAMAMOTO, E., NOJIMA, M., KAI, M., YAMANO, H. O., YOSHIKAWA, K., KIMURA, T., KUDO, T., HARADA, E., SUGAI, T., TAKAMARU, H., NIINUMA, T., MARUYAMA, R., YAMAMOTO, H., TOKINO, T., IMAI, K., TOYOTA, M. & SHINOMURA, Y. 2010. Methylation-associated silencing of microRNA-34b/c in gastric cancer and its involvement in an epigenetic field defect. *Carcinogenesis,* 31**,** 2066-73.

TAKAI, D. & JONES, P. A. 2002. Comprehensive analysis of CpG islands in human chromosomes 21 and 22. *Proc Natl Acad Sci U S A,* 99**,** 3740-5.

TAKAI, D. & JONES, P. A. 2003. The CpG island searcher: a new WWW resource. *In Silico Biol,* 3**,** 235-40.

TAKIGUCHI, Y., SEKINE, I., IWASAWA, S., KURIMOTO, R. & TATSUMI, K. 2014. Chronic obstructive pulmonary disease as a risk factor for lung cancer. *World J Clin Oncol,* 5**,** 660-6.

TRIPATHI, V., ELLIS, J. D., SHEN, Z., SONG, D. Y., PAN, Q., WATT, A. T., FREIER, S. M., BENNETT, C. F., SHARMA, A., BUBULYA, P. A., BLENCOWE, B. J., PRASANTH, S. G. & PRASANTH, K. V. 2010. The nuclear-retained noncoding RNA MALAT1 regulates alternative splicing by modulating SR splicing factor phosphorylation. *Mol Cell,* 39**,** 925-38.

TSAI, K. W., KAO, H. W., CHEN, H. C., CHEN, S. J. & LIN, W. C. 2009. Epigenetic control of the expression of a primate-specific microRNA cluster in human cancer cells. *Epigenetics,* 4**,** 587-92.

TSAI, K. W., LIAO, Y. L., WU, C. W., HU, L. Y., LI, S. C., CHAN, W. C., HO, M. R., LAI, C. H., KAO, H. W., FANG, W. L., HUANG, K. H. & LIN, W. C. 2011. Aberrant hypermethylation of miR-9 genes in gastric cancer. *Epigenetics,* 6**,** 1189-97.

VENTER, J. C., ADAMS, M. D., MYERS, E. W., LI, P. W., MURAL, R. J., SUTTON, G. G., SMITH, H. O., YANDELL, M., EVANS, C. A., HOLT, R. A., GOCAYNE, J. D., AMANATIDES, P., BALLEW, R. M., HUSON, D. H., WORTMAN, J. R., ZHANG, Q., KODIRA, C. D., ZHENG, X. H., CHEN, L., SKUPSKI, M., SUBRAMANIAN, G., THOMAS, P. D., ZHANG, J., GABOR MIKLOS, G. L., NELSON, C., BRODER, S., CLARK, A. G., NADEAU, J., MCKUSICK, V. A., ZINDER, N., LEVINE, A. J., ROBERTS, R. J., SIMON, M., SLAYMAN, C., HUNKAPILLER, M., BOLANOS, R., DELCHER, A., DEW, I., FASULO, D., FLANIGAN, M., FLOREA, L., HALPERN, A., HANNENHALLI, S., KRAVITZ, S., LEVY, S., MOBARRY, C., REINERT, K., REMINGTON, K., ABU-THREIDEH, J., BEASLEY, E., BIDDICK, K., BONAZZI, V., BRANDON, R., CARGILL, M., CHANDRAMOULISWARAN, I., CHARLAB, R., CHATURVEDI, K., DENG, Z., DI FRANCESCO, V., DUNN, P., EILBECK, K., EVANGELISTA, C., GABRIELIAN, A. E., GAN, W., GE, W., GONG, F., GU, Z., GUAN, P., HEIMAN, T. J., HIGGINS, M. E., JI, R. R., KE, Z., KETCHUM, K. A., LAI, Z., LEI, Y., LI, Z., LI, J., LIANG, Y., LIN, X., LU, F., MERKULOV, G. V., MILSHINA, N., MOORE, H. M., NAIK, A. K., NARAYAN, V. A., NEELAM, B., NUSSKERN, D., RUSCH, D. B., SALZBERG, S., SHAO, W., SHUE, B., SUN, J., WANG, Z., WANG, A., WANG, X., WANG, J., WEI, M., WIDES, R., XIAO, C., YAN, C., et al. 2001. The sequence of the human genome. *Science,* 291**,** 1304-51.

VERA, O., JIMENEZ, J., PERNIA, O., RODRIGUEZ-ANTOLIN, C., RODRIGUEZ, C., SANCHEZ CABO, F., SOTO, J., ROSAS, R., LOPEZ-MAGALLON, S., ESTEBAN RODRIGUEZ, I., DOPAZO, A., ROJO, F., BELDA, C., ALVAREZ, R., VALENTIN, J., BENITEZ, J., PERONA, R., DE CASTRO, J. & IBANEZ DE CACERES, I. 2017. DNA Methylation of miR-7 is a Mechanism Involved in Platinum Response through MAFG Overexpression in Cancer Cells. *Theranostics,* 7**,** 4118-4134.

VILA, M. R., LLORETA, J., SCHUSSLER, M. H., BERROZPE, G., WELT, S. & REAL, F. X. 1995. New pancreas cancers cell lines that represent distinct stages of ductal differentiation. *Lab Invest,* 72**,** 395-404.

VOLDERS, P. J., VERHEGGEN, K., MENSCHAERT, G., VANDEPOELE, K., MARTENS, L., VANDESOMPELE, J. & MESTDAGH, P. 2015. An update on LNCipedia: a database for annotated human lncRNA sequences. *Nucleic Acids Res,* 43**,** D174-80.

WANG, G., WANG, R., STRULOVICI-BAREL, Y., SALIT, J., STAUDT, M. R., AHMED, J., TILLEY, A. E., YEE-LEVIN, J., HOLLMANN, C., HARVEY, B. G., KANER, R. J., MEZEY, J. G., SRIDHAR, S., PILLAI, S. G., HILTON, H., WOLFF, G., BITTER, H., VISVANATHAN, S., FINE, J. S., STEVENSON, C. S. & CRYSTAL, R. G. 2015. Persistence of smoking-induced dysregulation of miRNA expression in the small airway epithelium despite smoking cessation. *PLoS One,* 10**,** e0120824.

WANG, J., DUNCAN, D., SHI, Z. & ZHANG, B. 2013. WEB-based GEne SeT AnaLysis Toolkit (WebGestalt): update 2013. *Nucleic Acids Res,* 41**,** W77-83.

WANG, K. C. & CHANG, H. Y. 2011. Molecular mechanisms of long noncoding RNAs. *Mol Cell,* 43**,** 904-14.

WANG, L., XIANG, S., WILLIAMS, K. A., DONG, H., BAI, W., NICOSIA, S. V., KHOCHBIN, S., BEPLER, G. & ZHANG, X. 2012. Depletion of HDAC6 enhances cisplatin-induced DNA damage and apoptosis in non-small cell lung cancer cells. *PLoS One,* 7**,** e44265.

WANG, Q., ZHONG, M., LIU, W., LI, J., HUANG, J. & ZHENG, L. 2011. Alterations of microRNAs in cisplatin-resistant human non-small cell lung cancer cells (A549/DDP). *Exp Lung Res,* 37**,** 427-34.

WANG, X., CHORLEY, B. N., PITTMAN, G. S., KLEEBERGER, S. R., BROTHERS, J., 2ND, LIU, G., SPIRA, A. & BELL, D. A. 2010. Genetic variation and antioxidant response gene expression in the bronchial airway epithelium of smokers at risk for lung cancer. *PLoS One,* 5**,** e11934.

WANG, Y., ZHANG, D., WU, K., ZHAO, Q., NIE, Y. & FAN, D. 2014. Long noncoding RNA MRUL promotes ABCB1 expression in multidrug-resistant gastric cancer cell sublines. *Mol Cell Biol,* 34**,** 3182-93.

WEBER, B., STRESEMANN, C., BRUECKNER, B. & LYKO, F. 2007. Methylation of human microRNA genes in normal and neoplastic cells. *Cell Cycle,* 6**,** 1001-5.

WEBER, M., BAKER, M. B., MOORE, J. P. & SEARLES, C. D. 2010. MiR-21 is induced in endothelial cells by shear stress and modulates apoptosis and eNOS activity. *Biochem Biophys Res Commun,* 393**,** 643-8.

WEBSTER, R. J., GILES, K. M., PRICE, K. J., ZHANG, P. M., MATTICK, J. S. & LEEDMAN, P. J. 2009. Regulation of epidermal growth factor receptor signaling in human cancer cells by microRNA-7. *J Biol Chem,* 284**,** 5731-41.

WILUSZ, J. E., SUNWOO, H. & SPECTOR, D. L. 2009. Long noncoding RNAs: functional surprises from the RNA world. *Genes Dev,* 23**,** 1494-504.

WRIGHT, A. A., BOHLKE, K., ARMSTRONG, D. K., BOOKMAN, M. A., CLIBY, W. A., COLEMAN, R. L., DIZON, D. S., KASH, J. J., MEYER, L. A., MOORE, K. N., OLAWAIYE, A. B., OLDHAM, J., SALANI, R., SPARACIO, D., TEW, W. P., VERGOTE, I. & EDELSON, M. I. 2016. Neoadjuvant Chemotherapy for Newly Diagnosed, Advanced Ovarian Cancer: Society of Gynecologic Oncology and American Society of Clinical Oncology Clinical Practice Guideline. *J Clin Oncol,* 34**,** 3460-73.

WU, C., WANGPAICHITR, M., FEUN, L., KUO, M. T., ROBLES, C., LAMPIDIS, T. & SAVARAJ, N. 2005. Overcoming cisplatin resistance by mTOR inhibitor in lung cancer. *Mol Cancer,* 4**,** 25.

YANG, H., LI, T. W., PENG, J., MATO, J. M. & LU, S. C. 2011. Insulin-like growth factor 1 activates methionine adenosyltransferase 2A transcription by multiple pathways in human colon cancer cells. *Biochem J,* 436**,** 507-16.

YANG, Y., CHEN, L., GU, J., ZHANG, H., YUAN, J., LIAN, Q., LV, G., WANG, S., WU, Y., YANG, Y. T., WANG, D., LIU, Y., TANG, J., LUO, G., LI, Y., HU, L., SUN, X., GUO, M., XI, Q., XI, J., WANG, H., ZHANG, M. Q. & LU, Z. J. 2017. Recurrently deregulated lncRNAs in hepatocellular carcinoma. *Nat Commun,* 8**,** 14421.

YANG, Y., LI, H., HOU, S., HU, B., LIU, J. & WANG, J. 2013. The noncoding RNA expression profile and the effect of lncRNA AK126698 on cisplatin resistance in non-small-cell lung cancer cell. *PLoS One,* 8**,** e65309.

YAO, H. & RAHMAN, I. 2012. Role of histone deacetylase 2 in epigenetics and cellular senescence: implications in lung inflammaging and COPD. *Am J Physiol Lung Cell Mol Physiol,* 303**,** L557-66.

YOUNG, R. P., HOPKINS, R. J., CHRISTMAS, T., BLACK, P. N., METCALF, P. & GAMBLE, G. D. 2009. COPD prevalence is increased in lung cancer, independent of age, sex and smoking history. *Eur Respir J,* 34**,** 380-6.

YTTERSTAD, E., MOE, P. C. & HJALMARSEN, A. 2016. COPD in primary lung cancer patients: prevalence and mortality. *Int J Chron Obstruct Pulmon Dis,* 11**,** 625-36.

ZAMPIERI, M., CICCARONE, F., CALABRESE, R., FRANCESCHI, C., BURKLE, A. & CAIAFA, P. 2015. Reconfiguration of DNA methylation in aging. *Mech Ageing Dev,* 151**,** 60-70.

ZHANG, S., HAO, J., XIE, F., HU, X., LIU, C., TONG, J., ZHOU, J., WU, J. & SHAO, C. 2011. Downregulation of miR-132 by promoter methylation contributes to pancreatic cancer development. *Carcinogenesis,* 32**,** 1183-9.

ZHOU, Y., XU, X., LV, H., WEN, Q., LI, J., TAN, L. & SHENG, X. 2016. The Long Noncoding RNA MALAT-1 Is Highly Expressed in Ovarian Cancer and Induces Cell Growth and Migration. *PLoS One,* 11**,** e0155250.

ANEXOS

PUBLICACIONES QUE HACEN PARTE DE LA TESIS / PUBLICATIONS THAT ARE PART OF THE THESIS

DNA methylation of miR-7 is a mechanism involved in platinum response through MAFG overexpression in cancer cells

IVYSPRING INTERNATIONAL PUBLISHER

Theranostics

2017; 7(17): 4118-4134. doi: 10.7150/thno.20112

Research Paper

DNA Methylation of miR-7 is a Mechanism Involved in Platinum Response through *MAFG* Overexpression in Cancer Cells

Olga Vera[1, 2*], Julia Jimenez[1, 2*], Olga Pernia[1, 2], Carlos Rodriguez-Antolin[1, 2], Carmen Rodriguez[1], Fatima Sanchez Cabo[3], Javier Soto[1, 2], Rocio Rosas[1, 2], Sara Lopez-Magallon[4], Isabel Esteban Rodriguez[2, 5], Ana Dopazo[6], Federico Rojo[7], Cristobal Belda[8], Rafael Alvarez[8], Jaime Valentin[9], Javier Benitez[10, 11], Rosario Perona[2, 11, 12], Javier De Castro[2]✉, Inmaculada Ibanez de Caceres[1, 2]✉

1. Cancer Epigenetics Laboratory, INGEMM, La Paz University Hospital, Madrid, Spain;
2. Biomarkers and Experimental Therapeutics in Cancer, IdiPAZ, Madrid, Spain;
3. Bioinformatics Unit, Centro Nacional de Investigaciones Cardiovasculares Madrid, Spain;
4. Department of Obstetrics and Gynecology, La Paz University Hospital, Madrid, Spain;
5. Department of Pathology, La Paz University Hospital, Madrid, Spain;
6. Genomics Unit, Centro Nacional de Investigaciones Cardiovasculares, Madrid, Spain;
7. Department of Pathology, University Hospital Fundación Jiménez Díaz, Madrid, Spain;
8. Department of Oncology, HM Hospitales, Madrid, Spain;
9. Translational Research in pediatric oncology Hematopoietic transplantation and cell Therapy, IdiPAZ, Madrid, Spain;
10. Human Genetics Group, Spanish National Cancer Research Center (CNIO);
11. Spanish Network on Rare Diseases (CIBERER), Madrid, Spain;
12. Department of Animal Models for Human Diseases, Institute for Biomedical Research CSIC/UAM, CIBER for Rare Diseases, Madrid, Spain.

* Both authors are first authors.

✉ Corresponding authors: Inmaculada Ibanez de Caceres and Javier de Castro, Cancer Epigenetics Laboratory, INGEMM, Biomarkers and Experimental Therapeutics in Cancer, IdiPAZ, Paseo de la Castellana 261, Madrid, 28046, Spain Phone 34-91-5854404 Fax 34-91-5854401 E-mail: inma.ibanezca@salud.madrid.org

© Ivyspring International Publisher. This is an open access article distributed under the terms of the Creative Commons Attribution (CC BY-NC) license (https://creativecommons.org/licenses/by-nc/4.0/). See http://ivyspring.com/terms for full terms and conditions.

Received: 2017.03.16; Accepted: 2017.07.04; Published: 2017.09.22

Abstract

One of the major limitations associated with platinum use is the resistance that almost invariably develops in different tumor types. In the current study, we sought to identify epigenetically regulated microRNAs as novel biomarkers of platinum resistance in lung and ovarian cancers, the ones with highest ratios of associated chemo-resistance.

Methods: We combined transcriptomic data from microRNA and mRNA under the influence of an epigenetic reactivation treatment in a panel of four paired cisplatin -sensitive and -resistant cell lines, followed by real-time expression and epigenetic validations for accurate candidate selection in 19 human cancer cell lines. To identify specific candidate genes under miRNA regulation, we assembled "in silico" miRNAs and mRNAs sequences by using ten different algorithms followed by qRT-PCR validation. Functional assays of site-directed mutagenesis and luciferase activity, miRNAs precursor overexpression, silencing by antago-miR and cell viability were performed to confirm their specificity in gene regulation. Results were further explored in 187 primary samples obtained from ovarian tumors and controls.

Results: We identified 4 candidates, miR-7, miR-132, miR-335 and miR-148a, which deregulation seems to be a common event in the development of resistance to cisplatin in both tumor types. miR-7 presented specific methylation in resistant cell lines, and was associated with poorer prognosis in ovarian cancer patients. Our experimental results strongly support the direct regulation of *MAFG* through miR-7 and their involvement in the development of CDDP resistance in human tumor cells.

Conclusion: The basal methylation status of miR-7 before treatment may be a potential clinical epigenetic biomarker, predictor of the chemotherapy outcome to CDDP in ovarian cancer patients. To the best of our knowledge, this is the first report linking the regulation of *MAFG* by miRNA-7 and its role in chemotherapy response to CDDP. Furthermore, this data highlights the possible role of *MAFG* as a novel therapeutic target for platinum resistant tumors.

Key words: miR-7, *MAFG*, DNA methylation, Cisplatin-resistance, cancer.

Introduction

Platinum-based chemotherapy, in combination with other anticancer drugs, is one of the most potent and widely used chemotherapeutic treatments. Platinum analogues display clinical activity against a broad spectrum of malignancies, including testis, ovary, head, neck and lung cancers. However, one of the major limitations of the use of platinum-based chemotherapy is that the disease almost invariably progresses to a platinum-resistant state, primarily in lung and ovarian cancers [1, 2]. In fact, it is common to find many studies enclosing both pathologies from researchers working in the field of drug-resistance [3-6]. A number of events have been proposed to explain the phenomenon of cisplatin resistance in cancer, including alterations in the epigenetic regulatory machinery, such as the silencing of gene expression through promoter methylation [7, 8]. This process has been also reported in the silencing of regulatory regions of tumor suppressor microRNAs (miRNAs), thereby increasing the expression of their target genes in cancer [9]. In fact, miRNAs are the most recently discovered mechanism of epigenetic inheritance that acting with messenger RNA can alter gene expression status [10]. miRNAs were first related to cancer in 2002; those that were downregulated were defined as tumor suppressor miRNAs, such as the miR-15a/16-1 cluster in chronic lymphocytic leukemia [11]. The gain or loss of these miRNAs can increase or decrease the activity of several signaling pathways in cancer cells [12]. For instance, a number of miRNAs are regulated by c-MYC, an oncogene that codes for a transcription factor involved in cancer and regulates processes such as cell cycle progression (miR-17, let-7), inhibition of apoptosis (miR-19a, miR-26a) and metastasis (miR-9) [13]. Moreover, miRNAs can regulate the action of DNA-methyltransferases, which has been associated with tumorigenesis in mice injected with lung cancer cell lines [14]. DNA methylation is one of the epigenetic regulators of miRNA expression and therefore, might be also responsible for the development of resistance to chemotherapy. The silencing though DNA methylation can be reverted by combination of demethylating drugs and histone deacetylase (HDAC) inhibitors such as 5 Aza-2deoxycytidine (5Aza-dC) and Trichostatine A (TSA). Both drugs act in synergy by depleting methyltransferase activity [15] and reversing the formation of transcriptionally repressive chromatin structure [16], Strategy previously described in many tumor types [17, 18]. However, our understanding of the regulation of miRNA expression and their role in chemoresistance is still poor [19]. In this study, we aimed to gain insight into the role of miRNA epigenetic regulation by DNA methylation over the response to cisplatin in cancer. We compared the global miRNA and mRNA expression profiles between sensitive/resistant-paired cancer cell lines under reactivation treatment and we analyzed whether those changes were due to DNA hypermethylation by further functional validation in different cell lines and cohorts of ovarian cancer patients.

Materials and Methods

Cell culture, treatments and viability to CDDP

Fifteen human cancer cell lines were purchased from ATCC (Manassas, VA) or ECACC (Sigma-Aldrich, Spain) and cultured as recommended. The CDDP-resistant variants A2780R and OVCAR3R were selected after a final exposure to 0.5 and 0.05 µg/ml cisplatin, respectively (Farma Ferrer, Spain), as previously described for H23R and H460R variants [20]. The additional 11 human cell lines, PC-3, LNCAP, H727, HT29, A549, BT474, LoVo, IMIM-PC-2, SKOV3, SW780 and IMR90, were used for further validations. For viability assays cells were treated with increasing doses of CDDP as described [21]. The epigenetic reactivation drugs 5Aza-2deoxycytidine (5Aza-dC) and trichostatin A (TSA) (Sigma-Aldrich, Spain) were used at 5µM and at 300nM respectively as described [22]. Cell authentication and treatments are described in Supplementary Material and Methods and Supplementary Table 1.

Clinical sample and data collection

Formalin-Fixed Paraffin embedded (FFPE) and fresh-frozen ovarian cancer samples were collected from untreated patients and associated clinical data were obtained from Hospital Parc de Salut Mar (83 patients) and Biobank of IDIS-CHUS-HULP (55 patients) representing the most frequent ovarian cancer subtypes; all the patients underwent chemotherapy treatment after sample collection. Seven patients were also selected from stage III/IV patients from Hospital Madrid Clara Campal with a platinum treatment response classified as refractory or resistant. In addition, 22 high-grade serous carcinoma (HGSOC), were obtained from the National Cancer Research Centre (CNIO) biobank in collaboration with Dr. J. Benitez, from a previously reported cohort of patients [23]. We also collected 10

normal ovarian samples from patients who had undergone a sex reassignment surgery or tubal ligation and 10 peripheral blood mononuclear cells (PBMCs) to discard genomic imprinting. Follow-up was conducted according to the criteria of the medical oncology divisions from each institution. All the samples were processed following the standard operating procedures with the appropriate approval of the Human Research Ethics Committees at each contributing center, including informed consent within the context of research. Clinical, pathological and therapeutic data were recorded by an independent observer, and a blind statistical analysis was performed on these data.

RNA extraction and miRNA/mRNA array preprocessing

RNA extraction, assessment of quality and hybridization into Agilent platforms for microRNA and mRNA microarrays and data normalization is deeply described in Supplementary Materials and Methods. The criteria used for filtering the miRNA/mRNA data were according to the packages recommended by Agilent, and were analyzed by two independent bioinformaticians. miRNA/mRNA experiments had an average expression over the 20th percentile of all average expressions and changed across the different conditions (i.e. with a coefficient of variation [CV] >5% across all samples). Global data were combined to identify those miRNAs, with inhibited expression after cisplatin treatment that were re-expressed after epigenetic reactivation, together with those genes that have *in silico* mRNA complementary sequences and opposite expression. Genes were considered as targets if selected with at least one of the 10 methods described by Alexiou *et al* [24]. For the inverse expression profiles, only those pairs (miRNA, gene) with a negative Spearman correlation coefficient and a p-value for this correlation <0.1 were considered as potential targets. The databases GeneCard (http://www.genecards.org) miRBase (www.mirbase.org), mirwalk (www.umm.uni-heidelberg.de/apps/zmf/mirwalk) and Web gestalt (www.bioinfo.vanderbilt.edu/webgestalt) were used for bioinformatics analysis [25-27]. (GEO reference: GSE84201).

RNA isolation and quantitative RT-PCR

Total RNA was retrotranscribed and quantitative RT-PCR analysis were performed as previously described [20, 22]. Samples were analyzed in triplicate using the HT7900Real-Time PCR system (Applied Biosystems, USA), and relative expression levels were calculated according to the comparative threshold cycle method ($2^{-\Delta\Delta Ct}$) using RNU48 or RNU6B as an endogenous control miRNAs and GADPH or β-actin as an endogenous control genes. Primers and probes for expression analysis were purchased from Applied Biosystems. miRNAs probes are detailed in Supplementary Table 2. Probes for gene expression are as follows: *MAFG*: Hs 01034678_g1; ELK1: Hs 00901847_m1; *MAPKAP1*: Hs 01118091_m1; *ABCA1*: Hs 01059118_m1; GADPH: Hs03929097_g1; β-actin: Hs99999903_m1. Data are presented as the "change of expression in number of times" (Log10-RQ) and the error bars are expressed as the maximum estimate (RQmax) and the minimum estimate (RQmin) expression levels, representing the standard deviation of the average expression level RQ. miRNAs from human HEK-293T cell line were isolated using the miRNeasy kit (Quiagen, USA) and miR-7 expression analysis was carried out as described before, using RNU48 as endogenous control and the experimental groups transfected with 3'-UTR plasmid control and miR-NC as calibrators.

Site-directed mutagenesis assay

The full length MAFG-3'-UTR sequence (NM_002359.3 OriGene, USA) was used as a template to generate the mutants MAFG 3´UTR. Two different regions were identified by more than six bioinformatical algorithms as seed region of miR-7 binding site. Seven nucleotides within each seed region were mutated. Site-directed mutagenesis was carried out with QuikChange lightning site-directed mutagenesis kit (Stratagene, USA) according to the manufacturer's instructions. The presence of both mutated seed regions and the integrity of the remaining MAFG 3ÚTR sequence of all constructs were validated by Sanger sequencing. The primers designed to introduce mutations were for Region2: Fw-5'-caagtaaaccatgatatat**agtgcta**cttccaccttaactttgcc-3'; Rv-5'-ggcaaagttaaggtggaag**tagcact**atatatcatggtttacttg-3'; and for Region8: Fw-5'-ggccaagcgttccctggcc **agtgcta**tctggcctcagctttgttc-3', Rv-5'-gaacaaagctgaggcc aga**tagcact**ggccagggaacgcttggcc-3'.

Cell Transfection and lentiviral transduction

miR-7 overexpression and silencing: Cell lines were seeded at 500,000 cells/p60 plate, then transfected with 40 or 50 nM of miR-7 precursor, anti-miR-7 or negative controls (AM17100, AM 17110, AM10047 and AM17010 Ambion, USA) and using Lipofectamine 2000 (Invitrogen, USA) according to the manufacturer's protocol.

Luciferase assay

HEK-293T cells were transfected with MAFG-3'-UTR, MAFG-3'-mutated-UTR, ABCA1-3'-UTR or ELK-1-3'-UTR plasmids (OriGene, USA), and PremiR-hsa-miR-7 or Negative Control as described

above. Luminiscence was assayed 24 hours later using the Kit Renilla Luciferase Assay System (Promega, USA), according to the manufacturer's instructions. Results were normalized to the Renilla luminescence from the same vector and shown as the ratio between the various treatments and cells transfected with control vector.

cDNA plasmids transfection

A Myc-DDK-tagged ORF clone of *MAFG*, *ELK-1* or *ABCA1* and the negative control pCMV6 were used for in transient transfection (OriGene, USA). H23 and A2780 cells were plated onto 60-mm dishes at 6x105 cells/dish and transfected with a negative control, *MAFG*, *ELK-1* or *ABCA1* vectors (IDs: RC221486; RC208921 and RC221861) using jet-PEI DNA Transfection Reagent (PolyPlus Transfection, USA). For stable overexpression, lentiviruses carrying *ELK-1* cDNA (Applied Biological Materials, Canada) were obtained by cotransfecting 15 µg of the specific lentiviral vector (pGIPZ-nonsilencing or pLenti-GIII-CMV-h*ELK-1*-GFP-2A-Puro) and 5 µg of each packaging vector (pCD-NL-BH and pMD2-VSV-G) in 10 million HEK 293T cells using Lipofectamine 2000 (Invitrogen, USA). Supernatants were taken at 48 hours posttransfection. A2780S cells were plated onto 60-mm dishes at 1x105 cells/dish and transduced with supernatant carrying nonsilencing or *ELK-1* lentivirus, and polybrene was added (5 µg/ml).

Transfection efficacy was measured by qRT-PCR, using the sensitive cell line transfected with the negative control as a calibrator. Two independent experiments were performed in quadruplicate.

Epigenetic validation: CpG island identification, DNA extraction, bisulfite modification, bisulfite sequencing and methylation-specific PCR

The occurrence of CpG islands (CGIs) encompassing microRNA genes or being located nearby as well as the identification of repetitive elements were assessed using various programs for CGI-revealing, listed and described in Supplementary Material and Methods. The possible gene in which the miRNA was encoded was also analyzed, searching for the presence of 5´ CGIs located in the transcriptional site. The DNA from a total of 151 samples, including tumors, controls and cultured cell was isolated, bisulfite modified and used for BS, as previously described [22]. Primers design, PCR and electrophoresis conditions are detailed in Supplementary Material and Methods. Primers are listed in Supplementary Table 3. For BS, we prefer direct sequencing, to subcloning of a mixed population of alleles to avoid potential cloning efficiency bias [28] and artifact [29].

Western blot analysis

Cell lines were cultured at a density of 600,000 cells per 60-mm plate, shifted into medium containing 10% fetal bovine serum for 24 h and 72 h. Twenty micrograms (20 µg) of whole-cell extracts were subjected to Western blot, performed as previously described [30]. The primary antibodies employed were the c-Myc-A14 (Santa Cruz, USA) and β-tubulin (Sigma, Spain) antibodies.

Statistical analysis

For the identification of differentially expressed miRNAs and genes from the microarray data, we used linear models [31] as implemented in the Limma Bioconductor package. The fixed effects were the origin of the tissue (lung/ovarian), the cell line (H460, H23, OVCAR3, A2780) and the condition (sensitive, resistant, resistant treated). The replicate is the random effect. To identify the downregulated miRNAs in resistant cells and their opposite expressed target genes, we performed the following contrasts for all the tissues (lung and ovarian) or for each tissue origin (lung or ovarian): resistant vs. sensitive and resistant-treated vs. resistant.

We then selected the candidates that fulfill the following conditions in at least 2 of the 4 cell lines interrogated: Log2(R/S) <0 AND Log2 (RT/R) >0; RvsS or RTvsR statistically different $p<0.05$. As a statistical method we used the unpaired T-test algorithm with Benjamini Hochberg (BH) as the FDR correction method for multiple testing corrections with statistical significance of $p<0.1$ in the miRNA approach and $p<0.05$ in the gene approach as an adjusted p-value.

Patient's clinical characteristics were described for the complete series with mean and standard deviation values or relative frequencies. The data were stratified for patients carrying methylated or unmethylated DNA, and their distributions compared with the chi-squared test or Fisher's exact test for qualitative variables, and Student's t test or the Wilcoxon-Mann-Whitney test (non-normal distribution) for quantitative variables. Overall survival and Progression free survival (PFS) were estimated according to the Kaplan-Meier method and compared between groups by means of the log-rank test. All the p-values were two-sided, and the type I error was set at 5 percent. Statistical analyses were performed using Stata 10 software.

Results

Establishment of ovarian human cancer cell lines resistant to CDDP

We have established 2 ovarian cancer cell lines resistant to CDDP, A2780-R and OVCAR3-R, that showed approximately three times more drug resistance than the paired parental cell line A2780 and OVCAR3 (3.00 and 2.96 Resistant-Index (RI); $p<0.001$) and a similar CDDP RI to H23R and H460R NSCLC cancer cells, that we established previously [20], (3.35 and 2.50 respectively; $p<0.001$) (Figure 2A and Supplementary Figure 1A).

Identification of candidate miRNAs

As a first step to identify candidate miRNAs under epigenetic regulation and involved in the CDDP response, we searched for miRNAs showing a decrease of the expression in R versus S cells and a recovered expression after epigenetic reactivation-treated (RT) versus R cells. First, 87 miRNAs identified on the expression arrays showed a significant expression change ($p<0.05$) in at least one of the following conditions: R < S or RT > R; while 28 changed their expression with a *p-value* adj<0.1 simultaneously in both situations. By analyzing the concurrence of CGIs with the characteristics described by Takai and Jones [32], candidates were reduced to 10 encompassing microRNA genes or being located nearby (less than 2000 bp 5´-upstream), together with the analysis of the presence of CGIs in the gene promoter region in which the miRNA is encoded. After a pair-base-complementarity analysis *in silico* between miRNA and the candidate target genes that showed an opposite expression profiles (Supplementary Database Information); we made a functional web-based enrichment analysis with the selected genes by GOTM. This approach identified 7 miRNAs which potential target genes were involved in tumor progression: miR-7, miR-132, miR-335, miR-148a, miR-10a, miR-124 and miR-9 (Figure 1 and Supplementary Table 4). Mature miR-7 is generated from three different miRNA precursors in the human genome, miR-7-1, miR-7-2, and miR-7-3; we assumed expression changes were tightly associated to miR-7-3 (hereafter called miR-7) as no changes were identified on miR-7-1 and miR-7-2 probes represented in the array and it is the only precursor that presents two CGIs surrounding its genome location. We also found that some of the miRNAs showing the strongest upregulation were located at the C19MC cluster, previously linked with carcinogenesis [33]. It presents a CGI located about 17kb from the first miRNA [34] that was included to analyze its potential epigenetic regulation in drug resistance.

miRNA-7 as potential chemoresistance candidate under epigenetic regulation

Firstly, we validated the expression profile of the 3 experimental conditions (S, R and RT) by qRT-PCR assay confirming the results from the microarray analysis for all 7 miRNAs in at least one of the four cell lines analyzed. Three of the seven miRNAs showed changes in their expression according to the microarray data in A2780 cells: miR-7, miR-132 and miR-10a, whereas no significant changes in expression between S and R cells were found for miR-124 (Figure 2B). The cell line OVCAR3 showed changes in miR-132 and -124, according to the array data. Although both increased expression in RT, no differences between S and R were reported (Figure 2C). For the lung cancer model, 6 miRNAs in H23 cells and 2 miRNAs in H460 cells miRNAs were fully validated (Supplementary figure 1B-C).

miR-132, miR-148a miR-335, and miR-7, were validated in at least 2 cell lines and further selected for epigenetic validation by bisulfite sequencing (BS), together with the C19MC cluster's CGI. This cluster is on the long arm of chromosome 19 and has a CGI of 2255 bp from which we analyzed 394 bp that comprises the area with the highest density of CG positions in H23, H460, A2780 and OVCAR3 cell lines. We also tested DNA from normal tissues from lung (LC), ovary (OC) and PMBCs to discard imprinting. All analyzed CpG positions were densely methylated (Supplementary Figure 2A), confirming a possible role in embryonic development as described [35, 36], but excluding a relation between acquisition of DNA hypermethylation and drug-response. Referred to miR-132, the area analyzed was 866 bp in length, at a CGI comprising -1847/+667bp at the short arm of chromosome 17. miR-148a is located on the short arm of chromosome 7, with a nearby CGI of 1663, located 137 bp upstream from the miRNA. A 560 bp area of the CGI was analyzed. No methylation was found for both miRNAs either on the tumor cell lines or controls samples analyzed (Supplementary Figure 2B and 2C). miR-335 is located on the long arm of chromosome 7, on the second intron of the MEST002 gene transcript. A 1123 bp CGI is located in the promoter region of this transcript. We analyzed a fragment of 528 bp initially in the H23S/R, H460S/R cells and LC. The results showed methylation only in H460S/R subtypes. We extended the analysis to the additional cell lines LoVo, OVCAR3 and PC-3, and control samples, and no methylation was found in any of them (Supplementary Figure 2D). Pairs of primers are listed in Supplementary Table 3.

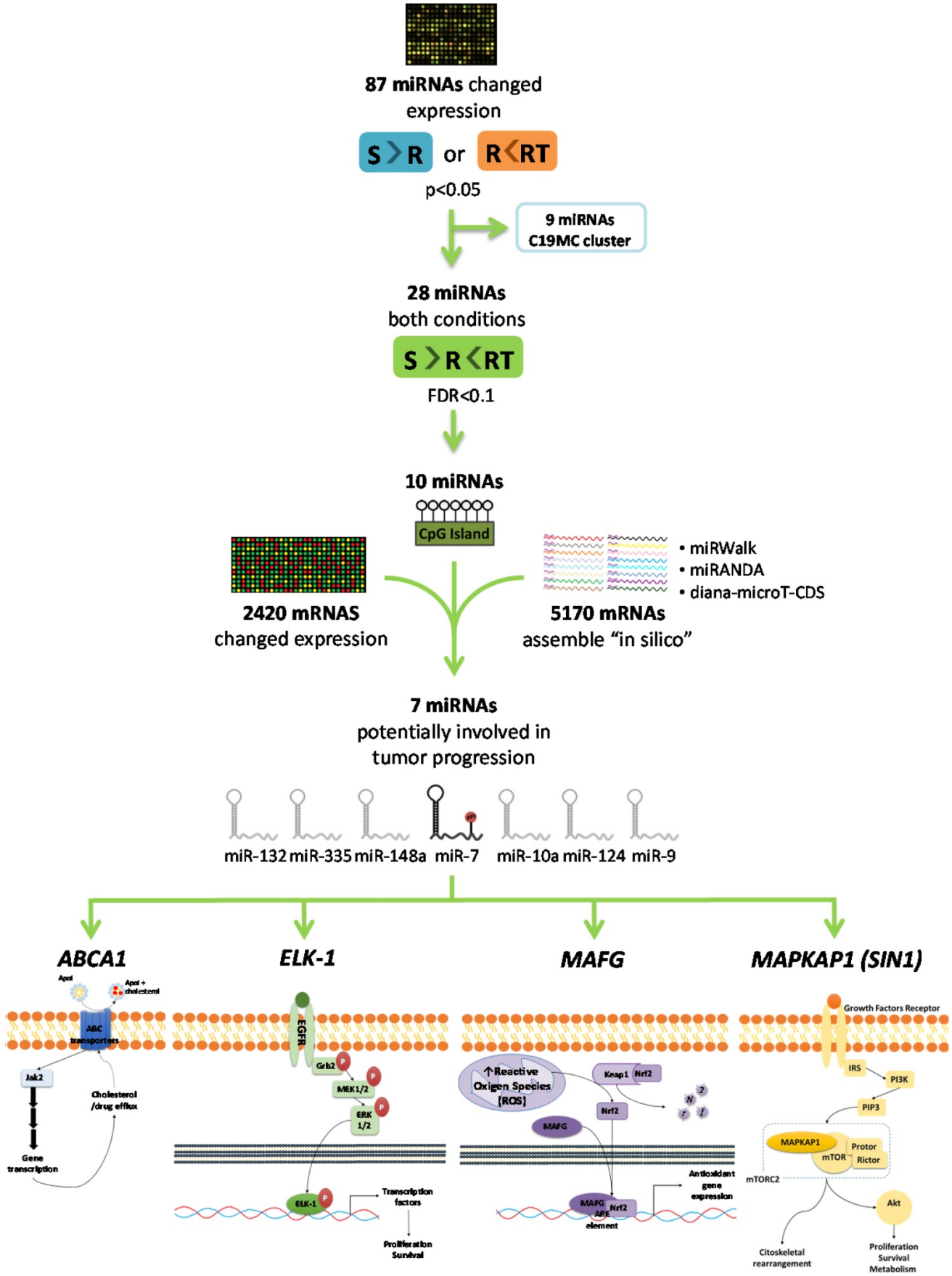

Figure 1. Selection of candidate miRNAs under epigenetic regulation and candidate target genes. The flowchart indicates the steps and criteria used for the selection of the final 7 candidate miRNAs under epigenetic regulation and the final 4 candidate genes under possible regulation of miR-7.

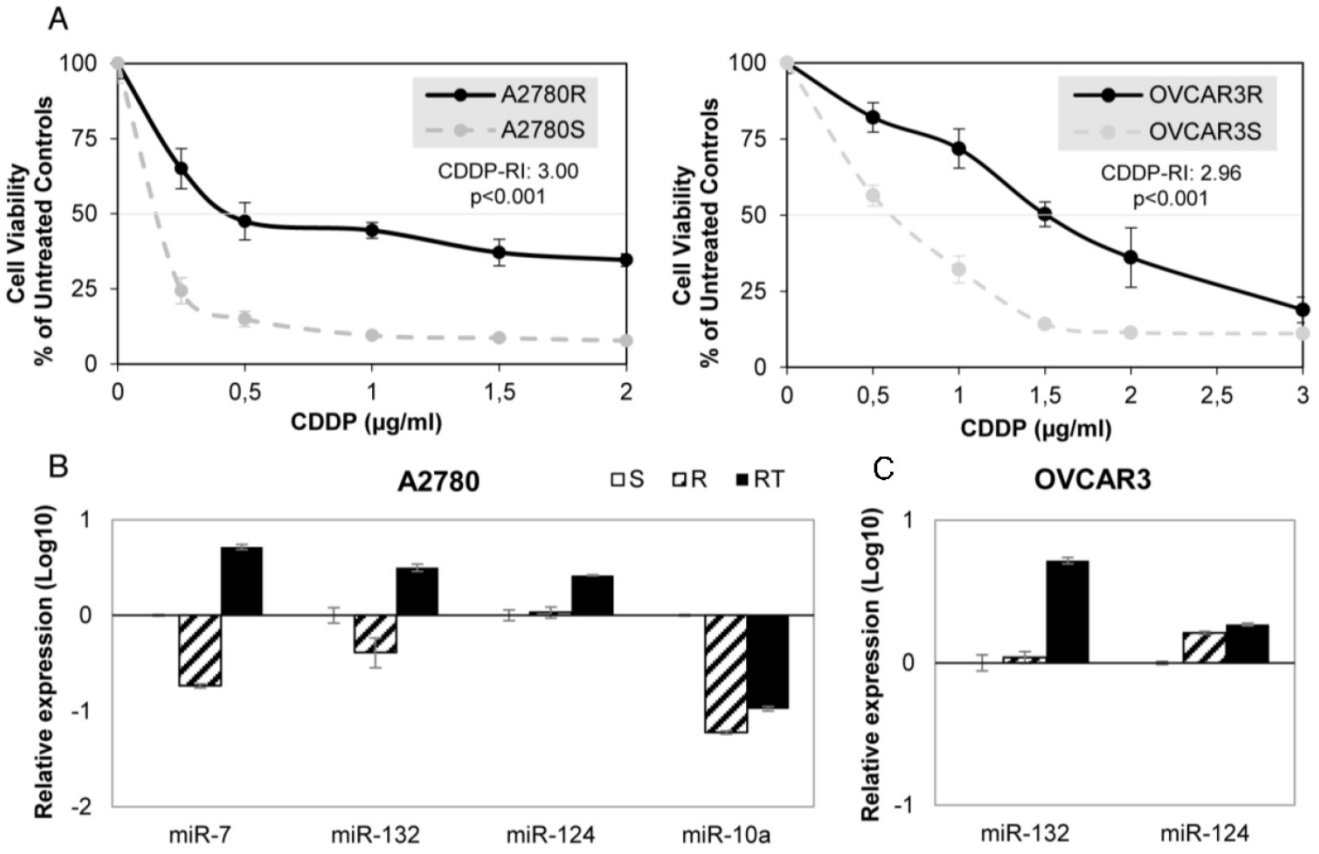

Figure 2: miRNA relative expression on CDDP-sensitive and -resistant ovarian cancer cell lines. (A) Viability curves showing the acquired resistance of A2780 and OVCAR3 cell lines; Cells were exposed for 72 h to each drug concentration. Data were normalized to the untreated control, which was set at 100% and represent the mean + SD of at least 3 independent experiments performed in quadruplicate at each drug concentration tested for every one cell analyzed. IC50, is the inhibitory concentration that kills 50% of the cell population. Resistant index (RI) calculated as IC50 resistant / IC50 sensitive cell line. $p<0.001$ was considered as a significant change in drug sensitivity (Student's t-test). (B-C) Relative expression levels of the selected miRNAs measured by qRT-PCR. Data are represented in log10 scale and are expressed using the corresponding sensitive (S) line as a calibrator. Each miRNA level was normalized to RNU48 as an endogenous control. Assays were made in the ovarian cancer cell lines A2780 (B) and OVCAR3 (C) in all experimental conditions: S, R and RT. S: sensitive; R: resistant; RT: resistant treated with epigenetic reactivation drugs (5-Aza and TSA). The expression number assays for each miRNA are indicated in Supplementary Table 2.

miR-7 is located on the short arm of chromosome 19, with 2 potential regulatory CGIs: one located 861 bp before the first nucleotide of the miRNA sequence with a length of 667 bp; the second has an extension of 269 bp and comprises the miRNA sequence (Figure 3). Two overlapping pairs of primers were used to analyze the first CGI, covering 776 bp, which included the entire CGI and adjacent areas (Supplementary Table 3). The analysis was performed on the ovarian cancer cells A2780S and A2780R. We found the presence of methylation specifically in the resistant cells. The specific aberrant methylation of miR-7 in resistance was confirmed in H23R cells as well as in the cisplatin resistant cell lines IMIM-PC2 and LoVo, which present an IC_{50} over 2µg/ml CDDP (Supplementary Figure 3). OC and LC were used as controls as well as nine additional tumor cell lines. In fact, the sensitive subtypes and controls presented an absence of methylation. A selection of these results is shown in Figure 3, left. This methylation pattern was used to design the MSP primers for the analysis of FFPE primary tumors. The second CGI, was fully methylated for all the samples tested (Figure 3, right). Therefore, the upstream CpG island of miRNA-7 was selected for our translational approach as it was the candidate downregulated through DNA methylation in CDDP-resistant cells.

miR-7 methylation is a potential predictive biomarker for recurrence and overall survival in patients with ovarian cancer treated with platinum

Response rates, overall survival or progression free survival are recommended by ASCO and ESMO Clinical Practice Guidelines Committees to assess the clinical benefit of chemotherapy treatment [37] [38]. Ovarian Cancer Consensus Meeting, defines 'platinum-refractory' as patients progressing during therapy or within 4 weeks after the last dose; 'platinum-resistant' patients progressing within 6 months of platinum-based therapy; 'partially platinum-sensitive, patients progressing between 6 and 12 months; and 'platinum-sensitive' patients progressing with an interval of more than 12 months

(GCIG Consensus) [39]. Following the international guidelines, we compared the miR-7 methylation levels with OS and PFS clinical parameters on two cohorts of 83 and 55 ovarian cancer patients all of them treated with platinum. We studied the OS for all patients and the PFS in those patients that had recurred at the end of the study to analyze the relationship between platinum response and miR-7 methylation.

We observed a 29% of methylation (24 out of 83 samples) in the cohort from Hospital del Mar (Table 1), which increased to 36% (20 out of 55) in the CHUS-HULP biobank samples, a cohort enriched in serous resistant tumors (Supplementary Table 5). We also observed a higher percentage of methylation in HGSOC samples from and additional cohort of patients from the CNIO (50% methylated samples) (Supplementary Table 6) and in a small group of the resistant/refractory samples from H. Madrid (57%). We also tested 10 ovarian control samples a non-tumor cell line (IMR90) and 10 PBMCs to discard imprinting and none of them were methylated (100% specificity) (Figure 4A). When correlating our results with the patient's clinical histories we obtained significant data correlating methylation and cisplatin response in the group of 33 patients that recurred. Kaplan-Meier curves show that patients relapsing before 10 months, carried preferentially methylated miR-7 tumors (80% methylated versus 14% unmethylated) (Figure 4B) (p=0.004). No differences

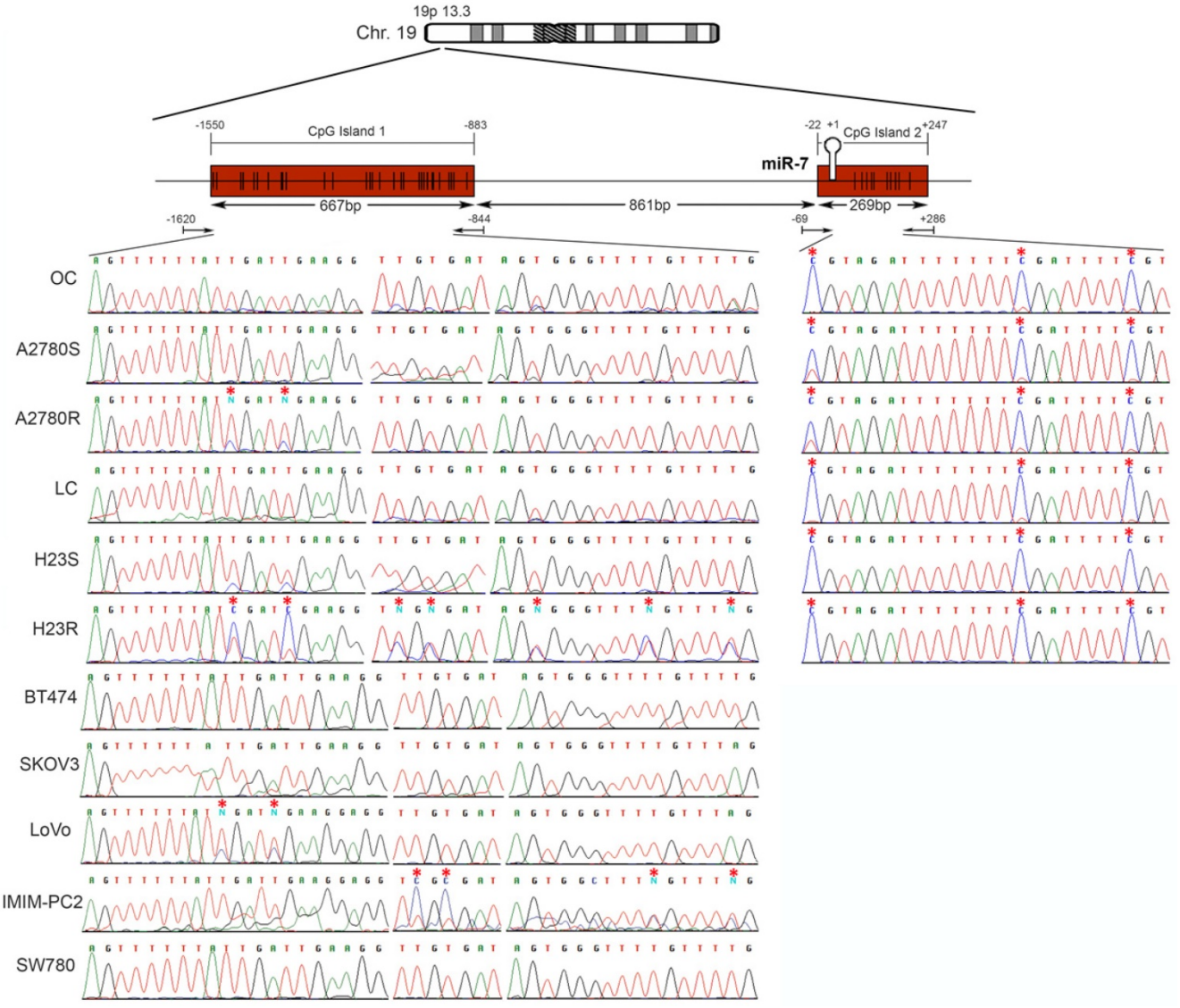

Figure 3. Bisulfite sequencing of miRNA-7 regulatory CGIs. Chromosomal location of miR-7 and their nearby CGIs, as well as representative images of corresponding bisulfite sequences (BS). CGIs are represented in red boxes; each CpG position is characterized by vertical black lines inside the boxes. The first nucleotide of each miRNA is indicated by +1. Facing arrows mark the primer positions used for BS. It is shown the methylation analysis of the two CGIs closely related to the encoded miR-7 region. For the first CGI, the 3 different fragments (left half of the Figure) corresponding to the most frequently methylated positions are shown. A representation of 5 of the 11 additional tumor cell lines interrogated, BT474, SKOV3, LoVo, IMIMPC2 and SW780, is also shown. All CpG positions interrogated at the second CGI were fully methylated in all the samples analyzed (right half of the Figure), as indicated by the presence of C preceding a G in the sites indicated by the asterisks. OC: ovary control; LC: lung control. Asterisks indicate methylated positions.

were found in CDDP-refractory and resistant patients. Moreover, after 3 years of follow up over the 83 patients cohort, the overall survival was significantly higher in the group of patients with an unmethylated tumor in comparison with those with a methylated one (67% vs 35%, p=0.004) (Figure 4C). Similar results showing a tendency in terms of PFS and OS were also observed in the CHUS-HULP biobank cohort, although these last results were not statically significant mainly because of a size-limitation (Supplementary Figure 5). Finally, we observed a decrease in the number of patients with higher ECOG status when the promoter region of miR-7 was unmethylated in the higher cohort of patients (p=0.025). Accordingly, 62.5% of the patients who harbored the methylated promoter presented ascites compared with 80% of the patients who did not develop ascites harboring an unmethylated promoter region (p=0.025) (Table 1). Those results indicate that patients carrying an unmethylated sample tended to have less aggressive tumors, with better progression free survival after platinum treatment and overall survival rates than those who carried the methylated DNA.

MAFG is a direct target gene of miRNA-7

To analyze if the methylation of miR-7 is affecting the cisplatin-cell viability through the silencing of its expression, we overexpressed miR-7 in the resistant subtypes at a final concentration of 40nM (Supplementary Figure 6A). No effect on drug sensitivity was observed although efficiency of the transfection was validated by qRT-PCR, confirming the miR-7 overexpression after 72h in both cell lines (Supplementary Figure 6B). The overexpression of higher concentration of pre-miR-7 (50nM) resulted in a decrease in cell viability, reaching levels of 63% and 52%, respectively, compared with their parental sensitive and resistant cell lines, transfected with the mimic negative control (Supplementary Figure 6C), making unfeasible to evaluate the response to CDDP, given no representative cell population was left from the cell culture after the miR-7 precursor overexpression. Thus, to fully understand the implication of miR-7 in the development of resistance, we investigated the role of the target candidate genes that showed a significant opposite expression to miR-7 and *in silico* complementarity (Figure 1). Out of the 1021 genes that accomplished both conditions we selected only those that were present in A2780 and H23 cell lines and which expression increased in R compared to S and RT subtypes, with a p-value<0.05 adjusted by FDR correction. Further functional web-based annotation using the Gene Ontology Tree Machine (GOTM) tool, grouped 149 genes in 20 significant functional groups, from which we selected *MAFG*, *MAPKAP1*, *ELK*-1 and *ABCA1* genes because of their implication in biological functions related to tumor progression (Figure 1, Supplementary Database information). The changes on the expression were confirmed by qRT-PCR in A2780 cells for *MAFG* and slighter but following the expected expression pattern for *ELK*-1 (Figure 5A) and in H23 cells for *MAFG* and *ABCA1* (Supplementary Figure 7A). To probe whether *MAFG*, *ELK*-1 and/or *ABCA1* are target genes of miR-7, we overexpressed a precursor of miR-7 in the resistant subtypes to assess the changes in expression of the candidate target genes by qRT-PCR. As expected, the overexpression of miR-7 in A2780R resulted in a decrease of the expression of *MAFG* and *ELK-1*, compared with the resistant cell line transfected with the negative control (Figure 5B). *MAFG* regulation was also confirmed in H23R cells, in which the miR-7 precursor lead also to the decrease of the potential candidate gene *ABCA1* (Supplementary Figure 7B). Efficiency of the miR-7 overexpresion was validated by qRT-PCR (Figure 5B and Supplementary Figure 7B). A summary of this selection in shown in Supplementary Table 7. Next, we cotransfected in HEK-293T cells the pre-miRNA-7 together with a luciferase reporter vector that carries the 3'-UTR region of each candidate gene. The cotransfection with the 3'-UTR region of *MAFG*, induced a reduction of the luciferase activity at both concentrations, 15 and 30nM of the precursor, effect that was not observed when cotransfecting 3'-UTR regions of *ELK*-1 and *ABCA1* (Supplementary Figure 8A, upper panel). Simultaneously, we confirmed through qRT-PCR that the pre-miR-7 was successfully transfected in the 293T cell line, for every experimental group (Supplementary Figure 8A, lower panel). To fully confirm that *MAFG* is a target gene of miR-7, we performed directed-site mutagenesis at the predicted binding sites of miR-7 in the 3' UTR of *MAFG*, at two different regions (Figure 6A), followed by luciferase reporter assays. The significant decrease of luciferase activity observed when using the WT 3'UTR of *MAFG*, disappeared when we cotransfected pre-miR-7 with both constructs containing the mutated regions (Figure 6B). Moreover, to ultimately confirm this regulation, we silenced the expression of miR-7 in A2780S that resulted in increased levels of *MAFG* (Figure 6C). A2780 cells express miR-7 at a low level, as we can observe in Supplementary Figure 8B compared with the control cell line HEK-293T, which explains the low efficiency decreasing the miR-7 levels at 48h, although it was sufficient enough to observe a strong change over *MAFG* expression.

Table 1. Demographic table with the clinicopathological characteristics of a cohort of 83 samples from Hospital del Mar.

Characteristics		Complete series (n=83)		Unmethylated (n=59)		Methylated (n=24)		
		No. of patients	%	No. of patients	%	No. of patients	%	*p*
Age (median, range)		55 (17-84)		59 (17-80)		55 (18-84)		0.880
Menopausal status								0.565
	Premenopausal	34	41.0	23	39.0	11	45.8	
	Postmenopausal	49	59.0	36	61.0	13	54.2	
Parity								0.974
	No	24	28.9	17	28.8	7	29.2	
	Yes	59	71.1	42	71.2	17	70.8	
Familiar history								0.684
	No	58	69.9	42	71.2	16	66.7	
	Yes	25	30.1	17	28.8	8	33.3	
ECOG								0.025
	0	21	25.3	20	33.9	1	4.2	
	1	36	43.4	22	37.3	14	58.3	
	2	20	24.1	12	20.3	8	33.3	
	3	6	7.2	5	8.5	1	4.2	
Ascites								0.025
	No	47	56.6	38	64.4	9	37.5	
	Yes	36	43.4	21	35.6	15	62.5	
Tumor Grade								0.35
	I	34	41	27	45.8	7	29.2	
	II	24	28.9	15	25.4	9	37.5	
	III	25	30.1	17	28.8	8	33.3	
Histology								0.883
	Serous	40	48.2	27	45.8	13	54.2	
	Mucinous	9	10.8	7	11.9	2	8.3	
	Clear cell	8	9.6	5	8.5	3	12.5	
	Endometroid	4	4.8	3	5.1	1	4.8	
	Others	22	26.5	17	28.8	5	20.8	
Chemotherapy								0.956
	Adjuvant	59	71.1	43	72.9	16	66.7	
	Neoadjuvant	6	7.2	3	5.1	3	12.5	
	Metastatic	18	21.7	13	22.0	5	20.8	
Platinum sensitivity								0.196
	Sensitive	21	63.6	15	71.4	6	50.0	
	Resistant	12	36.4	6	28.6	6	50.0	
Relapse								0.286
	No	49	59.0	37	62.7	12	50.0	
	Yes	34	41.0	22	37.3	12	50.0	
Death								0.119
	No	49	59	38	64.4	11	45.8	
	Yes	34	41	21	35.6	13	54.2	

The response to cisplatin is mediated by *MAFG* expression in human cancer cell lines

To determine if the expression of the miR-7 candidate target genes was linked to CDDP response, we conducted their *in transient* overexpression in the sensitive cells comparing their response to CDDP with their parental resistant and sensitive cell lines, both transfected with an empty vector.

MAFG overexpression resulted in an increase in the resistance to CDDP in A2780S cells compared with the sensitive cell line transfected with the empty vector, showing a resistance index of 1.6 ($p<0.001$) (Figure 7A). The same effect was also confirmed in the sensitive cell line H23S reaching a similar CDDP-RI of 1.7 ($p=0.01$) (Supplementary Figure 9A). The overexpression of *ABCA1* in H23S led to a RI of 1.5 compared with the sensitive cell line transfected with the empty vector, although it was not statistically significant ($p=0.796$) (Supplementary Figure 9B). *ELK-1* overexpression in A2780S did not change the response to CDDP after 48 h of exposure to the drug (Figure 7B).

In order to confirm the efficiency of the transfection, we analyzed the mRNA and protein levels by qRT-PCR and western blot of the overexpressed genes. Results confirmed ectopic overexpression of *MAFG*, *ELK-1* and *ABCA1* at 72 h in both cell lines (H23S-*MAFG*, A2780S-*MAFG*, H23S-*ABCA1* and A2780S-*ELK-1*) with an increase of 0.2, 7, 6416 and 28-folds respectively, compared with the sensitive cell lines transfected with the control vector. No changes at protein level were found between 24 and 72 hours when analyzing MAFG and ABCA1 overexpression (Figure 7C and Supplementary Figure 9C). However, we observed a

slightly protein levels of ELK1 at 24h that was not maintained at 72 h (Figure 7C). Therefore, we performed the stable overexpression of *ELK-1* by transduction assays with a lentiviral vector and compare the response to CDDP with the parental-sensitive and resistant subtypes harboring a nonsilencing vector (A2780S/R -NS). As previously observed in the "in transient" experimental assays, *ELK-1* overexpression did not change the sensitivity to CDDP; however, it induced an strongly increase in the number of cells at 0 μg/ml dose, that allowed to maintain higher ratios of survival fraction when treated with CDDP, compared with the control sensitive cell line. We also confirmed the success of the overexpression by qRT-PCR (Figure 7D).

Discussion

Epigenetic alterations by DNA methylation can reduce the expression of a number of miRNAs, altering the therapeutic response in tumor cells and contributing to the onset of more aggressive phenotypes. We intended to deepen our understanding of this aspect, identifying new miRNA-targets of promoter hypermethylation involved in the response to cisplatin, by using an experimental model of paired sensitive and CDDP-resistant tumor cell lines. We established the ovarian cancer cells A2780R and OVCAR3R, with a CDDP-RI in accordance with the previously established H23R and H460R cell lines, assuming that similar resistant events could follow [20]. Then, we combined an epigenetic reactivation therapy with a global transcriptomic-based strategy. The epigenetic therapy induced an expected reactivation percentage of 12% (87 of the 723 miRNAs), in accordance with published data, using the same technology and pharmacologic unmasking strategy [40]. The differential miRNA expression profile from sensitive, CDDP-resistant and resistant cells under epigenetic reactivation treatment was correlated with the expression of those genes from the same experimental groups that showed complementary sequences. This screening, included an ontological study of routes and processes related to tumor biology for all candidate target genes. We identified a set of 7 miRNAs containing a surrounding CGI that were complementary to target genes involved in cell growth, proliferation, cell migration, drug efflux, angiogenesis or apoptosis inhibition such *MAFG, ELK-1, RAB6B,CAMK2G, MAPKAP1, ABCA1, ABL1 or STAT3* [41, 42]. All these processes might influence the acquisition of drug-resistance in the CDDP treated cells through the potential miRNA silencing.

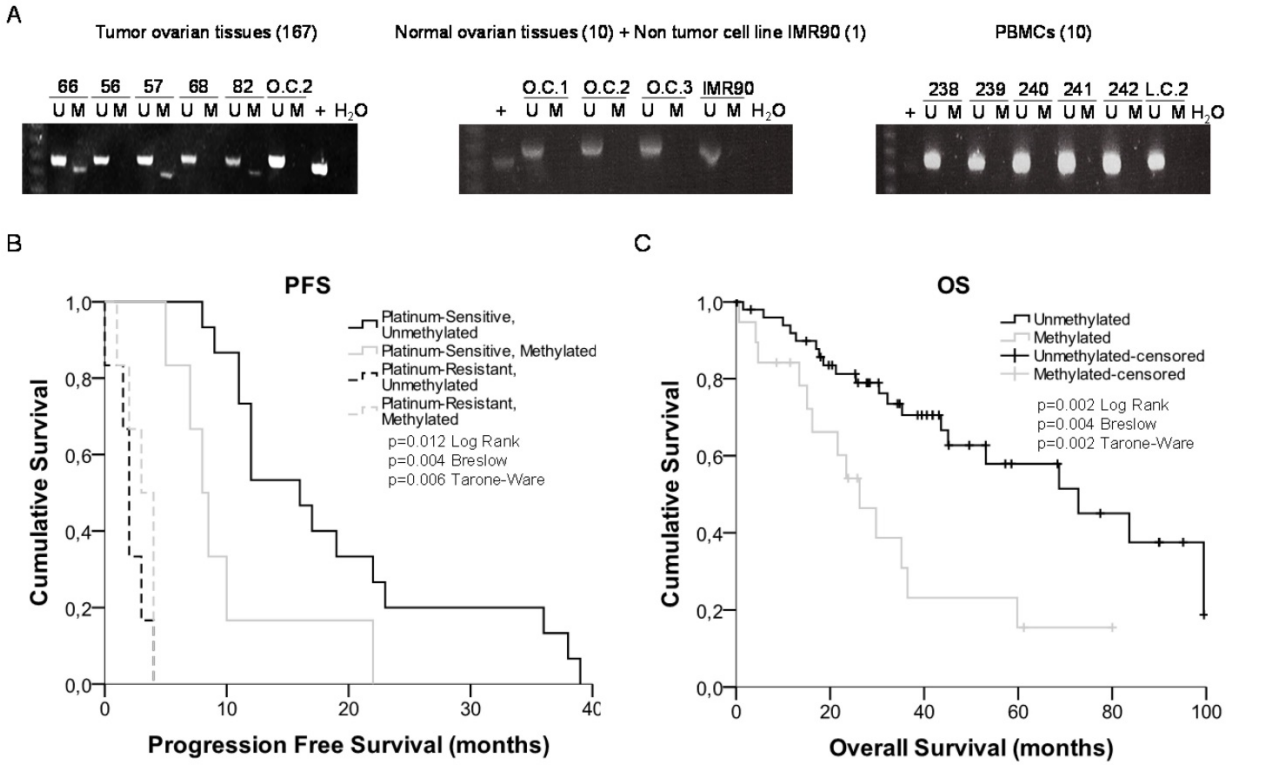

Figure 4. miRNA-7 methylation analysis in primary tumors and survival analysis. (A) Representative MSPs of miR-7 nearby CGI in DNA obtained from ovarian tumor tissues, normal ovarian tissues, non-tumor cell line and PBMCs from healthy donors. For each sample, the PCR product in the M lane was considered as the presence of methylated DNA, whereas the amplification product in the U lane was considered as the presence of unmethylated DNA. In vitro methylated DNA was used as a positive control (+). Uncropped gels of Figure 4a are included in Supplementary Figures (Supplementary Figure 4). (B) and (C) Kaplan-Meier comparison between cisplatin treatment and miR-7 proximal island methylation in ovarian cancer patients treated with platinum in terms of progression free survival (B) and overall survival in months (C). LogRank, Breslow and Tarone-Ware tests were used for comparisons and $p<0.05$ was considered as a significant change in OS or PFS. p values in (B) represent the significant difference between sensitive-unmethylated and sensitive-methylated patients

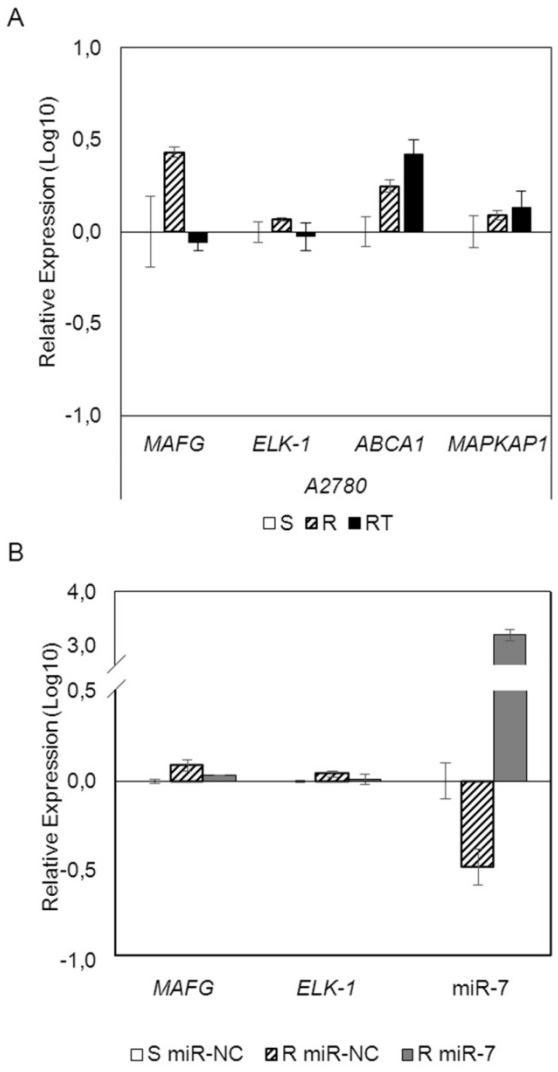

Figure 5. mRNAarrays data validation and effect of miRNA-7 over-expression on candidate target genes in the ovarian cancer cell line A2780. (A) Relative expression levels of the selected genes measured by qRT-PCR. Assays were made in all experimental conditions: S, R and RT. S: sensitive; R: resistant; RT: resistant treated with epigenetic reactivation drugs (5-Aza and TSA). Sensitive cells were used as calibrator. (B) Relative expression levels of *MAFG*, *ELK-1* and miR-7 measured by quantitative RT-PCR after miR-7 overexpression. The sensitive cell line transfected with the mimic negative control was used as a calibrator (S miR-NC, white). A2780R cells were transfected with same negative control (R miR-NC, stripped) or with miR-7 precursor (R miR-7, grey). For both (A) and (B), data are represented in Log10 scale obtained from the combined relative expression of 2 independent experiments measured in triplicate. Each gene expression level was normalized to *GAPDH* or *B-actin* as an endogenous control.

Changes in expression were validated for all 7 candidates, but not in all the expected paired cell lines, indicating that qRT-PCR is a valuable and necessary validation method more restrictive than microarray, that still keeps providing a powerful tool to study the involvement of a large number of miRNAs simultaneously [43, 44]. The expression changes were more significant after unmasking treatment, probably because the pharmacologic combination exerts a synergistic and specific influence in mRNA and miRNA global re-expression, as described in different tumor types [45]. This effect can be stronger than the silencing observed as a secondary effect of CDDP on DNA methylation.

The expression of miR-7, miR-132, miR-335 and miR-148a was validated in at least two paired cell lines. Epigenetic validation of those candidates revealed that only one miRNA from our panel, miR-7, had specific methylation in CDDP-resistance. miR-148a and miR-132 expression might be regulated by an upstream epigenetic mechanism or transcription factor reactivated by demethylation, as has been reported for other candidates [20, 22]. miR-335 epigenetic reactivation has been reported in breast cancer cells, confirming the relevance of our approach to identifying miRNAs under epigenetic regulation, although the response after platinum treatment was not studied [46]. We found specific methylation in both, H460S/R cells, but not in the controls and additional cell lines analyzed, suggesting that the downregulation in the resistant phenotypes is probably independent of the methylation profile. We cannot conclude that the downregulation of miR-335 is affecting the response to platinum, but the sensitivity to the drug seems not to be mediated by DNA methylation.

We focused on the epigenetic regulation of miR-7 at the upstream CpG island analyzed, as the one encompassing miR-7 showed constitutive methylation, suggesting the absence of a regulatory role, as reported for other potential regulatory CGIs [47]. The same methylation profile was found in ovarian, lung, colon and pancreatic cisplatin-resistant cell lines. These data suggest a potential epigenetic regulation of miR-7 at DNA methylation level for this second CGI, a relatively common event in various tumor types, which can present intrinsic resistance to CDDP by epigenetic regulation. We therefore tested the specificity of aberrant miR-7 hypermethylation as a potential epigenetic biomarker to detect the response to chemotherapy on 167 ovarian cancer patients, all of them treated with platinum-based therapy. An extensive clinical follow-up of 83 of those patients showed that those considered platinum-sensitive, harboring an unmethylated miR-7 had a better progression free survival rates than those patients with a methylated marker. These differences were not observed in platinum-resistant patients, probably because in these patients the recurrence develop in short-time periods and in a small number of cases. We confirmed the same tendency in an additional smaller cohort of 55 patients. Furthermore, our analysis indicated that those patients carrying an unmethylated marker tended to have less aggressive tumors, with three times more overall survival after platinum treatment than those who carried the

methylated DNA. In addition, the methylation percentage increased in tumor grades III/IV and when analyzing high-serous samples and Platinum-refractory/resistant tumors. Thus, miR-7 methylation could play a role as a clinical tool predicting the aggressive behavior of this malignancy and the poorer response to platinum-based treatment.

We sought then to confirm the role of miR-7 in the response to CDDP, in order to explore the potential therapeutic effect of miR-7 overexpression, as it has been developed for miR-34, the first microRNA mimic to be used in clinical testing as a theranostic marker (http://mirnatherapeutics.com). However, the ectopically overexpression of miRNA-7 in resistant cells did not change their sensitivity to CDDP, although it induced an increase in cell mortality; probably, due to the multifactorial effect that overexpression of miRNAs may cause on the cellular processes by regulating a high number of potential candidates genes. These results validate previous studies, which have shown its possible tumor suppressor role in cancer [48]. Its expression has been also linked with sensitization to paclitaxel [49], although its regulation in this process has not

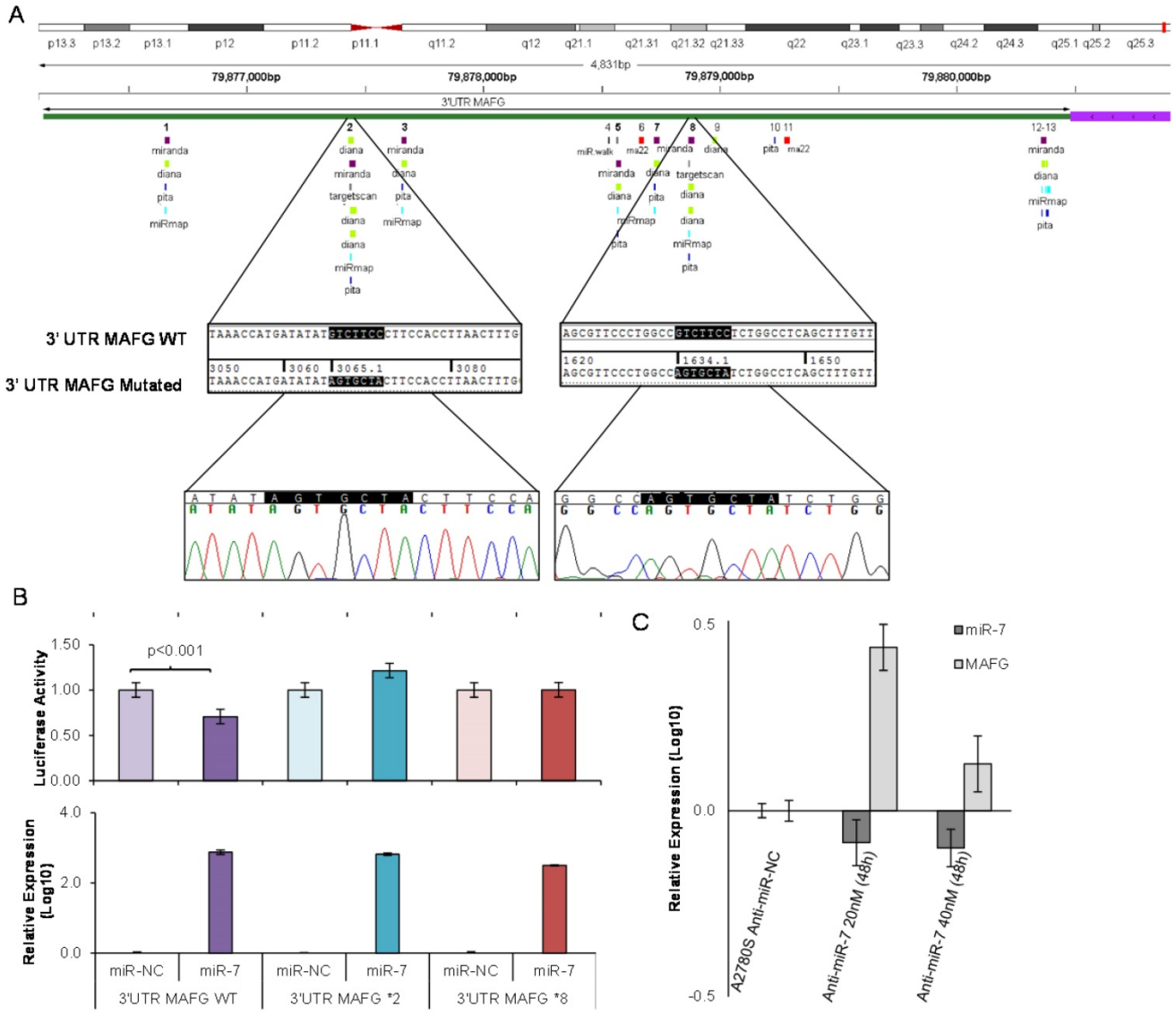

Figure 6. Site-directed mutagenesis for luciferase activity assay and effect of miR-7 silencing over MAFG expression. (A) Chromosomal localization of miR-7 predicted binding sites at 3'UTR of MAFG. Regions 2 and 8 were identified by six or more bioinformatical algorithms. Sanger sequencing showed that the seed sequence of miR-7 was fully mutated at regions 2 and 8 of the 3' UTR of MAFG. (B) Co-transfection of mimic miR-7 (miR-7) or mimic control (miR-NC) with the 3' UTR of MAFG WT, mutated on region 2 (MAFG 2*) and mutated on region 8 (MAFG 8*). Experiments were performed at 15nM and data was analyzed after 24h of co-transfection. (Upper panel) Relative luciferase activity. The figures represent the mean ± SD of at least 3 independent experiments after data normalization with Renilla and the data from the negative control 3'-UTR; p<0.01 was considered as significant change in Luciferase activity (Student's t-test). (Lower panel) Relative miR-7 expression levels measured by qRT-PCR after co-transfection, as an internal control for the mimic transfection. Each bar represents the combined relative expression of 2 independent experiments measured in triplicate. The miR-NC co-transfected with the 3'-UTR of each tested group was used as calibrator. (C) Relative miR-7 and *MAFG* expression levels measured by qRT-PCR after silencing of miR-7 with antago-miR in A2780S cells. Two different concentrations of Anti-miR-7 were tested, 20nM and 40 nM. Data was analyzed at 48h after transfection. Each bar represents the combined relative expression of 2 independent experiments measured in triplicate. A2780S cells transfected with the Anti-miR Negative Control was used as calibrator.

being defined. miR-7 might be involved in these processes through the regulation of its target genes, whose overexpression has been found in our experimental approach. Using a transcriptomic profile together with the *in silico* assembling of sequences, we identified a group of genes candidate to be targets of miR-7 that could provide cells with the oncogenic capabilities described by Hanahan and Weinberg [50]. Further analysis of molecular pathways and cellular functions, led us to the selection of *MAFG*, *ELK-1*, *ABCA1* and *MAPKAP1* genes. Validation by alternative techniques and overexpression of miR-7 in the resistant cell lines, revealed that *MAFG*, *ABCA1* and *ELK-1* recovered their levels of expression after epigenetic treatment and overexpression of miR-7, thus indicating a possible regulation of these genes by the methylation of this miRNA. However, our functional studies performed with luciferase vectors carrying a mutation in the conserved miR-7 binding site, revealed that only *MAFG* seems to be a direct candidate target gene under miR-7 regulation. Moreover, the silencing of miR-7 expression resulted in increased levels of *MAFG* and its overexpression is able to strongly increase the resistance to CDDP in sensitive cells. miR-7 may be an indirect regulator of *ABCA1* and *ELK-1*, in fact, it has been reported that miR-7 could act as modulator of chemoresistance by targeting the *MRP1/ABCC1*, a member of the ABC family proteins, and being involved in lung tumorogenesis by directly regulating the *EGFR* expression [51-53]. Moreover, *ABCA1* upregulation has been related to the decrease in chemotherapy response in breast cancer. However, we could not find a significant increase of resistance to CDDP after *ABCA1* overexpression, possibly because of the different schema of treatment used in this study, based on sequential paclitaxel/neoadjuvant chemotherapy [54]. The inhibition of *ELK-1* through the drug silodosin has been reported to increase the response to cisplatin in bladder cancer cells [55]. Its overexpression in ovarian cancer cells did not change the sensitivity to CDDP; nevertheless, we observed an increase in the cell survival fraction. As *ELK-1* is a nuclear target of the MAP-kinases cascade and the EGFR-signaling pathway, and miR-7 is a direct regulator of EGFR gene, we believe that our results are a consequence of the highly implication of *ELK-1* in cell proliferation and apoptosis though these signaling routes [56].

MAFG is associated with detoxification in oxidative stress situations. This leads us to believe that its involvement in the acquired resistance to platinum resides in the protection it confers against free radicals generated in the cell after the administration of this drug [57-61]. Despite the fact that sMafs family, to which *MAFG* belongs, have been associated with cellular response, little is known about their involvement in human diseases. A number of studies have however linked these proteins with cancer, such as the study by Schembri et al. on *MAFG* regulation by miR-218 as an indicator of smoking-induced disease processes in the lungs [62] and the study by Yang et al. on the relationship between increased *MAFG* and growth in colon cancer cell lines through the insulin-like growth factor-I actions [63]. Taken together, our experimental results strongly support the direct regulation of *MAFG* through miR-7 and their involvement in the development of CDDP resistance in human tumor cells.

In the present manuscript, we introduce the epigenetic regulation of miR-7 as a mechanism involved in platinum-resistance in cancer cell lines directly regulating the action of *MAFG*, which is overexpressed in resistant phenotypes. To the best of our knowledge, this is the first report linking the regulation of *MAFG* by miRNA-7 and its role in chemotherapy response to CDDP. Moreover, miR-7 methylation arises as a potential predictive biomarker for the identification of ovarian cancer patients that may present worst response to platinum-derived treatment in terms of OS and PFS. Furthermore, this data captures the interest of researchers due to the possible role *MAFG* plays as a novel therapeutic target for platinum resistant tumors.

Abbreviations

miRNAs: microRNAs; RI: Resistance Index; CGI: CpG island; CDDP: cisplatin; qRT-PCR: quantitative Real Time-PCR; BS: bisulfite sequencing; NSCLC: non-small cell lung cancer; PBMCs: peripheral blood mononuclear cells; mSP: Methylation Specific PCR.

Supplementary Material

Additional File 1:
Supplementary figures and tables.
http://www.thno.org/v07p4118s1.pdf
Additional File 2:
Supplementary database information.
http://www.thno.org/v07p4118s2.pdf

Acknowledgments

The authors thank ServingMed.com for the English language correction and D L for the biostatistical analysis. The authors also acknowledge Biobank from HULP for sample processing.

Financial support

FIS (ISCIII) and FEDER/FSE funds (PI12/00386, PI12/01463, PI14/01495, PI15/00186, and

FEDER/FSE, Una manera de hacer Europa support the study and contracts of I.I.C. and O.V. PTA2012/7141-I funds support OP contract and I.I.C. was financed by the ''Miguel Servet'' program (CP 14/00008). The authors gratefully acknowledge the Colombian Department for Science, Technology and Innovation (COLCIENCIAS), Cod.568-2012, for partially funding this work to J.S.

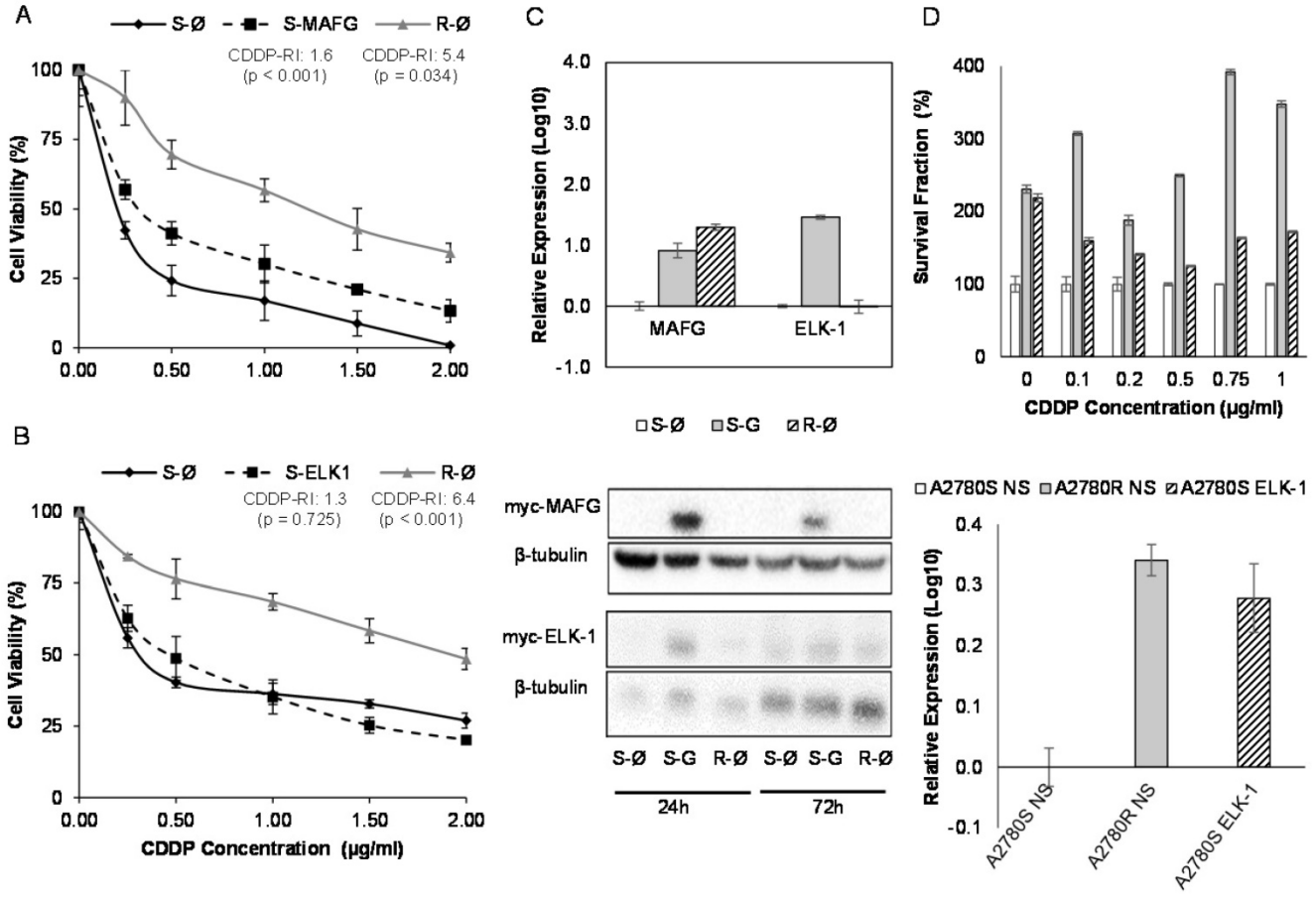

Figure 7. Effect of overexpression of *MAFG* and *ELK-1* on cell sensitivity to CDDP in A2780 cell lines. (A-B) Viability curves of A2780 cell lines transfected with pCMV6 (S-Ø and R-Ø) and with the overexpression vectors (S-*MAFG* and S-*ELK-1*). Each experimental group was exposed for 48 h to 6 different CDDP concentrations, and data were normalized to each untreated control, set to 100%. The data represent the mean ± SD of at least 3 independent experiments performed in quadruplicate at each drug concentration for each cell line analyzed. The CDDP-RI (Resistant Index to CDDP) was calculated as "IC50 from the R-Ø / IC50 from the S-Ø" and "IC50 from the S-transfected with the gene / IC50 from the S-Ø" ± SD. $p<0.01$ was considered as significant change in drug sensitivity (Student's t-test). (C) Validation of the transfection efficacy at mRNA and protein levels. Top, Relative expression levels of *MAFG* and *ELK-1* measured by quantitative RT-PCR, in the cell line A2780, represented in Log10 scale; In each experimental group, the sensitive cell line transfected with pCMV6 plasmid was used as a calibrator. Each bar represents the combined relative expression of 2 independent experiments measured in triplicate. Bottom, total cell protein (20µg) at 24 and 72 hours was subjected to WB, membranes were hybridized with antibodies against c-Myc and β-tubulin as loading control. S: Sensitive; S-G: Sensitive transfected with the gene; R: Resistant; β-tub: β-tubulin. (D) Stable overexpression of *ELK-1* in A2780S cell line. Top, Viability assay after the nonsilencing (NS) plasmid transductions (S-NS white; R-NS stripped) and overexpressing *ELK-1* plasmid (S-*ELK-1* grey). Each experimental group was exposed for 72 h to 6 different CDDP concentrations, and data were normalized to each sensitive subtype. Data represents the mean ± SD of at least 3 independent experiments performed with 4 wells at each drug concentration for each cell line analyzed. Bottom, relative *ELK-1* expression levels measured by qRT-PCR and represented in Log10 scale. The sensitive cell line with nonsilencing vector was used as a calibrator. Each bar represents the combined relative expression of 2 independent experiments measured in triplicate.

Author Contributions

IIC Conception and design.

OV, JJ, OP, CRA, CR, JS and IIC Development of methodology.

OV, JJ, OP, JS, RR, AD, IER and IIC acquisition of data.

OV, JJ, CRA, CR, JV, FR, RP, JDC analysis and interpretation of data.

SLM, RA, FR, CB, JB, IER and JDC provided clinical samples and histories.

All the authors Write, review and/or revised the manuscript.

Competing Interests

The authors have declared that no competing interest exists. Current state of intellectual property:

Spanish patent P201530997, PCT/ES2016/070516 (November 2016).

References

1. Kartalou M, Essigmann JM. Mechanisms of resistance to cisplatin. Mutat Res. 2001; 478: 23-43.
2. Ho GY, Woodward N, Coward JI. Cisplatin versus carboplatin: comparative review of therapeutic management in solid malignancies. Crit Rev Oncol Hematol. 2016.
3. Nogales V, Reinhold WC, Varma S, Martinez-Cardus A, Moutinho C, Moran S, et al. Epigenetic inactivation of the putative DNA/RNA helicase SLFN11 in human cancer confers resistance to platinum drugs. Oncotarget. 2016; 7: 3084-97.
4. Murphy M, Stordal B. Erlotinib or gefitinib for the treatment of relapsed platinum pretreated non-small cell lung cancer and ovarian cancer: a systematic review. Drug Resist Updat. 2011; 14: 177-90.
5. van Moorsel CJ, Pinedo HM, Veerman G, Bergman AM, Kuiper CM, Vermorken JB, et al. Mechanisms of synergism between cisplatin and gemcitabine in ovarian and non-small-cell lung cancer cell lines. Br J Cancer. 1999; 80: 981-90.
6. Woo EY, Chu CS, Goletz TJ, Schlienger K, Yeh H, Coukos G, et al. Regulatory CD4(+)CD25(+) T cells in tumors from patients with early-stage non-small cell lung cancer and late-stage ovarian cancer. Cancer Res. 2001; 61: 4766-72.
7. Heyn H, Esteller M. DNA methylation profiling in the clinic: applications and challenges. Nat Rev Genet. 2012; 13: 679-92.
8. Cortes-Sempere M, de Miguel MP, Pernia O, Rodriguez C, de Castro Carpeno J, Nistal M, et al. IGFBP-3 methylation-derived deficiency mediates the resistance to cisplatin through the activation of the IGFIR/Akt pathway in non-small cell lung cancer. Oncogene. 2013; 32: 1274-83.
9. Cao J, Song Y, Bi N, Shen J, Liu W, Fan J, et al. DNA methylation-mediated repression of miR-886-3p predicts poor outcome of human small cell lung cancer. Cancer Res. 2013; 73: 3326-35.
10. Weichenhan D, Plass C. The evolving epigenome. Hum Mol Genet. 2013; 22: R1-6.
11. Calin GA, Dumitru CD, Shimizu M, Bichi R, Zupo S, Noch E, et al. Frequent deletions and down-regulation of micro- RNA genes miR15 and miR16 at 13q14 in chronic lymphocytic leukemia. Proc Natl Acad Sci U S A. 2002; 99: 15524-9.
12. Mendell JT, Olson EN. MicroRNAs in stress signaling and human disease. Cell. 2012; 148: 1172-87.
13. Bui TV, Mendell JT. Myc: Maestro of MicroRNAs. Genes Cancer. 2010; 1: 568-75.
14. Fabbri M, Garzon R, Cimmino A, Liu Z, Zanesi N, Callegari E, et al. MicroRNA-29 family reverts aberrant methylation in lung cancer by targeting DNA methyltransferases 3A and 3B. Proc Natl Acad Sci U S A. 2007; 104: 15805-10.
15. Baylin SB, Herman JG, Graff JR, Vertino PM, Issa JP. Alterations in DNA methylation: a fundamental aspect of neoplasia. Advances in cancer research. 1998; 72: 141-96.
16. Marks PA, Richon VM, Miller T, Kelly WK. Histone deacetylase inhibitors. Advances in cancer research. 2004; 91: 137-68.
17. Xu S, Ren J, Chen HB, Wang Y, Liu Q, Zhang R, et al. Cytostatic and apoptotic effects of DNMT and HDAC inhibitors in endometrial cancer cells. Curr Pharm Des. 2014; 20: 1881-7.
18. Ibragimova I, Ibanez de Caceres I, Hoffman AM, Potapova A, Dulaimi E, Al-Saleem T, et al. Global reactivation of epigenetically silenced genes in prostate cancer. Cancer Prev Res (Phila). 2010; 3: 1084-92.
19. Chen DQ, Pan BZ, Huang JY, Zhang K, Cui SY, De W, et al. HDAC 1/4-mediated silencing of microRNA-200b promotes chemoresistance in human lung adenocarcinoma cells. Oncotarget. 2014; 5: 3333-49.
20. Ibanez de Caceres I, Cortes-Sempere M, Moratilla C, Machado-Pinilla R, Rodriguez-Fanjul V, Manguan-Garcia C, et al. IGFBP-3 hypermethylation-derived deficiency mediates cisplatin resistance in non-small-cell lung cancer. Oncogene. 2010; 29: 1681-90.
21. Chattopadhyay S, Machado-Pinilla R, Manguan-Garcia C, Belda-Iniesta C, Moratilla C, Cejas P, et al. MKP1/CL100 controls tumor growth and sensitivity to cisplatin in non-small-cell lung cancer. Oncogene. 2006; 25: 3335-45.
22. Ibanez de Caceres I, Dulaimi E, Hoffman AM, Al-Saleem T, Uzzo RG, Cairns P. Identification of novel target genes by an epigenetic reactivation screen of renal cancer. Cancer Res. 2006; 66: 5021-8.
23. Gayarre J, Kamieniak MM, Cazorla-Jimenez A, Munoz-Repeto I, Borrego S, Garcia-Donas J, et al. The NER-related gene GTF2H5 predicts survival in high-grade serous ovarian cancer patients. J Gynecol Oncol. 2016; 27: e7.
24. Alexiou P, Maragkakis M, Papadopoulos GL, Reczko M, Hatzigeorgiou AG. Lost in translation: an assessment and perspective for computational microRNA target identification. Bioinformatics. 2009; 25: 3049-55.
25. Wang J, Duncan D, Shi Z, Zhang B. WEB-based GEne SeT AnaLysis Toolkit (WebGestalt): update 2013. Nucleic Acids Res. 2013; 41: W77-83.
26. Dweep H, Gretz N. miRWalk2.0: a comprehensive atlas of microRNA-target interactions. Nat Methods. 2015; 12: 697.
27. Kozomara A, Griffiths-Jones S. miRBase: annotating high confidence microRNAs using deep sequencing data. Nucleic Acids Res. 2014; 42: D68-73.
28. Grunau C, Clark SJ, Rosenthal A. Bisulfite genomic sequencing: systematic investigation of critical experimental parameters. Nucleic Acids Res. 2001; 29: E65-5.
29. Sandovici I, Leppert M, Hawk PR, Suarez A, Linares Y, Sapienza C. Familial aggregation of abnormal methylation of parental alleles at the IGF2/H19 and IGF2R differentially methylated regions. Hum Mol Genet. 2003; 12: 1569-78.
30. Sanchez-Perez I, Murguia JR, Perona R. Cisplatin induces a persistent activation of JNK that is related to cell death. Oncogene. 1998; 16: 533-40.
31. Smyth GK. Linear models and empirical bayes methods for assessing differential expression in microarray experiments. Stat Appl Genet Mol Biol. 2004; 3: Article3.
32. Takai D, Jones PA. The CpG island searcher: a new WWW resource. In Silico Biol. 2003; 3: 235-40.
33. Augello C, Vaira V, Caruso L, Destro A, Maggioni M, Park YN, et al. MicroRNA profiling of hepatocarcinogenesis identifies C19MC cluster as a novel prognostic biomarker in hepatocellular carcinoma. Liver Int. 2012; 32: 772-82.
34. Tsai KW, Kao HW, Chen HC, Chen SJ, Lin WC. Epigenetic control of the expression of a primate-specific microRNA cluster in human cancer cells. Epigenetics. 2009; 4: 587-92.
35. Court F, Tayama C, Romanelli V, Martin-Trujillo A, Iglesias-Platas I, Okamura K, et al. Genome-wide parent-of-origin DNA methylation analysis reveals the intricacies of human imprinting and suggests a germline methylation-independent mechanism of establishment. Genome Res. 2014; 24: 554-69.
36. Noguer-Dance M, Abu-Amero S, Al-Khtib M, Lefevre A, Coullin P, Moore GE, et al. The primate-specific microRNA gene cluster (C19MC) is imprinted in the placenta. Hum Mol Genet. 2010; 19: 3566-82.
37. Wright AA, Bohlke K, Armstrong DK, Bookman MA, Cliby WA, Coleman RL, et al. Neoadjuvant Chemotherapy for Newly Diagnosed, Advanced Ovarian Cancer: Society of Gynecologic Oncology and American Society of Clinical Oncology Clinical Practice Guideline. J Clin Oncol. 2016; 34: 3460-73.
38. Ledermann JA, Raja FA, Fotopoulou C, Gonzalez-Martin A, Colombo N, Sessa C, et al. Newly diagnosed and relapsed epithelial ovarian carcinoma: ESMO Clinical Practice Guidelines for diagnosis, treatment and follow-up. Ann Oncol. 2013; 24 Suppl 6: vi24-32.
39. Friedlander M, Trimble E, Tinker A, Alberts D, Avall-Lundqvist E, Brady M, et al. Clinical trials in recurrent ovarian cancer. Int J Gynecol Cancer. 2011; 21: 771-5.
40. Lujambio A, Calin GA, Villanueva A, Ropero S, Sanchez-Cespedes M, Blanco D, et al. A microRNA DNA methylation signature for human cancer metastasis. Proc Natl Acad Sci U S A. 2008; 105: 13556-61.
41. Hanrahan V, Currie MJ, Gunningham SP, Morrin HR, Scott PA, Robinson BA, et al. The angiogenic switch for vascular endothelial growth factor (VEGF)-A, VEGF-B, VEGF-C, and VEGF-D in the adenoma-carcinoma sequence during colorectal cancer progression. J Pathol. 2003; 200: 183-94.
42. Iwasaki H, Okabe T, Takara K, Yoshida Y, Hanashiro K, Oku H. Down-regulation of lipids transporter ABCA1 increases the cytotoxicity of nitidine. Cancer Chemother Pharmacol. 2010; 66: 953-9.
43. Calura E, Fruscio R, Paracchini L, Bignotti E, Ravaggi A, Martini P, et al. MiRNA landscape in stage I epithelial ovarian cancer defines the histotype specificities. Clin Cancer Res. 2013; 19: 4114-23.
44. Wang G, Wang R, Strulovici-Barel Y, Salit J, Staudt MR, Ahmed J, et al. Persistence of smoking-induced dysregulation of miRNA expression in the small airway epithelium despite smoking cessation. PLoS One. 2015; 10: e0120824.
45. Adi Harel S, Bossel Ben-Moshe N, Aylon Y, Bublik DR, Moskovits N, Toperoff G, et al. Reactivation of epigenetically silenced miR-512 and miR-373 sensitizes lung cancer cells to cisplatin and restricts tumor growth. Cell Death Differ. 2015; 22: 1328-40.
46. Png KJ, Yoshida M, Zhang XH, Shu W, Lee H, Rimner A, et al. MicroRNA-335 inhibits tumor reinitiation and is silenced through genetic and epigenetic mechanisms in human breast cancer. Genes Dev. 2011; 25: 226-31.
47. Lopez-Lera A, Pernia O, Lopez-Trascasa M, Ibanez de Caceres I. Expression of the SERPING1 gene is not regulated by promoter hypermethylation in peripheral blood mononuclear cells from patients with hereditary angioedema due to C1-inhibitor deficiency. Orphanet J Rare Dis. 2014; 9: 103.
48. Ma J, Fang B, Zeng F, Pang H, Zhang J, Shi Y, et al. Curcumin inhibits cell growth and invasion through up-regulation of miR-7 in pancreatic cancer cells. Toxicol Lett. 2014; 231: 82-91.
49. Liu R, Liu X, Zheng Y, Gu J, Xiong S, Jiang P, et al. MicroRNA-7 sensitizes non-small cell lung cancer cells to paclitaxel. Oncol Lett. 2014; 8: 2193-200.
50. Hanahan D, Weinberg RA. Hallmarks of cancer: the next generation. Cell. 2011; 144: 646-74.
51. Liu H, Wu X, Huang J, Peng J, Guo L. miR-7 modulates chemoresistance of small cell lung cancer by repressing MRP1/ABCC1. Int J Exp Pathol. 2015; 96: 240-7.
52. Chou YT, Lin HH, Lien YC, Wang YH, Hong CF, Kao YR, et al. EGFR promotes lung tumorigenesis by activating miR-7 through a Ras/ERK/Myc pathway that targets the Ets2 transcriptional repressor ERF. Cancer Res. 2010; 70: 8822-31.
53. Webster RJ, Giles KM, Price KJ, Zhang PM, Mattick JS, Leedman PJ. Regulation of epidermal growth factor receptor signaling in human cancer cells by microRNA-7. J Biol Chem. 2009; 284: 5731-41.

54. Park S, Shimizu C, Shimoyama T, Takeda M, Ando M, Kohno T, et al. Gene expression profiling of ATP-binding cassette (ABC) transporters as a predictor of the pathologic response to neoadjuvant chemotherapy in breast cancer patients. Breast Cancer Res Treat. 2006; 99: 9-17.
55. Kawahara T, Ide H, Kashiwagi E, Patterson JD, Inoue S, Shareef HK, et al. Silodosin inhibits the growth of bladder cancer cells and enhances the cytotoxic activity of cisplatin via ELK1 inactivation. Am J Cancer Res. 2015; 5: 2959-68.
56. Smedberg JL, Smith ER, Capo-Chichi CD, Frolov A, Yang DH, Godwin AK, et al. Ras/MAPK pathway confers basement membrane dependence upon endoderm differentiation of embryonic carcinoma cells. J Biol Chem. 2002; 277: 40911-8.
57. Katsuoka F, Motohashi H, Engel JD, Yamamoto M. Nrf2 transcriptionally activates the mafG gene through an antioxidant response element. J Biol Chem. 2005; 280: 4483-90.
58. Katsuoka F, Yamamoto M. Small Maf proteins (MafF, MafG, MafK): History, structure and function. Gene. 2016; 586: 197-205.
59. Kilic U, Kilic E, Tuzcu Z, Tuzcu M, Ozercan IH, Yilmaz O, et al. Melatonin suppresses cisplatin-induced nephrotoxicity via activation of Nrf-2/HO-1 pathway. Nutr Metab (Lond). 2013; 10: 7.
60. Li W, Yu S, Liu T, Kim JH, Blank V, Li H, et al. Heterodimerization with small Maf proteins enhances nuclear retention of Nrf2 via masking the NEszip motif. Biochim Biophys Acta. 2008; 1783: 1847-56.
61. Motohashi H, Katsuoka F, Miyoshi C, Uchimura Y, Saitoh H, Francastel C, et al. MafG sumoylation is required for active transcriptional repression. Mol Cell Biol. 2006; 26: 4652-63.
62. Schembri F, Sridhar S, Perdomo C, Gustafson AM, Zhang X, Ergun A, et al. MicroRNAs as modulators of smoking-induced gene expression changes in human airway epithelium. Proc Natl Acad Sci U S A. 2009; 106: 2319-24.
63. Yang H, Li TW, Peng J, Mato JM, Lu SC. Insulin-like growth factor 1 activates methionine adenosyltransferase 2A transcription by multiple pathways in human colon cancer cells. Biochem J. 2011; 436: 507-16.

An epigenomic approach to identifying differential overlapping and cis-acting lncRNAs in cisplatin-resistant cancer cells

KEPI_A_1436364.3d (Compact Serif) (209.55×279.4mm) 07-03-2018 10:23

EPIGENETICS, 2018
VOL. 0, NO. 0, 1–13
https://doi.org/10.1080/15592294.2018.1436364

Taylor & Francis
Taylor & Francis Group

RESEARCH PAPER

OPEN ACCESS Check for updates

An epigenomic approach to identifying differential overlapping and *cis*-acting lncRNAs in cisplatin-resistant cancer cells

Olga Vera[a,b+], Carlos Rodriguez-Antolin[a,b+], Javier de Castro[a,b], Florian A. Karreth[c], Thomas A. Sellers[d] and Inmaculada Ibañez de Caceres[a,b]

[a]Cancer Epigenetics Laboratory, INGEMM, La Paz University Hospital, Madrid, Spain; [b]Biomarkers and Experimental Therapeutics in Cancer, IdiPAZ, Madrid, Spain; [c]Department of Molecular Oncology, H. Lee Moffitt Cancer Center and Research Institute, Tampa, USA; [d]Department of Cancer Epidemiology, H. Lee Moffitt Cancer Center and Research Institute, Tampa, USA

ABSTRACT

Long noncoding RNAs (lncRNAs) are critical regulators of cell biology whose alteration can lead to the development of diseases such as cancer. The potential role of lncRNAs and their epigenetic regulation in response to platinum treatment are largely unknown. We analyzed four paired cisplatin-sensitive/resistant non-small cell lung cancer and ovarian cancer cell lines. The epigenetic landscape of overlapping and *cis*-acting lncRNAs was determined by combining human microarray data on 30,586 lncRNAs and 20,109 protein coding mRNAs with whole-genome bisulfite sequencing. Selected candidate lncRNAs were further characterized by PCR, gene-ontology analysis, and targeted bisulfite sequencing. Differential expression in response to therapy was observed more frequently in *cis*-acting than in overlapping lncRNAs (78% vs. 22%, fold change $\geq$1.5), while significantly altered methylation profiles were more commonly associated with overlapping lncRNAs (29% vs. 8%; *P* value $<$0.001). Moreover, overlapping lncRNAs contain more CpG islands (CGIs) (25% vs. 17%) and the majority of CGI-containing overlapping lncRNAs share these CGIs with their associated coding genes (84%). The differences in expression between sensitive and resistant cell lines were replicated in 87% of the selected candidates ($P<0.05$), while our bioinformatics approach identifying differential methylation was confirmed in all of the selected lncRNAs (100%). Five lncRNAs under epigenetic regulation appear to be involved in cisplatin resistance (AC091814.2, AC141928.1, RP11-65J3.1-002, BX641110, and AF198444). These novel findings provide new insights into epigenetic mechanisms and acquired resistance to cisplatin that highlight specific lncRNAs, some with unknown function, that may signal strategies in epigenetic therapies.

Abbreviations: lncRNAs: long noncoding RNAs; WGBS: whole-genome bisulfite sequencing; NSCLC: non-small cell lung cancer; CGI: CpG island; DM: differential methylation; CDDP: cisplatin; qRT-PCR: quantitative real-time PCR; BS: bisulfite sequencing; GO: gene-ontology

ARTICLE HISTORY
Received 27 October 2017
Revised 29 December 2017
Accepted 26 January 2018

KEYWORDS
lncRNA; DNA methylation; cisplatin-resistance; lung/ovarian cancer

Introduction

The central dogma of molecular biology maintains that the RNA molecule is merely an intermediary between DNA and proteins, which are the main protagonists of cellular functions [1,2]. This idea was reinforced after completion of the Human Genome Project, which revealed a vast amount of genomic space with no apparent function because this space is not occupied by protein-coding genes [3].

However, data from the Encyclopedia of DNA Elements (ENCODE) project revealed that more than 70% of the genome is pervasively transcribed into noncoding RNAs. Many noncoding RNAs had been characterized prior to the ENCODE project, because they are involved in several cellular functions, such as ribosomal or transcriptional RNA [4]. ENCODE, however, contributed to the identification of novel groups of regulatory noncoding RNAs, including microRNAs and long noncoding RNAs (lncRNAs) [5].

lncRNAs are RNA transcripts of more than 200 nucleotides in length that lack evident open reading frames [6]. The first and best-known lncRNAs identified to date are involved in chromosome dosage compensation (e.g., Xist) and the genomic imprinting and silencing of maternal or paternal genes (e.g., H19), necessary for correct embryonic development [7–9]. Because lncRNAs are involved in several processes important to the normal functioning of the cell, alterations in lncRNAs have been shown to contribute to the development and progression of various human diseases, including cancer. One of the most studied cancer-associated lncRNAs is metastasis-associated lung adenocarcinoma transcript 1 (MALAT1), a lncRNA involved in the mRNA splicing process [10]. MALAT1 is overexpressed in non-small cell lung cancer (NSCLC) metastatic

CONTACT Inmaculada Ibañez de Caceres Inma.ibanezca@salud.madrid.org Cancer Epigenetics Laboratory, INGEMM, Biomarkers and Experimental Therapeutics in Cancer, IdiPAZ, Paseo de la Castellana 261, Madrid 28046 Spain
[+]These authors contributed equally to this work
Supplemental data for this article can be accessed at https://doi.org/10.1080/15592294.2018.1436364

© 2018 The Author(s). Published by Informa UK Limited, trading as Taylor & Francis Group.
This is an Open Access article distributed under the terms of the Creative Commons Attribution-NonCommercial-NoDerivatives License (http://creativecommons.org/licenses/by-nc-nd/4.0/), which permits non-commercial re-use, distribution, and reproduction in any medium, provided the original work is properly cited, and is not altered, transformed, or built upon in any way.

KEPI_A_1436364.3d (Compact Serif) (209.55×279.4mm) 07-03-2018 10:23

tumors and could be used as a prognostic biomarker in Stage I disease [11]. Overexpression of MALAT1 plays an oncogenic role in ovarian cancer, increasing cell viability, colony formation, and migration, together with a metastatic phenotype in patients with ovarian cancer [12].

Recent evidence suggests that lncRNAs are involved in chemoresistance to various anticancer therapies. One example is HOTTIP, a lncRNA regulating 5' HOXA gene transcription, which has been associated with cell proliferation, invasion and chemoresistance in osteosarcoma, liver, and pancreatic cancers [13,14]. Other lncRNAs, such as UCA1 and ROR, have been associated with the resistance of cancer cells to platinum-based treatments in bladder and nasopharyngeal cancers, respectively [15,16].

Cisplatin (CDDP) is the most widely used chemotherapeutic for solid tumors, such as lung, ovarian, testis, and head and neck cancers, among others. Although cisplatin is a first line cancer treatment, CDDP resistance develops in a high percentage of cancer patients [17–20]. It has been previously shown that CDDP treatment induces *de novo* methylation of gene and miRNA promoters, which contributes to the development of resistance to CDDP in several tumor types [21–24]. Although our understanding of lncRNAs is increasing, little is known of their regulation in the development of resistance to CDDP. In the present study, we integrated a global methylation analysis with lncRNA and mRNA transcriptomics to identify the epigenetic regulation of lncRNAs that could contribute to the development of acquired CDDP resistance in NSCLC and ovarian cancer cells.

Results

Approach to identify and validate lncRNAs regulated by CDDP resistance

All data are based on eight CDDP-sensitive and CDDP-resistant NSCLC (H23S/R and H460S/R) and ovarian cancer (A2780S/R and OVCAR3S/R) cell lines previously established in our laboratory [22,24] (Supplementary Figure 1). We generated a global transcriptome and DNA methylome profile of lncRNAs and mRNAs to identify those that had a change in expression levels after the development of platinum resistance (Figure 1(A)).

Among the 30,586 lncRNAs (19,590 intergenic lncRNAs and 10,996 overlapping) and the 20,109 mRNA transcripts, we found a percentage of expression changes of approximately 1.5% and 2.0%, respectively, for all the contrasts analyzed, with a fold change ≥1.5 (Table 1). We also compared the common lncRNAs or mRNAs with detectable changes in expression between sensitive and resistant cell lines and tissue type, and found a similar percentage change (Figure 1(B and C)).

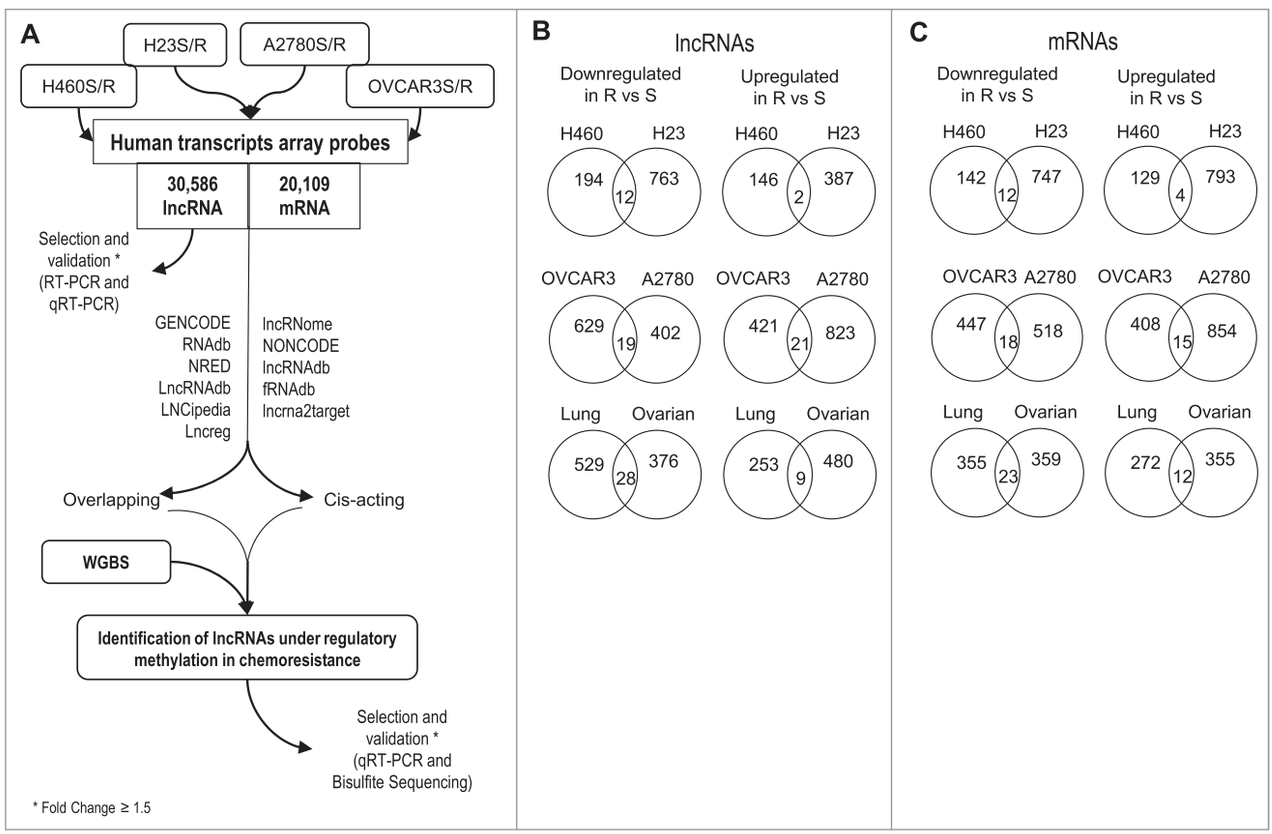

Figure 1. Experimental design and general overview of expression changes. (A) Pipeline of the followed steps for this study. Arrays combining lncRNAs and mRNAs probes were performed for four paired sensitive/resistant cell lines from lung and ovarian cancer. The threshold for selection was fold change ≥1.5. Inclusion of WGBS data was used to identify lncRNAs under epigenetic regulation by DNA methylation. Selection and further validation of lncRNAs was performed to confirm observed changes in expression and methylome analysis. (B and C) Venn diagram of shared lncRNAs (B) and mRNAs (C) that change in resistance in both lung cancer cell lines (top), both ovarian cancer cells (middle) or when comparing lung and ovarian cells (bottom).

KEPI_A_1436364.3d (Compact Serif) (209.55×279.4mm) 07-03-2018 10:23

Table 1. Overall view of changes for lncRNA (left) and mRNAs (right) observed in the arrays.

	lncRNAs				mRNAs			
Contrast	Downregulated		Upregulated		Downregulated		Upregulated	
H23R vs. H23S	763	2.5%	387	1.3%	747	2.9%	793	3.0%
H460R vs. H460S	194	0.6%	146	0.5%	142	0.5%	129	0.5%
A2780R vs. A2780S	402	1.3%	823	2.7%	518	2.0%	514	2.0%
OVCAR3R vs. OVCAR3S	629	2.1%	421	1.4%	447	1.7%	408	1.6%
Lung R vs. Lung S	529	1.7%	253	0.8%	355	1.4%	272	1.0%
Ovarian R vs. Ovarian S	376	1.2%	480	1.6%	359	1.4%	418	1.6%
All R vs. All S	363	1.2%	257	0.8%	290	1.1%	250	1.0%

We next selected a representative group of 30 lncRNA transcripts to validate the expression changes between resistant and sensitive cells observed in the array analysis by semi-quantitative PCR. Validation was successful in 11 out of 15 downregulated and 14 out of 15 upregulated lncRNAs in the cancer cell lines used for the array (Supplementary Figure 2(A and C)). We further tested the expression of six transcripts in a selection of two additional paired CDDP-resistant/sensitive cancer cell lines, a different pair A2780/A2780CP, and the pair OV2008/OVC13 (Supplementary Figure 2D). Table 2 summarizes the total lncRNAs analyzed and validated, as well as their associated coding genes. We performed a gene ontology analysis with the described associated coding genes of the 25 validated lncRNAs, which are included into the Arraystar platform. Most of the lncRNA probes included in the array have at least one associated coding gene. Based on this GO analysis we selected 16 lncRNAs due to biological plausibility for their involvement in cancer, or published evidence of a role in cancer, as is the case of CRNDE [25,26]. We were able to confirm the expression changes by quantitative RT-PCR for 6 out of 7 downregulated (Figure 2(A)) and 8 out of 9 upregulated lncRNA candidates (Figure 2(B)). A summary of the selection process is detailed in Supplementary Figure 2E.

Cis-*acting lncRNAs are more frequently altered in CDDP-resistant cells than overlapping lncRNAs*

Further bioinformatics analyses allowed us to classify the lncRNAs that changed in resistance into two groups according to their relationship with the mRNA of a coding gene [27,28]. These analyses included (a) transcript and lncRNA genomic annotations in order to designate their positional relation that could help determine their functional relationship with their possible associated coding gene (ACG) and (b) a restrictive statistical analysis selecting only those lncRNAs and mRNAs with statistically significant changes in expression (Figure 1(A)). Those lncRNAs sharing a genomic location with an ACG and both showing statistically significant expression changes in the array were classified as "overlapping lncRNAs," including sense, antisense, and bidirectional lncRNAs. This group was represented by 176 unique lncRNA transcripts, which were associated with 185 unique mRNA transcripts. lncRNAs encoded in the 1-300 kb upstream region that did not overlap with another coding gene were included in the "*cis*-acting lncRNA" group [29,30]. This group was represented by 613 lncRNA transcripts interacting with 662 mRNA transcripts (Figure 3(A)). Among the lncRNAs represented in the arrays with known genomic location, the observed vs. expected ratio was increased for *cis*-acting lncRNA (78% vs. 64%) but decreased for the overlapping lncRNAs (22% vs. 36%). When analyzing the global expression changes from both groups, we observed that the majority of the overlapping lncRNAs showed the same expression pattern as the associated mRNA (Figure 3(A), left panel). For *cis*-acting lncRNAs, we observed both similar and opposing expression changes with their associated mRNAs in resistant compared to sensitive cell lines (Figure 3(A), right panel).

CpG islands and aberrant methylation are more frequent in overlapping than cis-acting lncRNAs in CDDP resistance

To identify the role of epigenetic regulation of lncRNAs in CDDP resistance we interrogated the whole-genome bisulfite sequencing (WGBS) data obtained from our lung and ovarian experimental models (Supporting Dataset). We searched for canonical CpG islands (CGIs) and then classified the lncRNAs according to their island position. We first observed that 44 of the 176 overlapping lncRNAs (25%) have a defined CGI for themselves or for their ACG, whereas a defined CGI was found in only 17% (105 of 613) of the *cis*-acting lncRNAs. It is interesting to highlight that the majority of the overlapping lncRNAs with a defined CGI share this island with their ACG (84%). Those lncRNAs are increased in the downregulated group of lncRNAs (Figure 3(B)). Only 14% have an exclusive CGI and a small percentage of these lncRNAs (2%) belonged to a group with one CGI for the lncRNA and a different CGI for the ACG (Figure 3(B), left bars). Conversely, among the *cis*-acting lncRNAs, there was a small percentage of lncRNAs sharing the CGI with the ACG (1%), with 6% showing an exclusive CGI and the majority represented by lncRNAs that have CGIs different from the CGI of their ACG (10%). This association between the presence or absence of CGIs and the lncRNA location (overlapping or *cis*-acting) was statistically significant (Chi-square test, $P = 0.02$). Thus, to identify whether CGI methylation was associated with the observed changes in lncRNA expression, we divided them into lncRNAs carrying or not a CGI and another group based on where the CGI was located (Supplementary Figure 3A). For overlapping lncRNAs, we included all the lncRNAs with a possible CGI at their regulatory region or at their ACGs in the first group (Supplementary Figure 3A, top). For *cis*-acting lncRNAs, we included only those lncRNAs with a possible CGI in their regulatory region (Supplementary Figure 3A, bottom). This contrast revealed that the overlapping lncRNAs are similarly represented in both groups, with and without CGIs (42% and 58%, respectively), but *cis*-acting lncRNAs are richer in lncRNAs without CGIs (17% vs. 83%) (Figure 3(C)).

KEPI_A_1436364.3d (Compact Serif) (209.55×279.4mm) 07-03-2018 10:23

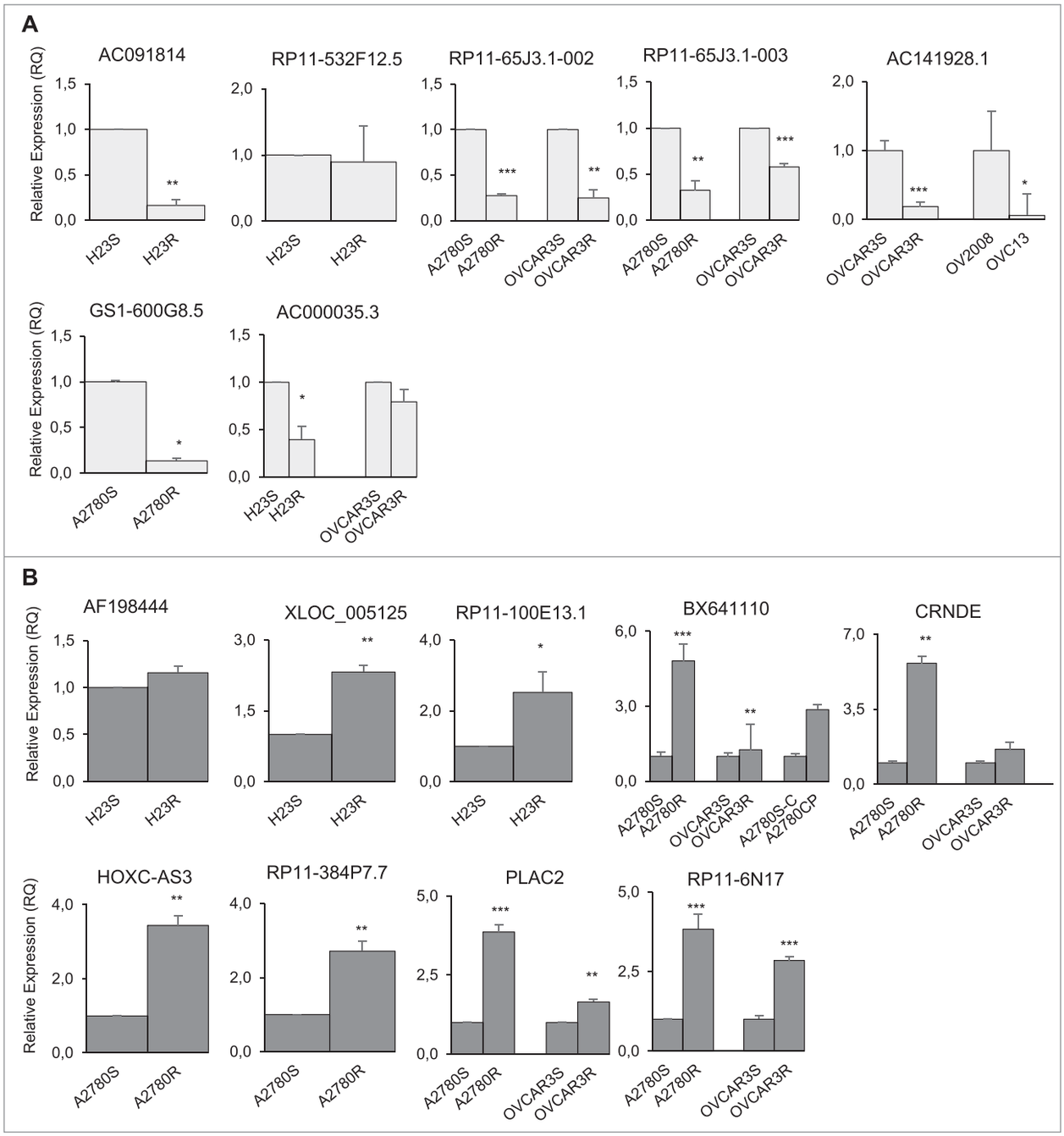

Figure 2. Quantitative validation of lncRNA microarray expression changes in 15 lncRNAs based on their possible biological implication in cancer. qRT-PCR to confirm the quantitative expression changes of the downregulated (A) and upregulated (B) lncRNAs that were validated in the resistant subtypes compared with the expression of the sensitive parental cells in the lung cancer model (H23S/R and H460S/), in the ovarian cancer model (A2780S/R and OVCAR3S/R) and two additional ovarian cancer cell lines (A2780S-C/A2780CP and OV2008/OVC13). The data represent the results from at least two different experiments measured by triplicate in Relative Quantification (RQ) scale ± SD. $^{*}P < 0.05$; $^{**}P < 0.01$; $^{***}P < 0.001$ (Student's T-test).

Following the identification of the possible CGIs that could be involved in the regulation of expression changes, we analyzed the differentially methylated CpG positions identified by WGBS. To avoid losing any possible methylated candidates, our bioinformatics study also included the analysis of a longer region starting at -2000 bp and ending at +500 bp from the lncRNA transcription start site (TSS) for those lncRNAs without a CGI (Supplementary Figure 3B, drawing). Among the overlapping lncRNAs with a CGI, 29% demonstrated differential methylation (DM) between resistant and sensitive cells at more than one position, compared with 8% of *cis*-acting lncRNAs (Figure 3(C)). The difference in methylation by location of the lncRNAs (overlapping or *cis*-acting) was statistically significant (Chi-square test P <0.001). For overlapping lncRNAs, the methylation pattern is associated with downregulation in platinum resistance, 73% of all differentially methylated overlapping lncRNAs in comparison with the 50% observed for *cis*-acting lncRNAs (Supplementary Figure 3C).

KEPI_A_1436364.3d (Compact Serif) (209.55×279.4mm) 07-03-2018 10:23

Table 2. Summary of selected lncRNAs.

Contrast	Cell line	Seq.name	GeneSymbol	Chromosome	Strand	RNA Length	Validation in Original/ Additional Cells	Associated Coding Gene (ACG)
Downregulated	H23	ENST00000412084	AC091814.2	chr12	–	979	H23R	*OLR1*
Downregulated	H23	ENST00000563217	RP11-532F12.5	chr15	–	250	H23R	*DNAJC17*
Downregulated	H23	ENST00000558382	RP11-522B15.3	chr15	+	501	Undetermined	*NR2F2*
Downregulated	A2780	ENST00000423122	RP11-65J3.1-002	chr9	+	545	A2780R & OVCAR3R	*IER5L*
Downregulated	Ovarian	ENST00000444125	RP11-65J3.1-003	chr9	+	783	A2780R & OVCAR3R	*IER5L*
Downregulated	OVCAR3	ENST00000511928	AC141928.1	chr4	–	4525	OVCAR3R/A2780CP & OVC13	*LRPAP1*
Downregulated	OVCAR3	ENST00000449073	AC007040.5	chr2	+	625	OVCAR3R	*FIGLA*
Downregulated	A2780R&OVCAR3R	ENST00000556071	RP11-1A16.1	chr14	+	554	A2780R & OVCAR3R	-
Downregulated	A2780R	ENST00000412485	GS1-600G8.5	chrX	–	1497	A2780R	*EGFL6*
Downregulated	OVCAR3R	ENST00000453395	LA16c-83F12.6	chr22	–	624	OVCAR3R	-
Downregulated	OVCAR3R	ENST00000490341	TUBA4B	chr2	+	1380	OVCAR3R	*TUBA4*
Downregulated	A2780R&OVCAR3R	ENST00000529081	CTD-2026G22.1	chr11	+	578	Undetermined/A2780CP	*FOLH1*
Downregulated	A2780R	ENST00000455275	AP001439.2	chr21	+	392	Undetermined	*APP*
Downregulated	A2780R	ENST00000577848	RP11-874J12.4	chr18	+	1455	Undetermined	*DLGAP1*
Downregulated	AllR_vs_All-S	ENST00000419368	AC000035.3	chr22	–	570	H23R & OVCAR3R	*NF2*
Upregulated	H23	uc021sxs.1	AF198444	chr15	+	3890	H23R & H460R	*ALDH1A3*
Upregulated	H23	TCONS_00011636	XLOC_005125	chr6	+	1366	H23R	*FOXC1*
Upregulated	Lung	ENST00000437416	RP11-100E13.1	chr1	–	403	H23R	*CNIH3*
Upregulated	A2780R&OVCAR3R	uc003jsd.1	BX641110	chr5	–	3720	A2780R & OVCAR3R/ A2780CP	*PDE4D*
Upregulated	A2780R&OVCAR3R	uc010vhb.2	CRNDE	chr16	–	838	A2780R & OVCAR3R	-
Upregulated	A2780R&OVCAR3R	NR_027064	PLAC2	chr19	–	3693	A2780R & OVCAR3R	*ZNRF4*
Upregulated	A2780R&OVCAR3R	ENST00000577279	RP11-6N17.4	chr17	–	374	A2780R & OVCAR3R	*SP2*
Upregulated	A2780R&OVCAR3R	ENST00000450535	ZNFX1-AS1	chr20	+	1075	A2780R & OVCAR3R	*ZNFX1*
Upregulated	OVCAR3R	ENST00000441539	AC007566.10	chr7	+	395	A2780R & OVCAR3R/ A2780CP	*PEX1*
Upregulated	A2780R	ENST00000567780	HOXC-AS3	chr12	–	2816	A2780R	*HOXC10*
Upregulated	A2780R	ENST00000520259	RP11-333A23.4	chr8	+	2367	A2780R	-
Upregulated	A2780R	ENST00000566968	RP11-384P7.7	chr9	+	3528	A2780R/A2780CP	*PRSS3*
Upregulated	OVCAR3R	ENST00000425587	RP11-561O23.8	chr9	+	340	OVCAR3R	-
Upregulated	OVCAR3R	ENST00000574086	RP11-760H22.2	chr8	+	522	OVCAR3R/A2780CP	-
Upregulated	A2780R&OVCAR3R	ENST00000417460	AC003986.7	chr7	+	692	Undetermined	*HDAC9*

Note: Contrast indicates lncRNA changes with statistical significance; Seq.name is the transcript name of the lncRNA; GeneSymbol is the name of the lncRNA.

The results show that the -2000/+500 bp region was essentially the same for overlapping lncRNAs and their ACG; while the -2000/+500 bp region for *cis*-acting lncRNAs is far away (>100,000 bp) from the -2000/+500 bp region observed in their ACG, assuming that the gene DM does not interfere with the *cis*-lncRNA epigenetic regulation. Analyses of the −2000/+500 bp region for those lncRNAs without CGI revealed similar percentages of differential methylation for overlapping (10%) and for *cis*-acting (8%) lncRNAs (Figure 3(C)).

Whole-genomic bisulfite sequencing validation confirms the selection criteria of our approach

Finally, we validated the methylation observed by WGBS in our cell lines. We selected eight candidates out of the 14 lncRNAs validated by qRT-PCR based on the bioinformatics analysis, the significant expression changes in both the lncRNA and the candidate ACG, and the differentially methylated positions observed by WGBS (Supplementary Figure 2E). These candidates were AC091814.2, AC141928.1, RP11-65J3.1-002, RP11-65J3.1-003, BX641110, AF198444, XLOC_005125, and RP11-100E13.1 (Table 3). Our first approach included the validation of general changes in expression after epigenetic reactivation treatment in the resistant cells, combining 5-Aza-2-deoxycytidine (5Aza-dC), a demethylating agent, and trichostatin A (TSA), a histone deacetylase inhibitor [24]. RT-PCR (Figure 4(A)) and qRT-PCR (Figure 4(B)) confirmed our first expression results observed in the cell lines for the six candidates, AC091814.2, AC141928.1, RP11-65J3.1-002, BX641110, AF198444, and XLOC_005125.

Bisulfite sequencing of the differentially methylated positions between sensitive (S) and resistant (R) cells confirmed the gain of methylation in the resistant subtypes for candidates AC091814.2, AC141928.1, and RP11-65J3.1-002, and loss of methylation for AF198444 and BX641110 (Figure 5).

Discussion

The main objective of the current study was to test the hypothesis that differential regulation of lncRNAs underlies CDDP resistance in NSCLC and ovarian cancer, which are frequently treated with platinum-derived therapies. We sought to identify lncRNAs whose expression is different and could be under epigenetic regulation when comparing CDDP-resistant with their CDDP-sensitive parental cells.

Consistent with previous reports on NSCLC [31] we observed a small percentage of expression changes among all the transcripts investigated, results that were consistent across bioinformatics contrasts. Moreover, we found a similar percentage change between ovarian and lung human cancer cell lines and limited to a relatively small number of transcripts. In fact, some of the common lncRNAs are associated with coding genes that belong to GO categories involved in cancer initiation and progression, such as the *PLCE* and *PDE11A* genes [32,33].

KEPI_A_1436364.3d (Compact Serif) (209.55×279.4mm) 07-03-2018 10:23

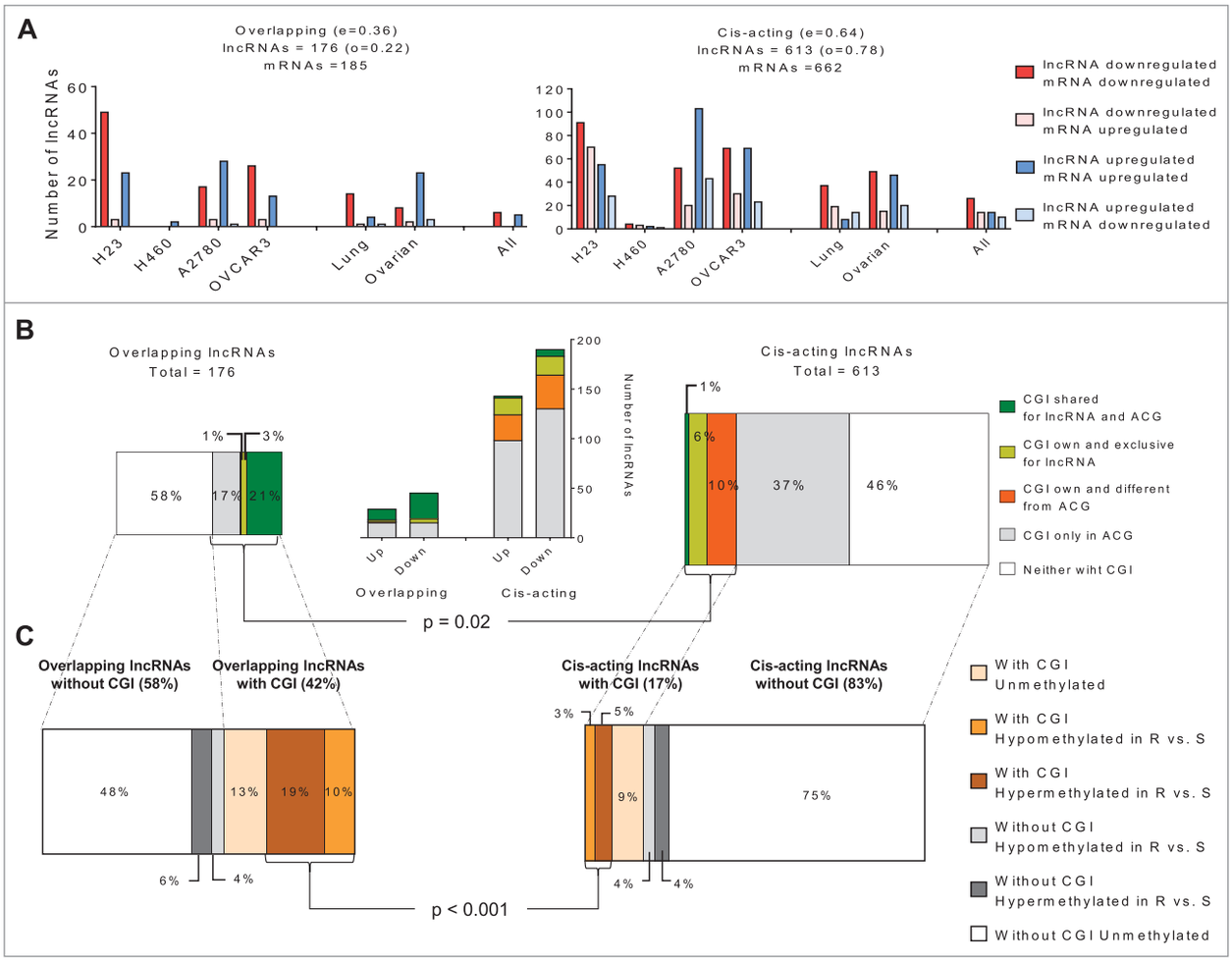

Figure 3. Bioinformatic and *in silico* analysis of lncRNA epigenetic regulation in resistance. (A) Overall view of the lncRNAs with significant changes in expression between resistant and sensitive cell lines, according to their relationship with the associated mRNA transcript identified in the array. The left panel represents overlapping lncRNAs, whereas the right panel represents *cis*-acting lncRNAs. (B) Identification of possible regulatory regions under methylation and distribution according to overlapping or *cis*-acting groups. The graphic in the middle represents the number of lncRNAs grouped by expression pattern and according to the location of their CGI. (C) Distribution of the methylation detected by WGBS in the six groups indicated with squares and comparison between *cis* and overlapping lncRNAs. Chi-squared test was used for statistical analysis and $P < 0.05$ was considered statistically significant.

The validation of the expression changes in a selected group of lncRNAs was successful in 87% of the candidates analyzed by quantitative methodology, which is similar to the percentage found in a previous study [34]. The remaining lncRNAs are novel, with unknown associated coding genes, highlighting the potential utility of the methodology employed. Although they were not included in the GO analysis, these lncRNAs cannot be completely refuted and additional research is needed to confirm the functional involvement of these candidates in cancer and chemoresistance. Some of the targets identified in the current study, AC091814.2, AC000035.3, XLOC_005125, BX641110, and RP11-384P7.7, are associated with coding genes that have been previously reported in the cancer literature; however, they have not been previously related to cancer development or cisplatin-resistance, which increases their interest for further studies.

Our bioinformatics analyses classified the lncRNAs that changed in resistance into overlapping and *cis*-acting lncRNAs according to their relationship with the mRNA of a coding gene [27–30]. One lncRNA transcript can be associated with one or more mRNA transcripts, and the number of *cis*-acting lncRNAs that change in the development of CDDP resistance is 3.5 times higher than the number of overlapping lncRNAs. This result is expected, because overlapping lncRNAs are encoded within the sequence of a coding gene, which represents less than 2% of the genome [35,36], whereas *cis*-acting lncRNAs can be found anywhere in a larger region (299 kb) on the same chromosome as an ACG. Trans-acting lncRNAs can exert a widespread action over the entire genome; thus, we limited our study to overlapping and *cis*-acting lncRNAs. The inclusion of *trans*-acting lncRNAs would necessitate a wider analysis in order to integrate all potential interactions between the transcriptome and the lncRNome, to discover new potential lncRNA-ACG pairs and to validate them. Therefore, this study is extensive and beyond the scope of the current work.

In terms of global expression changes, our results suggest that in the development of CDDP resistance the expression of a lncRNA overlapping with a coding gene is directly related to

KEPI_A_1436364.3d (Compact Serif) (209.55×279.4mm) 07-03-2018 10:23

Table 3. Main characteristics of the selected lncRNAs for methylation validation.

lncRNA			lncRNA							Differential Methylated Positions by WGBS			
lncRNA	mRNA	Contrast	Accession number	Symbol	Chromosomic location	Strand	ACG accession	ACG Symbol	Relationship	Possible Function	Analyzed region	Chromosomic location	Cell line	Number
Down	Up	H23	ENST00000412084	AC091814.2	12: 10089177-10096094	–	NM_001172632	*OLR1*	Cis-acting	upstream enhancer	-2000/+500 region	12: 10095915-10096112	H23	7
Down	Down	OVCAR3	ENST00000511928	AC141928.1	4: 3760474-3765117	–	NM_002337	*LRPAP1*	Cis-acting	downstream	lncRNA CpGi	4: 3768571-3769414	OVCAR3	37
Down	Down	A2780	ENST00000423122	RP11-65J3.1-002	9: 132104121-132121817	+	NM_203434	*IER5L*	Cis-acting	upstream enhancer	lncRNA CpGi	9: 132099124-132099573	A2780	23
Down	Down	Ovarian	ENST00000444125	RP11-65J3.1-003	9:132099157-132109743									
Up	Up	H23	uc021sxs.1	AF198444	15: 101449472-101453362	+	NM_000693	*ALDH1A3*	Overlapping	intron sense-overlapping	mRNA CpGi	15: 101419262-101420165	H23	15
Up	Up	H23	TCONS_00011636	XLOC_005125	6: 1605723-1607305	+	NM_001453	*FOXC1*	Cis-acting	downstream	lncRNA CpGi	6: 1605010-1611693	H23	13
Up	Up	Lung	ENST00000437416	RP11-100E13.1	1:22480997-224803922	–	NM_152495	*CNIH3*	Overlapping	bidirectional	-2000/+500 region	1:224804032-224804373	H460	8
Up	Up	OVCAR3	uc003jsd.1	BX641110	5: 58567936-58571656	–	NM_006203	*PDE4D*	Overlapping	intron sense-overlapping	mRNA CpGi	5: 59189120-59189507	OVCAR3	6

the expression of mRNA. Presumably, this is because their transcription is controlled by the same regulatory mechanisms. Conversely, *cis*-acting lncRNAs may promote or interfere with the expression of their ACG, as has been previously shown [37,38]. These results are in accordance with our bioinformatics methylation analysis performed on the data obtained from the WGBS, suggesting that the possible epigenetic regulation of overlapping lncRNAs can be mediated by CGIs located in their regulatory region or in one of their ACGs. By contrast, *cis*-acting lncRNAs could be primarily regulated by their own CGIs. Therefore, as overlapping lncRNA have a higher fraction of CGI, they are more likely to be unmethylated in normal/sensitive cells and more likely to be silenced by aberrant DNA methylation. Indeed, we found that the methylation in overlapping lncRNAs was more frequent than the *cis*-acting lncRNAs, reinforcing the idea that *cis*-acting lncRNAs could be regulated by mechanisms different from those of overlapping lncRNAs during the development of resistance to CDDP.

Although we observed that the occurrence of CpG islands in overlapping lncRNAs is higher than in *cis*-acting IncRNAs, this result does not reach the estimated 50%–60% of coding genes showing defined CGIs [39], suggesting that lncRNAs might be less regulated by DNA methylation. The inclusion of the -2000/+500 bp region surrounding the lncRNA and the mRNAs TSS in our analysis was an inefficient approach to increasing the number of possible candidates under epigenetic regulation because the scrutiny had to be extended to 508 *cis*-acting lncRNAs with a one-by-one candidate approach. All together, these results suggest that the overlapping lncRNAs could be epigenetically regulated through the ACG's CGIs, thus implying that these lncRNAs would be acting on regulatory loops with their ACG due to sequence complementarity. Conversely, *cis*-acting lncRNAs appear to be regulated by their own CGIs, being therefore able to regulate their ACG by other means. Although various studies have analyzed the epigenetic regulation by DNA methylation of lncRNAs in cancer [40,41] our results are the first to identify differential epigenetic regulation for overlapping and *cis*-acting lncRNAs in cancer chemoresistance.

Experimental validation at the level of lncRNA expression was successful for all the selected candidates, suggesting an epigenetic regulation of these lncRNAs in resistance. Furthermore, bisulfite sequencing of the regions identified by WGBS confirmed hypermethylation in resistance for AC091814.2, AC141928.1, and RP11-65J3.1-002 lncRNAs. In addition, we identified several positions that lost methylation in the resistant subtypes of our models in the regulatory regions of AF198444 and BX641110, suggesting that CDDP also leads to epigenetic changes that decrease methylation levels. We found more differentially methylated positions by Sanger sequencing than those first identified by WGBS. The more restrictive analysis of coverage and reads for WGBS showed no information for various regions along the genome. However, it has been reported that the methylation patterns show the same behavior in proximal regions, explaining the results in our cell lines [42,43]. We could not validate the methylated positions of XLOC_005125, because they were separately located along the CGI and no pair of primers was available to cover the entire region. However, we were able to validate the expected methylation pattern for 100% of the selected candidates.

KEPI_A_1436364.3d (Compact Serif) (209.55×279.4mm) 07-03-2018 10:23

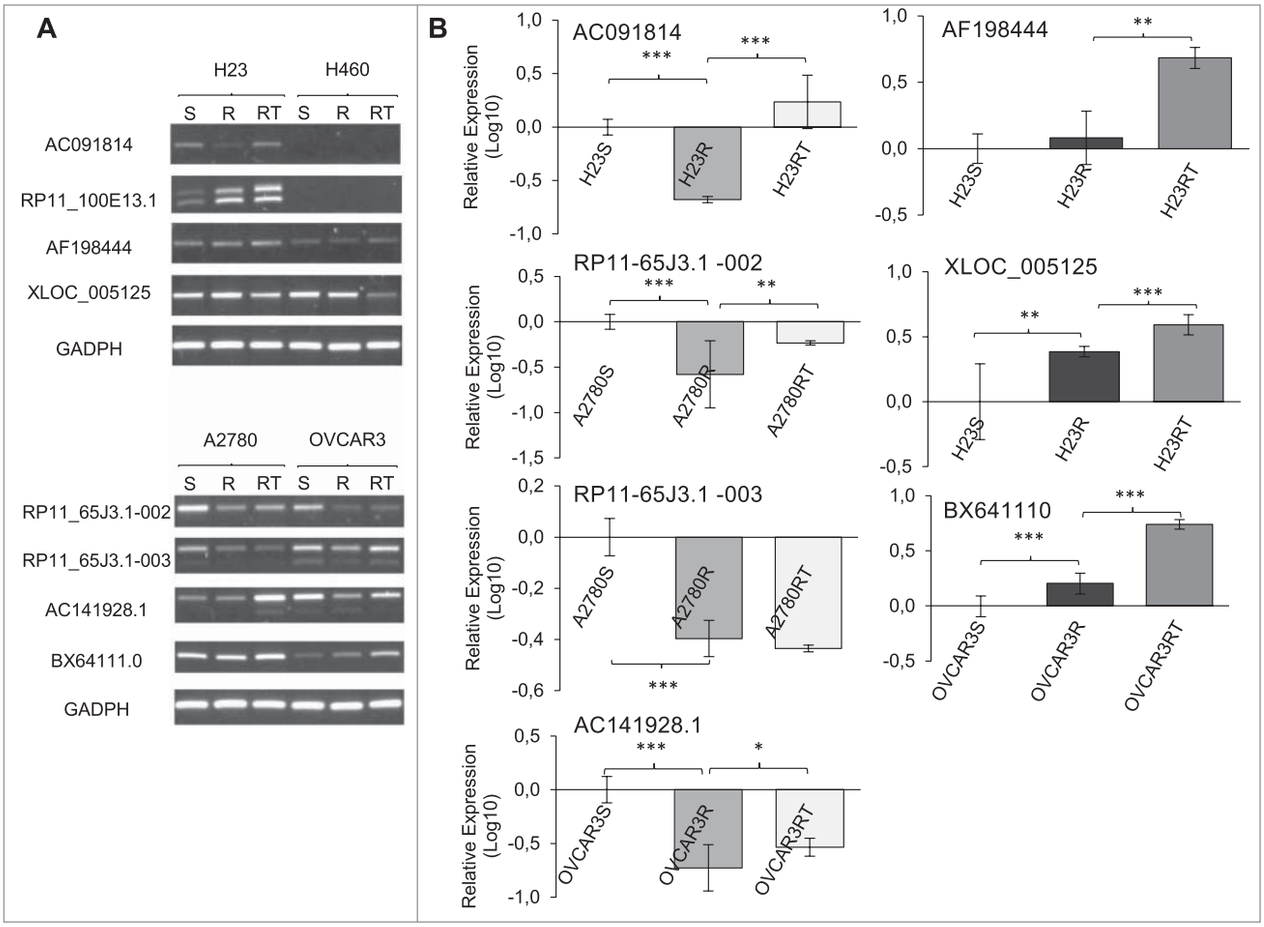

Figure 4. Validation of epigenetic changes in lncRNA expression. (A) RT-PCR comparing expression changes among sensitive (S), resistant (R), and resistant treated with epigenetic reactivation (RT). Each assay was performed at least three times to confirm the results. (B) qRT-PCR to confirm the quantitative expression changes in the same experimental groups, only for those samples that showed differentially methylated positions by WGBS. The data represent the results from two different experiments in triplicate in Log10 scale ± SD. $^{*}P < 0.05$; $^{**}P < 0.01$; $^{***}P < 0.001$ (Student's T-test).

Our approach has allowed us to identify and characterize the molecular behavior of lncRNAs in the development of CDDP resistance in cancer. We have first shown that variation in lncRNAs and mRNAs after CDDP treatment leads to similar ratios of differences, thus identifying a small group of candidates whose expression is altered in both NSCLC and ovarian tumor types as a result of platinum treatment. This outcome is of interest for future studies focused on the potential role of lncRNAs and mRNAs in acquired resistance. Moreover, our bioinformatics analyses have identified two groups of lncRNAs according to the relationship with their associated coding gene, indicating and reinforcing that overlapping and *cis*-acting lncRNAs could play different regulatory roles. Further, the whole-methylome scope of our study revealed differences in methylation patterns for overlapping and *cis*-acting lncRNAs. We clearly observed that overlapping and *cis*-acting lncRNAs are differentially regulated by DNA methylation, suggesting that overlapping lncRNAs that show a positive correlation of expression with their host gene are probably regulated by the shared CGI. This regulation has been shown for miRNAs, such as miR-335 and its host gene *MEST* and miR-31 and its host lncRNA LOC554202 [44,45]; however, to the best of our knowledge, this is the first report providing this finding for lncRNAs. Furthermore, our results indicate that *cis*-acting lncRNAs are probably regulated by transcriptional mechanisms other than DNA methylation and thus, alternative analyses are required to study the regulation of these lncRNAs. Our research could be of great importance for future analyses involving the identification of new diagnostic and predictive cancer biomarkers based on epigenetics and lncRNA regulation.

Materials and methods

Cell lines and reagents

A total of 12 cell lines were purchased from ATCC and ECACC (Sigma-Aldrich) and cultured as recommended. To analyze the changes in the transcriptome as a result of CDDP treatment, we established the CDDP-resistant variants of H23-R, H460-R, A2780-R, and OVCAR3-R from the parental-sensitive variants H23, H460, A2780, and OVCAR3, after exposure to increasing doses of CDDP treatment over a time period of 6-18 months [21,22]. In order to unmask epigenetic silencing caused by cisplatin, resistant cells received a combination of the epigenetic reactivation drugs 5-Aza-2-deoxycytidine (5Aza-dC) and trichostatin A (TSA) [as previously described [22,46] as an

KEPI_A_1436364.3d (Compact Serif) (209.55×279.4mm) 07-03-2018 10:23

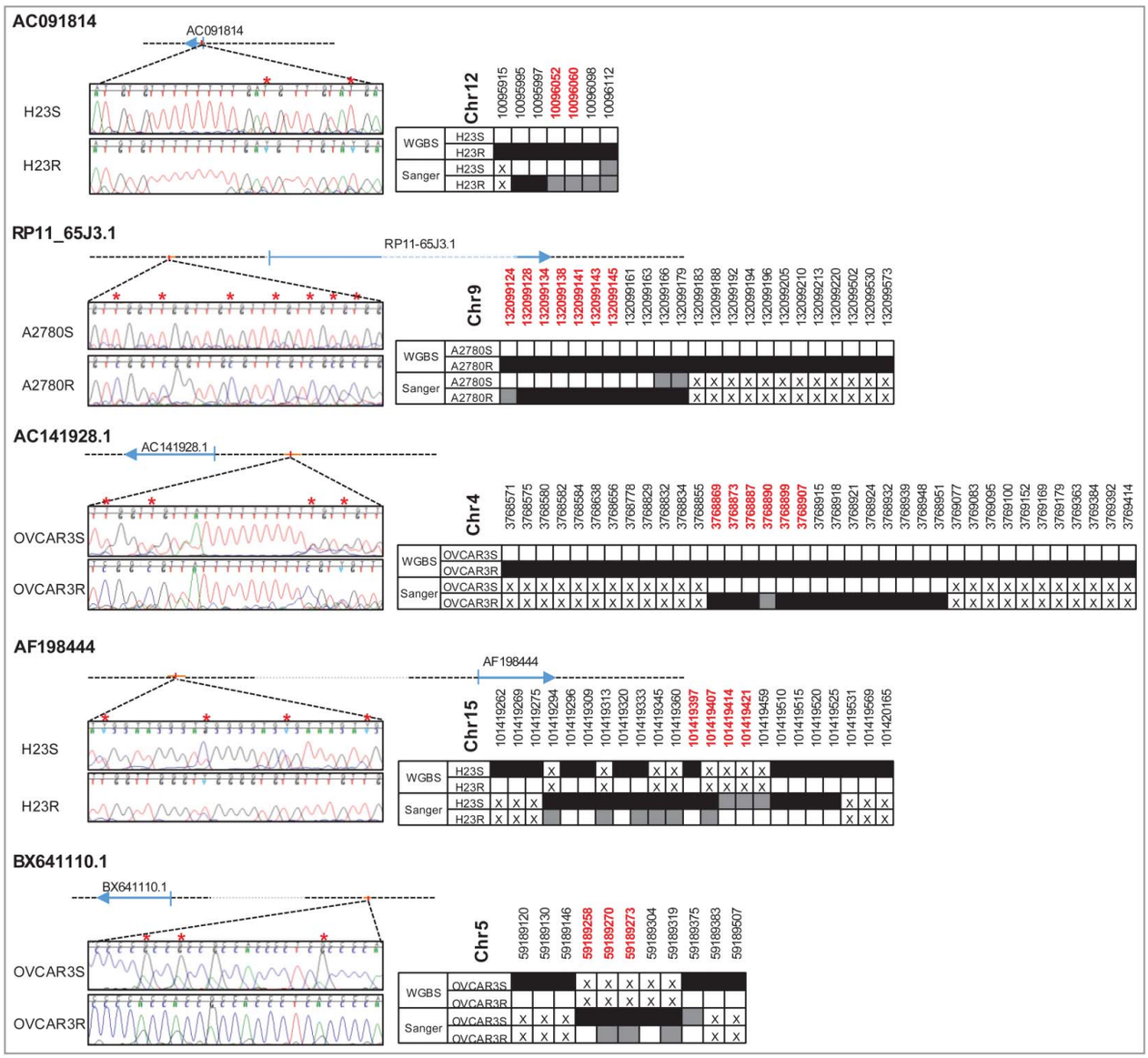

Figure 5. Bisulfite sequencing validation of the differentially methylated positions found by WGBS. Figure shows the genomic location of lncRNAs interrogated and the most representative positions after Sanger sequencing (left). Red asterisks indicate those positions with differential methylation between S and R cells. The right part of the panel shows the comparison with WGBS, where white squares indicate unmethylation, grey hemimethylation, and black shows methylated positions. The crosses indicate an absence of information. Red chromosomal positions are marked with an asterisk.

epigenetic reactivating treatment to generate the resistant-treated subtypes (H23RT, H460RT, A2780RT and OVCAR3RT)]. Cell authentication is provided in Supplementary Table S1.

RNA isolation and arraystar human LncRNA microarray V3.0

Total RNA from S and R cells was extracted by the guanidine thiocyanate method using TRIzol reagent (Invitrogen) and followed by a DNAse treatment (Qiagen). RNA integrity and concentration were assessed by Nanodrop ND-1000 and 2100 Bioanalyzer (Agilent Technologies).

mRNA and lncRNA expression profiling was performed using the Arraystar Human LncRNA Microarray V3.0 (Arraystar) in two independent biological replicates per sample (GSE108139). This lncRNA microarray interrogates lncRNAs, together with mRNAs on the same chip, which are labeled along the entire length without 3' bias, even for degraded RNA at low amounts. LncRNAs as a population are ~10x less represented than mRNA. The overlapping lncRNAs have partial or total regions in common with their host gene [47]. Thus, strand and transcript-specific detection is crucial to accurate detection of multiple transcript isoforms. The use of a specific exon or splice junction probe can specifically detect transcripts that overlap with other transcripts on the sense strand. The expression profiling was based on the manufacturer's standard protocols with minor modifications. Briefly, mRNA was purified from total RNA after removal of rRNA (mRNA-ONLY™ Eukaryotic mRNA Isolation Kit, Epicentre). Next, each sample was amplified and transcribed into fluorescent cRNA along the entire length of the transcripts without 3' bias, using a random

KEPI_A_1436364.3d (Compact Serif) (209.55×279.4mm) 07-03-2018 10:23

priming method (Arraystar Flash RNA Labeling Kit, Arraystar). The labeled cRNAs were hybridized onto the Human LncRNA Array v3.0 (8 × 60 K, Arraystar). The slides were washed and the arrays were scanned by the Agilent Scanner G2505C. Agilent Feature Extraction software (version 11.0.1.1) was used to analyze acquired array images. Quantile normalization and subsequent data processing were performed using the GeneSpring GX v12.1 software package (Agilent Technologies). After quantile normalization of the raw data, lncRNAs and mRNAs that, in at least 1 of 16 samples, had flags in Present or Marginal ("all targets value") were chosen for further data analysis. Differentially expressed lncRNAs and mRNAs with statistical significance between the two groups were identified through fold change ≥ 1.5, P value ≤ 0.05.

Semi-quantitative RT-PCR and quantitative RT-PCR

Total RNA was isolated using TRIzol reagent following the manufacturer's protocol and was used to generate cDNA with the High Capacity cDNA Reverse Transcription Kit (Life Technologies) and PrimeScript™ RT Master (Clontech-Takara). Briefly, 500 ng of total RNA were used for RT reaction, and 2 μl of the RT product (diluted 1:5) was used for subsequent semi-quantitative PCR or qPCR reactions with either Promega Green Mix or Promega PCR Mix (Promega) and SYBR Green PCR Mix (Applied Biosystems), respectively. Real-Time PCR was performed under the following conditions: (a) One cycle of 95°C for 2 min; (b) Number of amplification cycles are between 25 to 37 at 95°C for 1 min and annealing temperatures between 56°C to 62°C for 1 min depending on each pair of primers (detailed in Supplementary Table 2) and then 72°C for 1 min; (c) Extension of 5 min at 72°C. RT-PCR products were run on a 1.5% agarose gel, using the 100 bp Molecular size Marker (New England Biolabs) for appropriate identification of band size. qRT-PCR relative quantification was calculated according to the $2^{-\Delta\Delta Ct}$ using *GAPDH* as endogenous control and the sensitive-parental cell line as a calibrator and represents the change of expression in RQ and Log10. Deviation bars show the maximum estimate (RQ Max) and the minimum estimate (RQ Min) expression levels, representing the standard deviation of the average expression levels of two experiments measured by triplicate. Primers were designed flanking the probe on the array, when possible, and for specific lncRNAs transcripts that significantly showed changes in the arrays; *GAPDH* was used as an endogenous control; all primers and specific amplification conditions are listed in Supplementary Table 2. The RNA obtained from the paired A2780/A2780CP and OV2008/OVC13 cell lines was generously provided by Dr. Cheng (Moffitt Cancer Center) and was used for further validations.

Whole-genome bisulfite sequencing

The DNA from H23S/R, H460S/R, A2780S/R, and OVCAR3S/R was isolated as described [48] and sent to the National Centre for Genome Analysis [*Centro Nacional de Análisis Genómico* (CNAG)] for WGBS. Briefly, 2 μg of genomic DNA was mixed with unmethylated DNA from lambda phage in a proportion of 5 ng for each μg of genomic DNA. Libraries were prepared using the "preparation samples kit" TruSeq™ DNA v2 (Illumina, Inc.) following the manufacturer's indications with minimum changes. DNA was sonicated using Covaris E220 (Covaris, Inc.) to generate fragments of 50-500 bp. The selected size for library preparation was 150-300 bp. These fragments were purified using AMPure XP spheres (Agencourt Bioscience Corp). Following methodologies included end repair, adenylation and pairing with specific adaptors for the "paired-end" methodology from Illumina, as described previously in-depth [49]. After ligation, fragments were sodium-bisulfite modified using the EpiTect Bisulfite kit (Qiagen) following the manufacturer's protocol. DNA was amplified in 7 PCR cycles using DNA polymerase PfuTurboCx Hotstart (Agilent Technologies). Quality control of the library was performed by Bioanalyzer 75000 (Agilent Technologies). The library was sequenced on HiSeq2000 (Illumina, Inc.) following the manufacturer's protocol, in paired end mode with a read length of 2 × 101 bp. Images analysis, base calling and quality scoring of the run were processed using the manufacturer's software Real Time Analysis (RTA 1.13.48). The average million read-pairs was ~500 reads and the mean coverage was ~30X per sample. The mapping was carried out using GEM 1.242 and the methylation calling with BScall.

Epigenetic validation: bisulfite modification and bisulfite sequencing

Isolated DNA from the H23S/R, H460S/R, A2780S/R, and OVCAR3S/R samples was bisulfite-modified and used for bisulfite sequencing as previously described [50]. For bisulfite sequencing, primers were designed, when possible, to exclude binding to any CpG dinucleotides to ensure amplification of either methylated or unmethylated sequences. Primers are listed in Supplementary Table 3. PCR reactions were used for cell lines and were performed under the following conditions: (a) One cycle of 95°C for 5 min; (b) Number of amplification cycles are between 40 to 42 of 95°C for 1 min, annealing temperatures between 56°C to 62°C for 1 min depending on each pair of primers (detailed in Supplementary Table 3) and 72°C for 1 min; (c) Extension of 8 min at 72°C. The PCR products were run on a 1.5% agarose gel, using the 100 bp Molecular size Marker (New England Biolabs) for appropriate identification of band size, then cut and cleaned by the MinElute gel extraction kit (Qiagen). Direct sequencing was performed on all the genes, rather than subcloning of a mixed population of alleles, to avoid potential cloning efficiency bias [51] and artifacts [52].

Bioinformatics analysis of expression and methylation

To identify differentially expressed lncRNAs and mRNAs with *in silico* complementarity and under potential epigenetic regulation, we interrogated the available databases with lncRNAs annotations (GENCODE [53]; RNAdb [54]; NRED [55]; LncRNAdb [56]; LNCipedia [57], lncRNome [58]; NONCODE [59]; fRNAdb [60]; lncrna2target [61]) and selected those lncRNAs and mRNAs that changed significantly at three different contrasts: (1) resistant vs. sensitive for each cell line; (2) resistant vs. sensitive for each tumor type; and (3) resistant vs. sensitive for all. Based on the chromosomal relationship of the lncRNA with the mRNA, we defined as overlapping lncRNAs

KEPI_A_1436364.3d (Compact Serif) (209.55×279.4mm) 07-03-2018 10:23

those within the body of the gene or oriented head to head with a protein-coding gene within 1 kb; and as *cis*-acting lncRNAs those at least 1 kb away from the nearest protein-coding gene but no more than 300 kb [29, 30], including enhancer-like function LncRNAs [62] – excluding overlapping lncRNAs of this group. Finally, for the identification of CGIs based on the characteristics of Takai and Jones [63] in our WGBS data, we interrogated a region from 5000 bp upstream to the end of lncRNAs or mRNAs regions, and for individual CpGs from 2000 bp upstream to 500 bp downstream of TSS (Supporting Dataset, Sheets 2-5). The selection of differentially methylated (DM) CpG positions was based on previous results from our laboratory that established an experimentally validated cut-off point for the CpG site methylation level (ratio of reads with methylation out of the total number of reads covering this position). To be selected, the candidates must had to have a ratio of resistance >0.4 and sensitivity <0.23, with a minimum coverage of 10X, and at least five individuals DM CpGs. The association between qualitative variables was studied with the Chi-squared test with Yate's continuity correction and was considered statistically significant with P value <0.05.

Acknowledgments

The authors thank ServingMed.com and Hayley Pickett for editing services. The authors also acknowledge Dr. Jin Q. Cheng for his advice and total RNA provided from the A2780/A2780CP and OV2008/OVC13 cell lines.

Disclosure of potential conflicts of interest

All the authors have read the journal's authorship statement and have no conflicts of interest to declare.

Funding

Instituto de Salud Carlos III Instituto de Salud Carlos III Instituto de Salud Carlos III European Regional Development Fund. This work was supported by the 'Fondo de Investigación Sanitaria-Instituto de Salud Carlos III' under [grant number PI12/00386], [grant number PI15/00186] and [grant number CP 08/000689] to I.I.C.; and 'European Regional Development Fund/European Social Fund FIS' under the [grant number FEDER/FSE, Una Manera de Hacer Europa].

Data availability

All the data generated or analyzed during this study are included in this published article.

Author contributions

IIC: Conception and design
OV, CRA and IIC: acquisition, analysis and interpretation of data
OV: technical methodology
CRA: bioinformatic analysis
JdC: data interpretation
FAK, TAS data interpretation, and institutional support for the development of some experimental procedures
All authors wrote, reviewed, and/or revised the manuscript.

ORCID

Inmaculada Ibañez de Caceres http://orcid.org/0000-0001-9805-8486

References

[1] Crick F. Central dogma of molecular biology. Nature. 1970 Aug 08;227(5258):561–563. PubMed PMID: 4913914; eng. doi:10.1038/227561a0.

[2] Kung JT, Colognori D, Lee JT. Long noncoding RNAs: past, present, and future. Genetics. 2013 Mar;193(3):651–669. doi:193/3/651 [pii] 10.1534/genetics.112.146704. PubMed PMID: 23463798; eng.

[3] Mattick JS, Makunin IV. Non-coding RNA. Hum Mol Genet. 2006 Apr 15;15 Spec No 1:R17-29. doi:10.1093/hmg/ddl046. PubMed PMID: 16651366.

[4] Gibb EA, Brown CJ, Lam WL. The functional role of long non-coding RNA in human carcinomas. Mol Cancer. 2011 Apr 13;10:38. doi:10.1186/1476-4598-10-38. PubMed PMID: 21489289; PubMed Central PMCID: PMC3098824.

[5] Djebali S, Davis CA, Merkel A, et al. Landscape of transcription in human cells. Nature. 2012 Sep 06;489(7414):101–108. doi:nature11233 [pii] 10.1038/nature11233. PubMed PMID: 22955620; eng.

[6] Dey BK, Mueller AC, Dutta A. Long non-coding RNAs as emerging regulators of differentiation, development, and disease. Transcription. 2014;5(4):e944014. doi:10.4161/21541272.2014.944014. PubMed PMID: 25483404; eng.

[7] Bartolomei MS, Zemel S, Tilghman SM. Parental imprinting of the mouse H19 gene. Nature. 1991 May 09;351(6322):153–155. doi:10.1038/351153a0. PubMed PMID: 1709450; eng.

[8] Brannan CI, Dees EC, Ingram RS, et al. The product of the H19 gene may function as an RNA. Mol Cell Biol. 1990 Jan;10(1):28–36. PubMed PMID: 1688465; eng. doi:10.1128/MCB.10.1.28.

[9] Brown SD. XIST and the mapping of the X chromosome inactivation centre. Bioessays. 1991 Nov;13(11):607–612. doi:10.1002/bies.950131112. PubMed PMID: 1772416; eng.

[10] Tripathi V, Ellis JD, Shen Z, et al. The nuclear-retained noncoding RNA MALAT1 regulates alternative splicing by modulating SR splicing factor phosphorylation. Molecular cell. 2010 Sep 24;39(6):925–938. doi:10.1016/j.molcel.2010.08.011. PubMed PMID: 20797886; PubMed Central PMCID: PMC4158944.

[11] Ji P, Diederichs S, Wang W, et al. MALAT-1, a novel noncoding RNA, and thymosin beta4 predict metastasis and survival in early-stage non-small cell lung cancer. Oncogene. 2003 Sep 11;22(39):8031–8041. doi:10.1038/sj.onc.1206928 1206928 [pii]. PubMed PMID: 12970751; eng.

[12] Zhou Y, Xu X, Lv H, et al. The Long Noncoding RNA MALAT-1 Is Highly Expressed in Ovarian Cancer and Induces Cell Growth and Migration. PLoS One. 2016;11(5):e0155250. doi:10.1371/journal.pone.0155250 PONE-D-16-00259 [pii]. PubMed PMID: 27227769; eng.

[13] Li F, Cao L, Hang D, et al. Long non-coding RNA HOTTIP is up-regulated and associated with poor prognosis in patients with osteosarcoma. Int J Clin Exp Pathol. 2015;8(9):11414–20. PubMed PMID: 26617868; PubMed Central PMCID: PMC4637684.

[14] Quagliata L, Matter MS, Piscuoglio S, et al. Long noncoding RNA HOTTIP/HOXA13 expression is associated with disease progression and predicts outcome in hepatocellular carcinoma patients. Hepatology. 2014 Mar;59(3):911–923. doi:10.1002/hep.26740. PubMed PMID: 24114970; eng.

[15] Li L, Gu M, You B, et al. Long non-coding RNA ROR promotes proliferation, migration and chemoresistance of nasopharyngeal carcinoma. Cancer science. 2016 Sep;107(9):1215–1222. doi:10.1111/cas.12989. PubMed PMID: 27311700; PubMed Central PMCID: PMC5021023.

[16] Fan Y, Shen B, Tan M, et al. Long non-coding RNA UCA1 increases chemoresistance of bladder cancer cells by regulating Wnt signaling. FEBS J. 2014 Apr;281(7):1750–1758. doi:10.1111/febs.12737. PubMed PMID: 24495014; eng.

[17] Kartalou M, Essigmann JM. Mechanisms of resistance to cisplatin. Mutat Res. 2001 Jul 1;478(1-2):23–43. PubMed PMID: 11406167. doi:10.1016/S0027-5107(01)00141-5.

[18] Ho GY, Woodward N, Coward JI. Cisplatin versus carboplatin: comparative review of therapeutic management in solid malignancies. Crit

KEPI_A_1436364.3d (Compact Serif) (209.55×279.4mm) 07-03-2018 10:23

Rev Oncol Hematol. 2016 Mar 24; doi:10.1016/j.critrevonc.2016.03.014. PubMed PMID: 27105947.

[19] Lee SY, Jung DK, Choi JE, et al. PD-L1 polymorphism can predict clinical outcomes of non-small cell lung cancer patients treated with first-line paclitaxel-cisplatin chemotherapy. Scientific reports. 2016 May 16;6:25952. doi:10.1038/srep25952. PubMed PMID: 27181838; PubMed Central PMCID: PMC4867646.

[20] French JD, Johnatty SE, Lu Y, et al. Germline polymorphisms in an enhancer of PSIP1 are associated with progression-free survival in epithelial ovarian cancer. Oncotarget. 2016 Feb 9;7(6):6353–6368. doi:10.18632/oncotarget.7047. PubMed PMID: 26840454; PubMed Central PMCID: PMC4872719.

[21] Cortes-Sempere M, de Miguel MP, Pernia O, et al. IGFBP-3 methylation-derived deficiency mediates the resistance to cisplatin through the activation of the IGFIR/Akt pathway in non-small cell lung cancer. Oncogene. 2012 Mar 07;32(10):1274–1283. doi:onc2012146 [pii] 10.1038/onc.2012.146. PubMed PMID: 22543588; eng.

[22] Ibanez de Caceres I, Cortes-Sempere M, Moratilla C, et al. IGFBP-3 hypermethylation-derived deficiency mediates cisplatin resistance in non-small-cell lung cancer. Oncogene. 2010 Mar 18;29(11):1681–1690. doi:10.1038/onc.2009.454. PubMed PMID: 20023704.

[23] Heyn H, Esteller M. DNA methylation profiling in the clinic: applications and challenges. Nat Rev Genet. 2012 Oct;13(10):679–692. doi:10.1038/nrg3270. PubMed PMID: 22945394.

[24] Vera O, Jimenez J, Pernia O, et al. DNA Methylation of miR-7 is a Mechanism Involved in Platinum Response through MAFG Overexpression in Cancer Cells. Theranostics. 2017;7(17):4118–4134. doi:10.7150/thno.20112. PubMed PMID: 29158814; PubMed Central PMCID: PMC5695001.

[25] Ellis BC, Molloy PL, Graham LD. CRNDE: A Long Non-Coding RNA Involved in CanceR, Neurobiology, and DEvelopment. Front Genet. 2012;3:270. doi:10.3389/fgene.2012.00270. PubMed PMID: 23226159; PubMed Central PMCID: PMCPMC3509318.

[26] Graham LD, Pedersen SK, Brown GS, et al. Colorectal Neoplasia Differentially Expressed (CRNDE), a Novel Gene with Elevated Expression in Colorectal Adenomas and Adenocarcinomas. Genes Cancer. 2011 Aug;2(8):829–840. doi:10.1177/1947601911431081. PubMed PMID: 22393467; PubMed Central PMCID: PMCPMC3278902.

[27] Ma L, Bajic VB, Zhang Z. On the classification of long non-coding RNAs. RNA Biol. 2013 Jun;10(6):925–933. doi:24604 [pii] 10.4161/rna.24604. PubMed PMID: 23696037; eng.

[28] Wang KC, Chang HY. Molecular mechanisms of long noncoding RNAs. Mol Cell. 2011 Sep 16;43(6):904–914. doi:S1097-2765(11)00636-8 [pii] 10.1016/j.molcel.2011.08.018. PubMed PMID: 21925379; eng.

[29] Guttman M, Rinn JL. Modular regulatory principles of large non-coding RNAs. Nature. 2012 Feb 15;482(7385):339–346. doi:10.1038/nature10887. PubMed PMID: 22337053; PubMed Central PMCID: PMC4197003.

[30] Chen LL. Linking Long Noncoding RNA Localization and Function. Trends Biochem Sci. 2016 Sep;41(9):761–772. doi:10.1016/j.tibs.2016.07.003. PubMed PMID: 27499234.

[31] Yang Y, Li H, Hou S, et al. The noncoding RNA expression profile and the effect of lncRNA AK126698 on cisplatin resistance in non-small-cell lung cancer cell. PLoS One. 2013;8(5):e65309. doi:10.1371/journal.pone.0065309 PONE-D-12-23589 [pii]. PubMed PMID: 23741487; eng.

[32] Cui XB, Peng H, Li S, et al. Prognostic value of PLCE1 expression in upper gastrointestinal cancer: a systematic review and meta-analysis. Asian Pac J Cancer Prev. 2014;15(22):9661–9666. PubMed PMID: 25520085; eng. doi:10.7314/APJCP.2014.15.22.9661.

[33] Pathak A, Stewart DR, Faucz FR, et al. Rare inactivating PDE11A variants associated with testicular germ cell tumors. Endocr Relat Cancer. 2015 Dec;22(6):909–917. doi:ERC-15-0034 [pii] 10.1530/ERC-15-0034. PubMed PMID: 26459559; eng.

[34] Rajeevan MS, Vernon SD, Taysavang N, et al. Validation of array-based gene expression profiles by real-time (kinetic) RT-PCR. J Mol Diagn. 2001 Feb;3(1):26–31. doi:S1525-1578(10)60646-0 [pii] 10.1016/S1525-1578(10)60646-0. PubMed PMID: 11227069; eng.

[35] Venter JC, Adams MD, Myers EW, et al. The sequence of the human genome. Science. 2001 Feb 16;291(5507):1304–1351. doi:10.1126/science.1058040 291/5507/1304 [pii]. PubMed PMID: 11181995; eng.

[36] Jiang BC, Sun WX, He LN, et al. Identification of lncRNA expression profile in the spinal cord of mice following spinal nerve ligation-induced neuropathic pain. Mol Pain. 2015 Jul 17;11:43. doi:10.1186/s12990-015-0047-9 10.1186/s12990-015-0047-9 [pii]. PubMed PMID: 26184882; eng.

[37] Ozes AR, Miller DF, Ozes ON, et al. NF-kappaB-HOTAIR axis links DNA damage response, chemoresistance and cellular senescence in ovarian cancer. Oncogene. 2016 Oct 13;35(41):5350–5361. doi:onc201675 [pii] 10.1038/onc.2016.75. PubMed PMID: 27041570; eng.

[38] Wang Y, Zhang D, Wu K, et al. Long noncoding RNA MRUL promotes ABCB1 expression in multidrug-resistant gastric cancer cell sublines. Mol Cell Biol. 2014 Sep;34(17):3182–3193. doi:MCB.01580-13 [pii] 10.1128/MCB.01580-13. PubMed PMID: 24958102; eng.

[39] Deaton AM, Webb S, Kerr AR, et al. Cell type-specific DNA methylation at intragenic CpG islands in the immune system. Genome Res. 2011 Jul;21(7):1074–1086. doi:gr.118703.110 [pii] 10.1101/gr.118703.110. PubMed PMID: 21628449; eng.

[40] Yang Y, Chen L, Gu J, et al. Recurrently deregulated lncRNAs in hepatocellular carcinoma. Nat Commun. 2017 Feb 13;8:14421. doi:ncomms14421 [pii] 10.1038/ncomms14421. PubMed PMID: 28194035; eng.

[41] Hu H, Shu M, He L, et al. Epigenomic landscape of 5-hydroxymethylcytosine reveals its transcriptional regulation of lncRNAs in colorectal cancer. Br J Cancer. 2017 Feb 28;116(5):658–668. doi:bjc2016457 [pii] 10.1038/bjc.2016.457. PubMed PMID: 28141796; eng.

[42] Shoemaker R, Deng J, Wang W, et al. Allele-specific methylation is prevalent and is contributed by CpG-SNPs in the human genome. Genome Res. 2010 Jul;20(7):883–889. doi:10.1101/gr.104695.109. PubMed PMID: 20418490; PubMed Central PMCID: PMC2892089.

[43] Guo S, Diep D, Plongthongkum N, et al. Identification of methylation haplotype blocks aids in deconvolution of heterogeneous tissue samples and tumor tissue-of-origin mapping from plasma DNA. Nat Genet. 2017 Apr;49(4):635–642. doi:10.1038/ng.3805. PubMed PMID: 28263317; PubMed Central PMCID: PMC5374016.

[44] Dohi O, Yasui K, Gen Y, et al. Epigenetic silencing of miR-335 and its host gene MEST in hepatocellular carcinoma. Int J Oncol. 2013 Feb;42(2):411–418. doi:10.3892/ijo.2012.1724. PubMed PMID: 23229728; eng.

[45] Augoff K, McCue B, Plow EF, et al. miR-31 and its host gene lncRNA LOC554202 are regulated by promoter hypermethylation in triple-negative breast cancer. Mol Cancer. 2012 Jan 30;11:5. doi:1476-4598-11-5 [pii] 10.1186/1476-4598-11-5. PubMed PMID: 22289355; eng.

[46] Vera O, Jimenez J, Pernia O, et al. DNA Methylation of miR-7 is a Mechanism Involved in Platinum Response through MAFG Overexpression in Cancer Cells. Theranostics. 2017 Sept;7(17):4118–4134. doi:10.7150/thno.20112.

[47] Ning Q, Li Y, Wang Z, et al. The Evolution and Expression Pattern of Human Overlapping lncRNA and Protein-coding Gene Pairs [Article]. 2017 03/27/online.7:42775. doi:10.1038/srep42775 https://www.nature.com/articles/srep42775-supplementary-information. Q7

[48] Pernia O, Belda-Iniesta C, Pulido V, et al. Methylation status of IGFBP-3 as a useful clinical tool for deciding on a concomitant radiotherapy. Epigenetics. 2014 Nov;9(11):1446–1453. doi:10.4161/15592294.2014.971626. PubMed PMID: 25482372; PubMed Central PMCID: PMCPMC4622698.

[49] Soto J, Rodriguez-Antolin C, Vallespin E, et al. The impact of next-generation sequencing on the DNA methylation-based translational cancer research. Transl Res. 2014 Mar;169:1–18, e1. doi:S1931-5244(15)00407-7 [pii] 10.1016/j.trsl.2015.11.003. PubMed PMID: 26687736; eng.

[50] Ibanez de Caceres I, Dulaimi E, Hoffman AM, et al. Identification of novel target genes by an epigenetic reactivation screen of renal cancer. Cancer Res. 2006 May 15;66(10):5021–5028. doi:66/10/5021 [pii] 10.1158/0008-5472.CAN-05-3365. PubMed PMID: 16707423; eng.

KEPI_A_1436364.3d (Compact Serif) (209.55×279.4mm) 07-03-2018 10:23

[51] Grunau C, Clark SJ, Rosenthal A. Bisulfite genomic sequencing: systematic investigation of critical experimental parameters. Nucleic Acids Res. 2001 Jul 1;29(13):E65–E65. PubMed PMID: 11433041; PubMed Central PMCID: PMCPMC55789. doi:10.1093/nar/29.13.e65.

[52] Sandovici I, Leppert M, Hawk PR, et al. Familial aggregation of abnormal methylation of parental alleles at the IGF2/H19 and IGF2R differentially methylated regions. Hum Mol Genet. 2003 Jul 1;12(13):1569–1578. PubMed PMID: 12812984. doi:10.1093/hmg/ddg167.

[53] Harrow J, Frankish A, Gonzalez JM, et al. GENCODE: the reference human genome annotation for The ENCODE Project. Genome Res. 2012 Sep;22(9):1760–1774. doi:10.1101/gr.135350.111. PubMed PMID: 22955987; PubMed Central PMCID: PMCPMC3431492.

[54] Pang KC, Stephen S, Dinger ME, et al. RNAdb 2.0–an expanded database of mammalian non-coding RNAs. Nucleic Acids Res. 2007 Jan;35(Database issue):D178–D182. doi:10.1093/nar/gkl926. PubMed PMID: 17145715; PubMed Central PMCID: PMCPMC1751534.

[55] Dinger ME, Pang KC, Mercer TR, et al. NRED: a database of long noncoding RNA expression. Nucleic Acids Res. 2009 Jan;37(Database issue):D122–D126. doi:10.1093/nar/gkn617. PubMed PMID: 18829717; PubMed Central PMCID: PMCPMC2686506.

[56] Amaral PP, Clark MB, Gascoigne DK, et al. lncRNAdb: a reference database for long noncoding RNAs. Nucleic Acids Res. 2011 Jan;39(Database issue):D146–D151. doi:10.1093/nar/gkq1138. PubMed PMID: 21112873; PubMed Central PMCID: PMCPMC3013714.

[57] Volders PJ, Verheggen K, Menschaert G, et al. An update on LNCipedia: a database for annotated human lncRNA sequences. Nucleic Acids Res. 2015 Jan;43(Database issue):D174–D180. doi:10.1093/nar/gku1060. PubMed PMID: 25378313; PubMed Central PMCID: PMCPMC4383901.

[58] Bhartiya D, Pal K, Ghosh S, et al. lncRNome: a comprehensive knowledgebase of human long noncoding RNAs. Database (Oxford). 2013;2013:bat034. doi:10.1093/database/bat034. PubMed PMID: 23846593; PubMed Central PMCID: PMCPMC3708617.

[59] Bu D, Yu K, Sun S, et al. NONCODE v3.0: integrative annotation of long noncoding RNAs. Nucleic Acids Res. 2012 Jan;40(Database issue):D210–D215. doi:10.1093/nar/gkr1175. PubMed PMID: 22135294; PubMed Central PMCID: PMCPMC3245065.

[60] Kin T, Yamada K, Terai G, et al. fRNAdb: a platform for mining/annotating functional RNA candidates from non-coding RNA sequences. Nucleic Acids Res. 2007 Jan;35(Database issue):D145–D148. doi:10.1093/nar/gkl837. PubMed PMID: 17099231; PubMed Central PMCID: PMCPMC1669753.

[61] Jiang Q, Wang J, Wu X, et al. LncRNA2Target: a database for differentially expressed genes after lncRNA knockdown or overexpression. Nucleic Acids Res. 2015 Jan;43(Database issue):D193–D196. doi:10.1093/nar/gku1173. PubMed PMID: 25399422; PubMed Central PMCID: PMC4383967.

[62] Orom UA, Derrien T, Beringer M, et al. Long noncoding RNAs with enhancer-like function in human cells. Cell. 2010 Oct 01;143(1):46–58. doi:10.1016/j.cell.2010.09.001. PubMed PMID: 20887892; PubMed Central PMCID: PMCPMC4108080. doi:10.1016/j.cell.2010.09.001.

[63] Takai D, Jones PA. The CpG island searcher: a new WWW resource. In Silico Biol. 2003;3(3):235–240. PubMed PMID: 12954087.

PUBLICACIONES QUE NO HACEN PARTE DE LA TESIS / PUBLICATIONS THAT ARE NOT PART OF THE THESIS

Methylation status of IGFBP-3 as a useful clinical tool for deciding on a concomitant radiotherapy

Epigenetics 9:11, 1446–1453; November 2014; Published with license by Taylor & Francis Group, LLC

Methylation status of *IGFBP-3* as a useful clinical tool for deciding on a concomitant radiotherapy

Olga Pernía[1,2,†], Cristobal Belda-Iniesta[2,3,†], Veronica Pulido[1,2], María Cortes-Sempere[2,4], Carlos Rodriguez[1,2], Olga Vera[1,2], Javier Soto[1,2], Julia Jiménez[1,2], Alvaro Taus[5], Federico Rojo[5,6], Edurne Arriola[5], Ana Rovira[5], Joan Albanell[5], M Teresa Macías[7], Javier de Castro[2], Rosario Perona[2,4], and Inmaculada Ibañez de Caceres[1,2,*]

[1]Cancer Epigenetics Laboratory, INGEMM; University Hospital La Paz; Madrid, Spain; [2]Biomarkers and Experimental Therapeutics in Cancer; IdiPAZ; Madrid, Spain; [3]Department of Medical Oncology; University Hospital Madrid Norte Sanchinarro; Madrid, Spain; [4]Department of Animal Models for Human Diseases; Institute for Biomedical Research CSIC/UAM; CIBER for Rare Diseases; Valencia, Spain; [5]Department of Medical Oncology; Hospital del Mar-IMAS and Cancer Research Program; IMIM-Hospital del Mar; Barcelona, Spain; [6]Department of Pathology; IIS-Foundation Jimenez Diaz; Madrid, Spain; [7]Department of Radiobiology and Health Protection; Institute for Biomedical Research CSIC/UAM; Barcelona, Spain

Keywords: hypermethylation, IGFIR/AKT, IGFBP-3, NSCLC, radiotherapy

Abbreviations: ATCC, American Type Culture Collection; BS, bisulfite sequencing; CDDP cisplatin; ECACC, European Collection of Cell Cultures; IGFBP-3, insulin-like growth factor binding protein-3; IR, Ionizing radiation; NSCLC, non-small cell lung cancer; OS, overall survival; qMSP, quantitative methylation specific PCR.

Downloaded by [81.33.219.79] at 02:41 07 May 2016

The methylation status of the *IGFBP-3* gene is strongly associated with cisplatin sensitivity in patients with non-small cell lung cancer (NSCLC). In this study, we found *in vitro* evidence that linked the presence of an unmethylated promoter with poor response to radiation. Our data also indicate that radiation might sensitize chemotherapy-resistant cells by reactivating *IGFBP-3*-expression through promoter demethylation, inactivating the PI3K/AKT pathway. We also explored the *IGFBP-3* methylation effect on overall survival (OS) in a population of 40 NSCLC patients who received adjuvant therapy after R0 surgery. Our results indicate that patients harboring an unmethylated promoter could benefit more from a chemotherapy schedule alone than from a multimodality therapy involving radiotherapy and platinum-based treatments, increasing their OS by 2.5 y ($p = .03$). Our findings discard this epi-marker as a prognostic factor in a patient population without adjuvant therapy, indicating that radiotherapy does not improve survival for patients harboring an unmethylated *IGFBP-3* promoter.

Introduction

Non-small cell lung carcinoma (NSCLC) accounts for 1 of every 6 cancer-related deaths worldwide.[1] This mortality rate is due to the advanced stage of the disease at diagnosis and its resistance to all therapies. Surgery is the standard treatment in the early stages, and platinum-based adjuvant therapy has been shown to be effective in the advanced stages of the disease.[2] Multimodal therapy combining thoracic radiotherapy with chemotherapy after surgery also plays a role in the management of NSCLC,[3] primarily for patients at higher risk of local recurrence. However, treatment outcomes vary widely in terms of survival, and increased morbidity is strongly linked with therapy.

The mechanisms of drug resistance in cancer therapy have been widely analyzed, particularly for NSCLC, in which platinum-based therapy has often failed. In fact, we have previously reported that the loss of *IGFBP-3* expression by promoter hypermethylation results in reduced tumor cell sensitivity to cisplatin in NSCLC, an effect that is mediated by the activation of the IGF-IR/AKT pathway.[4,5] Despite the promising results regarding the usefulness of epigenetic alterations as potential markers in chemotherapy response,[6,7] these epi-markers have not been studied extensively in radiotherapy, leading to scarce data concerning epigenetics and radiosensitivity.[8] The radioresistance of tumor cells is a less explored and poorly defined field compared with drug resistance, and the role of the IGF-I/IGBP-3 axe on radiosensitivity in cancer is controversial because of the differing results when various tumor types are evaluated.[9–11] Furthermore, the relationship between *IGFBP-3* promoter hypermethylation and the response to radiotherapy in NSCLC is unknown. Recent studies have reported that radiotherapy induces global DNA hypomethylation,[12] which is why, in the present study, we evaluated both, the role of radiotherapy on the biology of *IGFBP-3* promoter methylation and its clinical value as a potential tool for deciding on a concomitant radiotherapy after NSCLC surgery.

© Olga Pernía, Cristobal Belda-Iniesta, Veronica Pulido, María Cortes-Sempere, Carlos Rodriguez, Olga Vera, Javier Soto, Julia Jiménez, Alvaro Taus, Federico Rojo, Edurne Arriola, Ana Rovira, Joan Albanell, M Teresa Macías, Javier de Castro, Rosario Perona, and Inmaculada Ibañez de Caceres
*Correspondence to: Inmaculada Ibañez de Caceres; Email: inma.ibanezca@salud.madrid.org
Submitted: 08/05/2014; Revised: 09/18/2014; Accepted: 09/29/2014
http://dx.doi.org/10.4161/15592294.2014.971626
This is an Open Access article distributed under the terms of the Creative Commons Attribution-NonCommercial License (http://creativecommons.org/licenses/by-nc/4.0/), which permits unrestricted non-commercial use, distribution, and reproduction in any medium, provided the original work is properly cited.

Methods

Cell lines and radiation-clonogenic cell survival assays

The resistant cell lines H23R and H460R were established previously in our laboratory from the parental H23S and H460S lung cell lines, and together with the cell line H1299 were purchased from the ATCC (Manassas, VA); all were maintained in RPMI supplemented with 10% FBS. The CDDP sensitive and resistant ovarian cancer cell lines 41M and 41MR, hereafter called 41S and 41R respectively, were provided by Dr. L Kelland and were maintained in DMEM supplemented with 10% FBS.[5] Each of the paired sensitive and resistant cell lines were irradiated at doses of 0, 2, 4, 6 and 8 Gy using a Cesium-137 irradiator Mark I30 (JL Shepherd and Associates, San Fernando, CA). Immediately following irradiation, the cells were trypsinized, diluted and seeded onto p100 plates. After 14 days, the cells were stained by crystal violet, and colonies with over 50 cells were counted with a ColCount colony counter (Optronix, Oxford, UK). Individual assays were performed in triplicate and repeated at least twice. The survival fraction was calculated as previously described.[13] For DNA, RNA and protein extraction, cell lines were cultured at a density of 400,000 cells by 60 mm plate for 72 h after irradiation.

NSCLC clinical samples and data collection

Formalin-fixed, paraffin-embedded (FFPE) surgical specimens were obtained from 40 NSCLC patients who received a chemotherapy schedule based on cisplatin/carboplatin with or without concomitant radiotherapy. Histological slides obtained from each block were reviewed by an expert pathologist (F. Rojo) to confirm diagnosis, and to guarantee at least 90% tumoral content. Follow-up was performed according the criteria used in the Medical Oncology Division from Hospital del Mar, including clinical assessments and thorax CT every 3 months for 2 y and every 6 months thereafter. Clinical, pathological, and radiological data were recorded by an independent observer at the H. del Mar and blinded for statistical analysis. In addition 10 samples obtained from pulmonary biopsies with non-neoplastic lung pathology were used as control tissues. We also included in the study clinical/pathological and *IGFBP-3* methylation data from an external group of 36 patients from La Paz University Hospital, as published previously,[4,5] who did not receive any therapy after surgery. The results from this group were adjusted by age, gender and stage to establish a control group.

Western-blot analysis

Whole-cell extracts from the human cancer cell lines and Western-Blot were performed as described.[14] Briefly, 20 μg from the 41S and 41R cell lines at 5 IR doses tested were subjected to western blot and the membranes were hybridized with antibodies against AKT (BD Biosciences, NJ, USA), pAKT-Ser473, pERK1/2-thr202/Tyr204 (E10) (Cell Signaling, MA, USA), ERK (C-14) (sc-154), IGFIR, anti-pIGFIR-Tyr1161 (Santa Cruz Biotechnology, Heidelberg, Germany), and anti-α-tubulin (Sigma Aldrich) as a loading control.

DNA and RNA extraction, bisulfite modification, quantitative methylation-specific PCR and qRT-PCR

DNA from human cancer cell lines, 40 paraffin-embedded NSCLC primary specimens, and 10 non-neoplastic lung tissues were isolated and bisulfite modified as described.[5] We then measured the *IGFBP-3* promoter methylation by qMSP using the following primer/probe set: F:5′-TTTTACGAGGTATATAC-GAATGC-3′; R:5′-TCTCGAAATAAAATCTCCCTACG-3′; Probe:5′FAM-CCGATATCGAAAAAACT-3′. A primer/probe set for the unmethylated *ACTB* gene promoter was used as reference.[15] Serial dilutions of bisulfite-modified DNA from the SW760 cell line that harbors a methylated promoter for *IGFBP-3* were used to construct calibration curves for *IGFBP-3* and *ACTB* genes. PCR reactions were performed in triplicate as described.[15]

Total RNA from human cancer cell lines was isolated as previously described.[16] Reverse transcription and qRT-PCR analysis were performed as described.[5] Samples were analyzed in triplicate using the HT7900 Real-Time PCR system (Applied Biosystems, USA), and relative gene expression quantification was calculated according to the comparative threshold cycle method ($2^{-\Delta\Delta Ct}$) using GADPH as an endogenous control gene. Primers and probes for *IGFBP-3* and *GADPH* expression analysis were purchased from Applied Biosystems (IGFBP-3: Hs 00365742_g1) *GADPH*: Hs03929097_g1).

Infinium humanmethylation27 annotation and TCGA NSCLC data

The Infinium HumanMethylation27 annotation (available at ftp://ftp.illumina.com/Methylation/InfiniumMethylation/HumanMethylation27/) used the National Center for Biotechnology Information (NCBI) relaxed definition of 200 bp length, 50% GC content and 0.6 ObsCpG/ExpCpG for identification of CpG islands in genes in the Consensus Coding Sequence (CCDS) database.[17] We first obtained the sequence of the probes from the TCGA Infinium HumanMethylation27 BeadChip annotation in order to determine the position of the probes within the gene *IGFBP-3*, and interrogate the Infinium probes located within the bona fide CpG island at the *IGFBP-3* promoter region. A probe was considered unmethylated if the β-value was ≤ 0.15, as previously described.[18] We correlate the methylation score (raw β-value) of the TCGA NSCLC patients with their clinical-pathological parameters.

Statistics and study approval

Discrete variables (histology, T, N, stage, gender, methylation status at the *IGFBP3* promoter and chemotherapy schedule) were compared with the Chi2 test and corrections with Fisher´s exact test were made when needed. DFS was defined as the time from surgery to clinical, radiological or histological evidence of relapse. Statistical significance was defined as $P < 0.05$.

Survival functions for patients diagnosed with NSCLC with an unmethylated *IGFBP3* promoter who were treated with chemotherapy or with chemo-radiotherapy were plotted using Kaplan-Meier methods, and were compared under 3 conditions the log-rank, Breslow and Tarone-Ware methods.

Downloaded by [81.33.219.79] at 02:41 07 May 2016

Downloaded by [81.33.219.79] at 02:41 07 May 2016

For patients without any evidence of survival at the time of analysis, data on OS were censored at the time of the last contact. Statistical analyses were done by use the SPSS software (version 17.0).

Samples were collected following the ethical and confidentiality issues by Dr. Rojo and Dr. De Castro. The present study is approved by the Idi-PAZ following rigorous biosecurity and ethical protocols in all procedures, in accordance with the Hospital's Local Ethic Committee.

Results and Discussion

Cell line data and discussion

To investigate the role of *IGFBP-3* methylation in radiosensitivity, we first developed radiation-clonogenic cell survival assays with 3 paired CDDP-sensitive and CDDP-resistant cell lines harboring various *IGFBP-3* methylation profiles: H23S/R, H460S/R and 41S/R.[4] Each of the paired cell lines was irradiated at doses of 0, 2, 4, 6 and 8 Gy. The unmethylated 41S cells showed lower sensitivity to radiotherapy than the H23S cells, which are semimethylated for *IGFBP-3*, whereas both the CDDP-resistant 41R and H23R cell lines that harbor an *IGFBP-3* hypermethylated promoter showed an increased sensitivity to radiotherapy (**Figs. 1A, B**) compared with their paired sensitive cell lines. These results agree with reported data that show that DNA hypermethylation of the tumor suppressor genes *TIMP3*, *CDH1* and *MGMT* predicts a better outcome in head and neck cell squamous cell carcinoma and glioblastoma when treated with radiotherapy.[19,20] There was no significant change in the radiotherapy sensitivity of the paired H460S/R cell lines, which were used as a negative control experimental group, given we

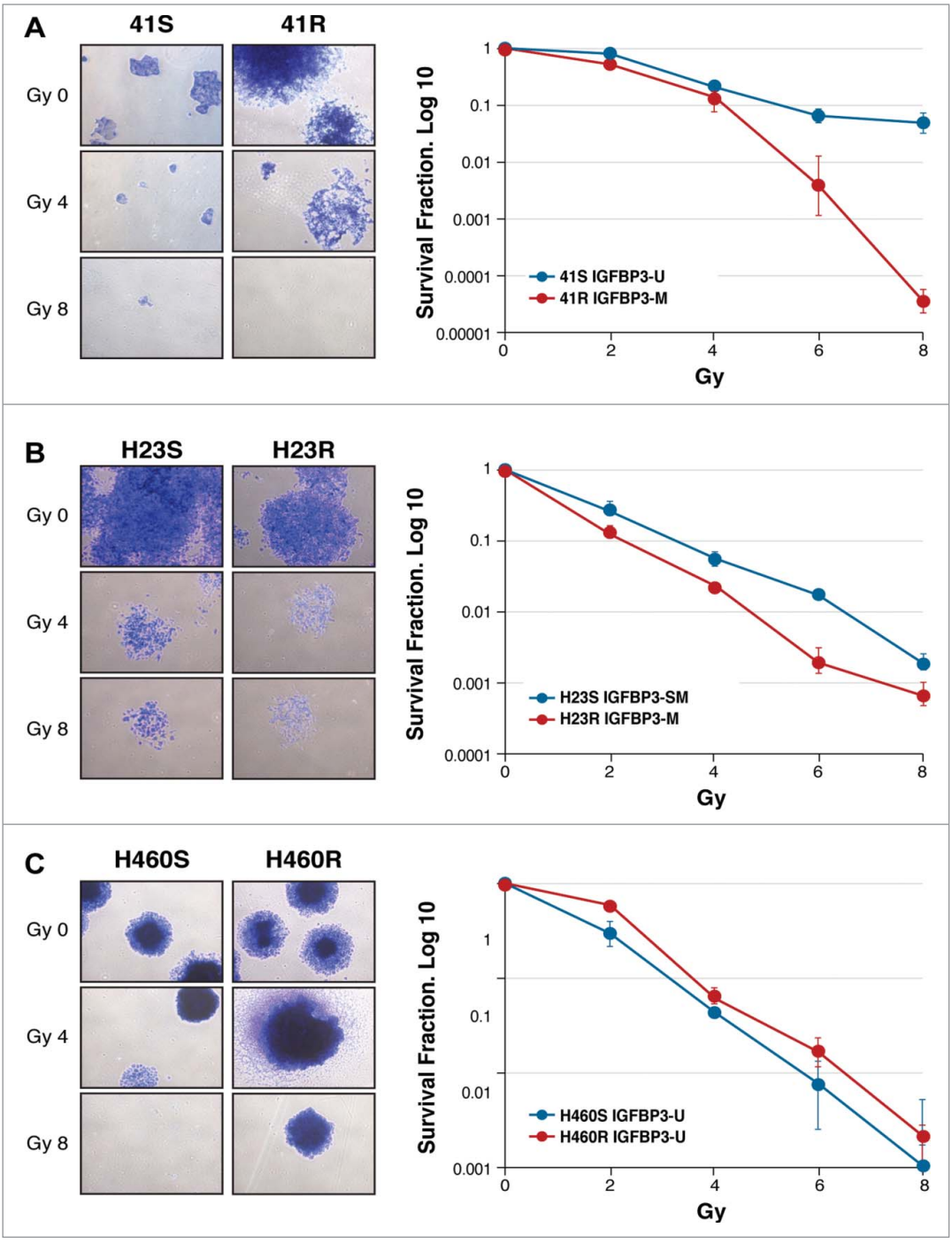

Figure 1. Radiation clonogenic cell survival assays with 3 paired CDDP-sensitive and CDDP-resistant cell lines, 41S/R (**A**), H23S/R (**B**) and H460S/R (**C**). The images are representative of 0, 4 and 8 Gy doses in each paired cell line using a cesium-137 irradiator Mark I30. Individual assays were performed in triplicate and repeated at least twice. The survival fraction (SF) was calculated by the following formula: SF = (number of colonies formed/number of cells seeded) x plating efficiency of the control group, in which plating efficiency was calculated as the ratio between the colonies observed and the number of cells plated. Dose-response clonogenic survival curves were plotted on a log-linear scale.

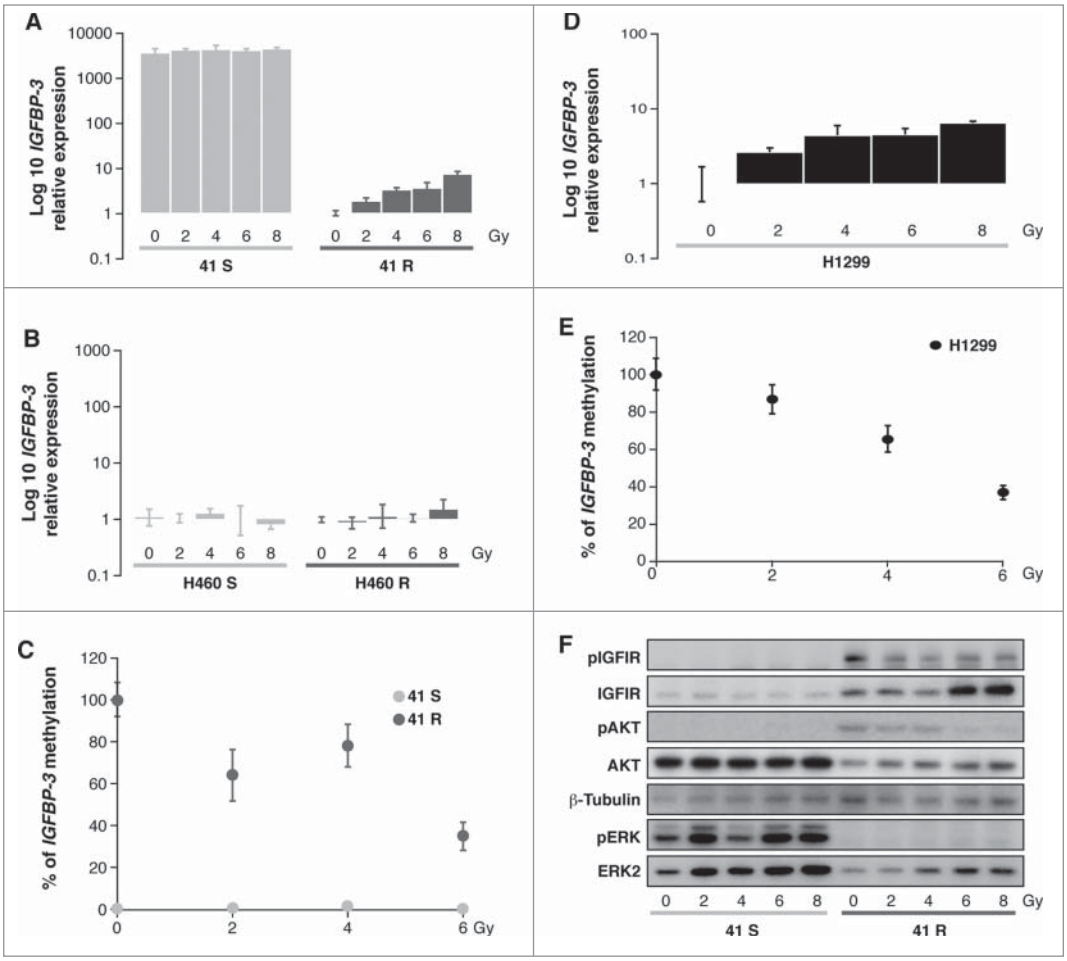

Figure 2. (**A**, **B**, **D**) Quantification of *IGFBP-3* expression levels in 41S/R, H460S/R and H1299 cells 72 h after IR treatment using the resistant untreated controls (0Gy) as calibrators. (**C**, **E**) Methylation levels of *IGFBP-3* in 41S, 41R and H1299 cells 72 h after irradiation.. The calculation of the *IGFBP-3* gene to β-actin ratios was based on the fluorescence emission intensity values for both genes at 0, 2, 4 and 6 Gy. The data were normalized to each untreated control, set to 100%, and represent the mean ± standard deviation of at least 3 independent experiments performed in triplicate at each concentration for every cell line analyzed. (**F**) Activation of the ERK and IGFIR/AKT axes 72 h after radiation in the 41S and 41R cell lines at 5 IR doses.

Downloaded by [81.33.219.79] at 02:41 07 May 2016

already reported that the resistance to cisplatin treatment in H460R cells is not mediated by changes in *IGFBP-3* expression and promoter methylation [4] (**Fig. 1C**). Our results indicate that those NSCLC cells harboring an *IGFBP-3* unmethylated promoter might receive less benefit from radiotherapy-based therapy than those cells with a hypermethylated promoter.

Radiotherapy is believed to function either by direct ionization or indirectly by DNA interaction of radicals formed by water ionization.[21] inducing DNA damage and mitochondrial production of ROS and RNS. The oxidative stress generated results in a complex cellular response, such as the activation of cell signaling, the inhibition of certain proteins and the increased metabolism of chemical compounds in the cells. All these events involve genetic and epigenetic alterations that lead the biological balance toward either death or survival of the treated malignant cells.[22] Therefore, to investigate whether the epigenetic regulation of the axis *IGFBP-3/IGFIR/AKT* is a mechanism that influences radiosensitivity in tumor cells, we studied the changes in the *IGFBP-3* expression and promoter methylation levels associated with radiotherapy treatment in the 41S/R and H460S/R paired cell lines. We also used the additional lung cancer cell line H1299, purchased from the American Type Culture Collection (ATCC), because these cells harbor a hypermethylated promoter for the *IGFBP-3* gene and present an elevated IC_{50} (6 ug/ml) to cisplatin.[5] We first observed a reactivation of *IGFBP-3* expression in a dose-response effect after radiotherapy treatment in the resistant cell line 41R, increasing from 10^2 (2 Gy) to $10^{7.8}$ times (at 8 Gy) in comparison with the sensitive cell line 41S treated at the same doses, in which there were no noticeable changes in *IGFBP-3* expression (**Fig. 2A**), probably due to the high basal levels of *IGFBP-3* expression in this cell line. As expected, there were no significant changes between the negative control cell lines H460S and H460R (**Fig. 2B**). These results are in agreement with previous findings that the hydroxyl radicals generated by radiation induce gene expression in mammalian cells.[23] The increase in *IGFBP-3* expression in the 41R cells is probably mediated by the decrease in *IGFBP-3* promoter hypermethylation observed in this cell line after ionizing radiation. *IGFBP-3* promoter hypermethylation decreases by approximately 30% at 2 and 4 Gy and 63% at 6 Gy compared with the non radiated cells (0Gy) (**Fig. 2C**). As expected, we did not find any decrease in the methylation levels in the cell line 41S after radiation therapy, probably because those cells harbor at baseline a completely unmethylated promoter for *IGFBP-3*[12] (**Fig. 2C**).

These results are not specific for the paired cell lines 41S and 41R because the results obtained from the additional cell

line H1299 also agree with these observations; there was an increase in the *IGFBP-3* mRNA levels that is a dose-response effect after radiotherapy treatment, increasing from $10^{2.6}$ at 2 Gy to $10^{6.4}$ times at 8 Gy in the H1299 cells (**Fig. 2D**). These results are concomitant with a reduction in the methylation levels of the *IGFBP-3* promoter after radiation exposure, reaching similar values to that observed in the 41R cells (75% and 63%, respectively) (**Fig. 2E**). In the 3 experimental groups treated at the higher concentration (8 Gy), we could not obtain a DNA template of sufficient quality to perform the qRT-MSP analysis. Supporting our observation, previous studies have shown that radiotherapy causes global hypomethylation *in vitro* and *in vivo*, possibly due to a decreased expression of epigenetic regulators[12,24]; we did not observe changes in the *DNMT3B* expression levels between the studied cell lines (data not shown), but in further studies, it would be necessary to get insight into the specific mechanisms responsible for *IGFBP-3* demethylation after radiotherapy treatment in cisplatin chemotherapy-resistant cells.

A

	N(%)
Methylation status for IGFBP3	
- Methylated	14 (35%)
- Unmethylated	26 (65%)
%Male	**85%**
Age (mean)	**63.6**
Smoker status	
- Current	19 (47.5%)
- Former	15 (37.5%)
- Never	6 (15%)
Histology	
- Adenocarcinoma	26 (64%)
-Squamous cell	12 (30%)
- Large cell	2 (5%)
Stages (TNM)	
-IB	8 (20%)
-IIA	3 (7.5%)
-IIB	8 (20%)
-IIIA	14 (35%)
-IIIB	5 (12.5%)
-IV	2 (5%)
Chemotherapy schedule	
- Cisplatin based	30 (75%)
- Carboplatin based	10 (25%)
% Radiotherapy	32.5%
DFS entire population	29.2 mo (CI95% 8.5-49.9)
OS entire population	74.6 mo (CI95% 28.7-120.5)

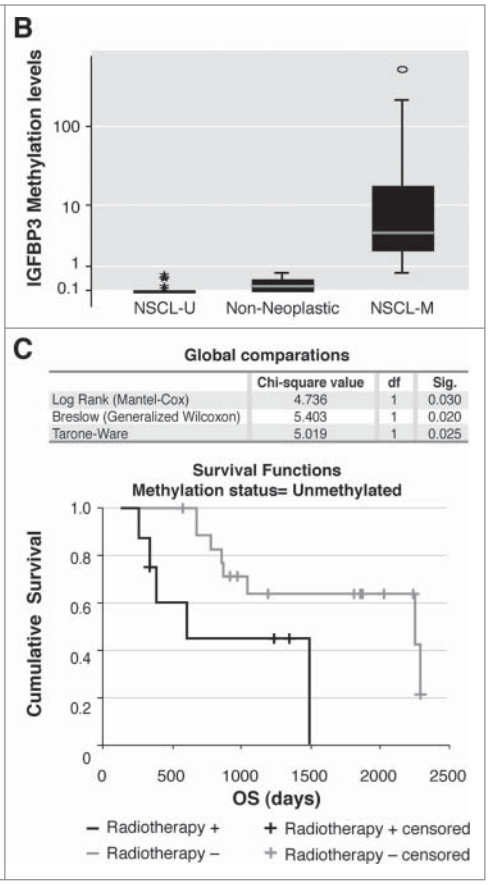

Figure 3. (**A**) Clinicopathological parameters of the entire population: Methylation status for the *IGFBP-3* promoter, gender, age, smoking status, histology, stages, chemo-radiotherapy schemes, disease-free survival (DFS) and overall survival (OS). (**B**) Box plot for the *IGFBP-3/ACTB* ratios determined by quantitative methylation-specific PCR (qMSP), in DNA from 40 paraffin-embedded tumors and 10 non-neoplastic lung tissue samples, the obtained ratios were multiplied by 1000 for easier tabulation, as described.[15] The values designated as 0.1 and 0.01 are zero values, which cannot be plotted correctly on a log scale. NSCLC-M: the samples considered methylated for *IGFBP-3*, with higher promoter methylation levels than the controls; NSCLC-U: the samples considered negative, with methylation levels less than or equal to those of the negative control group. (**C**) Kaplan-Meier. Comparison between *IGFBP-3* methylation status (unmethylated) and cumulative survival (days) in 40 patients diagnosed with NSCLC who were treated with chemotherapy (radiotherapy-) or with chemo-radiotherapy (radiotherapy+).

We then analyzed whether the observed changes in *IGFBP-3* expression and promoter methylation were linked to modifications affecting the activation of the IGFIR/AKT cellular pathway, which could explain the observed differential sensitivity to ionizing radiation. The results confirmed our previously published results, showing at 0 Gy the phosphorylation of both the IGFIR and AKT proteins in the resistant cell 41R compared with the sensitive cell line 41S at the same dose (**Fig. 2F**).[4] The exposure to ionizing radiation decreased the IGFIR and AKT phosphorylation levels in a dose response manner from 0 Gy to 8 Gy in the 41R cells. These results were concomitant with the dose-response increase in *IGFBP-3* expression we observed in the resistant cell line 41R at the same doses. This outcome indicates that the re-expression of *IGFBP-3* through promoter demethylation is probably mediating the decrease in the activation of the survival pathway IGF-IR/AKT by sequestering the IGF-I factor, a mechanism that we have already described in those cells.[4] The re-silencing of this survival pathway in cisplatin-resistant cells that initially harbored a methylated promoter for *IGFBP-3* could result in a gain in sensitivity to radiotherapy treatment. These findings open the door to exploring radiotherapy as an alternative treatment to cisplatin in those tumors that present the hypermethylated promoter of *IGFBP-3*.

As expected, IR-treatment induced a dose-response increase in the expression of ERK1/2 levels in both sensitive cells and cisplatin-resistant cells. In fact, MAPK signaling can be stimulated by treatment with IR in tumor cells,[25,26] probably promoting the activation of the ERBB family receptor, which in turn increases the activity of downstream molecules in the

Downloaded by [81.33.219.79] at 02:41 07 May 2016

Downloaded by [81.33.219.79] at 02:41 07 May 2016

Table 1. Clinicopathological parameters recorded from 40 NSCLC patients. Adeno, Adenocarcinoma; SCCA, Squamous Cell Carcinoma; M, Methylated; U, Unmethylated; 1, Cisplatin-Vinorelbine; 2, Carboplatin-Vinorelbine; 3, Cisplatin-Gemcitabine; 4, Carboplatin-Paclitaxel

Patient	Methylation levels (IGFBP3/ACTB)*1000	Methylation status	Age, y	Sex	Histology	Stage (TNM)	Chemotherapy	Radiotherapy	Start of Chemotherapy	End of Chemotherapy	Last contact	Status
1	496.148	M	58	Female	Adeno	IIIB	4	Yes	2002-06-20	2002-08-08	2003-07-19	Exitus
2	210.679	M	70	Female	SCCA	IIIA	1	No	2009-01-20	2009-04-14	2012-01-27	Alive
3	62.698	M	70	Female	SCCA	IB	1	No	2005-08-25	2005-09-22	2006-07-25	Exitus
4	18.000	M	65	Female	SCCA	IB	1	No	2009-05-26	2009-07-14	2012-05-08	Alive
5	15.546	M	61	Female	Adeno	IV	1	Yes	2009-02-26	2009-05-07	2012-05-17	Alive
6	7.550	M	73	Male	Adeno	IIIA	1	Yes	2007-09-17	2007-09-25	2012-02-09	Alive
7	4.377	M	70	Female	SCCA	IB	1	No	2006-05-11	2006-07-27	2006-10-05	Exitus
8	3.845	M	56	Female	Adeno	IIIA	2	No	2006-06-29	2006-09-07	2011-11-08	Alive
9	3.100	M	63	Female	Adeno	IIIA	1	Yes	2009-06-29	2009-09-07	2012-04-16	Alive
10	2.593	M	63	Female	SCCA	IV	1	No	2005-07-28	2005-08-26	2005-10-01	Exitus
11	2.088	M	68	Female	Adeno	IIA	1	No	2006-11-16	2007-01-25	2012-04-18	Alive
12	1.915	M	54	Female	Adeno	IIB	1	No	2009-12-14	2010-02-22	2012-05-31	Alive
13	1.507	M	56	Female	Adeno	IIB	1	No	2008-12-23	2009-03-12	2012-02-02	Alive
14	0.670	M	72	Female	Adeno	IIIA	2	Yes	2010-10-14	2010-12-02	2011-03-01	Exitus
15	0.555	U	63	Female	Adeno	IIB	1	Yes	2009-06-08	2009-08-17	2012-06-04	Alive
16	0.514	U	65	Female	Large Cell	IIIB	4	Yes	2006-01-02	2006-03-06	2006-04-18	Exitus
17	0.511	U	72	Female	Large Cell	IIIA	3	Yes	2003-01-30	2003-03-26	2004-04-24	Exitus
18	0.439	U	59	Female	Large Cell	IIIA	1	No	2005-11-24	2006-01-19	2012-01-18	Alive
19	0.169	U	79	Female	Adeno	IIIB	2	Yes	2008-04-11	2008-05-30	2011-09-16	Alive
20	0.077	U	69	Female	Adeno	IIIA	1	No	2010-03-23	2010-06-08	2011-08-21	Exitus
21	0.001	U	70	Male	Adeno	IB	1	No	2006-06-01	2006-07-20	2011-05-09	Alive
22	0.001	U	56	Female	SCCA	IIIA	1	No	2006-03-09	2006-05-22	2007-12-29	Exitus
23	0	U	72	Female	SCCA	IB	3	No	2006-01-19	2006-03-30	2007-12-13	Exitus
24	0	U	65	Female	Adeno	IIA	3	No	2007-01-26	2007-02-02	2012-06-14	Alive
25	0	U	67	Female	SCCA	IIIB	2	No	2009-04-16	2009-06-30	2012-03-30	Alive
26	0	U	75	Male	Adeno	II	2	No	2006-05-18	2006-07-27	2012-05-16	Alive
27	0	U	47	Male	Adeno	IB	1	No	2007-07-20	2007-09-07	2012-06-14	Alive
28	0	U	52	Male	Adeno	IIB	1	No	2007-08-06	2007-10-08	2012-04-20	Alive
29	0	U	61	Female	Adeno	IIIA	1	No	2007-12-03	2008-02-18	2009-02-12	Alive
30	0	U	73	Female	Adeno	IIIA	2	Yes	2009-10-01	2009-11-19	2010-03-23	Alive
31	0	U	55	Female	Adeno	IIB	1	No	2010-01-21	2010-04-06	2012-03-15	Alive
32	0	U	64	Female	SCCA	IIB	1	No	2010-01-22	2010-04-01	2012-05-21	Alive
33	0	U	69	Male	Adeno	IIIA	4	Yes	2002-06-13	2002-08-16	2006-05-17	Exitus
34	0	U	52	Female	Adeno	IB	3	No	2002-06-28	2002-08-26	2008-06-22	Exitus
35	0	U	61	Female	SCCA	IIB	3	No	2004-10-07	2004-12-23	2007-04-08	Exitus
36	0	U	50	Female	SCCA	IB	1	No	2008-03-17	2008-05-26	2010-03-06	Exitus
37	0	U	67	Female	SCCA	IIB	1	Yes	2009-05-28	2009-08-31	2009-11-23	Exitus
38	0	U	69	Female	Adeno	IIIA	1	No	2010-03-23	2010-06-08	2011-08-21	Exitus
39	0	U	57	Female	Adeno	IIIB	3	No	1999-05-07	1999-07-21	2005-05-17	Exitus
40	0	U	57	Female	Adeno	IIIA	4	Yes	2002-04-12	2002-05-23	2002-11-29	Exitus

RAS pathway such as RAF-1, MEK 1/2, ERK1/2 and $p90^{rsk}$.[27] The activation of the ERK pathway can either protect or enhance radiation sensitivity, depending on the cell type analyzed.[28-30] Our data indicate that this survival pathway is activated by radiotherapy treatment in *IGFBP-3* unmethylated 41S cells alone, and although the synthesis of the ERK protein is increased in 41R cells, its activation is inhibited. Therefore, the radioprotection observed in the 41S cells after radiotherapy exposure might be due to the activation of the ERK signaling pathway, as previously reported in the DU145 and A431 human cancer cell lines.[31,32] The ERK pathway activation observed in the 41S cells could also be secondarily regulated by the K-RaS/p38 pathway, given it has been proposed that a sublethal dose of radiation can enhance the metastatic potential of cancer cells via the K-Ras pathway.[33] These results indicate the possibility of alternative treatments with specific MERK inhibitors such as AZD6244, which enhance the radiation responsiveness of diverse tumor types, including lung and colorectal tumors.[30]

Primary tumor data and discussion

We next explored the *IGFBP-3* methylation effect on overall survival (OS) in a population of 40 patients with NSCLC who received a chemotherapy schedule based on cisplatin or carboplatin with or without concomitant radiotherapy (**Figs. 3A, B** and **Table 1**). We also included an external group of 36 patients with NSCLC who did not receive any therapy after surgery, whose results were published previously.[4,5] The NSCLC samples were separated into 2 groups based on their *IGFBP-3* methylation levels; patients with methylation levels equal to those of the negative control group were considered unmethylated (**Fig. 3B**). We then analyzed the patients' responses to radiotherapy and platinum-based treatments in terms of methylation levels. The survival functions were plotted using the Kaplan-Meier estimator and were compared using log-rank under 3 conditions (**Fig. 3C**). We found a statistically significant association ($p = .03$) between OS and evidence of *IGFBP-3* methylation. Twenty-6 of the 40 patients (65%), harbored an unmethylated promoter and, as expected, approximately, 31% of them underwent combined treatment with IR and Chemotherapy compared with the 69%, who underwent a chemotherapy regimen based on cisplatin or carboplatin without radiotherapy. Our results indicate that patients with an unmethylated *IGFBP-3* promoter had an OS of 6.57 y when receiving chemotherapy alone; however, when this group of patients also received radiotherapy, their OS decreased by approximately 2.5 y, confirming our experimental data from human cancer cells. This result could be associated with the initial stage at diagnosis, given that patients with locally advanced stages tend to receive radiotherapy; however, when we analyzed the stages of the patients who received radiotherapy, we found no correlation between stage at diagnosis and radiotherapy ($p = .329$). There were unfortunately no patients with a regimen of radiotherapy alone; therefore, although we observed a trend toward better survival when patients with a methylated promoter received a combined treatment with chemotherapy and radiotherapy, it was not a statistically significant event (data not shown).

We also interrogated the methylation status of IGFBP-3 *in silico* using The Cancer Genome Atlas (TCGA) database (http://cancergenome.nih.gov/). We found that most probes hybridized within the area located from −600 to −450 bp from the TSS, which is a hot spot for methylation at the CpG island located in the *IGFBP-3* promoter.[5] When we examined the raw β-value (probe methylation), the histology, the survival factors and the chemotherapy schedule in the TCGA dataset of 149 patients with NSCLC, (32 adenocarcinoma and 117 squamous cell carcinoma), we found that in the absence of methylation patients live longer when receiving chemotherapy as a unique treatment, whereas concomitant treatment with radiotherapy decreases the survival by half ($p = .034$).

Finally, the identification of a predictor for therapy could reflect biological changes in cancer cells that are independent of any type of therapy used. To evaluate this possibility, we tested *IGFBP-3* methylation status in a cohort of patients diagnosed with early-stage NSCLC who underwent an R0 resection without any adjuvant therapy. In this regard, there was no statistical significance ($p = .09$) in OS according to the methylation status (data not shown). In summary, our results indicate that the unmethylated *IGFBP-3* promoter is associated with resistance to radiotherapy in NSCLC. Specifically, the differences in survival suggest that patients harboring an unmethylated *IGFBP-3* promoter would not benefit from adding radiotherapy to adjuvant chemotherapy.

The limitations of this study are associated with the small number of patients analyzed, due mainly to different treatment arms, which limited the number of patients in each group; however, our findings are promising given there is currently no DNA methylation marker or marker panel that can predict radiotherapy response.[34] Future prospective multicentric studies including additional and larger NSCLC cohorts need to be performed in future. Nevertheless, *IGFBP-3* methylation status is worth considering prior to using radiation therapy after surgery for patients with NSCLC.

Disclosure of Potential Conflicts of Interest

No potential conflicts of interest were disclosed.

Acknowledgments

We gratefully acknowledge Javier Perez for the artwork and J. Siegfried for English grammar corrections.

Funding

Supported by FIS (ISCIII), PI12/00386, PI12/01463, PI11/00949; PI11/00537; PTA2012/7141-I, all supported by FEDER funds. IIC was supported by the "Miguel Servet" program (CP 08/000689).

Downloaded by [81.33.219.79] at 02:41 07 May 2016

Biomarcadores en cáncer. Contribución de la epigenética a la medicina personalizada

Rev Lab Clin. 2014;7(2):73–79

Revista del Laboratorio Clínico

www.elsevier.es/LabClin

REVISIÓN

Biomarcadores en cáncer. Contribución de la epigenética a la medicina personalizada

Olga Pernía[a,b,*], **Olga Vera**[a,b] **e Inmaculada Ibáñez de Cáceres**[a,b,*]

[a] *Laboratorio de Epigenética del Cáncer, Instituto de Genética Médica y Molecular, Hospital La Paz, MadridEspaña*
[b] *Terapias Experimentales y Nuevos Biomarcadores en Cáncer IdiPAZ, Hospital La Paz, Madrid, España*

Recibido el 8 de abril de 2014; aceptado el 15 de abril de 2014
Disponible en Internet el 18 de junio de 2014

PALABRAS CLAVE
Epigenética;
Cáncer;
Medicina personalizada;
Biomarcadores

Resumen En el contexto de la medicina personalizada, la epigenética cobra importancia como base de prevención, diagnóstico, prognosis y tratamiento de enfermedades como el cáncer. De los distintos procesos de control epigenético, el silenciamiento génico por metilación del ADN es el más frecuente en esta patología y aporta aplicaciones clínicas muy variadas como predicción de respuesta terapéutica, prognosis asociada a las características moleculares del tumor y el seguimiento de pacientes tras la intervención quirúrgica o el tratamiento con quimioterapia. Una de las principales ventajas clínicas de estas alteraciones epigenéticas es que pueden revertirse mediante tratamientos farmacológicos, aunque se asocien con múltiples efectos secundarios. Es por ello de gran importancia continuar con el estudio de la regulación epigenética en cáncer, complementado con la biología de sistemas, lo que aportaría conocimiento sobre la implicación biológica real de estos biomarcadores, y la identificación de fármacos específicos que disminuyan estos efectos adversos y nos acerquen a la realidad de una medicina personalizada.
© 2014 AEBM, AEFA y SEQC. Publicado por Elsevier España, S.L. Todos los derechos reservados.

KEYWORDS
Epigenetics;
Cancer;
Personalised medicine;
Biomarkers

Biomarkers in cancer. contribution of epigenetics in personalised medicine

Abstract In the context of personalised medicine, epigenetics has an important role as regards the prevention, diagnosis, prognosis, and treatment of diseases such as cancer. Of the different epigenetic control processes, gene silencing by DNA methylation is most frequent in this disease, and contributes to a wide variety of clinical applications such as, prediction of the therapeutic response, the prognosis associated with the molecular characteristics of the tumour, and the follow-up pf patients after treatment by surgery or chemotherapy. One of the main advantages of these epigenetic alterations is that they can be reversed with pharmacological treatments, although they are associated with multiple side effects. It for this reason, it

* Autor para correspondencia.
Correo electrónico: inma.ibanezca@salud.madrid.org (I. Ibáñez de Cáceres).

http://dx.doi.org/10.1016/j.labcli.2014.04.004
1888-4008/© 2014 AEBM, AEFA y SEQC. Publicado por Elsevier España, S.L. Todos los derechos reservados.

is of great importance to continue studying epigenetic regulation in cancer, complementing with biological systems, as well as the identification of specific drugs that may decrease these adverse effects, and which should help to determine the real biological implications of these biomarkers and may lead to achieving personalised medicine.
© 2014 AEBM, AEFA y SEQC. Published by Elsevier España, S.L. All rights reserved.

Introducción

El Instituto Nacional de Cáncer en Estados Unidos define la medicina personalizada como una forma de medicina que utiliza la información acerca de los genes y proteínas de un individuo y el ambiente que la rodea para prevenir, diagnosticar y tratar una enfermedad. La medicina personalizada utiliza conceptos tradicionales y conceptos emergentes sobre las bases genéticas de una enfermedad para individualizar la prevención, diagnóstico y tratamiento. Los resultados de multitud de proyectos de investigación sobre la relación entre los cambios genéticos y epigenéticos, así como en las rutas de señalización inducidas por los fármacos y aquellos presentes en tumores de los pacientes, han sido esenciales en la determinación de algunos marcadores de interés que han permitido administrar el mejor tratamiento oncológico para cada paciente.

Las aplicaciones de la genética y la epigenética en la medicina personalizada incluyen áreas básicas de la medicina como son la prevención, diagnóstico, prognosis y tratamiento (tabla 1). El trayecto que va desde un concepto hasta la aplicación clínica en cada una de estas áreas involucra investigación básica, traslacional, clínica y también aspectos regulatorios[1]. En el estudio de la relevancia de las terapias personalizadas en el tratamiento del cáncer y el impacto de estas nuevas alternativas terapéuticas hay que tener en cuenta, por una parte el valor que puede representar para el paciente en términos de sufrimiento (efectos secundarios, faltas de respuesta), para el sistema nacional de salud en términos de coste farmacéutico (terapias tradicionales vs. personalizadas que incluyen análisis genéticos, etc.) y por último el coste social y personal que implican las horas de trabajo no ejercido, horas de ocio no disfrutado, tiempo y dedicación de los familiares en el cuidado del paciente, etc.

Aporte de la epigenómica

Epigenómica

Los procesos epigenéticos tienen un papel fundamental en fenómenos fisiológicos como la embriogénesis, la impronta y la inactivación del cromosoma x, pero también en el desarrollo de enfermedades, entre ellas el cáncer. En esta última década, se han establecido los diferentes niveles mecanísticos que participan en la regulación epigenética, entre los que se incluyen la metilación del ADN, la modificación postraduccional de histonas y los micro ARN regulatorios de la expresión génica[2]. De todos estos mecanismos, el mejor conocido es la metilación del ADN.

Metilación y cáncer

La primera vez que se demostró una relación entre la metilación del ADN y el cáncer fue en 1983, cuando se observó que las células tumorales tenían un grado de metilación menor que las células originales no tumorales. Este fenómeno está relacionado con una pérdida de metilación en las regiones repetitivas del genoma provocando inestabilidad cromosómica en estas células tumorales. Sin embargo el principal evento que está involucrado en el origen de un gran número de cánceres es la hipermetilación de islas CpG en los promotores de genes supresores de tumores (GST)[3]. Estos genes pueden mediar diferentes funciones celulares implicadas en el desarrollo del cáncer, como son la regulación del ciclo celular, la reparación del ADN, la interacción célula-célula, la apoptosis y la angiogénesis[4].

Hoy en día, no hay duda de que alteraciones en la metilación del ADN tienen un papel importante en la tumorogénesis. Una metilación aberrante de las islas CpG de genes específicos, es un mecanismo epigenético tan común como las mutaciones puntuales o pérdidas de heterozigosidad (LOH) que causan el silenciamiento de los GST en cánceres humanos. Entre los diferentes genes alterados por la metilación en diversos tipos tumorales encontramos, *RASSF1, BRCA1, GSTP1, CDKN2A, CDH13, MLH1, VHL, APC, MGMT, DAPK, IGFBP-3 o TIMP3* entre otros (tabla 2).

ADN metilado como biomarcador

La contribución de la epigenética al estudio del cáncer es evidente, ya que la metilación aberrante de determinados genes ocurre muy temprano en la carcinogénesis, incluso cuando las muestras quirúrgicas son histológicamente negativas[5]. Los marcadores para ADN metilado son por tanto indicadores perfectos para la enfermedad ya establecida.

Además, debido a lo ubicuo que es el ADN hipermetilado y gracias a las nuevas tecnologías, capaces de detectar cambios de metilación en el ADN en diversos fluidos biológicos, hacen que este área de estudio se considere una de las grandes promesas no solo para la detección del cáncer, sino como fuente de identificación de biomarcadores para prognosis e incluso predicción de respuesta a fármacos. La epigenética proporciona gran flexibilidad biológica a la célula tumoral, sin embargo estas características pueden ser

Tabla 1 Biomarcadores genéticos/epigenéticos de uso clínico

Nombre	Aplicación clínica	Tipo tumoral	Resultado
BluePrint®	Predictivo	Mama	Diversas terapias individuales
BRCA1/2	Predictivo/pronóstico	Mama	Medida de riesgo presintomático
BRAF	Predictivo/pronóstico	Melanoma	Inhibidores de RAF
EGFR	Predictivo	Pulmón (CPNM)	Inhibidores tirosina quinasa (TKI) para EGFR
K-RAS	Pronóstico	Colorrectal	Elección de uso de cetuximab
MammaPrint®	Pronóstico	Mama	Estadio y agresividad del tumor
Therascreen MGMT PyroKit®	Predictivo	Glioblastoma	Decisión clínica sobre agentes alquilantes
OncoTypDX	Predictivo/pronóstico	Mama, ER+, HER2- y colon	Quimioterapia sí/no
VeriStrat®	Pronóstico	Pulmón con bevacizumab y erlotinib en primera línea	Decisión clínica sobre TKIs para EGFR

modificadas farmacológicamente gracias al uso de agentes desmetilantes e inhibidores de acetilasas de histonas. Esta posibilidad nos permite identificar dianas terapéuticas con uso potencial en clínica, ya que existen en la actualidad cuatro fármacos distintos aprobados con estas características, de los que hablaremos más adelante.

Las características que han de tener las secuencias de ADN metilado para poder ser consideradas biomarcadores clínicos se han definido conjuntamente por el National Cancer Institute's y el Early Detection Research Network[6].

La mayoría de los marcadores epigenéticos se han identificado mediante aproximaciones puntuales a genes candidatos; sin embargo en los últimos años, han surgido numerosos estudios combinando arrays de expresión con tratamientos epigenéticos de reactivación de la expresión génica. Estos estudios permiten identificar nuevos genes bajo regulación epigenética con significado en progresión tumoral, que pudieran eventualmente comportarse como biomarcadores en diferentes tipos tumorales como el de vejiga, colorrectal esofágico, renal o pulmón[7]. Recientemente se han sumado a estas aproximaciones otros estudios apoyados en técnicas de secuenciación masiva del genoma completo, combinada con perfiles de expresión diferencial, que se han enfocado en tumores de origen epitelial, identificando marcadores que pudieran iluminar las rutas moleculares involucradas en tumorogénesis. De los diferentes estudios realizados podemos resaltar los siguientes candidatos: *BCN1, MSX1, CCNA1, ALDH1A3*, genes cuya

Tabla 2 Genes supresores tumorales bajo regulación epigenética en diferentes tipos tumorales

Gen	Función	Tipos tumorales
APC	Regulatión negativa del ciclo celular	esofágo, renal, mama, pulmón, colon y otros
ATM	Respuesta a daño en el ADN	linfoma, leucemia
BRCA1	Regulatión negativa del ciclo celular	mama, ovario
CDH1	Adhesión celular	gastrico. endmetrio, vejiga
CDH13	Adhesión celular	mama, ovario, pulmón
CHFR	Regulatión mitótica	Gastrico, Colon
DAPK1	Apoptosis	Pulmón. cervix, próstata, mama, esofágo y otros
ESR1	Receptor de estrógenos	Prostate, ovario
FHIT	Regulatión de ciclo celular	esofágo, gástrrico, colon, pulmón
GSTP1	Transformatión de sustancias electrofílicas	Prostate, gástrico, hígado
HIC1	Factor de Transcriptión	mama, pulmón, liver, medulloblastoma
hMLHl	Reparación del ADN	Colorectal, endometrio, astrocitoma
IGFBP3	Señalización de fatores de crecimiento	Pulmón, renal, próstata, ovario, gástrico, hígado
MGMT	Reparación de guaninas metiladas	pulmón, colon, cabeza y cuello
pl4NK4a	Regulación del ciclo celular	Colon, astrocitoma, mama
pl5NK4a	Regulación del ciclo celularr	Leucemia, linfoma, vejiga
pl6NK4a	Regulación del ciclo celular	pulmón, renal, colorectal
RARbeta	Regulación del crecimiento y ciclo celular	próstata, vejiga, mama, pulmón
RASSF1A	Homologo de RASS	renal, mama
S0CS2	Supresor de citoquinas	ovario, mama, melanoma
TIG1	Regulación negativa del proliferation celular	próstata, digestivo
VHL	Regulación negativa del ciclo celular	renal

expresión está bajo regulación epigenética, y que han sido validados en más de cien muestras quirúrgicas procedentes de diferentes tipos tumorales como mama, colon, próstata y pulmón. Estos resultados indicarían que diversos tipos tumorales de origen epitelial pueden compartir alteraciones en las mismas rutas celulares. Actualmente se argumenta que los patrones de ADN metilado podrían estratificar el cáncer de pulmón no microcítico en dos subtipos fenotípicamente diferentes capaces de predecir respuesta a inhibidores de la ruta del *EGFR*[8].

Por otra parte, la eficacia de un ensayo con biomarcadores viene determinada por su sensibilidad y especificidad. Para un ensayo con biomarcadores de hipermetilación del ADN, la sensibilidad se describe como la cantidad mínima de ADN metilado (diana) capaz de ser detectada por el ensayo. En términos clínicos, se describe como la proporción de pacientes con enfermedad confirmada, para los cuales el test con el biomarcador resulta positivo; mientras que la especificidad del ensayo viene determinada por la proporción de sujetos controles para los que el test resulta negativo. La sensibilidad óptima se alcanza cuando el número de falsos negativos se aproxima a cero. Por otra parte, la especificidad es alta cuando el número de falsos positivos es bajo.

Actualmente, la sensibilidad en cuanto a la detección de los biomarcadores de metilación de ADN recae principalmente en las técnicas de PCR de metilación específica (MSP) o en la versión cuantitativa de esta técnica (qMSP), junto con el origen y la calidad del ADN de la muestra de partida. La orina o la saliva, parecen ser los fluidos biológicos que proporcionan mayor sensibilidad clínica para detectar cánceres de vejiga y de pulmón respectivamente; sin embargo, son el suero y el plasma las fuentes que mejores datos proporcionan en cuanto a la especificidad tumoral. Desafortunadamente, surge un problema inherente asociado a la alta sensibilidad que proporcionan estos biomarcadores de ADN metilado, y es que esta es mayor que la que actualmente proporcionan los métodos diagnósticos por lo que se podrían tener casos de falsos positivos. Por lo que si un caso clínico es detectado por un marcador de metilación de alta sensibilidad, antes que por cualquier otra tecnología existente, lo más frecuente es que este caso sea clasificado como un falso positivo, restándole futura aplicabilidad al biomarcador identificado.

Modificación de histonas y cáncer

Las modificaciones de histonas consisten en reacciones covalentes que afectan a sus regiones amino-terminales. Estas modificaciones incluyen la acetilación, la metilación, la fosforilación, la ubiquitinación, la sumoilación, y la ADP-ribosilación y pueden tener efectos directos sobre diferentes procesos nucleares, incluyendo la transcripción génica, la reparación y replicación del ADN y la organización de cromosomas. Las enzimas que catalizan estas reacciones son las histonas acetiltransferasas (HAT), las desacetilasas de histonas (HDAC), las histonas metiltransferasas (HMT) y las histonas desmetilasas (HDMT). Estas pueden funcionar como activadores o represores transcripcionales dependiendo del residuo sobre el que actúen. Generalmente la acetilación de histonas está asociada con la activación transcripcional, en cambio la metilación de histonas depende del tipo de aminoácido que se metile y de su posición. En cáncer, la modificación más común de histonas es la reducción en la acetilación de la lisina 16 de la histona H4[9], reacción mediada por las HDAC, que se encuentran sobreexpresadas o mutadas en diferentes tipos tumorales[10,11]. Además en algunos tipos de cáncer (colon, útero, pulmón y leucemia) se han observado translocaciones que dan lugar a la formación de proteínas aberrantes, mutaciones o deleciones de *HAT* y de genes relacionados, contribuyendo a una acetilación aberrante de histonas[12]. Las modificaciones postranscripcionales de histonas están íntimamente relacionadas con metilación y participan en la regulación de la expresión génica, mostrando un valor pronóstico y predictivo en muchos tipos de cáncer, entre los que se encuentra el cáncer de pulmón y ovario. En los últimos años se ha visto como estas modificaciones pueden contribuir a la tumorogénesis y se ha comprobado la existencia de un patrón de expresión alterado de enzimas modificadoras de histonas en los tumores humanos.

miARN y cáncer

El control epigenético más recientemente descubierto es la regulación génica postranscripcional mediada por miARN[13]. Esta regulación se lleva a cabo gracias a la unión por complementariedad de secuencias del miARN a la región 3'UTR de sus ARNm diana, provocando la degradación de dicho ARNm o inhibiendo la traducción proteica. Existen más de 1.000 miARN maduros en el genoma humano (*mirbase.org*), cada uno de los cuales presenta múltiples tránscritos diana. La especificidad entre miARN y ARNm diana viene determinada por la complementariedad de secuencia entre ambas moléculas. Un solo miARN puede tener como diana cientos de ARN mensajeros que pueden estar implicados en numerosos procesos biológicos incluidos diferenciación, ciclo celular, y apoptosis[14]. A su vez, un ARNm puede ser diana de distintos miARN. Por lo tanto, la capacidad de alterar la expresión en una célula que posee un solo miARN depende tanto de su propia concentración como de la concentración de sus ARNm diana, y pequeños cambios en la expresión de un miARN puede tener efectos importantes sobre el fenotipo, puesto que puede influir simultáneamente en la expresión de cientos de genes.

La primera evidencia de la correlación entre cáncer y miARN apareció en el año 2002 cuando se observó que el miR-15a y el miR16-1 estaban codificados por una región frecuentemente delecionada del cromosoma 13, en leucemia linfocítica crónica de células B. Actualmente se conocen miARN que se expresan de forma aberrante o que están mutados en una gran variedad de tumores, lo cual sugiere su implicación en iniciación y progresión del cáncer, además estos tienen una función dual, ya que pueden actuar como oncogenes o genes supresores de tumores en función de sus ARNm diana.

Las alteraciones en la expresión de los miARN se han estudiado en diversos tipos tumorales como en cáncer de pulmón[15] y ovario[14], permitiendo distinguir entre subtipos celulares. Los miARN no solo sirven para perfilar distintos tipos tumorales, sino que también pueden servir para predecir respuesta a fármacos. Se ha comprobado que en tumores

de ovario aparecen regulados negativamente el miR-100 y miR-214, habiéndose demostrado que este último tiene como diana al gen supresor tumoral *PTEN* asociado con la resistencia a platino[16]. También se ha descrito el papel de determinados miARN, como el miR-34c, como posibles biomarcadores de riesgo en estudios de quimio-prevención en cáncer de pulmón[17]. Es necesario remarcar que la expresión de los miARN puede estar regulada epigenéticamente a través de la metilación de islas CpG localizadas en regiones reguladoras de la expresión del miARN, pero a su vez, los miARN pueden actuar regulando la maquinaria epigenética. Por ejemplo, en CNMP se encuentra disminuida la expresión de la familia miR-29, que tiene como diana el ARNm de las metiltransferasas DNMT3A y -3B. Cuando se restablecen los valores normales de estos miR-29s se obtienen unos patrones normales de metilación de ADN, inhibiendo en parte la tumorigenicidad celular.

Aplicaciones clínicas

Detección y estratificación del cáncer

Entre las aplicaciones clínicas de los marcadores de metilación se incluyen la predicción de respuesta terapéutica (marcadores predictivos), la capacidad pronóstica, asociada con las características intrínsecas de cada tumor (marcadores pronósticos) y la monitorización de pacientes para identificar la presencia de recidivas de la enfermedad tras intervención quirúrgica, o tras tratamiento con quimioterapia para evaluar su efectividad, especialmente si se ha definido el biomarcador de antemano por biopsia.

Se han descrito unos 30 GST regulados epigenéticamente, aunque pocos de ellos son específicos para un tipo tumoral en concreto, por ejemplo, *DAPK* y *p16* son posibles marcadores pronósticos de fenotipos más agresivos en cáncer de pulmón, colorrectal y tumores cerebrales; mientras que *VHL* por ejemplo parece específico de carcinoma de células renales y *BRCA1* de cáncer de mama y de ovario. Sin embargo, algunos genes muestran diferentes grados de metilación según el tipo tumoral: *GSTP1* está metilado en un 90% de cáncer de próstata, 30% de cáncer de mama y 25% de cáncer hepático. Esta última característica de algunos marcadores de metilación ha permitido a los científicos desarrollar paneles de metilación con GST diferentes, cubriendo en la mayoría de los casos la detección del 100% de las muestras tumorales; por ejemplo, para la detección precoz del *cáncer de mama* se han testado diferentes paneles de metilación en muestras con diferente origen como aspirado de mama, lavado ductal o suero. Evron et al[18], compararon la metilación de los promotores de *ciclina D2*, *Twist* y *RAR-β* utilizando células procedentes de lavado ductal. Estos investigadores encontraron metilación anormal en las células de algunas mujeres sanas, que luego desarrollaron cáncer de mama, proporcionando una evidencia directa del uso de los marcadores de metilación para la detección del cáncer en individuos asintomáticos. El cáncer de mama también se ha podido identificar a través del análisis de los genes *RASSF1A*, *APC*, *DAPK*, *GSTP1*, *beta RAR*, *p16* y *p14* en muestras de suero y aspirado de mama. También se han descrito diferentes aproximaciones para la detección molecular de cáncer de ovario. El estado de hipermetilación de los genes *BRCA1* y *RASFF1A* se ha valorado en 50 pacientes con cáncer de ovario o con tumores primarios peritoneales. La hipermetilación de uno o ambos genes se encontró en un 68% del ADN tumoral. Un examen adicional de uno o más de los siguientes GST; *APC, p14, ARF, p16 y DAPK* completó el 100% de cobertura, encontrándose un patrón idéntico de hipermetilación del gen en el ADN de origen sérico (82% de sensibilidad), incluyendo estadios de enfermedad I y II[19].

La alteración epigenética más común en el *cáncer de próstata* es la pérdida de la expresión del gen *GSTP1* asociada a la presencia de hipermetilación en su promotor. Esta puede valorarse en orina, pudiendo discriminar entre diferentes grados de malignidad tumoral[20]. También se ha descrito la correlación entre metilación del gen *RARb* y discriminación entre tejido neoplásico o no neoplásico.

Uno de los problemas asociados al *cáncer de pulmón* es el fracaso en su diagnóstico temprano. Sin embargo, el material biológico presente en esputo o en aspirado bronquial permite nuevas aproximaciones diagnósticas. Los genes *APC, p16 y RARβ* están frecuentemente metilados en este tipo tumoral, lo que ha hecho que se diseñen diferentes ensayos utilizando la técnica de MSP para diagnóstico temprano en pacientes con este tipo tumoral. Por ejemplo, la metilación aberrante en los genes *p16* y *MGMT* en el ADN de esputo se identificó en un 100% de los pacientes con carcinoma de pulmón de células escamosas hasta 3 años antes de su diagnóstico clínico. Por otra parte, el descenso en la expresión del gen *IGFBP3*, mediada por la metilación de su promotor es un evento temprano en la carcinogénesis de pulmón. Más recientemente se ha descrito que la metilación de este gen, no solo sirve para detección temprana de cáncer de pulmón, sino que también es un marcador de respuesta terapéutica al agente CDDP[7].

La alteración epigenética más común en *gliomas* afecta a la enzima O^6-metilguanina-ADN metiltransferasa *MGMT*, esta actúa eliminando el grupo metilo añadido a la posición O^6 de las guaninas del ADN. Se ha descrito que la metilación de las islas CpG localizadas en la zona del promotor de este gen reprime la expresión génica; en el caso de los gliomas malignos, el promotor de *MGMT* está metilado en un 40-68% de los casos por lo que gana eficacia en tratamiento quimioterápico basado en agentes alquilantes y metilantes[21].

La ventaja clínica que tiene la pérdida de la expresión génica por metilación del ADN es, en contraste con las mutaciones genéticas, la posibilidad de revertir el estado de metilación mediante tratamiento farmacológico con inhibidores de la desacetilación de histonas y agentes desmetilantes. En la actualidad hay cuatro medicamentos aprobados por la FDA con acción epigenética: los inhibidores de la ADN metiltransferasa 5-azacitidina (Vidaza) y decitabina (2-desoxi-5-azacitidina, Dacogen) y los inhibidores de acetilasas de histonas (HDAC), ácido hidroxámicosuberoilanilida (SAHA, Zolinza) y romidepsina (Istodax). Varios fármacos adicionales desmetilantes e inhibidores de HDAC se están evaluando en estudios preclínicos y en ensayos clínicos. Sin embargo, no hay en la actualidad ningún ensayo clínico con fármacos candidatos dirigidos contra otros objetivos epigenéticos.

Tanto 5-azacitidina como decitabina han demostrado un beneficio clínico significativo en el tratamiento del síndrome mielodisplásico y en leucemia mieloide. Aunque se haya confirmado por varios estudios que se produce una desmetilación en los pacientes tratados, sin embargo, aún

no se ha podido demostrar una relación directa entre la desmetilación del ADN y la respuesta clínica, ya que no hay establecidos biomarcadores de metilación del ADN que predigan con precisión las respuestas del paciente[22]. Este hecho tan relevante tiene abiertos muchos frentes de estudio en busca de biomarcadores para establecer la prueba de concepto que falta con la terapia epigenética de estos fármacos.

Los fármacos epigenéticos más utilizados en la clínica son 5-azacitidina y decitabina. La incorporación de las bases de azacitosina en el ADN y ARN induce la formación de aductos covalentes con las metiltransferasas, resultando en la depleción de las DNMT, y en la consecuente reducción global de la metilación del ADN. Este descenso en los niveles globales de metilación tiene efectos antitumorales según se ha descrito en diferentes modelos murinos. En general se supone que el beneficio terapéutico de la desmetilación global del ADN está relacionado con la desmetilación y la reactivación de los genes aberrantemente silenciados. Sin embargo, como veremos más adelante, la desmetilación global no es selectiva de los marcadores tumorales que se encuentran metilados en cáncer, efecto que podría restringir severamente la especificidad de la terapia con estos fármacos.

Los inhibidores de HDAC, SAHA y romidepsina se han aprobado para el tratamiento de linfoma cutáneo de células T[23]. En la actualidad hay numerosos inhibidores de HDAC que se están testando en diferentes ensayos clínicos, debido a la gran farmacobilidad de la familia de enzimas HDAC, que permite el desarrollo de potentes inhibidores específicos. Es importante resaltar que la desacetilación de histonas interactúa sinérgicamente con la metilación del ADN en el silenciamiento epigenético en cáncer, por lo que se han justificado diferentes ensayos clínicos combinando inhibidores de HDAC y DNMT. Sin embargo, los estudios no han revelado efectos clínicos sinérgicos, que podrían estar relacionados con la complejidad de los modos de acción de los fármacos que aún no se han dilucidado. Por una parte, cada vez está más claro que la actividad enzimática de HDAC no está restringida a las proteínas histonas, ya que el tratamiento de líneas celulares de cáncer humano con inhibidores de HDAC altamente específicos, inducen la hiperacetilación de 1.750 proteínas[24]. Este hallazgo sugiere fuertemente que la gran mayoría de los sustratos de los fármacos de HDAC son proteínas no-histonas.

Efectos secundarios sobre la desmetilación global del ADN

El tratamiento de reactivación epigenética basado en agentes desmetilantes, puede inducir como efectos secundarios inestabilidad genómica y/o aumento de la expresión de protooncogenes como resultado de la hipometilación inducida por estos fármacos.

Además, la hipometilación global del DNA se ha asociado tradicionalmente con inestabilidad cromosómica y propensión al desarrollo de neoplasias, y también se ha relacionado más recientemente, una desregulación en los elementos repetitivos del genoma[25]. La desmetilación de una región LINE-1 situada en un intrón del protooncogen *cMet*, resulta en un transcrito aberrante de *cMET*, que se asocia con la reducción de la expresión de la proteína y de la señalización del receptor de *cMET*. Estos resultados proporcionan una importante fuente de información, por ejemplo sobre la alteración de la regulación transcripcional que se induce por la desmetilación de elementos repetitivos, lo que sugiere que muchos loci genómicos podrían estar sujetos a los efectos secundarios de la desmetilación epigenética global del ADN[26]. Por otra parte, es bien sabido que la desmetilación de ADN está estrechamente controlada durante la diferenciación celular, por lo que la desmetilación global que inducen estos fármacos epigenéticos y/o la pérdida de las modificaciones de histonas podrían afectar negativamente a las funciones en las poblaciones de células progenitoras en los pacientes[27]. Por lo que es crítico la identificación de drogas epigenéticas con dianas más específicas que no actuaran sobre las DNMT, sino sobre otros factores o rutas epigenéticas, como podrían ser enzimas que actúan sobre metilación *de novo* específica en cáncer. Por ejemplo, la metiltransferasa EZH2 es una enzima crítica en la metilación de la lisina 27 de la histona 3, involucrada en el desarrollo de distintos tipos tumorales. Una terapia dirigida contra esta diana podría redirigir el establecimiento de programas epigenéticos específicos en cáncer[28].

La medicina personalizada está tomando cada vez más fuerza dentro de los sistemas hospitalarios público y privados, ya que su uso permite optimizar e implementar tratamientos que disminuyen tanto el coste de los gastos médicos asociados a la quimioterapia como al coste personal y social que deriva de estos tratamientos y del desarrollo de la enfermedad. Gracias a la introducción de las nuevas técnicas genómicas y epigenómicas de nueva generación como la secuenciación masiva, se está acelerando exponencialmente la identificación de nuevos parámetros moleculares; sin embargo sigue siendo de gran importancia dedicarle tiempo y esfuerzo al estudio de la biología de sistemas, ya que puede explicar la implicación biológica real de cada uno de estos potenciales biomarcadores, así como las rutas celulares que se alteran en cada caso, que en definitiva es lo que puede permitir la identificación y selección de fármacos específicos.

Financiación

Financiado por FIS PS09/00472 y PI12/00386, Ibanez de Cáceres I, disfruta de un contrato «Miguel Servet» del ISCIII (CP 08/000689; PI-717). O. Pernía disfruta de un contrato con el Ministerio de Economía y Competitividad PTA2012/7141-I.

Conflicto de intereses

Los autores declaran no tener ningún conflicto de intereses.

Bibliografía

1. Hamburg MA, Collins FS. The path to personalized medicine. N Engl J Med. 2010;363:301–4. Epub 2010 Jun 15.
2. Jones PA, Baylin SB. The fundamental role of epigenetic events in cancer. Nat Rev Genet. 2002;3:415–28.
3. Herman JG, Baylin SB. Gene silencing in cancer in association with promoter hypermethylation. N Engl J Med. 2003;349:2042–54.

4. Esteller M. Epigenetics in cancer. N Engl J Med. 2008;358:1148–59.
5. Brock MV, Hooker CM, Ota-Machida E, Han Y, Guo M, Ames S, et al. DNA methylation markers and early recurrence in stage I lung cancer. N Engl J Med. 2008;358:1118–28.
6. Kagan J, Srivastava S, Barker PE, Belinsky SA, Cairns P. Towards clinical application of methylated DNA sequences as cancer biomarkers: a joint NCI's EDRN and NIST works hopon standards, methods, assays, reagents and tools. Cancer Res. 2007;67: 4545–9.
7. Ibanez de Caceres I, Cortes-Sempere M, Moratilla C, Machado-Pinilla R, Rodriguez-Fanjul V, Manguán-García C, et al. IGFBP-3 hypermethylation-derived deficiency mediates cisplatin resistance in non-small-cell lung cancer. Oncogene. 2010;18(29(11)):1681–90. Epub 2009 Dec 21.
8. Walter K, Holcomb T, Januario T, Du P, Evangelista M, Kartha N, et al. DNA methylation profiling defines clinically relevant biological subsets of non-small cell lung cancer. Clin Cancer Res. 2012;18:2360–73. Epub 2012 Jan 19.
9. Fraga MF, Ballestar E, Villar-Garea A, Boix-Chornet M, Espada J, Schotta G, et al. Loss of acetylation at Lys16 and trimethylation at Lys20 of histone H4 is a common hallmark of human cancer. Nat Genet. 2005;37:391–400.
10. Ropero S, Fraga MF, Ballestar E, Hamelin R, Yamamoto H, Boix-Chornet M, et al. A truncating mutation of HDAC2 in human cancers confers resistance to histone deacetylase inhibition. Nat Genet. 2006;38:566–9.
11. Zhu P, Martin E, Mengwasser J, Schlag P, Janssen KP, Gottlicher M. Induction of HDAC2 expression upon loss of APC in colorectal tumorigenesis. Cancer Cell. 2004;5:455–63.
12. Portela A, Esteller M. Epigenetic modifications and human disease. Nat Biotechnol. 2010;28:1057–68.
13. Schickel R, Boyerinas B, Park SM, Peter ME. MicroRNAs: keyplayers in the immune system, differentiation, tumorigenesis and cell death. Oncogene. 2008;27:5959–74.
14. Iorio MV, Visone R, Di Leva G, Donati V, Petrocca F, Casalini P, et al. MicroRNA signatures in human ovarian cancer. Cancer Res. 2007;67:8699–707.
15. Du L, Schageman JJ, Irnov I, Girard L, Hammond SM, Minna JD, et al. MicroRNA expression distinguishes SCLC from NSCLC lung tumor cells and suggests a possible pathological relationship between SCLCs and NSCLCs. J Exp Clin Cancer Res. 2010;29:75.
16. Yang H, Kong W, He L, Zhao JJ, O'Donnell JD, Wang J, et al. MicroRNA expression profiling in human ovarian cancer: miR-214 induces cell survival and cisplatin resistance by targeting PTEN. Cancer Res. 2008;68.:425–33.
17. Mascaux C, Keith RL, Feser WJ, Lewis MT, Barón AE, Merrick DT, et al. miR-34c is a potential biomarker for histological response in lung cancer chemoprevention studies. Abstract 790.Translational research, biology and pathology. ESMO European Lung Cancer Conference). 2012.
18. Evron E, Dooley WC, Umbricht CB, Rosenthal D, Sacchi N, Gabrielson E, et al. Detection of breast cancer cells in ductal lavage fluid by methylation-specific PCR. Lancet. 2001;357:1335–6.
19. Ibanez de Caceres I, Battagli C, Esteller M, Herman JG, Dulaimi E, Edelson MI, et al. Tumor cell-specific BRCA1 and RASSF1A hypermethylation in serum, plasma, and peritoneal fluid from ovarian cancer patients. Cancer Res. 2004;64:6476–81.
20. Henrique R, Jeronimo C. Molecular detection of prostate cancer: a role for GSTP1 hypermethylation. EurUrol. 2004;46:660–9.
21. Esteller M, Garcia-Foncillas J, Andion E, Goodman SN, Hidalgo OF, Vanaclocha V, et al. Inactivation of the DNA-repair gene MGMT and the clinical response of gliomas to alkylating agents. N Engl J Med. 2000;343:1350–4.
22. Fandy TE, Herman JG, Kerns P, Jiemjit A, Sugar EA, Choi SH, et al. Early epigenetic changes and DNA damage do no predict clinical response in anoverlapping schedule of 5-azacytidine and entinostat in patients with myeloid malignancies. Blood. 2009;114:2764–73.
23. Piekarz RL, Frye R, Turner M, Wright JJ, Allen SL, Kirschbaum MH, et al. Phase II multi-institutional trial of the histone deacetylase inhibitor omidepsin as monotherapy for patients with cutaneous T-cell lymphoma. J Clin Oncol. 2009;27:5410–7.
24. Choudhary C, Kumar C, Gnad F, Nielsen ML, Rehman M, Walther TC, et al. Lysine acetylation targets protein complexes and co regulates major cellular functions. Science. 2009;325:834–40.
25. Wolff EM, Byun HM, Han HF, Sharma S, Nichols PW, Siegmund KD, et al. Hypomethylation of a LINE-1 promoter activates an alternate transcript of the MET oncogene in bladders with cancer. PLoS Genet. 2010;6:e1000917.
26. Lizardi PM. As we bringde methylating drugs to the clinic, we better know the DICE being cast. Oncogene. 2010;29:5772–4.
27. Hansen KD, Timp W, Bravo HC, Sabunciyan S, Langmead B, McDonald OG, et al. Increased methylation variation in epigenetic domains across cancer types. Nat Genet. 2011;43:768–75.
28. Simon JA, Lange CA. Roles of the EZH2 histone methyltransferase in cancer epigenetics. Mutat Res. 2008;647:21–9.

PATENTES/PATENTS

PATENT COOPERATION TREATY

From the INTERNATIONAL SEARCHING AUTHORITY

PCT

To:
Arias Sanz, Juan
ABG Patentes, S.L.
Avenida de Burgos 16D
Edificio Euromor
28036 Madrid
ESPAGNE

RECEIVED
25 OCT. 2016
ABG Patentes, S.L.

NOTIFICATION OF TRANSMITTAL OF THE INTERNATIONAL SEARCH REPORT AND THE WRITTEN OPINION OF THE INTERNATIONAL SEARCHING AUTHORITY, OR THE DECLARATION

(PCT Rule 44.1)

	Date of mailing *(day/month/year)*: 20 October 2016 (20-10-2016)
Applicant's or agent's file reference: P11783PC00	**FOR FURTHER ACTION** See paragraphs 1 and 4 below
International application No.: PCT/ES2016/070516	International filing date *(day/month/year)*: 8 July 2016 (08-07-2016)
Applicant: FUNDACION PARA LA INVESTIGACION BIOMEDICA DEL...	

1. [X] The applicant is hereby notified that the international search report and the written opinion of the International Searching Authority have been established and are transmitted herewith.

   Filing of amendments and statement under Article 19:
   The applicant is entitled, if he so wishes, to amend the claims of the International Application (see Rule 46):

   When? The time limit for filing such amendments is normally two months from the date of transmittal of the International Search Report.

   How? Directly to the International Bureau of WIPO, 34 chemin des Colombettes 1211 Geneva 20, Switzerland, Fascimile No.: (41-22) 338.82.70

   For more detailed instructions, see *PCT Applicant's Guide*, International Phase, paragraphs 9.004 - 9.011.

2. [ ] The applicant is hereby notified that no international search report will be established and that the declaration under Article 17(2)(a) to that effect and the written opinion of the International Searching Authority are transmitted herewith.

3. [ ] **With regard to any protest** against payment of (an) additional fee(s) under Rule 40.2, the applicant is notified that:

   [ ] the protest together with the decision thereon has been transmitted to the International Bureau together with any applicant's request to forward the texts of both the protest and the decision thereon to the designated Offices.

   [ ] no decision has been made yet on the protest; the applicant will be notified as soon as a decision is made.

4. **Reminders**

   The applicant may **submit comments on an informal basis on the written opinion of the International Searching Authority** to the International Bureau. These comments will be made available to the public after international publication. The International Bureau will send a copy of such comments to all designated Offices unless an international preliminary examination report has been or is to be established.

   Shortly after the expiration of **18 months from the priority date, the international application will be published** by the International Bureau. If the applicant wishes to avoid or postpone publication, a notice of withdrawal of the international application, or of the priority claim, must reach the International Bureau before the completion of the technical preparations for international publication (Rules 90*bis*.1 and 90*bis*.3).

   Within **19 months** from the priority date, but only in respect of some designated Offices, a demand for international preliminary examination must be filed if the applicant wishes to postpone the entry into the national phase **until 30 months** from the priority date (in some Offices even later); otherwise, the applicant must, **within 20 months** from the priority date, perform the prescribed acts for **entry into the national phase** before those designated Offices. In respect of other designated Offices, the time limit of **30 months** (or later) will apply even if no demand is filed within 19 months. For details about the applicable time limits, Office by Office, see www.wipo.int/pct/en/texts/time_limits.html and the *PCT Applicant's Guide*, National Chapters.

   Within **19 months from the priority date, the applicant may request that a supplementary international search be carried out** by a different International Searching Authority that offers this service (Rule 45*bis*.1). The procedure for requesting supplementary international search is described in the *PCT Applicant's Guide*, International Phase, paragraphs 8.006-8.032.

Name and mailing address of the International Searching Authority	Authorized officer
European Patent Office, P.B. 5818 Patentlaan 2 NL-2280 HV Rijswijk Tel. (+31-70) 340-2040 Fax: (+31-70) 340-3016	EMERY, Carole Tel: +31 (0)70 340-2848

PATENT COOPERATION TREATY

PCT

INTERNATIONAL SEARCH REPORT

(PCT Article 18 and Rules 43 and 44)

Applicant's or agent's file reference	**FOR FURTHER ACTION**	see Form PCT/ISA/220 as well as, where applicable, item 5 below.
P11783PC00		
International application No.	International filing date *(day/month/year)*	(Earliest) Priority Date *(day/month/year)*
PCT/ES2016/070516	8 July 2016 (08-07-2016)	9 July 2015 (09-07-2015)
Applicant		
FUNDACION PARA LA INVESTIGACION BIOMEDICA DEL...		

This international search report has been prepared by this International Searching Authority and is transmitted to the applicant according to Article 18. A copy is being transmitted to the International Bureau.

This international search report consists of a total of 6 sheets.

[X] It is also accompanied by a copy of each prior art document cited in this report.

1. **Basis of the report**
   a. With regard to the **language,** the international search was carried out on the basis of:
      [X] the international application in the language in which it was filed
      [ ] a translation of the international application into _____, which is the language of a translation furnished for the purposes of international search (Rules 12.3(a) and 23.1(b))
   b. [ ] This international search report has been established taking into account the **rectification of an obvious mistake** authorized by or notified to this Authority under Rule 91 (Rule 43.6*bis*(a)).
   c. [X] With regard to any **nucleotide and/or amino acid sequence** disclosed in the international application, see Box No. I.

2. [ ] **Certain claims were found unsearchable** (See Box No. II)

3. [ ] **Unity of invention is lacking** (see Box No III)

4. With regard to the **title,**
   [ ] the text is approved as submitted by the applicant
   [X] the text has been established by this Authority to read as follows:

   DETERMINATION OF METHYLATION AND MIRNA-7 LEVELS FOR PREDICTING THE RESPONSE TO A PLATINUM-BASED ANTITUMOR COMPOUND

5. With regard to the **abstract,**
   [X] the text is approved as submitted by the applicant
   [ ] the text has been established, according to Rule 38.2, by this Authority as it appears in Box No. IV. The applicant may, within one month from the date of mailing of this international search report, submit comments to this Authority

6. With regard to the **drawings,**
   a. the figure of the **drawings** to be published with the abstract is Figure No. _____
      [ ] as suggested by the applicant
      [ ] as selected by this Authority, because the applicant failed to suggest a figure
      [ ] as selected by this Authority, because this figure better characterizes the invention
   b. [X] none of the figures is to be published with the abstract

MINISTERIO
DE INDUSTRIA, ENERGÍA
Y TURISMO

Oficina Española
de Patentes y Marcas

Acknowledgement of receipt

We hereby acknowledge receipt of your request for grant of a European patent as follows:

Submission number	300247372	
Application number	EP17382610.8	
File No. to be used for priority declarations	EP17382610	
Date of receipt	15 September 2017	
Your reference	902 444	
Applicant	Fundación para la Investigación Biomédica del Hospital Universitario La Paz (FIBHULP)	
Country	ES	
Title	MAFG as a potential therapeutic target to restore chemosensitivity in platinum-resistant cancer cells	
Documents submitted	package-data.xml	ep-request.xml
	application-body.xml	ep-request.pdf (4 p.)
	SPECEPO-2.pdf\902 444 Claims.pdf (3 p.)	SPECEPO-4.pdf\902 444 Figures.pdf (8 p.)
	SPECEPO-3.pdf\902 444 Abstract.pdf (1 p.)	SPECEPO-1.pdf\902 444 Description.pdf (40 p.)
	OLF-ARCHIVE.zip\902 444 Text ready to file.zip	f1002-1.pdf (2 p.)
	feesheetint.pdf (1 p.)	
Submitted by	CN=Gustavo Fuster 26814	
Method of submission	Online	
Date and time receipt generated	15 September 2017, 13:43:29 (CEST)	

Official Digest of Submission	A4:84:41:5D:A3:78:F3:98:11:8B:43:FB:AF:D3:35:01:22:CB:AF:E3

/Madrid, Oficina Receptora/